Protected areas and Andean ecosystems in Colombia under land-use/land-cover and climate change: habitat loss, connectivity decline, and hydroclimatic vulnerability

Autor

Kristian David Rubiano Calderón

Director

Nicola Clerici, PhD.

Título a obtener

Doctor en Ciencias Biomédicas y Biológicas

Escuela de Medicina y Ciencias de la Salud

Doctorado en Ciencias Biomédicas y Biológicas

Universidad del Rosario

Bogotá – Colombia

2026

Protected areas and Andean ecosystems in Colombia under land-use/land-cover and climate change: habitat loss, connectivity decline, and hydroclimatic vulnerability

Kristian Rubiano

Thesis committee

Thesis director
Nicola Clerici, PhD.
School of Sciences and Engineering, Universidad del Rosario
Bogotá, Colombia

Advisors
Fernando Jaramillo, PhD.
Department of Physical geography, Stockholm University
Stockholm, Sweden

Adriana Sánchez, PhD.
School of Sciences and Engineering, Universidad del Rosario
Bogotá, Colombia

Luigi Boschetti, PhD.
College of Natural Resources, University of Idaho
Moscow, Idaho, US

Marius Bottin, PhD.
Instituto de Investigación de Recursos Biológicos Alexander von Humboldt
Bogotá, Colombia

Examiners
Camilo Correa, PhD.
Faculty of environmental and rural studies, Pontificia Universidad Javeriana
Bogotá, Colombia

Cristian Echeverría, PhD.
Faculty of Forest Sciences, Universidad de Concepción
Concepción, Chile

Benjamin Quesada, PhD.
School of Sciences and Engineering, Universidad del Rosario
Bogotá, Colombia

Table of contents

Chapter 1

General introduction

1. Armed conflict, post-agreement, and landscape transformation in Colombia

Armed conflict is one of the most pervasive forms of human disturbance, with profound and lasting ecological consequences. Over time, recurrent warfare has shaped ecosystems across the globe, prompting the emergence of *warfare ecology* as a field dedicated to understanding the environmental dimensions of conflict and the mechanisms through which it alters ecological systems (Machlis & Hanson, 2008). Research has shown that these impacts are highly context-dependent, ranging from severe degradation to temporary ecological recovery, depending on the conflict's nature, intensity, and socio-political conditions (Dudley et al., 2002; Gaynor et al., 2016; Hanson, 2018; Suarez et al., 2018). Deforestation, a key indicator of landscape transformation, may either increase or decline during wartime, reflecting the complex interplay between economic, political, and geographic drivers (Álvarez, 2003; Grima & Singh, 2019; Machlis & Hanson, 2008; Suarez et al., 2018).

Warfare often weakens institutional capacity for environmental governance, reduces the enforcement of conservation laws, and disrupts resource management systems (Adano et al., 2012; Reuveny et al., 2010). At the same time, population displacement and restricted land access can temporarily reduce human pressures in some regions, creating unintended refuges for biodiversity (Aide & Grau, 2004; Dudley et al., 2002; Ordway, 2015; Suarez et al., 2018). Yet, the transition from conflict to peace frequently reverses these dynamics. In many post-conflict contexts, such as Rwanda, Angola, or Sri Lanka, demobilization, population return, and renewed economic activity have led to rapid forest loss and poorly planned land-use expansion (Grima & Singh, 2019; Kanyamibwa, 1998; Mason, 2014; Suarez et al., 2018). These patterns highlight that the post-conflict phase constitutes a critical ecological turning point, where governance reconstruction determines whether landscapes degrade further or begin to recover.

Colombia provides one of the most illustrative examples of these dynamics. Its internal armed conflict, rooted in ideological struggles and rural inequality since the 1960s, involved guerrilla groups, paramilitaries, and the national army, displacing millions of people and leaving nearly six million hectares of abandoned land (Suarez et al., 2018). Environmentally, the conflict produced both negative and unintended positive effects (Figure 1; Álvarez, 2001, 2003; Landholm et al., 2019; Murillo-Sandoval et al., 2020). Forests, present in roughly one-third of conflict-affected territories, served as both battlegrounds and buffers (Álvarez, 2003). In areas under FARC control, practices of *gunpoint conservation* imposed de facto land-use restrictions, while landmines and isolation limited access, allowing vegetation recovery in several regions (Álvarez, 2001, 2003; Murillo-Sandoval et al., 2020; Negret et al., 2017, 2019). Similarly, large-scale displacement fostered forest regrowth through agricultural abandonment (Aide & Grau, 2004; Sánchez-Cuervo et al., 2012).

Conversely, the conflict also intensified deforestation, largely driven by the expansion of illicit crops, especially coca (*Erythroxylum coca*) and poppy (*Papaver somniferum*), that financed armed groups (Cavelier & Etter, 1995; Dávalos et al., 2011; Landholm et al., 2019; Negret et al., 2019). Following the 2016 Peace Agreement and the demobilization of the FARC, Colombia entered a "post-conflict" period marked by rapid and spatially uneven landscape transformation. As restricted areas reopened, deforestation surged, particularly in former conflict strongholds where new actors seized control of land and resources (Murillo-Sandoval et al., 2020; Suarez et al., 2018). Weak governance and the emergence of new armed groups have fueled renewed

violence and expansion of illicit economies, accelerating forest loss in several regions, including PAs and their buffer zones (Armenteras et al., 2019; Clerici et al., 2020; Mendoza, 2020; Negret et al., 2019).

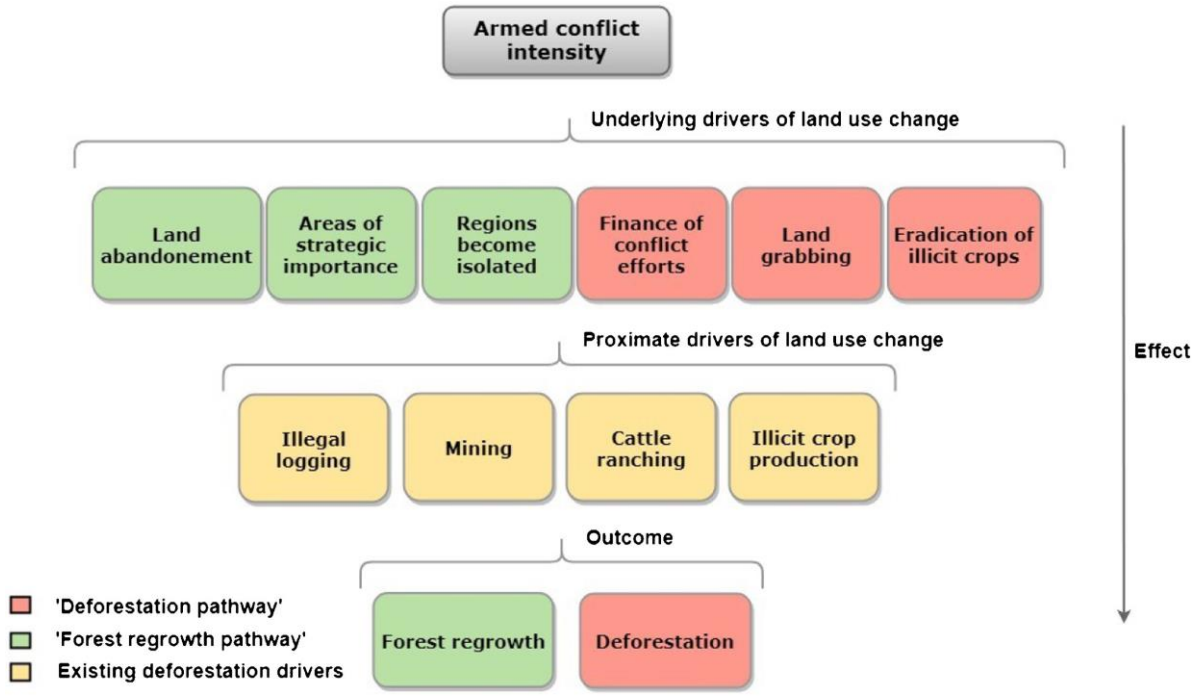

Figure 1. Conceptual pathways through which armed conflict affects forest ecosystems. Armed conflict influences forests by modifying the underlying drivers of land-use change, such as population displacement, restricted land access, or the need to finance military activities, which, in turn, intensify or reduce the proximate drivers of land conversion (e.g., illicit crop cultivation, cattle ranching). Mechanisms shown in red increase deforestation pressure ("deforestation pathway"), whereas those in green reduce it ("forest regrowth pathway"). Adapted from Landholm et al. (2019).

Recent analyses warn that deforestation continues to rise in post-conflict Colombia and may persist without structural reforms (Armenteras et al., 2019; Clerici et al., 2020; Murillo-Sandoval et al., 2020). Two central components of the 2016 Peace Agreement, land tenure reform and the substitution of illicit crops (Presidencia de la República & FARC-EP, 2016), remain only partially implemented, constrained by institutional weakness, security instability, and political shifts. Their effective realization is essential to achieve sustainable land management and prevent further forest degradation. In this context, Colombia's post-conflict transition represents not only a social and political challenge but also an ecological test, determining whether peace will enable the recovery of ecosystems or lead to a new phase of environmental deterioration, underscoring the need for rigorous territorial planning, integrated land governance, and sustainable rural development.

2. Landscape transformation within Colombia's National System of Protected Areas

Numerous studies have analyzed landscape transformation processes within Colombia's protected areas (PAs), evaluating their capacity to mitigate deforestation and identifying the main

drivers shaping these dynamics. Most investigations have focused on individual parks or specific regions, particularly the Andes and Amazon, while relatively few have adopted a nationwide perspective encompassing sites distributed across the country. Within the National System of Protected Areas (SINAP), research has concentrated mainly on the National Natural Parks System (SPNN), especially the National Natural Parks (NNP). Temporal analyses typically covered the period 1985–2016, with some recent extensions, and rely largely on the interpretation of medium (30 m) and coarse-resolution (250 m) satellite imagery, as well as open-access datasets such as IDEAM's deforestation reports (Cabrera et al., 2019) and the Global Forest Change dataset (Hansen et al., 2013).

At the national scale, evidence consistently indicates that Colombian PAs have generally been effective in reducing deforestation, although their performance varies considerably among regions and management categories, and depends on ecological, social, and institutional conditions (Bonilla-Mejía & Higuera-Mendieta, 2019; Negret et al., 2020). Despite overall positive trends, substantial forest losses persist in several PAs. Between 2001 and 2010, about 4 % of national deforestation hotspots overlapped with ten PAs, mostly in Urabá and the Magdalena Valley, whereas forest regeneration hotspots were concentrated in the Colombian Massif and Caribbean coast (Sánchez-Cuervo & Aide, 2013). From 2000 to 2015, SINAP lost roughly 1.5 % of its forest cover, affecting 82 % of NNPs, with the most severe losses in Tinigua, Nevado del Huila, Las Hermosas, Los Colorados, and Sanquianga. Deforestation was highest in the Pacific region but decreased in the Caribbean (Negret et al., 2020).

More recent analyses show that the post-conflict period (2013–2018) brought a sharp escalation of deforestation, with forest loss occurring in 79 % of NNPs and reserves. Deforestation rates rose by 177 % inside PAs and 158 % in buffer zones, totaling approximately 33,000 ha of lost forest, particularly in Tinigua, Cordillera de los Picachos, Sierra de la Macarena, Sierra Nevada de Santa Marta, Paramillo, and Catatumbo Barí National Parks (Clerici et al., 2020). These patterns reveal marked spatial disparities linked to governance and accessibility: national-level PAs have generally performed better than regional ones, and effectiveness tends to be higher in areas with stronger institutions, higher population density, and lower violence. In contrast, PAs in remote or conflict-affected regions remain highly vulnerable to pressures from coca cultivation, illegal mining, and weak law enforcement (Bonilla-Mejía & Higuera-Mendieta, 2019).

Overall, research indicates that SINAP has contributed significantly to moderating deforestation at the national level, yet its effectiveness remains heterogeneous, reflecting pronounced regional contrasts in institutional capacity, socioeconomic pressures, and land-use dynamics. These disparities underscore the need for comprehensive assessments that encompass protected areas across all biogeographical regions, enabling spatial and temporal comparability of conservation outcomes. Addressing this gap is particularly critical in the current post-conflict context, where rapid landscape transformations and shifting socio-institutional conditions demand an integrated, long-term understanding of how Colombia's protected areas respond to renewed anthropogenic pressures and evolving governance frameworks.

3. Biodiversity threats from land-use changes in PAs and surrounding buffer zones

The loss and fragmentation of natural habitats currently represent some of the primary drivers of biodiversity decline at the global scale (Newbold et al., 2015; Pereira et al., 2012). Human-induced land-cover and land-use changes not only reduce biodiversity but also undermine the provision of key ecosystem services that sustain human well-being (Foley et al., 2005; Haines-Young, 2009; Nagendra, Reyers et al., 2013). As habitats shrink and become increasingly fragmented, the risk of local extinction rises for species that depend on them, primarily due to the ecological isolation of populations (Prugh et al., 2008).

As natural habitat area decreases, landscape structure and connctivity are progressively disrupted, constraining the flows of matter, energy, and information due to the barriers imposed by the surrounding landscape matrix (Correa et al., 2016). Tropical regions are particularly vulnerable to these threats because they harbor exceptionally high biodiversity levels while being subject to some of the world's highest rates of habitat conversion, with a global annual net forest loss estimated at ~42,000 km^2 (Lambin et al., 2003; Wright, 2010).

In this context, PAs constitute critical refuges for threatened species and key providers of ecosystem services by restricting land transformation and preserving habitat quality and ecological processes in highly biodiverse regions (Watson et al., 2014). The areas surrounding PAs play an equally important role in maintaining long-term conservation effectiveness by buffering transformation pressures at their boundaries and mitigating the ecological isolation of protected ecosystems (DeFries et al., 2005; Laurance et al., 2012). PAs are ecologically linked to the transformation processes occurring around them through several interrelated mechanisms that can be grouped into four main categories: (i) reduction of the effective area of the ecosystem encompassed by the PAs, (ii) alteration of ecological flows, (iii) disruption of source–sink dynamics, and (iv) edge effects that increase exposure to anthropogenic pressures (Figure 2; Hansen & DeFries, 2007).

4. Landscape connectivity

Landscape ecology has long recognized that biodiversity persistence depends not only on how much habitat remains, but also on how that habitat is spatially arranged across the landscape. Within this field, connectivity has been classically defined as the degree to which the landscape facilitates or impedes movement among habitat or resource patches, linking landscape pattern with dispersal, recolonization, and persistence processes (Taylor et al., 1993; Tischendorf & Fahrig, 2000). Its importance goes well beyond movement itself: connectivity underpins dispersal, recolonization, gene flow, persistence, and ecological function, and is therefore central to biodiversity conservation, ecological resilience, and restoration in fragmented landscapes (Beger et al., 2022; Brodie et al., 2025; Rudnick et al., 2012; Hilty et al., 2020).

Although connectivity is often discussed as a single concept, some authors distinguish between habitat connectivity, landscape connectivity, and ecological connectivity. These concepts are related but not fully equivalent and differ in scope and level of inference (Tischendorf & Fahrig, 2000; Kindlmann & Burel, 2008). Ecological connectivity is the broadest concept, as it includes not only spatial continuity and movement potential, but also ecological flows and processes such as gene flow, demographic exchange, recruitment, and broader ecosystem functioning (Fu et al., 2009; Oettel et al., 2025). Within this broader domain,

landscape connectivity refers more specifically to the degree to which the spatial arrangement of landscape elements, together with organism responses to that arrangement, facilitates or impedes movement across space; it therefore integrates both structural and functional dimensions and may also incorporate temporal dynamics (Tischendorf & Fahrig, 2000; Oettel et al., 2025). At the most specific level, habitat connectivity focuses on the arrangement and connection of habitat patches that enable movement, often from a species-oriented perspective and with emphasis on patch accessibility and dispersal among suitable habitats (Tischendorf & Fahrig, 2000; Calabrese & Fagan, 2004). In this sense, habitat connectivity can be seen as a more patch-focused expression within the broader domain of landscape connectivity, whereas ecological connectivity extends further by incorporating process-based ecological relationships (Kindlmann & Burel, 2008; Oettel et al., 2025).

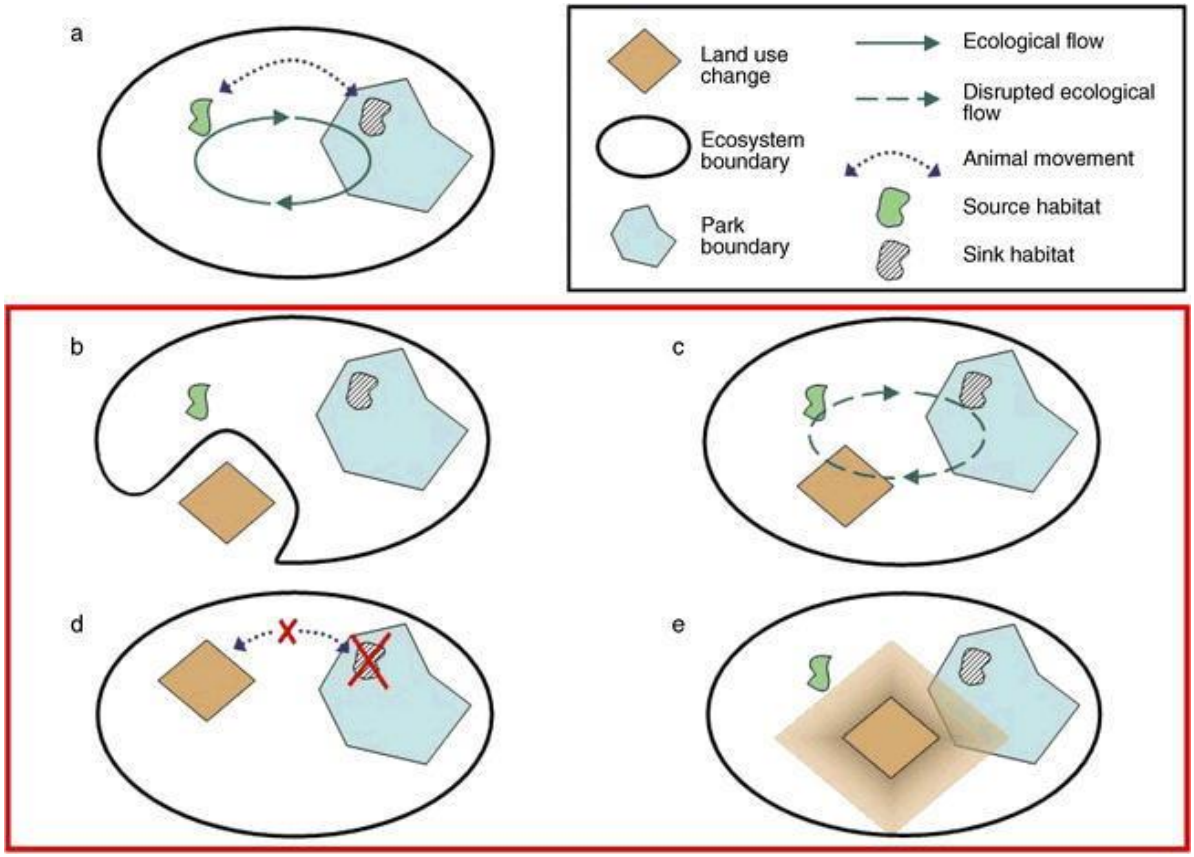

Figure 2. Conceptual framework depicting how land-use change influences ecosystem functioning. (a) Protected areas are embedded within broader ecosystems where energy, materials, and organisms flow. (b) Land-use change reduces the ecosystem's effective extent. (c) Land-use change modifies ecological flows. (d) Land-use change removes unique habitats and disrupts source–sink relationships. (e) Edge effects arising from land use exert negative impacts on the protected area. Adapted from Hansen & DeFries (2007).

A foundational distinction is between structural connectivity and functional connectivity. Structural connectivity refers to the physical arrangement of habitat patches, whereas functional connectivity refers to connectivity as experienced by organisms according to their movement abilities and responses to the surrounding matrix (Tischendorf & Fahrig, 2000). A second distinction is between potential and actual connectivity. Potential connectivity is inferred from

habitat pattern and modeled dispersal assumptions, while actual connectivity is supported by direct evidence such as movement data or gene flow (Calabrese & Fagan, 2004; Lowe & Allendorf, 2010). This distinction is especially important in graph-based studies, where connectivity is usually modeled rather than directly observed, and where metric choice constrains the level of ecological inference that can be drawn (Calabrese & Fagan, 2004; Keeley et al., 2021).

Within landscape ecology, one of the most influential approaches for assessing connectivity is the graph-based habitat-availability framework. In this framework, habitat patches are represented as nodes and the possible movement links among them as edges (Urban & Keitt, 2001). Saura and Pascual-Hortal argued that connectivity should be understood within the broader concept of habitat availability, because habitat amount and among-patch accessibility jointly determine how much habitat is effectively reachable in a landscape (Saura & Pascual-Hortal, 2007). This is the conceptual context in which the Integral Index of Connectivity (IIC) and the Probability of Connectivity (PC) were developed. IIC uses a binary representation of links, whereas PC uses a probabilistic formulation that better captures gradual variation in dispersal feasibility among patches (Pascual-Hortal & Saura, 2006; Saura & Rubio, 2010).

Within this same framework, Equivalent Connected Area (ECA) is derived directly from PC and represents the area of a single maximally connected habitat patch that would provide the same connectivity as the observed landscape (Saura et al., 2011). This gives ECA a major interpretive advantage: unlike a purely probabilistic index, it is expressed in area units, which makes it easier to compare connectivity with total habitat amount and with habitat change through time. ECA is therefore especially useful for distinguishing simple habitat loss from the loss of connected habitat, and for evaluating whether changes in landscape pattern have disproportionately strong effects on connectivity. In addition, the PC framework can separate the contribution of habitat area, dispersal flux, and stepping-stone roles, which strengthens its usefulness for conservation planning, restoration, and the identification of priority landscape elements (Saura & Rubio, 2010; Saura et al., 2011).

Conceptually, ECA estimated from PC is best interpreted as a metric of functional potential connectivity. It is functional because it incorporates dispersal assumptions and estimates reachable habitat rather than only patch adjacency. However, it is potential rather than actual because the links among patches are modeled from assumed dispersal distances or probabilities, not from direct observations of movement, colonization, or gene flow (Calabrese & Fagan, 2004; Saura & Rubio, 2010). This becomes especially relevant when multiple dispersal distances are considered. Rather than being a limitation, the use of several distances is one of the strengths of the approach, because it makes species- and scale-dependence explicit and allows connectivity to be evaluated across a range of biologically plausible movement scenarios (Baguette et al., 2013; Keeley et al., 2021). Recent syntheses likewise stress the value of integrating structural and functional perspectives, temporal change, and explicit assumptions in connectivity assessments (Auffret et al., 2015; Oettel et al., 2025; Keeley et al., 2021).

The importance of connectivity analysis is particularly clear in protected-area networks and under climate change. Protected areas often function as core habitat nodes, but their conservation value depends strongly on whether they remain connected to one another and to surrounding landscapes (Hilty et al., 2020; Keeley et al., 2021). Under climate change, connectivity increasingly determines whether species can shift their distributions, maintain

demographic exchange, and persist in changing environments (Schloss et al., 2022; Brodie et al., 2025). At the same time, recent evidence suggests that many protected areas may be too isolated or climatically mismatched to serve effectively as stepping stones for climate-driven range shifts (Parks et al., 2023). This makes connectivity analysis essential not only for describing present-day fragmentation, but also for identifying landscapes and corridors that can support long-term conservation under uncertain futures (Rudnick et al., 2012; Schloss et al., 2022; Hilty et al., 2020).

Applications in Colombia and other tropical regions illustrate the practical value of this framework. In the Colombian Andes–Amazon, connected habitat loss between 2000 and 2020 exceeded habitat loss, showing that area-based assessments alone can underestimate the magnitude of ecological degradation (Murillo-Sandoval et al., 2022). At the national scale, graph-based functional approaches have been used to identify priority areas for maintaining bird connectivity among protected areas in Colombia (Linero-Triana et al., 2023). In tropical Borneo, ECA-based analyses have shown strong declines in functionally connected habitat for forest vertebrates under long-term forest loss (Ocampo-Peñuela et al., 2020). Together, these studies show that ECA is not only conceptually robust, but also operationally useful for monitoring fragmentation, comparing dispersal scenarios, and informing conservation and restoration decisions in fragmented tropical landscapes (Keeley et al., 2021; Rudnick et al., 2012).

5. Colombian Andean Forests overview: ecology, pressures, and global change scenarios

The Colombian Andes form part of the Tropical Andes biodiversity hotspot (Myers et al., 2000; Orme et al., 2005). In this region, Andean forests occupy a broad elevational band shaped by steep temperature and moisture gradients, complex topography, and frequent cloud immersion at higher elevations (Cárdenas et al., 2017; Espinoza et al., 2020; Helmer et al., 2019). Floristic assemblages include diverse tree and shrub guilds and rich epiphyte communities that enhance canopy water interception and nutrient retention (Bruijnzeel et al., 2011). At the canopy and soil interface, cloud water interception, enhanced infiltration, and moderated evapotranspiration regulate flow paths and buffer hydrological extremes (Cárdenas et al., 2017; Helmer et al., 2019). On steep slopes, deep root systems stabilize soils and reduce erosion (Quintero-Gallego et al., 2018; Restrepo et al., 2015; Restrepo & Escobar, 2018). Across the landscape, contiguous habitat strata enable species movement and maintain genetic exchange (Ruíz-Diaz et al., 2025). These coupled functions support high endemism in plants, amphibians, birds, and small mammals, while also securing carbon storage in biomass and organic soils, maintaining cool, humid microclimates critical for downstream agriculture, and sustaining reliable baseflows for cities and irrigation (Aparecido et al., 2018; Castillo-Figueroa, 2021; Duque et al., 2021; Myster, 2021). Conserving these forests safeguards biodiversity and secures critical regulating services that support water security and climate mitigation at regional scales (Buytaert & Bievre, 2012; Ochoa-Tocachi et al., 2016; Quesada et al., 2017, 2018).

Decades of land conversion have fragmented Andean forests into increasingly isolated (Correa Ayram et al., 2020; Etter et al., 2008). Current pressures are dominated by agricultural expansion, road development, mining, and settlement growth, which amplify edge effects, reduce interior habitat, and disrupt species interactions (Aide et al., 2019; Armenteras et al., 2011; Etter & Van Wyngaarden, 2000; Rubiano et al., 2017). These trends can weaken cloud

interception, modify streamflow seasonality, and raise disturbance risks (e.g., landslides; Báez et al., 2016; Buytaert et al., 2007; Helmer et al., 2019; Tovar et al., 2022). Robust projections of land-use scenarios are therefore essential to anticipate habitat loss, connectivity decline, potential interactions with climate change, and degradation of ecosystem services provision (Bax et al., 2021; Castellanos-Mora & Agudelo-Hz, 2021; Clerici et al., 2019; González-González et al., 2021). This kind of information is thus essential to guide restoration, protected-area design, and landscape planning (Cuykens et al., 2024; Rodríguez Eraso et al., 2013).

6. Colombian Páramos overview: ecology, pressures, and global change scenarios

Within the Colombian Andes, páramos form a distinctive tropical alpine belt above the upper forest limit (≈3,000–4,500 m a.s.l.), characterized by cold temperatures, high UV radiation, large diurnal temperature ranges, and persistent humidity (Llambí & Rada, 2019; Valencia et al., 2020). Vegetation mosaics, tussock grasses, cushions, shrubs, and rosette forms such as *Espeletia*, exhibit morphological and biochemical adaptations that confer tolerance to frost, desiccation, and oxidative stress (Rada et al., 2019; Sanchez et al., 2014; Sanchez & Rada, 2023; Sandoval et al., 2019). Hydrologically, páramos function as "water towers": organic-rich Andosols with exceptional porosity and water-holding capacity buffer rainfall variability, while occult precipitation augments inputs, sustaining baseflows to major Andean basins (Buytaert & Bievre, 2012; Cárdenas et al., 2017; Célleri & Feyen, 2009). These ecosystems also store substantial soil carbon, protect headwater soils from erosion, and support specialized biota with high endemism (Hribljan et al., 2016; Merckx et al., 2015; Sklenář et al., 2014). Their conservation is directly linked to downstream water security, climate regulation, and the persistence of unique evolutionary lineages (Dimitrov et al., 2012; Viviroli et al., 2020).

Land-use change, particularly conversion to potato and vegetable cropping, pasture, and associated burning, degrades páramo soils, reduces organic matter, and lowers infiltration and storage capacity, weakening dry-season flows (Bonnesoeur et al., 2019; Buytaert et al., 2007; Crespo et al., 2010). Climate change is shifting thermal isotherms upslope, facilitating forest encroachment into high-elevation grasslands and altering the balance between evapotranspiration, fog interception, and soil moisture (Cárdenas et al., 2017, 2018; Tovar et al., 2013, 2022). Projections indicate substantial contractions of climatically suitable páramo area under warming scenarios, with implications for both biodiversity and hydrologic regulation (Cresso et al., 2020; Helmer et al., 2019; Marengo et al., 2011; Pabón-Caicedo et al., 2020). Prospective assessments that integrate land-use trajectories with high-resolution climate projections are thus crucial to estimate thresholds of soil degradation, losses in baseflow regulation, and range shifts for páramo specialists (La Sorte & Jetz, 2010; Lenoir & Svenning, 2015; Pecl et al., 2017; Perugini et al., 2017; Quesada et al., 2017). Such projections can inform zoning, restoration of degraded soils, and the protection of elevational gradients that maintain ecological and hydrological resilience in Colombia (Christmann & Menor, 2021; Gleeson et al., 2016).

7. Aim of this work

The aim of this work was to assess how land-use/land-cover change and climate change affect habitat loss, landscape connectivity, and the extent and spatial distribution of Andean ecosystems in Colombia, emphasizing forest and páramo ecosystems, and to evaluate these dynamics in protected areas and their buffer zones across all Colombian biogeographical regions to inform conservation planning.

8. Specific objectives of this work

1. Evaluate changes in natural habitat loss and landscape connectivity within Colombia's protected areas and their buffer zones between the conflict (2009–2016) and post-conflict (2016–2023) periods.

2. Estimate deforestation by forest typology across the Colombian Andes and its protected areas under Business-as-Usual and Governance scenarios for 2018–2030 and 2030–2050, drawing on published spatially explicit projections.

3. Assess the potential impacts of future climate change on the extent and spatial distribution of humid high-elevation tropical ecosystems worldwide, with particular emphasis on Andean páramo ecosystems, by contrasting a historical hydroclimatic baseline (1985–2014) with late-century projections (2071–2100) under SSP5-8.5.

9. Thesis outline

This doctoral thesis comprises 5 chapters: a general introduction (Chapter 1), three research chapters (Chapters 2-4), and a general conclusions chapter (Chapter 5).

Chapter 2 evaluates how habitat loss and landscape connectivity have changed across 50 Colombian protected areas and their 10-km and 20-km buffer zones amid rapid socio-ecological shifts. Leveraging the MapBiomas Colombia v2.0 land use/land cover dataset and the Equivalent Connected Area (ECA) index, it quantifies spatiotemporal dynamics of deforestation and natural non-forest vegetation loss alongside landscape connectivity across the conflict (2009–2016) and post-conflict (2016–2023) periods. The chapter establishes a spatially explicit baseline of recent anthropogenic impacts, revealing emerging patterns of habitat loss and connectivity change in ecologically important areas. It delivers decision-ready indicators and maps to inform buffer governance, targeted restoration, and connectivity-aware landscape planning that sustain ecological flows and the long-term functionality of the protected areas network.

Chapter 3 estimates projected deforestation in the Colombian Andes and within Andean National Natural Parks for 2018–2030 and 2030–2050 under two alternative pathways: Business-as-Usual and Governance. Using spatially explicit models, national ecosystem maps and forest-type stratification, it quantifies trajectories of forest conversion across Andean sub-regions and protected areas and evaluates implications for conservation planning. The chapter elucidates how differing policy and enforcement pathways could reshape habitat amount in future decades. It delivers decision-ready maps and indicators to support conservation planning and policy design under contrasting governance futures.

Chapter 4 assesses how future climate change may alter the extent and spatial distribution of humid high-elevation tropical ecosystems, with particular emphasis on Andean páramos, under the high-emissions scenario SSP5-8.5. Building on CMIP6 downscaled climate data, it contrasts a historical hydroclimatic baseline (1985–2014) with late-century projections (2071–2100) to quantify potential breaching of current hydroclimatic spaces defined by long-term means, extremes, and seasonality of temperature and precipitation. The chapter operationalizes the concept of hydroclimatic space, details metrics for breaching and spatial reconfiguration, and frames adaptation-oriented outputs for conservation policy and management.

Chapter 5 provides the general conclusions of this thesis.

Chapter 2

Post-agreement acceleration of habitat loss and landscape connectivity decline in and around Colombian protected areas

Accepted for publication in *Environmental Research Communications* (2026): In press, https://doi.org/10.1088/2515-7620/ae69a5

Post-agreement acceleration of habitat loss and landscape connectivity decline in and around Colombian protected areas

Kristian Rubiano[1,*], Nicola Clerici[1], Marius Bottin[2], Luigi Boschetti[3]

[1]School of Sciences and Engineering, Universidad del Rosario. Kr 26 No 63B-48, Bogotá – Colombia.
[2]Independent researcher, Bogotá – Colombia.
[3]Department of Forest, Rangeland and Fire Sciences, College of Natural Resources, University of Idaho, Moscow, ID 83844, USA.
[*]Corresponding Author – Kristian Rubiano, kristian.rubiano@urosario.edu.co

Abstract

Protected areas (PAs) are increasingly exposed to land-use pressures that erode habitat and landscape connectivity. In Colombia, rapid socio-ecological changes following the 2016 peace agreement marked a major territorial and governance transition and have been associated with heightened habitat loss in and around PAs, yet the magnitude and spatial configuration of habitat and connectivity change across the Colombian System of National Natural Parks (SPNN) remain insufficiently quantified. In this work, we combined the MapBiomas Colombia v2.0 land-use/land-cover dataset with the Equivalent Connected Area (ECA) index to evaluate deforestation, loss of natural non-forest vegetation (NNFV), and landscape connectivity dynamics for 50 PAs and their immediate surroundings (0–10 km buffers), and broader surroundings (10–20 km buffers) across two periods bracketing the peace agreement (2009–2016 and 2016–2023). We found that deforestation and NNFV loss intensified after 2016 across most regions, with particularly pronounced signals in the Andes–Amazon transition. Overall, landscape connectivity declined across all zones and periods. Within PAs, reductions were comparatively modest, and most habitat remained connected by 2023, suggesting some persistence of internal structural integrity. In surrounding buffers, declines were stronger and not fully explained by habitat amount alone, as connectivity fell faster than area loss, indicating stronger configuration effects and increasing fragmentation of natural-vegetation networks. Taken together, these results suggest that the post-agreement period coincided with intensified habitat and disproportionate connectivity erosion in landscapes surrounding PAs. By extending national-scale monitoring through 2023 and, most importantly, by evaluating how habitat-loss trajectories translated into connectivity outcomes across 50 strictly PAs and two surrounding buffer bands, this study provides an updated basis for identifying where habitat conversion and isolation pressures are most strongly concentrated.

Keywords

Colombia, post-agreement, protected areas, land-use/land-cover change, deforestation, natural non-forest vegetation loss, landscape connectivity.

1. Introduction

Habitat loss and degradation caused by anthropogenic land use are widely recognized as the main drivers of global biodiversity decline (Newbold et al., 2015; Pereira et al., 2012). Tropical ecosystems are particularly vulnerable, as they harbor more than 60% of global biodiversity (Bradshaw et al., 2009) and continue to experience some of the highest deforestation rates worldwide, with an average annual loss of 7.29 million ha of tropical moist forest between 1990 and 2019 (Vancutsem et al., 2021). In response, the number and extent of protected areas (PAs), key strategies for biodiversity conservation, have increased substantially across the tropics over recent decades (Jenkins & Joppa, 2009; Watson et al., 2014). However, PAs are often exposed to multiple anthropogenic pressures that compromise their effectiveness in conserving biodiversity and sustaining ecosystem services (Laurance et al., 2012). Habitat and connectivity loss around PAs is of particular concern because these areas are linked to surrounding lands by key biotic and abiotic processes. Buffer areas play a crucial role in maintaining ecological flows, contributing strongly to PA integrity and counteracting ecological isolation (DeFries et al., 2005; Hansen & DeFries, 2007; Prugh et al., 2008). Monitoring PAs and their surroundings jointly is thus essential for detecting threats, assessing the progress of conservation goals, and guiding management decisions (Willis, 2015). Remote sensing–based LULC monitoring platforms provide critical spatial information for decision-makers and PA managers, offering valuable insights into habitat change, degradation, and connectivity loss (Nagendra et al., 2013).

Colombia is one of the megadiverse countries, harboring around 10% of global biodiversity (Convention on Biological Diversity, 2025; Moreno et al., 2018), largely as a result of its geomorphological and climatic heterogeneity, which has fostered complex biogeographic diversification processes and a wide variety of ecosystems (Hazzi et al., 2018; Kattan et al., 2004). These features make Colombia a country with exceptional natural capital and of major global importance for biodiversity conservation (Bax & Francesconi, 2019; Ocampo-Peñuela & Winton, 2017). Currently, about 17% of the national territory is protected under the Colombian National System of Protected Areas (SINAP), encompassing about 1,800 PAs (PNNC, 2025) that harbor more than 70% of the country's bird species and approximately 39% of its vascular plants (Franco et al., 2007; Mendoza-Cifuentes et al., 2018). PAs with the most restrictive IUCN protection categories (IA, IB, II, and III) are grouped under the System of National Natural Parks (SPNN), which is managed by the national government. The SPNN includes 61 PAs covering nearly 146,200 km^2 of territory (PNNC, 2025). PAs under these more restrictive conservation categories do not allow productive activities and are open only to tourism and recreation, while others serve as reference areas for strict protection and scientific research (Dudley, 2008).

Despite this extensive protected area network, Colombia's natural capital faces increasing anthropogenic pressures (Correa Ayram et al., 2020), including illegal cattle ranching, agricultural expansion, illicit crop cultivation, and mining, all of which have been identified as important drivers of habitat loss and declining landscape connectivity in and around PAs (Dávalos et al., 2011; González-González et al., 2021). For instance, between 2023 and 2024, about 1,930 km^2 of forest were lost in Colombia, of which around 8% occurred inside PAs (IDEAM & MADS, 2025). These long-standing pressures have interacted with changing patterns of territorial control, governance, and accessibility, particularly in remote areas historically affected by armed conflict.

More broadly, transitions from armed conflict to ceasefire, demobilization, or peace-agreement settings can trigger major socioecological reorganization. Research framed within warfare ecology has shown that such transitions may alter territorial control, governance, access, migration, infrastructure expansion, and the intensity and geography of natural-resource use, with consequences that can either increase or reduce environmental degradation depending on local institutional and political conditions (Gaynor et al., 2016; Hanson, 2018; Hanson et al., 2009; Landholm et al., 2019; Machlis & Hanson, 2008; Suarez et al., 2018). In Colombia, the 2016 final peace agreement between the national government and the FARC-EP marked a major territorial and institutional transition that reshaped land-use dynamics in many remote regions. In this study, we use the term post-agreement to refer specifically to the period following the 2016 peace agreement as a temporal and political reference point. This terminology acknowledges that armed violence persisted and reconfigured after the accord and avoids implying that Colombia entered a fully settled post-conflict condition.

The Colombian armed conflict had diverging effects on land-use and land-cover (LULC) dynamics. On the one hand, some authors have described a form of *gunpoint conservation*, whereby the territorial presence of armed groups restricted access, limited extractive activities, and constrained infrastructure expansion in remote areas (Murillo-Sandoval et al., 2020). Forced displacement from rural to urban areas also promoted ecosystem regeneration in many areas previously used for agriculture (Sánchez-Cuervo et al., 2013a). On the other hand, illicit cropping, cattle ranching, and other activities used to finance armed groups also promoted deforestation in several regions (Dávalos et al., 2011; Mendoza, 2020; Negret et al., 2019). These contrasting dynamics were particularly common in remote PAs and surrounding landscapes historically occupied by guerrilla groups (Canavire-Bacarreza et al., 2018; Hoffmann et al., 2018).

Remote-sensing studies have documented rapid forest loss after 2016, particularly in the Amazon and Andean–Amazon foothills, and have linked these patterns to land grabbing, agricultural expansion, weak governance, and shifting territorial control (Armenteras et al., 2019; Clerici et al., 2020; Mendoza, 2020; Murillo-Sandoval et al., 2020, 2021; Negret et al., 2019). Illegal crop expansion has also been reported in several regions (Mendoza, 2020; Negret et al., 2019; UNODC-SIMCI, 2021), and forest connectivity has declined sharply across the Colombian arc of deforestation (López et al., 2024; Murillo-Sandoval et al., 2022). These studies provide an essential basis for understanding environmental change after 2016. However, most studies have focused primarily on deforestation, have evaluated a limited number of PAs, and have rarely integrated habitat-conversion trajectories with landscape connectivity outcomes across immediate and broader PA surroundings. While increases in forest loss after 2016 are already well documented, comparatively little is known about how habitat-loss patterns observed during the post-agreement period translated into connectivity outcomes for PAs and their surrounding landscapes at the national scale. Comparatively less attention has also been given to natural non-forest vegetation (NNFV), explicit transition destinations, and to whether connectivity decline tracked or exceeded habitat loss across different surrounding landscapes.

Accordingly, this study addresses three main gaps. First, it extends national-scale monitoring through 2023 across 50 strictly protected areas and their surrounding landscapes. Second, it evaluates a broader set of habitat-conversion trajectories by jointly assessing deforestation, loss of NNFV, and combined natural-vegetation (NV) loss, together with their main

destination land-use classes. Third, and most importantly, it integrates these habitat-loss trajectories with landscape connectivity metrics to evaluate how habitat loss during the post-agreement period translates into connectivity outcomes across PA cores, the immediate surroundings (0–10 km buffers), and the broader surroundings (10–20 km buffers). This is important because similar amounts of habitat loss can generate very different connectivity outcomes depending on where habitat is removed and how remaining natural vegetation is spatially configured. Together, these gaps limit the ability to identify which PAs and surrounding zones are most exposed not only to habitat loss but also to ecological isolation and fragmentation during the post-agreement period. Such information is crucial, as it can inform land-use planning and strengthen conservation strategies (Sierra et al., 2017; Suarez et al., 2018; Torres et al., 2020).

Specifically, we ask: (1) how did deforestation, NNFV loss, and total NV loss differ between the conflict (2009–2016) and post-agreement (2016–2023) periods? (2) how did these changes differ among PAs, immediate surroundings (0–10 km buffers), and broader surroundings (10–20 km buffers)? (3) how did these habitat-loss trajectories translate into changes in landscape connectivity across PAs and their surroundings, and to what extent did connectivity decline track or exceed habitat loss? By addressing these questions, we provide an updated national-scale assessment of habitat loss and changes in connectivity in and around Colombian PAs and discuss the implications of these patterns for biodiversity conservation and land-use planning within the country's broader post-agreement context.

2. Materials and methods

2.1. Study area

This study included 50 of the 61 PAs in the SPNN (see Table S1). The PAs excluded from the study (see Table S2) were either predominantly covering water bodies (terrestrial area < 5% of the extent of the PA), very small (< 1 km^2), or established after the beginning of the analysis time window (year of establishment > 2009). The size of 1 km^2 was set to minimize the effects of the 30 m spatial resolution of the LULC dataset (see section 2.2). Collectively, the 50 selected PAs cover about 144,000 km^2 of land. Also, to evaluate how land-use pressure and connectivity change with distance from PA boundaries, we included two non-overlapping buffers, 0–10 km and 10–20 km, around the 50 PAs (hereinafter, the 10-km and 20-km buffers, respectively; Figure 1). These buffers were not intended to reproduce reserve-specific legal or management zones, which vary among PAs, but rather to provide standardized analytical units that distinguish the immediate from the broader surrounding landscape under a consistent national-scale framework. This design is supported by ecological theory, which shows that PA integrity depends on surrounding lands through effects on habitat area, ecological flows, crucial habitats outside reserve boundaries, and edge-related human pressures (DeFries et al., 2010; Hansen & DeFries, 2007). It is also consistent with classic buffer-based analyses of PA isolation in tropical forests (DeFries et al., 2005) and with applied studies that have used 10-km surrounding buffers or broader multi-distance approaches to quantify conservation-relevant pressures around PAs (Geldmann et al., 2013), including post-conflict deforestation in Colombia (Clerici et al., 2020), built-up expansion around protected areas globally (de la Fuente et al., 2020), degradation of tropical buffer zones (de Almeida-Rocha & Peres, 2021), and heterogeneous spillover effects within 20-km surrounding

landscapes (Shen et al., 2022). PAs boundaries in vector format were obtained from the Colombian National Natural Parks institution (PNNC, 2024). The dataset was filtered according to the study areas' selection criteria of this study, using the continental administrative boundaries of Colombia from the Colombian SIGOT system (Instituto Geográfico Agustin Codazzi, 2019). The buffer areas around PAs were produced as non-overlapping surrounding bands for contiguous protected areas by removing overlaps among adjacent buffers (see Figure 1). A detailed description of the workflow is provided in Bottin (2022), and it is briefly summarized here for completeness. First, influence zones were generated for each PA using a Voronoi/Thiessen approach based on points extracted along PA boundaries; these influence zones were then clipped to continental Colombia and the PA polygons themselves were removed. Finally, the resulting influence zones were intersected with the 0–10 km and 10–20 km buffers around each PA so that overlapping portions between adjacent parks were assigned to the nearest PA, yielding non-overlapping buffer bands. The workflow was implemented in PostgreSQL/PostGIS, with data handling and verification supported in R.

2.2. LULC data

We used data from the MapBiomas Colombia Collection 2.0 dataset (Souza et al., 2020; MapBiomas Colombia, 2024) as the reference to extract trajectory statistics and analyze connectivity changes. This dataset consists of annual national LULC maps for the period 1985-2023 generated through cloud-based processing. Each annual map is a raster grid with a 30 m spatial resolution, produced from the classification of Landsat TM, ETM+, and OLI imagery mosaics. For every year, mosaics were created by spatial and temporal integration of multiple scenes representing optimal phenological conditions to minimize cloud and seasonal variability. Classification relies on Random Forest algorithms trained with more than 140 predictor variables, including spectral bands, indices, spectral fractions, topographic metrics, and ancillary variables (Souza et al., 2020; Fundación Gaia Amazonas, 2024).

The MapBiomas Colombia Collection 2.0 product adopts a hierarchical LULC legend comprising 21 classes at level 2, aggregated into five level-1 categories. This legend is derived from the National Land Cover Legend adapted from CORINE methodology, and the FAO land cover typologies (Di Gregorio & Jansen, 2005; IDEAM, 2010). Mean annual overall accuracy reported for MapBiomas Colombia is 97.9% (±0.5% SD) at level 1 and 91.2% (±1.8% SD) at level 2 (MapBiomas Colombia, 2026). These values reflect overall product performance and should not be interpreted as class-specific validation of the aggregated categories used in this study. Table S3 summarizes the publicly accessible user's and producer's accuracies of the main Level 1 classes most relevant to this study for 2009 and afterward. To date, it constitutes one of the most comprehensive, spatially explicit, and temporally consistent sources of land use and land cover information available for Colombia, serving as the foundation for the subsequent LULC and connectivity analyses (Fundación Gaia Amazonas, 2024; Xu et al., 2025).

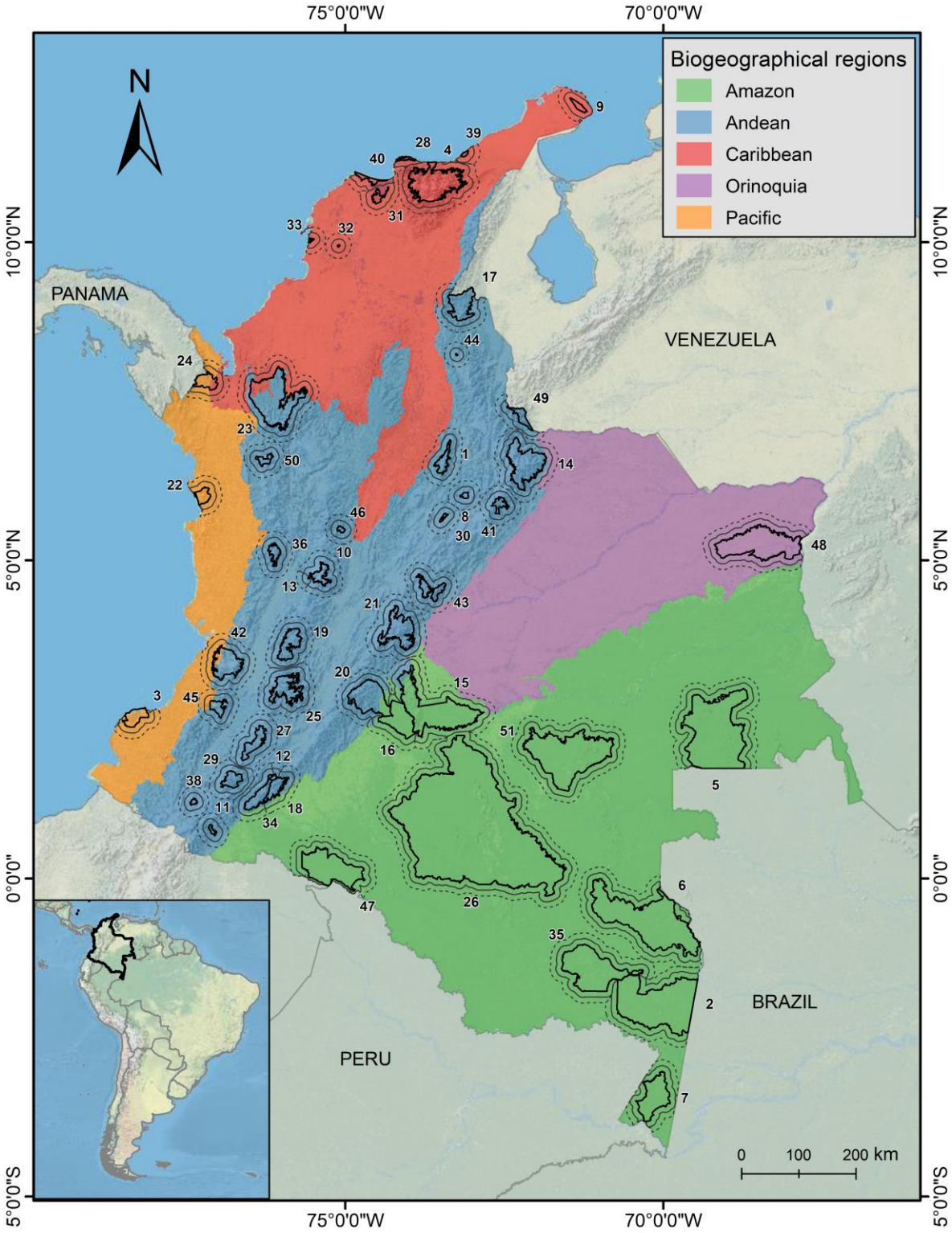

Figure 1. Colombian PAs considered in this study (solid lines) and their surrounding non-overlapping 10-km (lighter lines) and 20-km buffers (dotted lines). PAs are labeled with their IDs. See Table S1 for PA names and IUCN categories. Biogeographical regions according to Chaves & Arango (1998).

2.3. Data processing

All processing of the MapBiomas Colombia Collection 2.0 dataset was carried out on the cloud-based Google Earth Engine (GEE) platform (Gorelick et al., 2017) to access, filter, and extract both

raster and tabular data required for subsequent analyses. First, the national LULC raster collection was filtered to select annual maps from 2009 to 2023, which represent land-cover conditions at the end of each year. This temporal range was chosen to encompass both the Colombian conflict (2009–2016) and post-agreement (2016–2023) periods of interest. To spatially constrain the analysis, we used the vector boundaries of PAs previously filtered according to the selection criteria described in Section 2.1, together with their 10-km and 20-km buffers generated using a non-overlapping buffer algorithm (see section 2.1). All geometries were dissolved to create a single external boundary corresponding to the 20-km buffer limit, and the annual LULC rasters were clipped to this extent.

Subsequently, the original LULC legend of the dataset was reclassified into four level-1 categories to emphasize distinctions among habitat, anthropogenic land use, and non-vegetated natural areas (Table 1). Natural vegetation classes were grouped into two categories: Forest formation (hereafter Forest) and Natural non-forest vegetation (NNFV) based on physiognomic and structural criteria that reflect major differences in vegetation form, such as canopy height, cover density, and the dominance of woody versus non-woody life forms (e.g., shrubs, grasses, or open herbaceous cover). Anthropogenic land-use classes were grouped into a single category, Human-modified areas (HMA), encompassing all non-natural classes associated with landscape transformation and human activity. Finally, the Non-vegetated natural area and waterbody (NNW) category includes all non-vegetated natural areas and waterbodies. This reclassification served as the analytical framework for subsequent LULC change and landscape connectivity assessments.

2.4. LULC statistics extraction

We used the reclassified annual LULC maps, along with the PAs' boundaries and their 10-km and 20-km buffers, to extract statistics describing LULC change trajectories. As we aimed to assess transitions directly attributable to anthropogenic pressures, our analysis focused on two forms of anthropogenic natural-vegetation conversion: deforestation, defined as the direct conversion of forest to human-modified areas (HMA; Table 1), consistent with the IPCC definition of direct human-induced conversion of forested land to non-forested land (IPCC, 2006), and NNFV loss, defined analogously as the conversion of NNFV to HMA. Therefore, transitions between natural vegetation types (e.g., from forest to NNFV or vice versa) or toward NNW were not considered deforestation or NNFV loss events.

To quantify cumulative gross anthropogenic conversion within each period while avoiding multiple counting of the same pixel, we applied a monotonic non-increasing loss-accounting approach, following the logic of gross cover loss commonly used in large-scale remote-sensing assessments (Curtis et al., 2018; Hansen et al., 2013). Specifically, once a pixel classified as forest or NNFV at the beginning of a period underwent a transition to HMA, it was counted as a single loss event and remained flagged as lost for the remainder of that period for accounting purposes. This rule was not applied to transitions between natural vegetation classes, which were excluded from the loss analysis.

Table 1. Level-1 reclassification scheme proposed for LULC change and landscape connectivity assessments, based on the original MapBiomas Colombia Collection 2.0 LULC thematic legend (LU, land-use; LC, land-cover).

Habitat/No habitat	Level-1 reclassified class	Level-1 original MapBiomas class	Level-2 original MapBiomas class	LU/ LC
Habitat	Forest	Forest formation	Forest	LC
			Mangrove	LC
			Floodable forest	LC
			Wooded sandbank vegetation	LC
	Natural non-forest vegetation (NNFV)	Natural non forest formation	Wetland	LC
			Grassland	LC
			Herbaceous sandbank vegetation	LC
			Other non forest formation	LC
No habitat	Human-modified areas (HMA)	Agricultural and livestock area	Forest plantation	LU
			Palm oil	LU
			Mosaic of agriculture and pasture	LU
		Non-vegetated area	Urban infrastructure	LU
			Mining	LU
			Other non-vegetated area	LU
	Non-vegetated natural area and waterbody (NNW)	Natural non forest formation	Hypersaline tidal flat	LC
			Rocky outcrop	LC
		Non-vegetated area	Beach, dune and sand spot	LC
			Other natural non-vegetated area	LC
		Water body	River, lake or ocean	LC
			Aquaculture	LC
			Glacier	LC

Annual estimates of deforestation and NNFV loss were generated for every year as first detected transitions from forest or NNFV to HMA, and cumulative totals for the conflict and post-agreement periods were obtained by summing these annual first-loss events, with each pixel counted at most once per period. Accordingly, period totals represent cumulative gross anthropogenic loss rather than net end-of-period change. To better understand the trajectories of land-cover change, we identified the main destination land-use classes associated with deforestation and NNFV loss and evaluated their relative contributions between the two periods using both level-1 and disaggregated level-2 LULC classes.

Furthermore, to complement the separate assessments of deforestation and NNFV loss, we analyzed overall natural vegetation (NV) loss by combining both metrics into a unified indicator of total habitat conversion (hereafter referred to as NV loss). This allowed an objective comparison between predominantly forested and non-forested PAs and an evaluation of

differences in habitat and connectivity outcomes between the conflict and post-agreement periods.

Temporal trend analyses were then performed to evaluate changes in loss rates between the conflict and post-agreement periods. To quantify these changes, we calculated the percentage difference between periods for each PA and buffer zone as the relative change of post-agreement values with respect to conflict-period values (Clerici et al., 2020). Percentage changes were also computed by aggregating PAs and buffer zones according to biogeographical regions, following the regionalization proposed by Chaves & Arango (1998).

2.5. Landscape connectivity analysis

We used the Equivalent Connected Area (ECA) index (Saura et al., 2011) to quantify the effects of habitat conversion during the conflict and post-agreement periods on the connectivity of natural-vegetation networks within PAs and their surrounding buffer zones. ECA represents the area of a single, hypothetical, fully connected habitat patch that would provide the same probability of connectivity as the actual configuration of habitat patches in the landscape. In this sense, ECA expresses the effective amount of connected habitat, integrating both intra-patch area, and the probability of connection among patches under a defined dispersal-distance threshold into a single, ecologically meaningful metric (Saura & Pascual-Hortal, 2007; Saura et al., 2011). This makes ECA particularly useful for multitemporal comparisons, because it captures not only changes in habitat amount or spatial subdivision, as purely structural connectivity and fragmentation metrics do, but also their implications for potential functional connectivity (Tischendorf & Fahrig, 2000; Calabrese & Fagan, 2004; Oettel et al., 2025).

To assess connectivity change between years within each zone type, we used the Makurhini v3.0 R package (Godínez-Gómez et al., 2025; R Core Team, 2024) to compute the ECA index for the aggregated extent of all PAs combined, and separately for the 10-km and 20-km buffer zones. This zone-specific approach was intended to compare changes in the internal connectivity of natural-vegetation networks within PAs and within their surrounding buffer landscapes. It was not designed to quantify connectivity between buffer habitats and PA cores. We reclassified the 2009, 2016, and 2023 LULC maps to a binary habitat map (Forest and NNFV classes combined; see table 1) and delineated habitat nodes as contiguous habitat patches. Because the connectivity analysis was based on a binary natural-vegetation layer (Forest + NNFV) and Euclidean inter-patch distances, the results represent generic natural-vegetation connectivity under a homogeneous-matrix assumption rather than species-specific habitat connectivity. Pairwise Euclidean distance matrices among were generated with the *Generate Near Table* tool in ArcMap 10.8. Accordingly, this analysis does not explicitly account for variation in movement costs or permeability among different HMA types.

To assess the sensitivity of connectivity patterns to alternative generic dispersal assumptions, we computed ECA using six median dispersal distances (d = 1, 5, 10, 30, 50, and 70 km), spanning thresholds commonly used in Colombia (Castillo et al., 2020; Correa-Ayram et al., 2025; Murillo-Sandoval et al., 2022). We adopted 10 km as the reference d for result interpretation, as it represents a central benchmark within the tested range of dispersal distances and has been widely used in large-scale connectivity analyses (see e.g., Correa-Ayram et al.,

2025; Martensen et al., 2017; Murillo-Sandoval et al., 2017; Saura et al., 2017). ECA was calculated in absolute units (km^2) and later normalized by the total habitat area to obtain the normalized ECA (ECA_{norm}).

We also calculated other ECA-derived metrics helpful to assess spatiotemporal patterns of landscape connectivity. To assess trends in connectivity across periods and zone types, we computed the percentage change in the ECA (dECA) for the conflict and post-agreement periods as the difference between ECA values over time, expressed as a percentage of the initial value (Saura et al., 2011). Negative dECA values indicate a loss of connectivity, whereas positive values indicate a gain in connectivity over the corresponding period. To identify how connectivity changes are related to changes in habitat area, we also estimated the relativized ECA (rECA), by dividing the dECA by the change in habitat area (dA) (Dilts et al., 2016; Liang et al., 2021). rECA values greater than 1 indicate that habitat changes result in a disproportionately large change in habitat connectivity, whereas values lower than 1 indicate lower impacts of habitat loss on connectivity (Godínez-Gómez et al., 2025; Saura et al., 2011).

Subsequently, the ECA and related connectivity metrics were also calculated for each individual PA and buffer zone, using 10 km as *d* value. The multi-distance analysis was used to assess sensitivity at the overall scale, whereas the PA-level analysis was performed only for the 10-km reference distance as a common benchmark for spatial prioritization. Finally, to compare connectivity outcomes between the post-agreement and conflict periods, we calculated the inter-period change in connectivity as:

$$\Delta dECA = dECA_{2009-2016} - dECA_{2016-2023}$$

Where $dECA_{2009\text{-}2016}$ and $dECA_{2016\text{-}2023}$ correspond to the percentage change in ECA during the conflict and post-agreement periods, respectively. Negative ΔdECA values indicate that connectivity outcomes became more negative in the post-agreement period (i.e., connectivity loss intensified or connectivity gains weakened), whereas positive ΔdECA values indicate that connectivity outcomes became less negative or more positive in the post-agreement period (i.e., connectivity loss was reduced or connectivity gains increased).

Because identical ΔdECA values may arise from different combinations of period-specific dECA values, inter-period changes were interpreted jointly with the sign of dECA in each period. To facilitate interpretation, inter-period connectivity outcomes were also classified into six qualitative change categories based on the sign of dECA in each period and on the sign of ΔdECA: intensified loss, reduced loss, shift from loss to gain, shift from gain to loss, stronger gain, and weakened gain (Table S4). These categories were used to identify the most vulnerable and most improved areas in terms of connectivity outcomes during the post-agreement period.

2.6. Statistical analysis

To evaluate temporal and spatial differences in patterns of habitat loss, we analyzed deforestation, NNFV loss, and NV loss for the conflict and post-agreement periods. For between-period comparisons within each zone type (PAs, 10-km buffers, and 20-km buffers), we used paired Wilcoxon signed-rank tests. Because our a priori expectation was that habitat loss would be greater during the post-agreement period than during the conflict period, we used a one-tailed

test. This resulted in 9 one-tailed Wilcoxon tests for habitat-loss metrics (3 response variables × 3 zone types). To assess differences among the three zone types within each period, we applied the Friedman test to each response variable and period separately. When the omnibus Friedman test was significant, it was followed by three pairwise Wilcoxon signed-rank tests comparing PAs vs. 10-km buffers, PAs vs. 20-km buffers, and 10-km vs. 20-km buffers. Holm-adjusted p-values were applied only within each response-variable × period family of post hoc comparisons. Nonparametric methods were selected because of nonnormal residuals (Dytham, 2011). These analyses allowed us to identify both the magnitude and direction of habitat change across spatial contexts and time periods.

An equivalent statistical approach was applied to the dECA data to assess variations in connectivity change between the conflict and the post-agreement periods. For between-period comparisons within each zone type, we used three one-tailed paired Wilcoxon signed-rank tests to assess whether dECA values were more negative during the post-agreement than during the conflict period, indicating less favorable connectivity outcomes. To examine differences among zone types within each period, we applied Friedman tests, followed, when significant, by pairwise Wilcoxon signed-rank tests, with Holm-adjusted p-values applied within each period-specific post hoc family. All statistical analyses were conducted in R (R Core Team, 2024).

3. Results

3.1. Overall and regional patterns of deforestation and NNFV loss

Within PAs, annual deforestation exhibited a slight increase during the conflict period, averaging 134 ± 15 km^2 (Fig. 2A). After 2016, deforestation sharply increased, peaking at 316 km^2 in 2018. Similar increases in annual deforestation were observed in the 10-km (Fig. 2B) and 20-km buffers (Fig. 2C), where mean annual forest loss during the conflict (463 ± 41 km^2 and 523 ± 57 km^2, respectively) increased after 2016, reaching maximum values of 834 km^2 and 828 km^2 in 2018.

Annual NNFV loss also intensified across periods, exhibiting spatial and temporal patterns similar to those of deforestation. Within PAs, maximum annual NNFV loss during the conflict was 21 km^2 in 2016 and grew nearly fourfold during the post-agreement period, reaching 81 km^2 in 2023 (Fig. 2D). In the 10-km buffers, losses decreased during the conflict and peaked in 2017 and 2023 (Fig. 2E), whereas in the 20-km buffers, they consistently declined during the conflict (from a maximum in 2010 to a minimum in 2016) but rapidly increased again after 2016 (Fig. 2F).

Deforestation increased across all biogeographical regions from the conflict to the post-agreement period, with the most pronounced growth occurring in the Amazon region (Table 2; Figs. 2, S1). Within PAs, deforestation in the Amazon rose from 431 km^2 to 1196 km^2 (+765 km^2), accounting for the largest absolute increase among all regions. Similar increases in deforestation were recorded in the surrounding 10-km and 20-km buffers, where deforestation more than doubled between periods (+1336 km^2 and +803 km^2, respectively). In the Andean region, deforestation also increased notably within PAs (+181 km^2) and in the 10-km and 20-km buffers (+362 km^2 and +204 km^2, respectively). Smaller yet consistent increases were detected in the

Caribbean and Pacific regions, whereas the Orinoquia showed a marked relative rise despite its small absolute area (from 3.8 km^2 to 33.2 km^2 within PAs; see Figure S1 for relative changes).

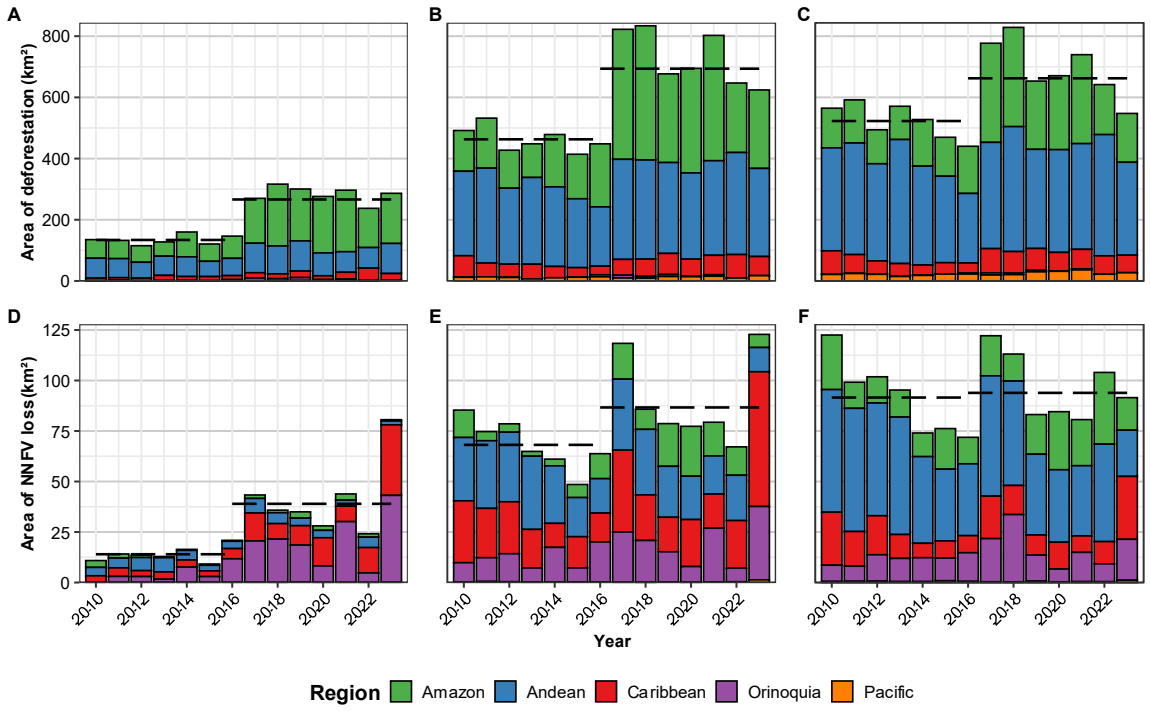

Figure 2. Trends of annual deforestation and NNFV loss in Colombian PAs and their surrounding buffers. Panels A–C show deforestation within PAs (A), 10-km buffers (B), and 20-km buffers (C). Panels D–F display NNFV loss for the same zones. Bars represent annual values as stacked bar plots, with colors indicating each biogeographical region's contribution to total deforestation or NNFV loss. Dashed black horizontal lines indicate the mean annual values for the conflict (2009–2016) and post-agreement (2016–2023) periods.

Table 2. Deforestation and NNFV loss within PAs and their surrounding 10-km and 20-km buffers, by biogeographical region, during the conflict (t_0) and post-agreement (t_1) periods, and their absolute difference ($t_1 - t_0$). n indicates the number of PAs in every region.

Region	n	PA			10-km buffer			20-km buffer		
		t_0	t_1	t_1-t_0	t_0	t_1	t_1-t_0	t_0	t_1	t_1-t_0
					Deforestation (km^2)					
Amazon	10	431.4	1196.2	764.8	1052.8	2388.3	1335.5	923.9	1726.9	802.9
Andean	28	412.6	593.4	180.8	1797.5	2159.9	362.4	2257.0	2460.6	203.6
Caribbean	8	82.9	150.6	67.7	302.5	435.4	132.9	326.0	461.9	135.8
Orinoquia	1	3.8	33.2	29.4	8.3	28.8	20.5	7.0	23.0	16.0
Pacific	3	7.4	10.6	3.2	79.4	89.6	10.2	145.0	186.5	41.5
					NNFV loss (km^2)					
Amazon	10	8.9	13.7	4.8	46.8	110.8	63.9	111.2	156.0	44.8
Andean	28	33.5	30.0	-3.5	200.4	167.6	-32.8	349.6	293.0	-56.6
Caribbean	8	25.3	100.2	74.8	141.6	210.7	69.1	98.7	109.0	10.3
Orinoquia	1	29.8	146.5	116.6	86.0	138.1	52.1	77.2	117.4	40.2
Pacific	3	0.4	0.4	0.05	2.2	2.4	0.2	4.2	3.8	-0.5

Patterns of NNFV loss differed among regions (Table 2; Fig. 2, S2). In the Amazon, NNFV loss intensified across all spatial zones, particularly within the 10-km buffer (+63.9 km^2). The Caribbean and Orinoquia regions also exhibited substantial increases (+74.8 km^2 and +116.6 km^2 within PAs, respectively), while the Andean and Pacific regions showed slight declines or negligible changes. Notably, the Andean region displayed a reduction of NNFV loss across all spatial scales, suggesting conversion dynamics distinct from the deforestation trends observed in the same area. Relative changes of NNFV loss across regions are shown in Figure S2.

3.2. Dynamics of LULC transitions

Analysis of land-use trajectories revealed that most deforestation and NNFV losses were driven by conversions to agricultural and pasture lands (Table 3). During both periods, this class accounted for over 95 % of all deforestation and more than 85 % of NNFV loss across spatial zones. Within PAs, 96.4 % of deforestation during 2009–2016 and 95.5 % during 2016–2023 transitioned to this class while smaller proportions shifted toward forest plantations (0.1–0.04 %) or mining areas (0.1–0.02 %). A similar dominance was observed in the 10-km and 20-km buffers, where agricultural and pasture lands accounted for approximately 98 % of total forest conversion. Oil palm expansion increased notably in the post-conflict period within PAs, rising from 0.2 % to 2.3 % of total deforestation, while remaining below 1 % in surrounding buffers. Mining and infrastructure maintained low, relatively stable proportions (<0.2 %), suggesting limited influence on the direct processes of habitat loss. Losses of NNFV followed comparable trajectories, with the mosaic of agriculture and pasture remaining the primary destination (86–93 %) across all zones. However, compared to the forest, a larger proportion of NNFV moved to other non-vegetated areas, with increases within PAs and declines in buffers between periods.

3.3. Changes in natural vegetation loss

Statistical analysis revealed significant increases in deforestation during the post-agreement period across PAs, and their surrounding 10-km and 20-km buffer, with moderate to large effect sizes (Table 4; Figure 3A). Overall, 34 of the 50 PAs (68%) experienced higher deforestation rates, representing an additional 1046 km^2 (+111%) of forest loss compared with the conflict period (Table S5; Figure S1). The largest absolute increases occurred in the Tinigua (447 km^2), Sierra de la Macarena (222 km^2), and Serranía de Chiribiquete (85 km^2) National Natural Parks, all located in the Amazon region.

In the 10-km buffers, 29 areas (58 %) showed increased deforestation, totaling an additional 1862 km^2 (+57 %). The most affected were those surrounding Serranía de Chiribiquete (617 km^2), Sierra de la Macarena (496 km^2), and Cordillera de los Picachos (210 km^2) NNPs. A comparable pattern emerged in the 20-km buffers, where 30 zones exhibited deforestation increases amounting to 1200 km^2 (+33 %). Again, buffers around Serranía de Chiribiquete (700 km^2), Sierra de la Macarena (471 km^2), and Cordillera de los Picachos (216 km^2) NNPs recorded the highest increments.

Table 3. Percentage of deforestation and NNFV loss in PAs and their surrounding 10-km and 20-km buffers during 2009–2016 and 2016–2023, disaggregated by destination land-use class.

Destination land-use class	2009-2016			2016-2023		
	Protected areas	10-km buffers	20-km buffers	Protected areas	10-km buffers	20-km buffers
			Deforestation (%)			
Forest plantation	0.1	0.04	0.3	0.04	0.1	0.3
Infrastructure	0.001	0.02	0.01	0.001	0.004	0.01
Mining	0.1	0.1	0.1	0.02	0.1	0.2
Mosaic of agriculture and pasture	96.4	97.6	98.1	95.5	98.1	98.1
Oil palm	0.2	0.3	0.2	2.3	0.5	0.3
Other non-vegetated area*	3.2	1.9	1.2	2.1	1.2	1.0
			Natural non-forest vegetation loss (%)			
Forest plantation	0.05	0.7	1.2	0.002	0.5	1.5
Infrastructure	0.001	0.3	0.1	0.01	0.2	0.1
Mining	0.002	0.1	0.3	0.005	0.1	0.2
Mosaic of agriculture and pasture	93.5	90.2	86.2	89.8	91.2	90.6
Oil palm	0.0	0.3	0.3	0.001	0.4	0.3
Other non-vegetated area*	6.5	8.4	12.0	10.2	7.63	7.2

*Areas of anthropogenic origin (infrastructure, urban expansion, or mining) not mapped within their respective classes and soils devoid of vegetation or sparse vegetative cover. It also includes burned areas and agricultural lands under preparation or fallow (Fundación Gaia Amazonas, 2024).

Table 4. Results of statistical tests comparing deforestation, NNFV loss, and NV loss between periods (2010–2016 vs. 2017–2023; Wilcoxon signed-rank test) across zones and between zones (protected areas, 10-km buffers, 20-km buffers; Friedman test) across periods. Statistically significant results ($p < 0.05$) are highlighted in bold. r_{rb} = rank-biserial correlation (effect size for Wilcoxon test); W = Kendall's W (effect size for Friedman test).

LULC change trajectory	Between periods			Between zones	
	Protected areas	10-km buffers	20-km buffers	2010–2016	2017–2023
Deforestation	**V=993; p<0.001; r_{rb}=0.56**	**V=853; p=0.019; r_{rb}=0.34**	**V=836; p=0.028; r_{rb}=0.31**	**χ^2=59.1; p<0.001; W=0.59**	**χ^2=44.3; p<0.001; W=0.44**
NNFV loss	V=542; p=0.204; r_{rb}=0.15	V=657; p=0.241; r_{rb}=0.12	V=515; p=0.882; r_{rb}=−0.19	**χ^2=51.1; p<0.001; W=0.51**	**χ^2=42.71; p<0.001; W=0.43**
NV loss	**V=996; p<0.001; r_{rb}=0.56**	**V=821; p=0.039; r_{rb}=0.29**	V=786; p=0.077; r_{rb}=0.23	**χ^2=59.1; p<0.001; W=0.59**	**χ^2=46.8; p<0.001; W=0.47**

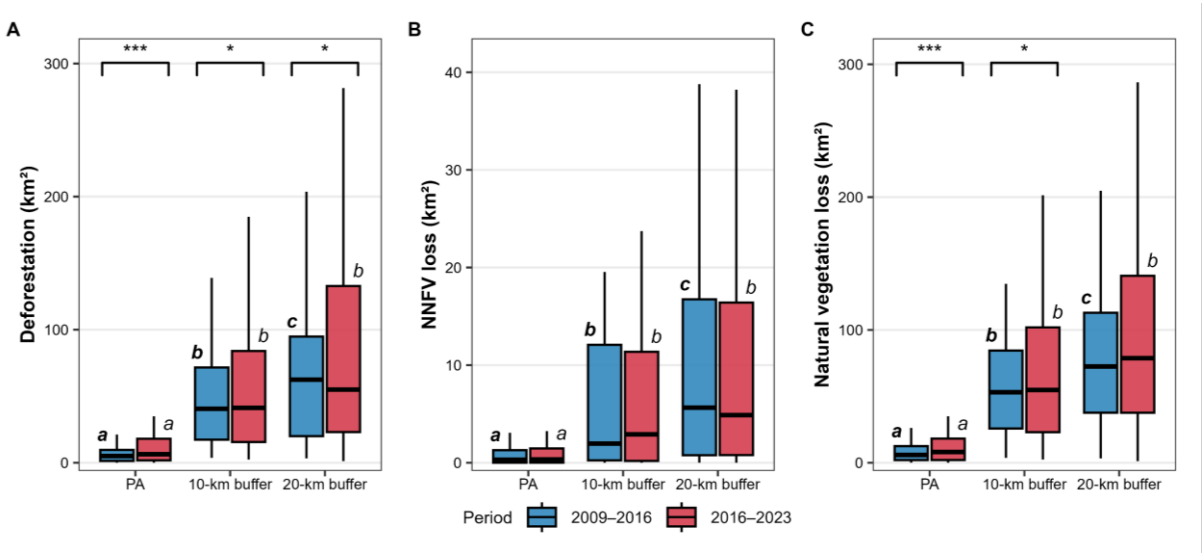

Figure 3. Boxplots of deforestation (A), NNFV loss (B), and NV loss (C) in PAs and their surrounding 10-km and 20-km buffers (n = 50) for the periods 2010–2016 (before the peace agreement) and 2017–2023 (after the peace agreement). Asterisks and brackets indicate significant differences between periods according to Wilcoxon signed-rank tests (*p < 0.05; **p < 0.01; ***p < 0.001). Different letters indicate statistically significant differences among zones within each period (p < 0.05) based on post hoc tests: letters in bold italics correspond to comparisons before the peace agreement, and letters in italics correspond to comparisons after the peace agreement. See Tables S5–S7 for detailed values and Figures S1–S3 for percentage changes between periods.

Loss of NNFV also increased between periods within PAs and 10-km buffers, though changes were not statistically significant (Table 4; Fig. 3B). Among the 50 PAs, 22 (44 %) showed higher NNFV losses during the post-agreement period, totaling 193 km^2 (+197 %), while 25 (50 %) of the 10-km buffers exhibited an additional 153 km^2 (+32 %) of loss (Table S6; Fig. S2). In contrast, NNFV loss decreased by 20 (40 %) of the 20-km buffers. Although not significant overall, these variations reveal considerable spatial heterogeneity, with some PAs experiencing marked post-agreement increases in NNFV loss.

NV loss (combining deforestation and NNFV loss) showed significant increases between periods in both PAs (+1239 km^2; 120%) and 10-km buffers (2014 km^2; 54%), with large and moderate effect sizes, respectively (Table 4). In 34 PAs (68%), NV loss rates intensified, with the steepest increases in Tinigua (447 km^2; 397%), Sierra de la Macarena (222 km^2; 166%) y El Tuparro (146 km^2; 434%) NNPs (Table S7, Figure S3).

Comparisons between zones across periods (Friedman tests) revealed significant differences with moderate to large effect sizes for all three LULC change trajectories (Table 4; Figure 3C). Post-hoc analyses showed consistent differences between PAs and their buffer zones in both periods, whereas contrasts between 10-km and 20-km buffers were evident only during the conflict period (Figure 3).

3.4. Overall changes in landscape connectivity

PAs and their surrounding 10-km and 20-km buffer zones experienced overall declines in landscape connectivity during both the conflict and post-agreement periods (Figure 4; Table S8).

Between 2009 and 2023, habitat connectivity within PAs decreased by 1.2% (1688 km^2), with a sharper decline in ECA following the peace agreement (-0.9%) compared to the conflict period (-0.3%). In these zones, habitat loss closely matched connectivity loss (rECA = 1) during the entire analysis time window, but with variations in specific periods rECA (Table S8). The outcome by 2023 was 95.6% of the landscape covered by connected habitat (Figure 4A).

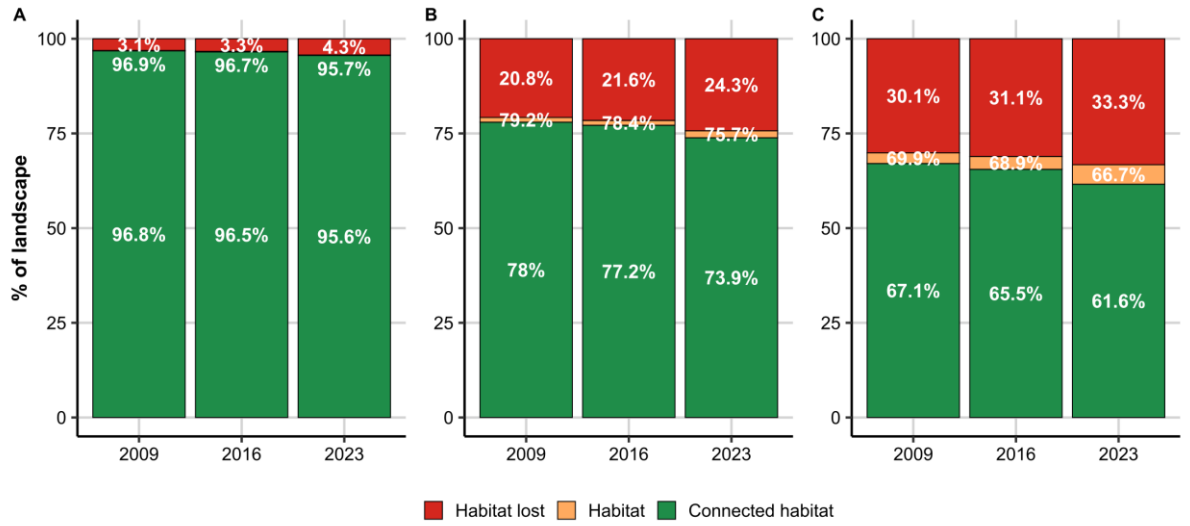

Figure 4. Changes in habitat and connected habitat for 2009, 2016, and 2023 in Colombian PAs (A), and in their surrounding 10-km (B) and 20-km (C) buffers. Values are expressed as the percentage of the total landscape area. Table S8 displays the extended results of the landscape connectivity analysis at the overall scale. Results shown here correspond to a dispersal distance of 10 km; see Figure S4 for connectivity analysis results using alternative dispersal distances.

In contrast, buffer zones exhibited more pronounced spatial and temporal fluctuations in both habitat area and connectivity. By 2023, the 10-km buffers had lost 3875 km^2 of habitat and 4326 km^2 of connected habitat relative to 2009, representing reductions of 4.4% and 5.3%, respectively. Connected habitat loss intensified after the peace agreement, when 4.3% of connected areas disappeared compared to only 1% during the conflict period. By the end of the study period, connected habitat covered 74% of the 10-km buffer landscapes (Figure 4B).

Similarly, the 20-km buffers lost 3473 km^2 of habitat (0.3%) and 6062 km^2 of connected habitat (8.9%) between 2009 and 2023. Connected habitat declined more rapidly after the peace agreement, with dECA values of 6% post-agreement and 2.3% during the conflict. Corresponding rECA values of 1.7 and 1.9 suggest that connected habitat loss exceeded the rate of habitat loss. By 2023, only 61.6% of the outer buffer landscapes remained as connected habitat (Figure 4C).

Figure S4 shows the results of the overall landscape connectivity analysis using alternative dispersal values (*d*). Across these alternative dispersal distances, the broad direction of change remained consistent. Connectivity declines were comparatively small within PAs and stronger in the surrounding 10-km and 20-km buffers, although the absolute amount of connected habitat varied with *d*.

Although statistical differences were not significant (Wilcoxon V = 525, p = 0.140, r_{rb} = -0.176; Figure 5), individual PAs exhibited heterogeneous inter-period connectivity outcomes (Figure 6; Tables S9-S10). 22 of them showed positive ΔdECA values, indicating reductions in connectivity loss between periods, and whereas the remaining 28 showed negative ΔdECA values. The strongest deteriorations were observed in Tinigua NNP and Los Flamencos FFS (ΔdECA = -24.8% and -12.0%, respectively), whereas Los Estoraques and Isla de Salamanca showed the largest improvements relative to the conflict period (ΔdECA = 36.6% and 31.8%, respectively).

Regarding the 10-km buffers, no significant differences were detected between periods (Wilcoxon V = 534, p = 0.160, rrb = –0.162; Figure 5). In total, 29 buffers exhibited positive ΔdECA values, indicating less negative or more positive post-agreement connectivity outcomes, whereas 21 showed negative ΔdECA values, indicating more negative post-agreement outcomes. The strongest deteriorations were concentrated around the Tinigua and Sierra de la Macarena NNPS (ΔdECA = -28.9% and -23.6%, respectively). In contrast, the buffers surrounding Los Estoraques and Galeras showed the largest improvements relative to the conflict period (ΔdECA = 15.3% and 15.1%, respectively).

For the 20-km buffers, differences between periods were statistically significant (Wilcoxon V = 416, p = 0.016, rrb = –0.347; Figure 5). 29 buffers showed negative ΔdECA values and 21 showed positive ΔdECA values (Figure 6; Tables S9–S10), confirming heterogeneous inter-period connectivity outcomes. The strongest deteriorations were observed around the Tinigua and Paramillo NNPs (ΔdECA = -30.6% and -23.1%, respectively). In contrast, the buffers of Los Estoraques and Los Colorados registered notable connectivity gains (+16.2% and +11.7%), reflecting localized recovery processes.

Differences between zones among periods were significant for both 2009-2016 (Friedman χ^2 = 7.96, p = 0.019, W = 0.08) and 2016-2023 (Friedman χ^2 = 9.64, p = 0.008, W = 0.096) periods, but with low size effects (Figure 5; Figure S5). Nevertheless, post-hoc analysis showed significant differences between PAs and buffer zones only after the agreement.

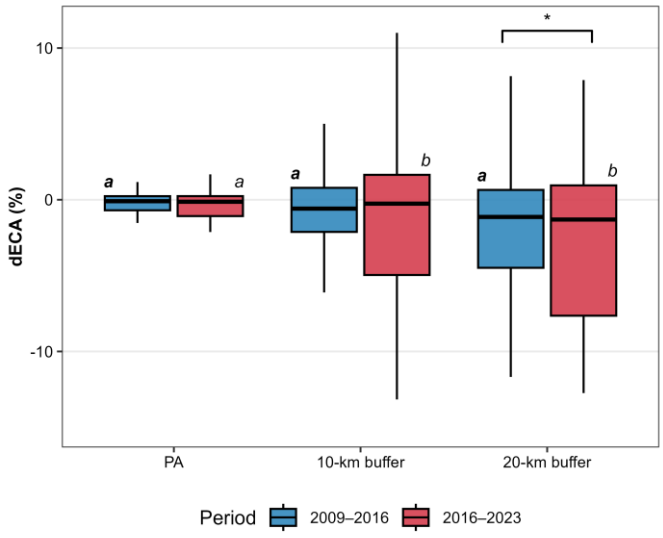

Figure 5. Boxplots of dECA in protected areas (PAs) and their surrounding 10-km and 20-km buffers (n = 50) for the periods 2009–2016 (before the peace agreement) and 2016–2023 (after the peace agreement). Asterisks and brackets

indicate significant differences between periods according to Wilcoxon signed-rank tests (*p < 0.05). Different letters indicate statistically significant differences among zones within each period (p < 0.05) based on post hoc tests: letters in bold italics correspond to comparisons before the peace agreement, and letters in italics correspond to comparisons after the peace agreement. See Tables S9–S10 for detailed values and Figure S5 for the spatial distribution of dECA.

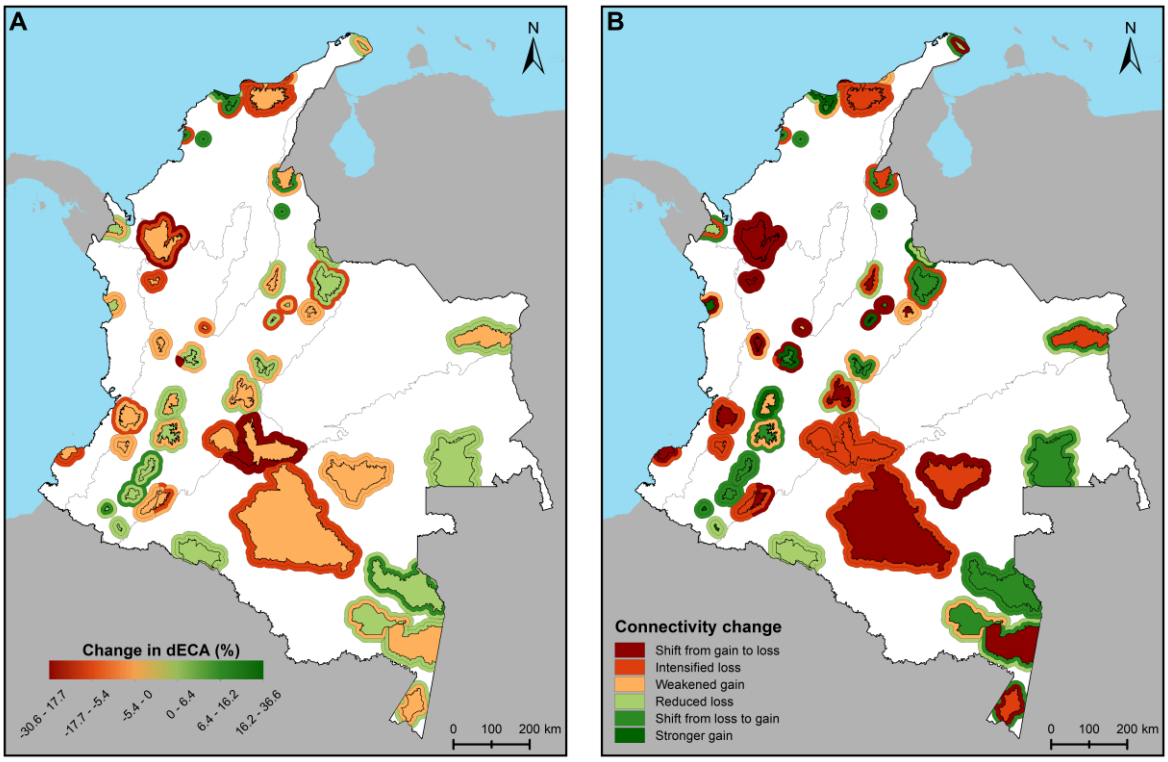

Figure 6. Inter-period change in landscape connectivity outcomes across PAs and their surrounding buffers. (A) Spatial distribution of ΔdECA. Positive values indicate less negative or more positive connectivity outcomes in the post-agreement period relative to the conflict period, whereas negative values indicate more negative connectivity outcomes in the post-agreement period. (B) Qualitative categories of inter-period connectivity change derived from the sign of dECA in each period and the sign of ΔdECA, distinguishing intensified loss, reduced loss, shift from loss to gain, shift from gain to loss, stronger gain, and weakened gain. See Figure S5 for the spatial distribution of dECA among periods. Inter-period connectivity change category definitions are provided in Table S4.

4. Discussion

4.1. Regional patterns of vegetation loss

Our results showed different levels of change in natural vegetation loss across biogeographical regions, reflecting heterogeneous socioecological and institutional contexts that condition PAs' ability to prevent habitat conversion (González-González et al., 2021). In general, previous studies have identified that Colombian PAs located closer to human settlements or within municipalities with better governance and public services tend to better mitigate deforestation, whereas remote areas are often more vulnerable to illegal ranching, coca cultivation, and gold mining, among other drivers of land-use change (Bonilla-Mejía & Higuera-Mendieta, 2019).

The Amazon region experienced the most pronounced post-agreement surge in deforestation, with losses inside PAs more than doubling relative to the conflict period. This

escalation was particularly severe around major PAs of the Andes Amazon Transition Belt (AATB), which were strategic territories under FARC control for several years due to their remoteness and limited accessibility (Canavire-Bacarreza et al., 2018; Hoffmann et al., 2018). After the withdrawal of FARC, these landscapes faced rapid forest loss, particularly within PAs, associated with the reoccupation of previously restricted zones, weak institutions, the emergence of illegal land markets, and the expansion of cattle ranching, agriculture, illicit crops, and infrastructure (Armenteras et al., 2019; Bonilla-Mejía & Higuera-Mendieta, 2019; Clerici et al., 2020; Mendoza, 2020; Murillo-Sandoval et al., 2020, 2021; Negret et al., 2019). This pattern illustrates the dual role of armed conflict in shaping land-use trajectories, where conflict-driven isolation once constrained deforestation but subsequent peace-time accessibility accelerated landscape transformation (Landholm et al., 2019; Suarez et al., 2018).

Although other regions exhibited smaller absolute increases, the consistent upward trends within PAs and surrounding buffers indicate that forest pressures are spreading beyond traditional Amazonian hotspots. For instance, the sharp deforestation relative increase in the Orinoquia likely reflects the growing pressures from oil palm cultivation, petroleum extraction, and illicit crops (Armenteras et al., 2009; Romero-Ruiz et al., 2012). Two PAs from the Caribbean region registered the most substantial relative increase in deforestation (see Fig. S1), which agrees with other studies that have reported PAs such as Los Colorados and Sierra Nevada de Santa Marta as the most transformed in the last two decades (Latorre Parra et al., 2022), sharpening pressures on the last remnants of Colombia's tropical dry forest (García et al., 2014). In the Andean region, the observed increases likely reflect the intensification of smallholder agriculture, cattle ranching, and urban expansion in peri-urban and montane areas where remaining forest remnants are highly fragmented and ecologically critical (Etter et al., 2006).

Patterns of NNFV loss displayed greater heterogeneity among regions, suggesting that open vegetation formations respond differently to post-agreement land-use pressures. NNFV loss intensified in the Amazon, Orinoquia, and Caribbean regions, driven by the conversion of savannas and shrublands into pastures and mixed agricultural mosaics, while declining or stabilizing in the Andean and Pacific regions, possibly due to secondary succession, land abandonment, or stricter land-use regulation (Sánchez-Cuervo & Aide, 2013). These contrasts indicate that habitat degradation processes extend beyond forests, with Amazonian and Orinoquian PAs emerging as critical frontiers of natural vegetation loss.

4.2. Dominant land-use transitions and emerging pressures

The dominance of agricultural and pasture mosaics as the main destination of both deforestation and NNFV loss underscores the influence of extensive ranching and low-intensity agriculture as the leading proximate drivers of land-cover change across Colombia's PAs and their surroundings. These findings are consistent with previous national-scale assessments (Clerici et al., 2020) but further reveal that conversion to productive land uses remains the primary mechanism of natural vegetation loss even within legally protected landscapes. The persistence of this trend across spatial scales and periods suggests that the peace process did not alter the proximate drivers of habitat transformation but rather sharpened them and enabled their spatial expansion into previously inaccessible areas by modifying underlying drivers (Landholm et al.,

2019). Beyond these dominant agricultural dynamics, our results also suggested localized post-agreement habitat conversions to oil palm and, to a lesser extent, mining, indicating an emerging diversification and intensification of land-use pressures near PAs.

Colombia is currently the world's fourth-largest oil palm producer, and further expansion of oil palm cultivation is expected, driven by rising global demand for this commodity and the country's extensive areas suitable for cultivation (Castiblanco et al., 2013; Garcia-Ulloa et al., 2012). For instance, in the Amazon, oil palm has become the dominant industrial crop and an increasingly important driver of deforestation (Molina, 2024). Assessments have identified South American forests as particularly vulnerable to oil-palm-related biodiversity loss, with regions such as the Serranía de la Macarena among the most at risk in Colombia (Ocampo-Peñuela et al., 2018; Vijay et al., 2016). Although our findings suggest emerging oil palm-related habitat loss within PAs, to the best of our knowledge, such processes have not been previously documented in Colombia. Therefore, these results should be interpreted cautiously, as they may partly reflect misclassification or thematic uncertainty in the LULC dataset.

4.3. Dynamics of natural vegetation loss in the post-agreement period

The significant increase in deforestation observed during the post-agreement period is consistent with multiple regional and national analyses reporting accelerated forest loss after 2016 (Armenteras et al., 2019; Clerici et al., 2020; Murillo-Sandoval et al., 2020, 2021; Negret et al., 2019). As in those studies, the sharpest increases were concentrated in the Amazonian foothills and the AATB, where weak governance, land grabbing, and expanding agricultural frontiers have rapidly transformed landscapes previously constrained by armed territorial control. By extending the temporal window of analysis to seven years before and after the 2016 peace agreement (2009–2023), increasing the number of protected areas examined, and explicitly distinguishing PA cores from immediate and broader surrounding landscapes, our results provide an updated national-scale picture of how habitat conversion evolves after 2016. These patterns are consistent with a sustained intensification of deforestation within PAs and their buffers after 2016, but they should be interpreted as descriptive evidence within a broader post-agreement context rather than as a strict causal attribution to the agreement itself.

Results related to NNFV add an additional, but more uncertain, dimension to this picture. Although NNFV loss increased in several PAs and regions, and the relative increase within PAs was larger than that of deforestation, these patterns were more heterogeneous and should be interpreted with greater caution than deforestation results. Even so, they highlight that after 2016, habitat conversion pressures extended beyond forests into open natural ecosystems such as shrublands, savannas, páramos, and other non-forest formations, components of Colombia's protected landscapes that have received comparatively less attention in national post-2016 assessments. For example, this trend was evident in PAs such as El Tuparro PNN in the Orinoquia and Sierra Nevada de Santa Marta PNN in the Caribbean region, where NNFV loss increased sharply between periods, reflecting the growing vulnerability of open natural formations even within PAs.

These findings are particularly relevant for biodiversity conservation within PAs dominated by non-forest ecosystems, such as high-Andean páramos and Orinoquian savannas,

which sustain unique species assemblages, regulate hydrology, store carbon, and maintain landscape connectivity. The intensification of NNFV loss suggests that these habitats are increasingly exposed to anthropogenic disturbance and land-use conversion following rapid socioecological shifts in the post-agreement period. Recognizing and incorporating NNFV dynamics into conservation monitoring frameworks is therefore essential to safeguard the integrity of these ecosystems and to ensure that post-agreement restoration and land-management policies effectively address the full spectrum of Colombia's natural vegetation types.

When considered together, the combined increase in NV loss provides a more integrated view of habitat transformation across Colombia's PAs. This metric captures both the rapid and extensive clearing of forests and the more diffuse transformation of open natural formations, revealing a cumulative erosion of ecological integrity that extends across all spatial zones. The significant rise in NV loss during the post-agreement period indicates that the effects of land-use expansion have transcended vegetation types and administrative boundaries, undermining the protected area network's ability to maintain ecosystem functionality and connectivity. These results underscore the need for conservation and restoration strategies that operate at the landscape scale, addressing both forested and non-forested habitats within a unified framework capable of mitigating the diverse, interlinked drivers of natural vegetation loss in post-agreement Colombia.

4.4. Dynamics of landscape connectivity in the post-agreement period

Connected area declined across PAs and their surrounding buffers. Although PAs retained relatively high levels of connected habitat (>95%), dECA values were generally more negative in the post-agreement period, indicating less favorable connectivity outcomes after 2016. These patterns suggest that the post-2016 intensification of habitat conversion coincided with increasing fragmentation and isolation of natural-vegetation networks around PAs, especially in broader surrounding landscapes. Spatially, the connected area decreased with increasing distance from PAs' boundaries, and losses in surrounding buffers were often disproportionate to habitat-area reduction alone. These patterns suggest that after 2016, the intensification of habitat conversion coincided with increasing fragmentation and isolation of natural-vegetation networks around PAs, especially in broader surrounding landscapes. Such declines have the potential to promote ecological isolation and disrupt key ecological processes linking protected habitats with surrounding landscapes and other PAs, including species dispersal, gene flow, and biogeochemical exchanges (DeFries et al., 2010; Hansen & DeFries, 2007; Laurance et al., 2012). This progressive disconnection indicates increasing spatial separation among natural-vegetation patches surrounding PAs, weakening the role of buffers in maintaining habitat continuity and likely amplifying edge-related disturbances that further erode landscape integrity.

Beyond these overall patterns, changes in rECA values provide insights into the processes driving connectivity loss. The increase in rECA within PAs (from 0.9 to 1.3) indicates a shift from transformations primarily associated with habitat reduction (e.g., perforation or shrinkage) toward those linked to habitat isolation (e.g., fragmentation or attrition). In contrast, buffer zones exhibited more pronounced and heterogeneous declines, with connectivity losses exceeding

habitat losses, particularly in the outer 20-km buffers (rECA > 1.7). This decoupling implies that land-use transitions not only reduced the amount of habitat but also disrupted its spatial configuration, increasing habitat isolation and fragmentation. Such structural degradation likely intensifies edge effects and constrains species movement (Haddad et al., 2015; Laurance et al., 2011). These findings reinforce that maintaining habitat extent alone is insufficient to preserve connectivity within natural-vegetation networks; spatial arrangement is also critical.

At finer spatial scales, the heterogeneous trajectories observed among individual PAs and buffers underscore the context-dependent nature of connectivity responses. Some landscapes exhibited localized recovery, while others continued to experience accelerated isolation. This variability likely reflects differences in land-use history, accessibility, governance capacity, and the scope of ongoing restoration or conservation actions. For instance, areas such as Los Estoraques, Los Colorados, and Isla de Salamanca showed positive ΔdECA values, likely associated with reduced NV loss or active restoration, whereas Paramillo, Otún Quimbaya, Sierra de la Macarena, and particularly Tinigua exhibited negative ΔdECA values consistent with advancing deforestation fronts. Recent analyses have similarly identified the Eje Cafetero, where Otún Quimbaya SFF is located, as a hotspot of connectivity decline in Andean forests (Correa-Ayram et al., 2025). Similarly, PAs within the AATB have been repeatedly reported as critical areas of connectivity loss during the post-agreement period (López et al., 2024; Murillo-Sandoval et al., 2022). Together, this evidence highlights the growing vulnerability of the northern Andes–Amazon biodiversity bridge (Clerici et al., 2018; Murillo-Sandoval et al., 2022) and underscores the urgent need to integrate connectivity restoration and landscape governance into post-agreement conservation and land-governance agendas (Calle-Rendón et al., 2018; Linero-Triana et al., 2023; Negret et al., 2021).

4.5. Study limitations

This study is based on a descriptive before-and-after comparison and does not isolate the specific causal effect of the 2016 peace agreement from other concurrent processes, such as market dynamics, governance shifts, infrastructure expansion, enforcement changes, or climate variability. Accordingly, the observed patterns are best interpreted as changes occurring across the conflict and post-agreement periods within a broader socioecological transition, rather than as effects attributable solely to the agreement itself. In addition, potential residual temporal inconsistencies in annual LULC products arising, for example, from sensor transitions (TM, ETM+, and OLI), image availability, or differences in classification performance may influence apparent changes in time series as previously observed on the Global Forest Change dataset (Ceccherini et al., 2021; Hansen et al., 2013; Palahí et al., 2021). However, the methodology used by MapBiomas to produce its annual LULC dataset includes spatiotemporal filtering rules designed to reduce implausible year-to-year transitions (Fundación Gaia Amazonas, 2024; Souza et al., 2020).

Results related to NNFV loss should be interpreted more cautiously than those for deforestation. The overall MapBiomas accuracy values reported here reflect product-wide performance rather than direct validation of the aggregated NNFV category used in this study, and the class-level accuracies indicate greater thematic uncertainty for Natural non-forest formation

than for Forest formation MapBiomas classes (Table S3). Finally, the connectivity analysis represents generic natural-vegetation connectivity rather than species-specific or resistance-weighted connectivity. Habitat was defined as a binary natural-vegetation layer (Forest + NNFV), and connectivity was estimated from Euclidean inter-patch distances under a homogeneous-matrix assumption. Therefore, the analysis captures changes associated with habitat amount and spatial configuration, but it does not model differential matrix permeability among HMA types, quantify connectivity between buffer habitats and PA cores, or support species-level inference (Saura & Pascual-Hortal, 2007; Saura et al., 2011).

5. Conclusion

The period following the 2016 peace agreement coincided with more intense habitat conversion in and around PAs, with the Andes–Amazon transition showing the strongest signals. By integrating habitat-loss trajectories and connectivity metrics across 50 strictly protected areas and two non-overlapping buffer bands, this study shows that connectivity remained comparatively stable inside PA cores but declined much more strongly in surrounding landscapes, where configuration effects often outpaced habitat loss. These results indicate that safeguarding PA cores alone is insufficient to maintain ecological flows across the national network. Strengthening buffer governance, targeted restoration, and connectivity-aware land-use planning at ecologically meaningful landscape scales will be essential for reducing isolation of PA cores and enhancing the long-term functionality of Colombia's protected-area system.

6. Data statement

The minimum derived datasets required to replicate the analyses, figures, and results presented in this manuscript are openly available at Zenodo: https://doi.org/10.5281/zenodo.19445808 (Rubiano et al. 2026).

7. Acknowledgements

The research work was supported by institutional funding from the Dirección de Investigación e Innovación, Universidad del Rosario (Grant IV-FGD004).

8. Supplementary information

Table S1. Summary information of the protected areas (PAs) included in the analysis (n = 50), showing the SINAP category (NNP: National Natural Park; FFS: Fauna and Flora Sanctuary; NNR: National Natural Reserve; FS; UNA: Unique Natural Area; VP: Via Park), and the IUCN Category (IA: Strict Nature Reserve; IB: Wilderness Area; II: National Park; III: Natural Monument).

ID	Name	SINAP Category	IUCN Category	Biogeographical Region*	Geographical area (km²)†
1	Serranía De Los Yariguies	NNP	II	Andean	597.0
2	Rio Pure	NNP	II	Amazon	9,876.7
3	Sanquianga	NNP	II	Pacific	865.6
4	Sierra Nevada De Santa Marta	NNP	II	Caribbean	4,014.5
5	Puinawai	NNR	IA	Amazon	10,956.5
6	Yaigojé Apaporis	NNP	II	Amazon	10,560.2
7	Amacayacu	NNP	II	Amazon	2,624.8
8	Guanentá Alto Río Fonce	FFS	IB	Andean	102.7
9	Macuira	NNP	II	Caribbean	240.5
10	Los Nevados	NNP	II	Andean	614.2
11	Plantas Medicinales Orito Ingi-Ande	FS	IB	Andean	104.0
12	Cueva De Los Guácharos	NNP	II	Andean	71.3
13	Otún Quimbaya	FFS	IB	Andean	4.5
14	El Cocuy	NNP	II	Andean	3,063.3
15	Sierra De La Macarena	NNP	II	Amazon	6,205.8
16	Tinigua	NNP	II	Amazon	2,143.6
17	Catatumbo Barí	NNP	II	Andean	1,609.8
18	Alto Fragua Indi Wasi	NNP	II	Andean	761.3
19	Las Hermosas	NNP	II	Andean	1,247.7
20	Cordillera De Los Picachos	NNP	II	Andean	2,879.4
21	Sumapaz	NNP	II	Andean	2,217.5
22	Utría	NNP	II	Pacific	643.3
23	Paramillo	NNP	II	Andean	5,040.1
24	Los Katíos	NNP	II	Pacific	779.7
25	Nevado Del Huila	NNP	II	Andean	1,638.4
26	Serranía De Chiribiquete	NNP	II	Amazon	42,681.0
27	Puracé	NNP	II	Andean	918.4
28	Tayrona	NNP	II	Caribbean	193.1
29	Complejo Volcánico Dona Juana Cascabel	NNP	II	Andean	658.6
30	Iguaque	FFS	IB	Andean	68.9
31	Ciénaga Grande De Santa Marta	FFS	IB	Caribbean	270.2
32	Los Colorados	FFS	IB	Caribbean	10.4
33	El Corchal El Mono Hernández	FFS	IB	Caribbean	38.7
34	Serranía De Los Churumbelos Auka Wasi	NNP	II	Andean	972.4
35	Cahuinarí	NNP	II	Amazon	5,586.6
36	Tatamá	NNP	II	Andean	435.1
38	Galeras	FFS	IB	Andean	83.3
39	Los Flamencos	FFS	IB	Caribbean	70.3

40	Isla De Salamanca	VP	III	Caribbean	565.9
41	Pisba	NNP	II	Andean	352.4
42	Farallones De Cali	NNP	II	Andean	1,963.6
43	Chingaza	NNP	II	Andean	774.1
44	Los Estoraques	UNA	III	Andean	6.6
45	Munchique	NNP	II	Andean	469.8
46	Selva De Florencia	NNP	II	Andean	100.2
47	La Paya	NNP	II	Amazon	4,401.2
48	El Tuparro	NNP	II	Orinoquia	5,549.1
49	Tamá	NNP	II	Andean	511.3
50	Las Orquídeas	NNP	II	Andean	287.5
51	Nukak	NNR	IA	Amazon	8,756.5

* According to (Chaves & Arango, 1998).

† According to (PNNC, 2024).

Table S2. General features of the PAs excluded from the analysis.

Name	SINAP Category	IUCN Category	Establishment year	Geographical area (km^2)	Terrestrial area (km^2)
Bahía Portete - Kaurrele	NNP	II	2014	140.6	27
Corales de Profundidad	NNP	II	2013	1,423.5	0
Cordillera Beata	NNR	IA	2022	33,125.3	0
Gorgona	NNP	II	1984	605	0
Isla de la Corota	FS	IB	1977	0.2	0.2
Los Corales del Rosario y de San Bernardo	NNP	II	1977	1,234.8	2.6
Malpelo	FFS	IB	1995	48,151.1	0
Old Providence Mc Bean Lagoon	NNP	II	1995	16.4	0.9
Serranía de Manacacías	NNP	II	2023	680.3	680.3
Uramba Bahía Málaga	NNP	II	2010	468.9	5

Table S3. User's and producer's accuracy (UA and PA, respectively) of the main Level 1 classes most relevant to this study for 2009 and afterward. Values are summarized as mean annual accuracy and standard deviation (SD) across years. Based on data from MapBiomas Colombia (2026).

MapBiomas level 1 class	Mean annual UA (%)	SD	Mean annual PA (%)	SD
Forest formation	98.4	0.4	99.6	0.6
Natural non forest formation	74.9	19.8	12.1	0.2
Agricultural and livestock area	90.8	3.7	92.1	15.8

Table S4. Definition of qualitative inter-period connectivity change categories used to interpret ΔdECA. Categories are based on the sign of dECA during the conflict period (2009–2016), the sign of dECA during the post-agreement period (2016–2023), and the sign of ΔdECA. The table summarizes the logical condition and ecological interpretation associated with each category.

Category of connectivity change	Condition	Interpretation
Shift from gain to loss	$dECA_{2009\text{-}2016} > 0$, $dECA_{2016\text{-}2023} < 0$	Connectivity shifted from gain to loss
Intensified loss	$dECA_{2009\text{-}2016} < 0$, $dECA_{2016\text{-}2023} < 0$, $\Delta dECA < 0$	Connectivity loss occurred in both periods and became more severe in the post-agreement period
Weakened gain	$dECA_{2009\text{-}2016} > 0$, $dECA_{2016\text{-}2023} > 0$, $\Delta dECA < 0$	Connectivity gain occurred in both periods, but became weaker in the post-agreement period
Reduced loss	$dECA_{2009\text{-}2016} < 0$, $dECA_{2016\text{-}2023} < 0$, $\Delta dECA > 0$	Connectivity loss occurred in both periods, but became less severe in the post-agreement period
Shift from loss to gain	$dECA_{2009\text{-}2016} < 0$, $dECA_{2016\text{-}2023} > 0$	Connectivity shifted from loss to gain
Stronger gain	$dECA_{2009\text{-}2016} > 0$, $dECA_{2016\text{-}2023} > 0$, $\Delta dECA > 0$	Connectivity gain occurred in both periods and became stronger in the post-agreement period

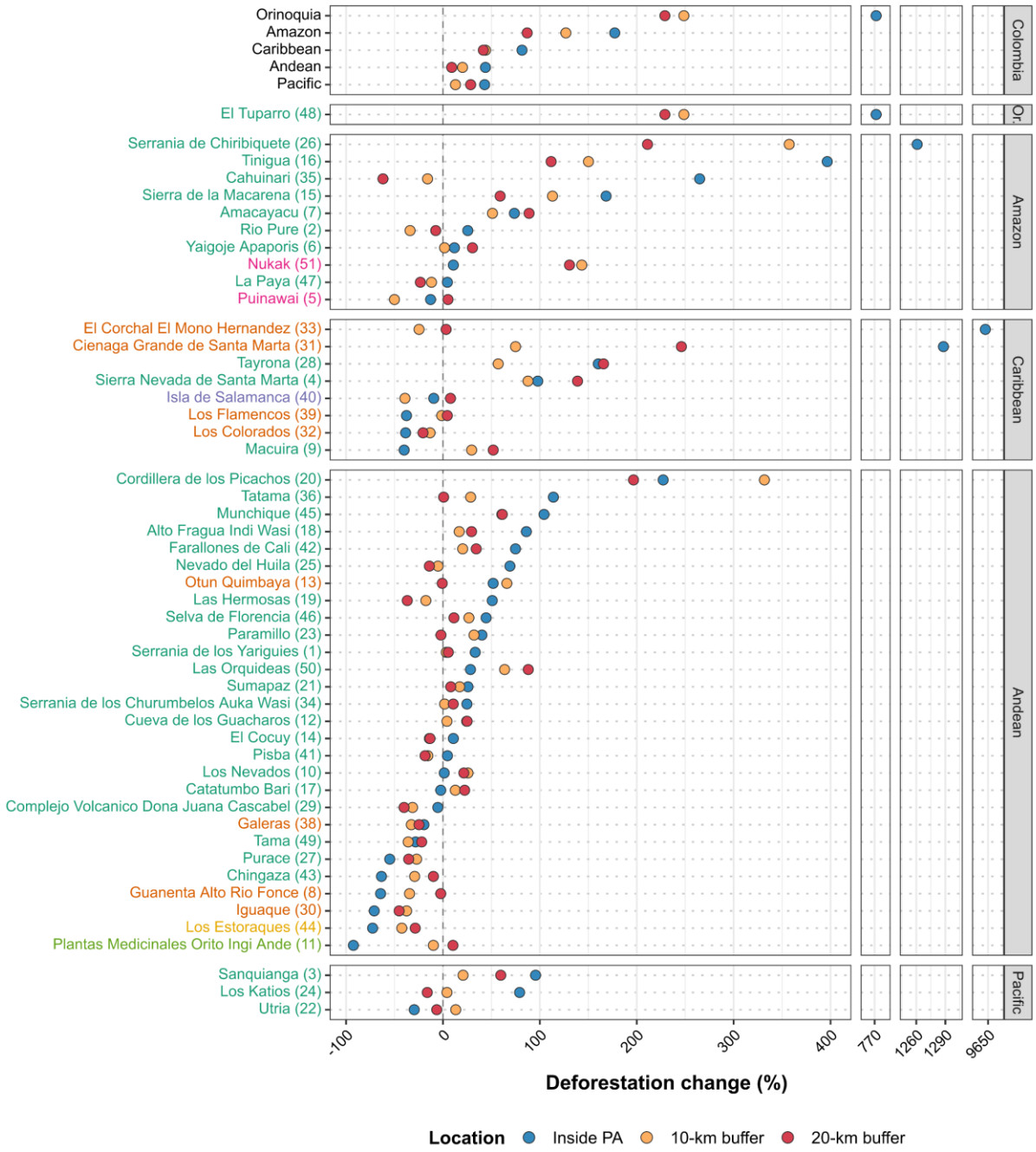

Figure S1. Deforestation change (%) between the 2009–2016 and 2016–2023 periods in PAs and their surrounding 10-km and 20-km buffers. The first panel shows aggregated values by biogeographical region (Or = Orinoquia), while subsequent panels present percentage change by individual PA grouped by biogeographical region. PAs are sorted decreasingly by deforestation change inside them. Labels are colored according to SINAP category, with numbers in parentheses indicating PA IDs (see Table S1).

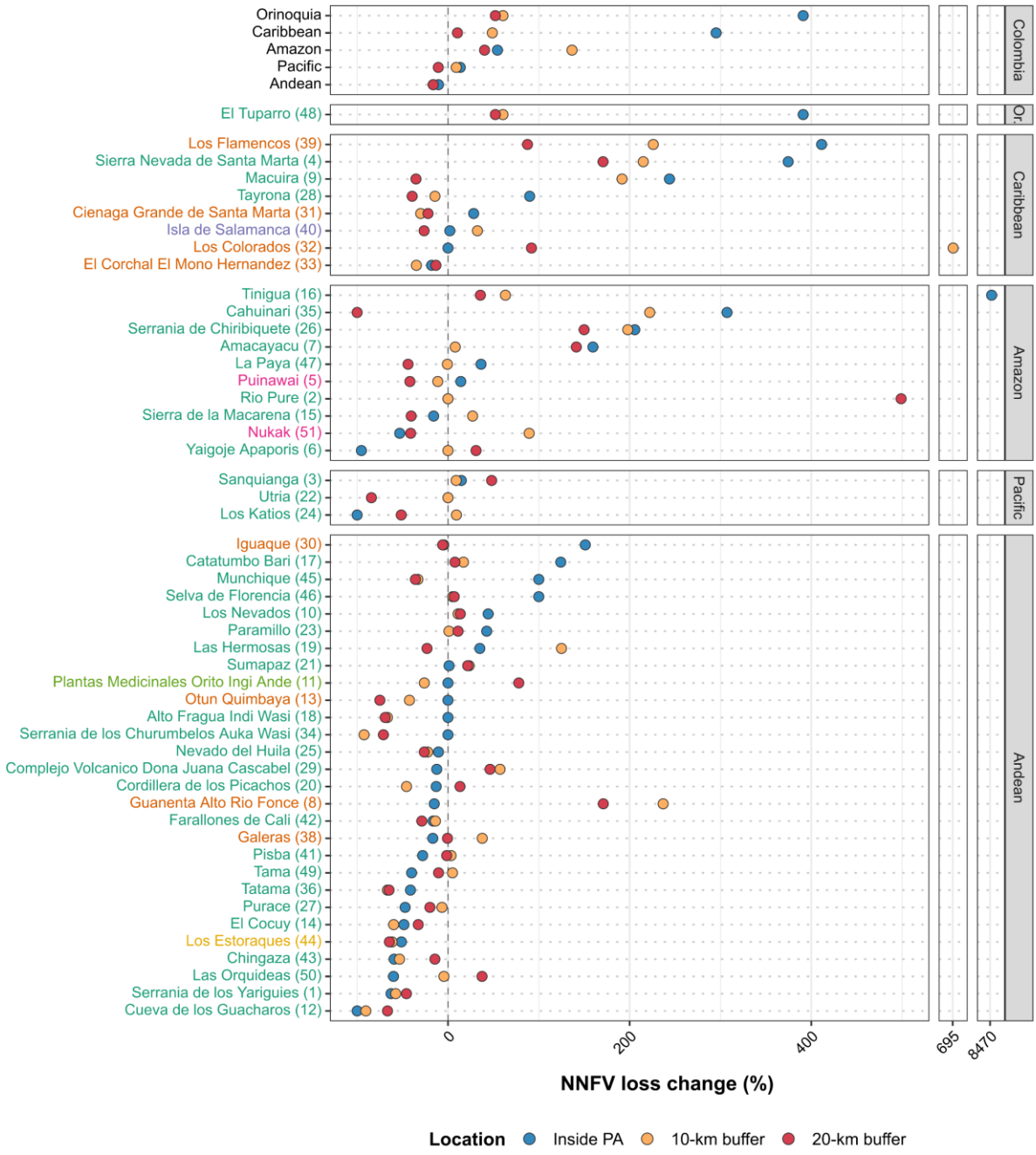

Figure S2. NNFV loss change (%) between the 2009–2016 and 2016–2023 periods in PAs and their surrounding 10-km and 20-km buffers. The first panel shows aggregated values by biogeographical region (Or = Orinoquia), while subsequent panels present percentage change by individual PA grouped by biogeographical region. PAs are sorted decreasingly by NNFV loss change inside them. Labels are colored according to SINAP category, with numbers in parentheses indicating PA IDs (see Table S1).

Table S5. Deforested area in PAs and their surrounding 10-km and 20-km buffers for 2009–2016 (t_0) and 2016–2023 (t_1).

ID	Name	Deforestation (km²)								
		PAs			10-km buffers			20-km buffers		
		t_0	t_1	t_1-t_0	t_0	t_1	t_1-t_0	t_0	t_1	t_1-t_0
1	Serranía De Los Yariguies	4.7	6.3	1.6	123.0	127.2	4.2	122.4	129.0	6.7
2	Rio Pure	5.7	7.1	1.4	3.7	2.4	-1.3	7.5	7.0	-0.6
3	Sanquianga	3.3	6.5	3.2	34.5	41.6	7.1	84.0	134.1	50.1
4	Sierra Nevada De Santa Marta	68.7	135.8	67.2	139.0	260.9	122.0	95.0	227.0	132.0
5	Puinawai	36.2	31.5	-4.6	21.4	10.7	-10.7	3.6	3.7	0.2
6	Yaigojé Apaporis	31.2	34.9	3.7	23.9	24.3	0.4	17.9	23.4	5.5
7	Amacayacu	2.0	3.4	1.4	5.7	8.6	2.9	4.8	9.0	4.2
8	Guanentá Alto Río Fonce	0.6	0.2	-0.4	16.8	11.0	-5.8	23.7	23.2	-0.5
9	Macuira	6.5	3.9	-2.6	31.6	41.0	9.4	12.4	18.8	6.4
10	Los Nevados	1.7	1.7	0.02	49.1	61.8	12.7	112.8	137.0	24.3
11	Plantas Medicinales Orito Ingi-Ande	0.04	0.003	-0.03	24.9	22.5	-2.5	73.6	81.1	7.6
12	Cueva De Los Guácharos	0.1	0.2	0.03	8.5	8.9	0.4	18.5	23.1	4.6
13	Otún Quimbaya	0.1	0.1	0.03	9.7	16.1	6.4	37.4	37.1	-0.3
14	El Cocuy	7.7	8.5	0.8	46.9	40.3	-6.6	62.5	54.2	-8.4
15	Sierra De La Macarena	132.1	354.5	222.4	438.5	934.1	495.6	296.2	471.0	174.8
16	Tinigua	112.6	559.4	446.8	129.1	322.9	193.8	93.7	198.3	104.6
17	Catatumbo Barí	51.6	50.4	-1.2	176.1	198.4	22.4	230.1	281.6	51.5
18	Alto Fragua Indi Wasi	7.3	13.6	6.3	70.7	82.6	11.8	62.4	80.7	18.4
19	Las Hermosas	5.3	8.0	2.7	50.6	41.6	-8.9	44.7	28.3	-16.5
20	Cordillera De Los Picachos	32.2	105.3	73.1	63.4	273.6	210.2	72.7	215.7	143.0
21	Sumapaz	3.6	4.5	0.9	89.0	104.4	15.3	130.4	140.9	10.5
22	Utría	3.0	2.1	-0.9	13.6	15.4	1.8	12.4	11.6	-0.8
23	Paramillo	204.8	287.1	82.3	309.3	408.3	99.0	242.6	237.6	-5.1
24	Los Katíos	1.1	2.0	0.9	31.3	32.6	1.3	48.6	40.7	-7.9
25	Nevado Del Huila	2.8	4.7	1.9	71.9	68.3	-3.7	64.9	55.7	-9.1
26	Serranía De Chiribiquete	6.7	91.4	84.7	172.7	789.6	617.0	224.9	699.5	474.6
27	Puracé	1.2	0.6	-0.7	43.9	32.0	-11.9	126.3	81.6	-44.7
28	Tayrona	2.9	7.5	4.6	19.0	29.9	10.8	3.6	9.5	5.9
29	Complejo Volcánico Dona Juana Cascabel	4.4	4.1	-0.2	73.7	50.5	-23.1	109.9	65.8	-44.2
30	Iguaque	0.7	0.2	-0.5	6.3	4.0	-2.4	19.1	10.5	-8.7
31	Ciénaga Grande De Santa Marta	0.002	0.02	0.02	7.2	12.5	5.4	4.4	15.1	10.7
32	Los Colorados	0.9	0.5	-0.3	53.4	46.3	-7.1	114.9	91.3	-23.7
33	El Corchal El Mono Hernández	0.003	0.3	0.3	14.8	11.1	-3.7	31.5	32.6	1.0
34	Serranía De Los Churumbelos Auka Wasi	7.7	9.6	1.9	107.0	108.8	1.8	130.2	144.0	13.8
35	Cahuinarí	0.6	2.2	1.6	4.2	3.5	-0.7	3.3	1.3	-2.0
36	Tatamá	5.7	12.2	6.5	54.7	70.3	15.6	67.6	68.1	0.5
38	Galeras	2.0	1.6	-0.4	31.3	21.1	-10.2	63.6	47.9	-15.7
39	Los Flamencos	4.0	2.5	-1.5	28.7	28.3	-0.4	48.0	50.1	2.2
40	Isla De Salamanca	0.014	0.01	0.0	8.8	5.4	-3.5	16.2	17.5	1.3
41	Pisba	6.1	6.4	0.3	31.0	26.1	-4.9	33.7	27.5	-6.2
42	Farallones De Cali	11.2	19.5	8.3	60.3	72.6	12.3	40.4	54.3	13.9
43	Chingaza	21.2	7.7	-13.5	94.6	66.9	-27.7	94.2	84.9	-9.3

44	Los Estoraques	0.1	0.02	-0.1	15.7	9.1	-6.7	42.4	30.3	-12.1
45	Munchique	6.2	12.6	6.4	52.6	84.5	31.9	69.2	111.6	42.4
46	Selva De Florencia	7.4	10.7	3.3	59.9	75.9	16.0	91.1	101.4	10.3
47	La Paya	60.7	63.4	2.8	209.7	184.9	-24.8	203.7	156.2	-47.5
48	El Tuparro	3.8	33.2	29.4	8.3	28.8	20.5	7.0	23.0	16.0
49	Tamá	5.9	4.2	-1.7	19.4	12.5	-7.0	22.6	17.7	-5.0
50	Las Orquídeas	10.3	13.2	2.9	37.1	60.8	23.6	47.8	89.8	42.1
51	Nukak	43.7	48.4	4.7	44.1	107.3	63.2	68.3	157.5	89.2
	Total	938.1	1984.0	1045.9	3240.5	5102.0	1861.5	3658.9	4858.7	1199.8

Table S6. Area of NNFV loss in PAs and their surrounding 10-km and 20-km buffers for 2009–2016 (t_0) and 2016–2023 (t_1).

ID	Name	Natural non-forest vegetation loss (km2)								
		PAs			10-km buffers			20-km buffers		
		t_0	t_1	t_1-t_0	t_0	t_1	t_1-t_0	t_0	t_1	t_1-t_0
1	Serranía De Los Yariguies	0.2	0.06	-0.1	11.8	5.0	-6.8	37.4	20.3	-17.1
2	Rio Pure	0	0	0	0	0	0	0.1	0.3	0.3
3	Sanquianga	0.3	0.4	0.1	1.6	1.8	0.1	1.7	2.6	0.8
4	Sierra Nevada De Santa Marta	19.3	91.7	72.4	35.9	113.2	77.3	16.7	45.1	28.5
5	Puinawai	1.1	1.2	0.2	0.3	0.3	-0.04	0.3	0.2	-0.1
6	Yaigojé Apaporis	1.6	0.07	-1.5	0.1	0.1	0.0	0.04	0.1	0.01
7	Amacayacu	0.03	0.1	0.1	0.2	0.3	0.02	0.1	0.2	0.1
8	Guanentá Alto Río Fonce	0.1	0.1	0.0	1.2	3.9	2.8	6.2	16.7	10.5
9	Macuira	0.4	1.2	0.9	5.1	14.9	9.8	7.5	4.9	-2.7
10	Los Nevados	3.2	4.7	1.4	14.8	16.4	1.6	3.4	3.8	0.5
11	Plantas Medicinales Orito Ingi-Ande	0	0	0.0	0.1	0.1	-0.02	2.1	3.7	1.6
12	Cueva De Los Guácharos	0.01	0	-0.01	0.3	0.03	-0.3	2.1	0.7	-1.4
13	Otún Quimbaya	0	0	0.0	0.03	0.02	-0.01	0.02	0.004	-0.01
14	El Cocuy	3.8	2.0	-1.9	38.2	15.3	-22.8	35.3	23.7	-11.6
15	Sierra De La Macarena	1.4	1.1	-0.2	12.2	15.5	3.3	59.6	35.5	-24.1
16	Tinigua	0.001	0.1	0.1	1.7	2.7	1.0	5.1	7.0	1.8
17	Catatumbo Barí	0.2	0.3	0.2	2.5	3.0	0.4	4.5	4.9	0.3
18	Alto Fragua Indi Wasi	0	0	0	0.01	0.004	-0.01	0.5	0.2	-0.4
19	Las Hermosas	2.3	3.1	0.8	7.0	15.7	8.7	14.1	10.8	-3.3
20	Cordillera De Los Picachos	0.05	0.04	-0.01	6.3	3.4	-2.9	19.7	22.3	2.6
21	Sumapaz	9.3	9.4	0.1	19.3	23.7	4.5	11.1	13.5	2.4
22	Utría	0	0	0	0	0	0	0.05	0.01	-0.04
23	Paramillo	0.3	0.4	0.1	0.8	0.8	0.01	10.1	11.2	1.1
24	Los Katíos	0.004	0	-0.004	0.5	0.6	0.05	2.4	1.2	-1.2
25	Nevado Del Huila	2.2	2.0	-0.2	10.9	8.5	-2.4	32.6	24.1	-8.5
26	Serranía De Chiribiquete	3.1	9.4	6.3	30.0	89.5	59.4	44.9	112.2	67.3
27	Puracé	0.6	0.3	-0.3	9.4	8.8	-0.6	11.4	9.2	-2.3
28	Tayrona	0.8	1.5	0.7	11.5	9.9	-1.7	6.9	4.2	-2.7
29	Complejo Volcánico Dona Juana Cascabel	0.4	0.4	-0.1	1.8	2.8	1.0	9.5	14.0	4.4
30	Iguaque	0.6	1.5	0.9	12.4	11.9	-0.6	16.1	15.1	-0.9
31	Ciénaga Grande De Santa Marta	1.0	1.2	0.3	59.2	41.4	-17.8	34.2	26.7	-7.5
32	Los Colorados	0	0	0	0.02	0.2	0.1	0.6	1.1	0.5
33	El Corchal El Mono Hernández	0.8	0.6	-0.1	13.4	8.8	-4.7	9.2	7.9	-1.2
34	Serranía De Los Churumbelos Auka Wasi	0	0	0	0.4	0.03	-0.4	0.4	0.1	-0.3
35	Cahuinarí	0.002	0.01	0.01	0.03	0.1	0.1	0.003	0	-0.003
36	Tatamá	0.1	0.1	-0.04	0.02	0.01	-0.01	0.7	0.2	-0.4
38	Galeras	0.1	0.1	-0.02	5.7	7.8	2.1	16.8	16.7	-0.1
39	Los Flamencos	0.2	0.8	0.7	0.4	1.2	0.8	1.4	2.7	1.3
40	Isla De Salamanca	2.9	3.0	0.1	16.0	21.2	5.2	22.3	16.4	-5.9
41	Pisba	4.5	3.2	-1.3	18.3	18.9	0.6	38.8	38.2	-0.6
42	Farallones De Cali	0.1	0.1	-0.02	10.7	9.2	-1.5	8.1	5.8	-2.3

43	Chingaza	5.0	2.0	-3.0	7.9	3.7	-4.2	19.1	16.3	-2.7
44	Los Estoraques	0.3	0.2	-0.2	19.6	7.5	-12.0	42.1	14.9	-27.1
45	Munchique	0	0.004	0.004	0.3	0.2	-0.1	3.3	2.1	-1.2
46	Selva De Florencia	0	0.005	0.01	0.2	0.2	0.01	0.9	1.0	0.1
47	La Paya	1.0	1.4	0.4	2.1	2.1	-0.01	1.0	0.6	-0.4
48	El Tuparro	29.8	146.5	116.6	86.0	138.1	52.1	77.2	117.4	40.2
49	Tamá	0.02	0.01	-0.01	0.4	0.4	0.02	2.7	2.4	-0.3
50	Las Orquídeas	0.004	0.002	-0.003	0.12	0.1	-0.01	0.7	1.0	0.3
51	Nukak	0.7	0.3	-0.4	0.14	0.3	0.1	0.1	0.1	-0.04
	Total	98.0	290.8	192.9	477.0	629.5	152.5	640.9	679.1	38.2

Table S7. Area of NV loss in PAs and their surrounding 10-km and 20-km buffers for 2009–2016 (t_0) and 2016–2023 (t_1).

ID	Name	Natural vegetation loss (km²)								
		PA			10-km buffer			20-km buffer		
		t_0	t_1	t_1-t_0	t_0	t_1	t_1-t_0	t_0	t_1	t_1-t_0
1	Serranía De Los Yariguies	4.9	6.4	1.5	134.7	132.1	-2.6	159.7	149.3	-10.4
2	Rio Pure	5.7	7.1	1.4	3.7	2.4	-1.3	7.6	7.3	-0.3
3	Sanquianga	3.7	6.9	3.2	36.1	43.4	7.3	85.8	136.7	51.0
4	Sierra Nevada De Santa Marta	88.0	227.5	139.5	174.9	374.1	199.2	111.7	272.1	160.4
5	Puinawai	37.2	32.8	-4.5	21.7	11.0	-10.7	3.8	3.9	0.1
6	Yaigojé Apaporis	32.8	35.0	2.2	23.9	24.3	0.4	18.0	23.4	5.5
7	Amacayacu	2.0	3.5	1.5	5.9	8.8	2.9	4.9	9.2	4.4
8	Guanentá Alto Río Fonce	0.7	0.3	-0.4	18.0	14.9	-3.0	29.9	39.8	10.0
9	Macuira	6.9	5.2	-1.7	36.7	55.8	19.1	19.9	23.7	3.8
10	Los Nevados	4.9	6.4	1.5	63.9	78.2	14.3	116.1	140.9	24.7
11	Plantas Medicinales Orito Ingi-Ande	0.04	0.003	-0.03	25.0	22.5	-2.5	75.7	84.8	9.2
12	Cueva De Los Guácharos	0.1	0.2	0.02	8.9	8.9	0.04	20.6	23.8	3.2
13	Otún Quimbaya	0.1	0.1	0.03	9.7	16.1	6.4	37.4	37.1	-0.3
14	El Cocuy	11.5	10.5	-1.0	85.1	55.7	-29.4	97.8	77.9	-19.9
15	Sierra De La Macarena	133.5	355.7	222.2	450.7	949.6	498.9	355.8	506.5	150.7
16	Tinigua	112.6	559.5	446.8	130.7	325.6	194.9	98.8	205.2	106.4
17	Catatumbo Barí	51.8	50.8	-1.0	178.6	201.4	22.8	234.7	286.5	51.8
18	Alto Fragua Indi Wasi	7.3	13.6	6.3	70.7	82.6	11.8	62.9	80.9	18.0
19	Las Hermosas	7.6	11.2	3.5	57.5	57.3	-0.2	58.8	39.1	-19.7
20	Cordillera De Los Picachos	32.2	105.4	73.1	69.7	277.0	207.3	92.4	238.0	145.6
21	Sumapaz	12.8	13.8	1.0	108.3	128.1	19.8	141.5	154.4	12.9
22	Utría	3.0	2.1	-0.9	13.6	15.4	1.8	12.5	11.6	-0.8
23	Paramillo	205.1	287.5	82.4	310.1	409.2	99.0	252.7	248.8	-3.9
24	Los Katíos	1.1	2.0	0.9	31.8	33.2	1.3	51.0	41.9	-9.1
25	Nevado Del Huila	5.0	6.7	1.7	82.9	76.8	-6.1	97.4	79.8	-17.6
26	Serranía De Chiribiquete	9.8	100.8	91.0	202.7	879.1	676.4	269.7	811.7	541.9
27	Puracé	1.9	0.9	-1.0	53.3	40.7	-12.6	137.7	90.7	-47.0
28	Tayrona	3.7	9.0	5.3	30.6	39.7	9.2	10.5	13.7	3.2
29	Complejo Volcánico Dona Juana Cascabel	4.8	4.5	-0.3	75.5	53.4	-22.1	119.5	79.7	-39.8
30	Iguaque	1.2	1.7	0.4	18.8	15.8	-3.0	35.2	25.6	-9.6
31	Ciénaga Grande De Santa Marta	1.0	1.3	0.3	66.3	53.9	-12.4	38.5	41.8	3.2
32	Los Colorados	0.9	0.5	-0.3	53.4	46.4	-7.0	115.5	92.4	-23.2
33	El Corchal El Mono Hernández	0.8	1.0	0.2	28.2	19.9	-8.3	40.7	40.5	-0.2
34	Serranía De Los Churumbelos Auka Wasi	7.7	9.6	1.9	107.4	108.9	1.4	130.6	144.1	13.5
35	Cahuinarí	0.6	2.2	1.6	4.2	3.6	-0.6	3.3	1.3	-2.0
36	Tatamá	5.8	12.2	6.4	54.7	70.3	15.6	68.3	68.3	0.02
38	Galeras	2.2	1.7	-0.4	37.0	28.9	-8.1	80.4	64.6	-15.8
39	Los Flamencos	4.2	3.3	-0.9	29.1	29.5	0.5	49.4	52.8	3.4
40	Isla De Salamanca	3.0	3.0	0.1	24.9	26.6	1.7	38.5	33.9	-4.6
41	Pisba	10.6	9.6	-1.0	49.3	45.1	-4.2	72.5	65.7	-6.8
42	Farallones De Cali	11.3	19.6	8.3	71.0	81.8	10.8	48.5	60.0	11.5
43	Chingaza	26.2	9.8	-16.4	102.5	70.6	-31.9	113.3	101.3	-12.1

44	Los Estoraques	0.4	0.2	-0.2	35.3	16.6	-18.7	84.5	45.2	-39.3
45	Munchique	6.2	12.6	6.4	52.9	84.7	31.8	72.5	113.7	41.2
46	Selva De Florencia	7.4	10.7	3.3	60.1	76.1	16.0	92.1	102.4	10.4
47	La Paya	61.7	64.8	3.1	211.8	187.0	-24.8	204.8	156.8	-48.0
48	El Tuparro	33.6	179.7	146.0	94.3	166.9	72.6	84.2	140.4	56.2
49	Tamá	5.9	4.3	-1.7	19.8	12.9	-7.0	25.4	20.1	-5.3
50	Las Orquídeas	10.3	13.2	2.9	37.3	60.9	23.6	48.5	90.8	42.3
51	Nukak	44.4	48.7	4.3	44.3	107.6	63.3	68.4	157.6	89.1
	Total	1036.1	2274.9	1238.8	3717.4	5731.5	2014.1	4299.9	5537.9	1238.0

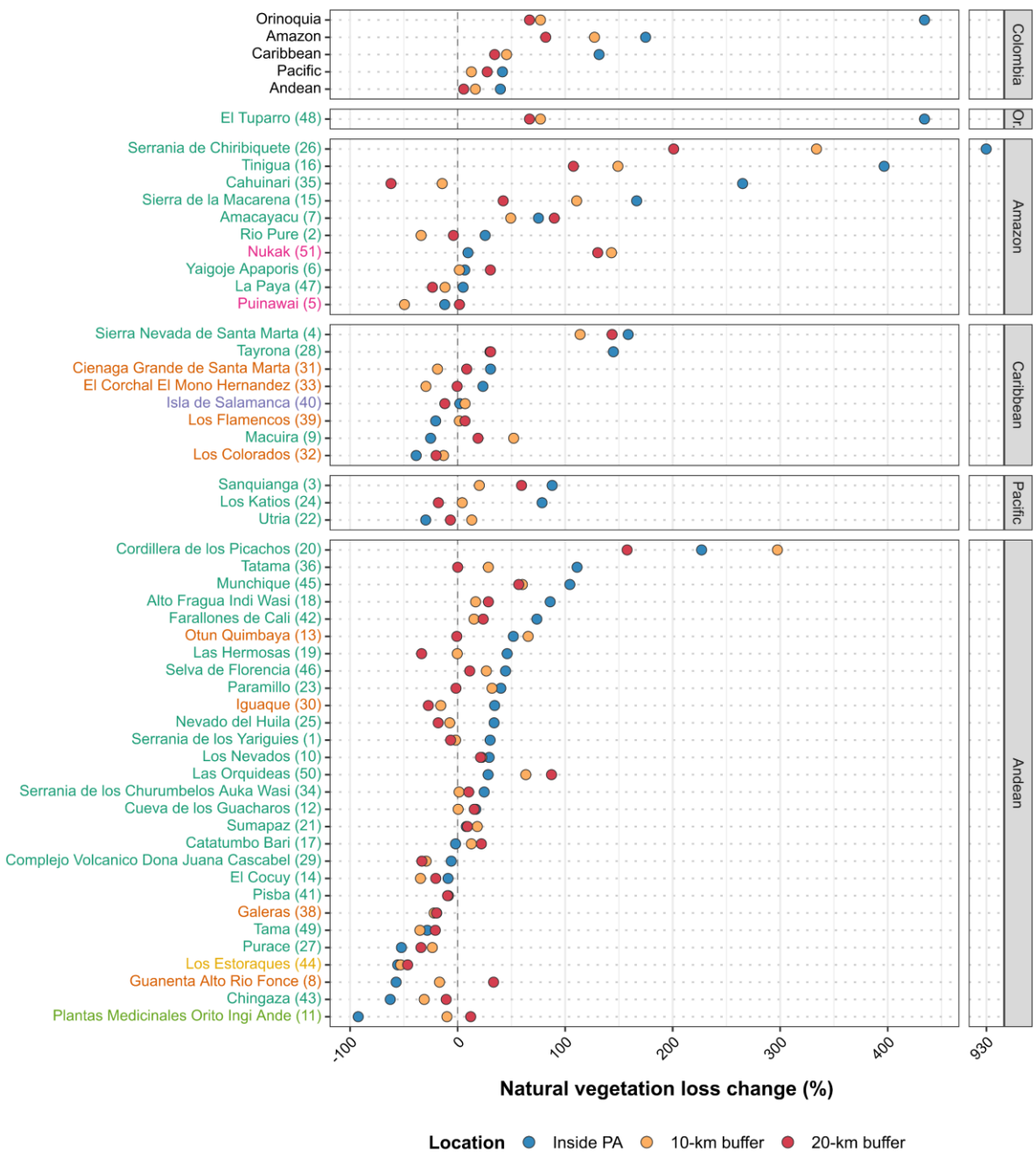

Figure S3. NV loss change (%) between the 2009–2016 and 2016–2023 periods in PAs and their surrounding 10-km and 20-km buffers. The first panel shows aggregated values by biogeographical region (Or = Orinoquia), while subsequent panels present percentage change by individual PA grouped by biogeographical region. PAs are sorted decreasingly by NV loss change inside them. Labels are colored according to SINAP category, with numbers in parentheses indicating PA IDs (see Table S1).

Table S8. Extended results of landscape connectivity analysis at overall scale using *d* = 10 km.

Year	Landscape area (km^2)	Habitat area (km^2)	ECA (km^2)	Normalized ECA (% of LA)	Normalized ECA (% of habitat area)	dA (%)	dECA (%)	rECA
Protected areas								
2009	144,023	139,553	139,397	96.8	99.9	-3.1	-3.2	1.0
2016	144,023	139,236	138,994	96.5	99.8	-0.2	-0.3	1.3
2023	144,023	137,848	137,709	95.6	99.9	-1.0	-0.9	0.9
10-km buffers								
2009	110,346	87,412	86,041	78.0	98.4	-20.8	-22.0	1.1
2016	110,346	86,554	85,152	77.2	98.4	-1.0	-1.0	1.1
2023	110,346	83,537	81,516	73.9	97.6	-3.5	-4.3	1.2
20-km buffers								
2009	111,006	77,568	74,448	67.1	96.0	-30.1	-32.9	1.1
2016	111,006	76,513	72,742	65.5	95.1	-1.4	-2.3	1.7
2023	111,006	74,095	68,386	61.6	92.3	-3.2	-6.0	1.9

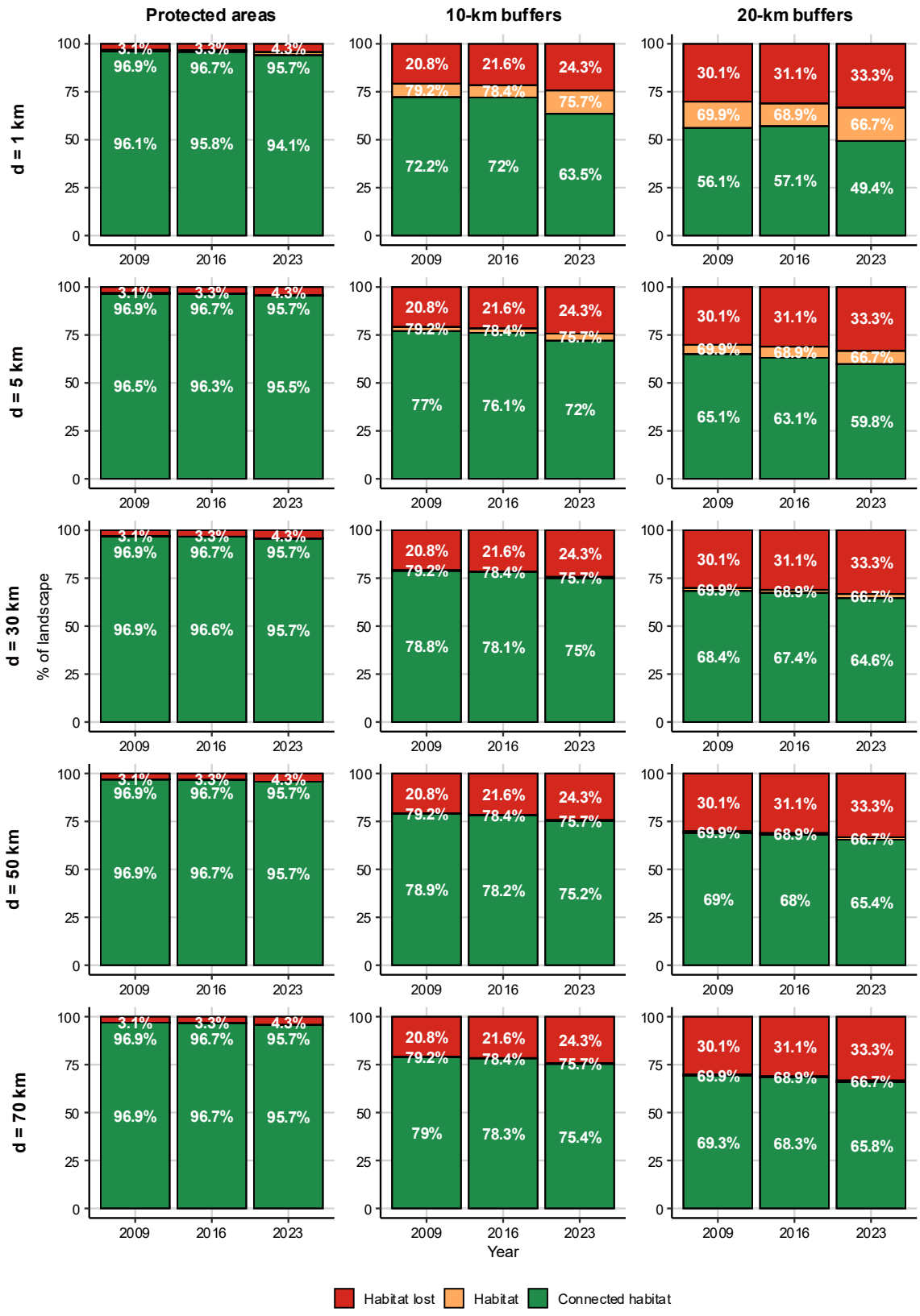

Figure S4. Changes in habitat and connected habitat for 2009, 2016, and 2023 in PAs, and in their surrounding 10-km and 20-km buffers using alternative dispersal distances (d). Values are expressed as the percentage of total landscape area.

Table S9. Changes in ECA in area units for 2009–2016 (t_0) and 2016–2023 (t_1) periods in PAs and in their surrounding 10-km and 20-km buffers.

ID	Name	ECA (km²)								
		PA			10-km buffer			20-km buffer		
		t_0	t_1	t_1-t_0	t_0	t_1	t_1-t_0	t_0	t_1	t_1-t_0
1	Serranía De Los Yariguies	0.9	-3.4	-4.3	-35.7	-61.2	-25.6	-90.8	-75.5	15.3
2	Rio Pure	2.1	-1.2	-3.3	-1.4	0.3	1.7	-4.7	-2.3	2.4
3	Sanquianga	12.4	-5.6	-18.0	15.8	-58.2	-73.9	-22.4	-109.8	-87.4
4	Sierra Nevada De Santa Marta	-49.4	-178.1	-128.7	-35.3	-256.7	-221.4	-5.8	-157.1	-151.2
5	Puinawai	-13.2	18.3	31.5	-15.0	3.8	18.8	-6.9	-1.0	6.0
6	Yaigojé Apaporis	-13.8	10.4	24.2	-344.8	329.8	674.6	-54.0	41.1	95.1
7	Amacayacu	-0.1	-2.1	-2.0	4.3	-0.8	-5.0	-6.8	3.3	10.1
8	Guanentá Alto Río Fonce	-0.2	0.1	0.3	4.0	-0.7	-4.7	21.3	-17.8	-39.1
9	Macuira	-1.6	-0.9	0.7	10.7	-11.3	-22.0	-9.6	13.4	23.0
10	Los Nevados	-3.5	5.9	9.4	9.6	18.2	8.6	23.4	-5.6	-28.9
11	Plantas Medicinales Orito Ingi-Ande	0.03	0.1	0.02	-18.0	-8.3	9.7	-51.7	-38.4	13.3
12	Cueva De Los Guácharos	0.1	-0.05	-0.2	0.5	-1.1	-1.6	2.6	-5.8	-8.4
13	Otún Quimbaya	0.2	-0.1	-0.3	10.8	-7.7	-18.5	-3.9	-17.4	-13.5
14	El Cocuy	-19.5	13.4	32.9	-32.3	42.8	75.1	-31.4	-167.4	-136.0
15	Sierra De La Macarena	-52.2	-314.0	-261.8	-310.3	-919.2	-608.9	-133.4	-366.8	-233.4
16	Tinigua	-101.3	-556.3	-455.1	-112.5	-324.6	-212.0	-68.4	-218.8	-150.4
17	Catatumbo Barí	-9.0	-23.1	-14.1	-34.7	73.4	108.1	-139.7	-143.0	-3.3
18	Alto Fragua Indi Wasi	0.9	-9.3	-10.2	-6.4	-42.0	-35.6	7.0	-4.8	-11.8
19	Las Hermosas	5.5	1.6	-4.0	1.9	28.2	26.3	-15.3	52.3	67.6
20	Cordillera De Los Picachos	-19.9	-99.5	-79.5	-18.1	-237.3	-219.2	-19.1	-190.7	-171.5
21	Sumapaz	1.1	-3.8	-4.9	-13.4	-39.6	-26.1	-50.3	-13.7	36.6
22	Utría	0.2	1.3	1.1	8.8	-0.02	-8.9	4.9	3.1	-1.8
23	Paramillo	24.7	-79.8	-104.5	28.2	-131.1	-159.3	191.9	-80.9	-272.8
24	Los Katíos	-1.0	-0.8	0.3	-13.6	-14.3	-0.6	-55.7	10.8	66.5
25	Nevado Del Huila	-0.2	1.5	1.8	8.5	7.0	-1.4	-12.6	22.5	35.1
26	Serranía De Chiribiquete	1.9	-86.0	-88.0	-187.3	-943.6	-756.3	-159.6	-820.8	-661.2
27	Puracé	-0.3	1.4	1.7	-11.3	12.6	23.9	-69.1	13.8	82.9
28	Tayrona	1.4	-6.6	-8.0	-2.9	-26.2	-23.2	-0.8	-8.0	-7.2
29	Complejo Volcánico Dona Juana Cascabel	-2.7	0.8	3.6	-38.6	12.0	50.5	-85.4	23.6	108.9
30	Iguaque	1.5	-0.3	-1.8	0.8	3.2	2.4	18.0	-15.2	-33.2
31	Ciénaga Grande De Santa Marta	-6.1	22.9	29.0	3.0	43.6	40.6	14.8	12.5	-2.2
32	Los Colorados	-0.3	0.4	0.6	-7.7	6.7	14.3	-17.2	25.4	42.6
33	El Corchal El Mono Hernández	-0.5	0.2	0.8	-10.7	11.2	21.9	-1.7	-11.3	-9.7
34	Serranía De Los Churumbelos Auka Wasi	-3.4	-4.4	-0.9	-49.3	-59.5	-10.2	-61.5	-61.4	0.1
35	Cahuinarí	-50.6	57.2	107.8	1.0	0.1	-0.9	-38.3	-9.7	28.6
36	Tatamá	4.4	-4.9	-9.4	28.4	-10.9	-39.3	15.1	4.0	-11.1
38	Galeras	0.2	1.9	1.7	-5.4	16.5	21.9	-7.4	18.4	25.8
39	Los Flamencos	5.4	2.3	-3.1	29.7	17.1	-12.6	13.8	6.6	-7.2
40	Isla De Salamanca	-12.7	26.8	39.6	7.8	34.9	27.1	-6.3	-1.3	4.9
41	Pisba	9.1	-0.9	-10.0	22.1	3.8	-18.3	7.2	0.3	-6.9
42	Farallones De Cali	7.0	-11.3	-18.2	-11.7	-48.1	-36.5	-25.5	-150.2	-124.7

43	Chingaza	-4.0	12.2	16.2	-1.0	25.4	26.5	45.7	45.7	0.04
44	Los Estoraques	-0.1	0.7	0.8	-17.1	21.0	38.1	-49.3	43.1	92.4
45	Munchique	-1.2	-9.7	-8.5	-8.6	-56.4	-47.8	-22.0	-91.8	-69.9
46	Selva De Florencia	0.8	0.4	-0.5	17.9	-11.0	-28.9	8.0	-10.0	-18.0
47	La Paya	-48.1	-46.6	1.5	-170.0	-136.9	33.1	-200.8	-170.6	30.2
48	El Tuparro	-26.5	-26.7	-0.2	-54.7	5.7	60.4	-33.1	-2.4	30.6
49	Tamá	-2.2	-0.8	1.3	-6.7	-2.2	4.5	1.8	5.5	3.7
50	Las Orquídeas	1.4	-3.7	-5.1	33.1	-29.6	-62.7	93.4	-49.9	-143.3
51	Nukak	-6.1	-13.9	-7.8	21.2	-81.8	-103.0	3.7	-154.4	-158.1

Table S10. Changes in ECA (dECA) for 2009–2016 (t_0) and 2016–2023 (t_1) periods in PAs and in their surrounding 10-km and 20-km buffers.

ID	Name	dECA (%)								
		PA			10-km buffer			20-km buffer		
		t_0	t_1	t_1-t_0	t_0	t_1	t_1-t_0	t_0	t_1	t_1-t_0
1	Serranía De Los Yariguies	0.2	-0.6	-0.7	-3.5	-6.3	-2.8	-9.1	-8.3	0.8
2	Rio Pure	0.02	-0.01	-0.03	-0.04	0.01	0.05	-0.2	-0.1	0.1
3	Sanquianga	2.4	-1.0	-3.4	2.0	-7.3	-9.3	-2.3	-11.6	-9.3
4	Sierra Nevada De Santa Marta	-1.5	-5.6	-4.1	-1.4	-10.7	-9.2	-0.4	-11.9	-11.5
5	Puinawai	-0.1	0.2	0.3	-0.3	0.1	0.4	-0.1	-0.02	0.1
6	Yaigojé Apaporis	-0.1	0.1	0.2	-6.1	6.2	12.3	-1.1	0.9	2.0
7	Amacayacu	-0.004	-0.1	-0.1	0.2	-0.03	-0.2	-0.4	0.2	0.6
8	Guanentá Alto Río Fonce	-0.2	0.1	0.3	0.8	-0.1	-0.9	3.5	-2.8	-6.3
9	Macuira	-0.7	-0.4	0.3	1.2	-1.2	-2.4	-1.3	1.9	3.2
10	Los Nevados	-0.7	1.2	1.9	0.9	1.7	0.8	3.1	-0.7	-3.8
11	Plantas Medicinales Orito Ingi-Ande	0.03	0.1	0.0	-2.3	-1.1	1.2	-4.2	-3.3	0.9
12	Cueva De Los Guácharos	0.2	-0.1	-0.2	0.5	-1.0	-1.5	2.7	-5.9	-8.7
13	Otún Quimbaya	5.1	-1.3	-6.4	13.5	-8.4	-22.0	-5.6	-26.6	-21.0
14	El Cocuy	-0.7	0.5	1.2	-1.4	1.9	3.2	-1.8	-9.8	-8.0
15	Sierra De La Macarena	-0.9	-5.4	-4.5	-10.3	-33.9	-23.6	-8.8	-26.5	-17.7
16	Tinigua	-5.2	-29.9	-24.8	-12.6	-41.5	-28.9	-11.7	-42.3	-30.6
17	Catatumbo Barí	-0.6	-1.5	-0.9	-3.0	6.6	9.7	-10.7	-12.2	-1.6
18	Alto Fragua Indi Wasi	0.1	-1.2	-1.4	-1.1	-7.6	-6.5	2.0	-1.3	-3.3
19	Las Hermosas	0.5	0.1	-0.3	0.1	1.9	1.8	-1.2	4.3	5.5
20	Cordillera De Los Picachos	-0.7	-3.6	-2.9	-1.0	-13.2	-12.2	-1.3	-12.7	-11.5
21	Sumapaz	0.1	-0.2	-0.2	-0.5	-1.6	-1.1	-2.9	-0.8	2.1
22	Utría	0.04	0.3	0.2	1.0	-0.003	-1.0	0.4	0.3	-0.2
23	Paramillo	0.5	-1.7	-2.2	1.0	-4.8	-5.8	17.0	-6.1	-23.1
24	Los Katíos	-0.1	-0.1	0.0	-1.3	-1.4	-0.1	-5.3	1.1	6.4
25	Nevado Del Huila	-0.02	0.1	0.1	0.4	0.3	-0.1	-0.9	1.7	2.6
26	Serranía De Chiribiquete	0.005	-0.2	-0.2	-1.6	-8.4	-6.8	-1.7	-8.6	-7.0
27	Puracé	-0.03	0.2	0.2	-0.7	0.7	1.4	-5.6	1.2	6.8
28	Tayrona	1.2	-5.5	-6.7	-1.2	-10.7	-9.5	-0.7	-7.6	-6.9
29	Complejo Volcánico Dona Juana Cascabel	-0.4	0.1	0.5	-3.5	1.1	4.6	-8.7	2.6	11.3
30	Iguaque	2.5	-0.4	-2.9	0.4	1.4	1.1	5.2	-4.1	-9.3
31	Ciénaga Grande De Santa Marta	-3.3	12.7	15.9	0.8	11.0	10.2	23.3	16.0	-7.3
32	Los Colorados	-3.3	4.8	8.1	-5.0	4.5	9.5	-4.6	7.1	11.7
33	El Corchal El Mono Hernández	-1.5	0.7	2.2	-5.7	6.3	12.0	-1.2	-7.9	-6.7
34	Serranía De Los Churumbelos Auka Wasi	-0.4	-0.5	-0.1	-4.4	-5.5	-1.2	-5.4	-5.7	-0.3
35	Cahuinarí	-0.9	1.1	2.0	0.03	0.004	-0.02	-1.0	-0.3	0.8
36	Tatamá	1.0	-1.1	-2.2	2.7	-1.0	-3.7	1.4	0.4	-1.0
38	Galeras	0.3	2.6	2.3	-3.7	11.6	15.3	-1.7	4.4	6.1
39	Los Flamencos	18.9	6.9	-12.0	18.7	9.0	-9.6	7.0	3.1	-3.9
40	Isla De Salamanca	-9.5	22.2	31.8	4.3	18.4	14.2	-6.1	-1.4	4.7
41	Pisba	3.7	-0.4	-4.1	2.5	0.4	-2.1	0.7	0.03	-0.7
42	Farallones De Cali	0.4	-0.6	-1.0	-0.6	-2.6	-2.0	-1.5	-9.1	-7.6

43	Chingaza	-0.5	1.7	2.2	-0.1	2.1	2.1	6.7	6.3	-0.4
44	Los Estoraques	-5.0	31.6	36.6	-6.5	8.6	15.1	-8.3	7.9	16.2
45	Munchique	-0.3	-2.1	-1.9	-0.8	-5.0	-4.3	-1.7	-7.1	-5.4
46	Selva De Florencia	0.9	0.4	-0.5	5.0	-2.9	-7.9	1.0	-1.3	-2.3
47	La Paya	-1.1	-1.1	0.02	-6.8	-5.9	0.9	-8.3	-7.6	0.6
48	El Tuparro	-0.5	-0.5	-0.01	-1.4	0.1	1.5	-0.8	-0.1	0.8
49	Tamá	-0.5	-0.2	0.3	-1.2	-0.4	0.8	0.3	1.0	0.7
50	Las Orquídeas	0.6	-1.5	-2.0	3.6	-3.1	-6.7	8.1	-4.0	-12.2
51	Nukak	-0.1	-0.2	-0.1	0.4	-1.5	-1.9	0.1	-2.9	-3.0

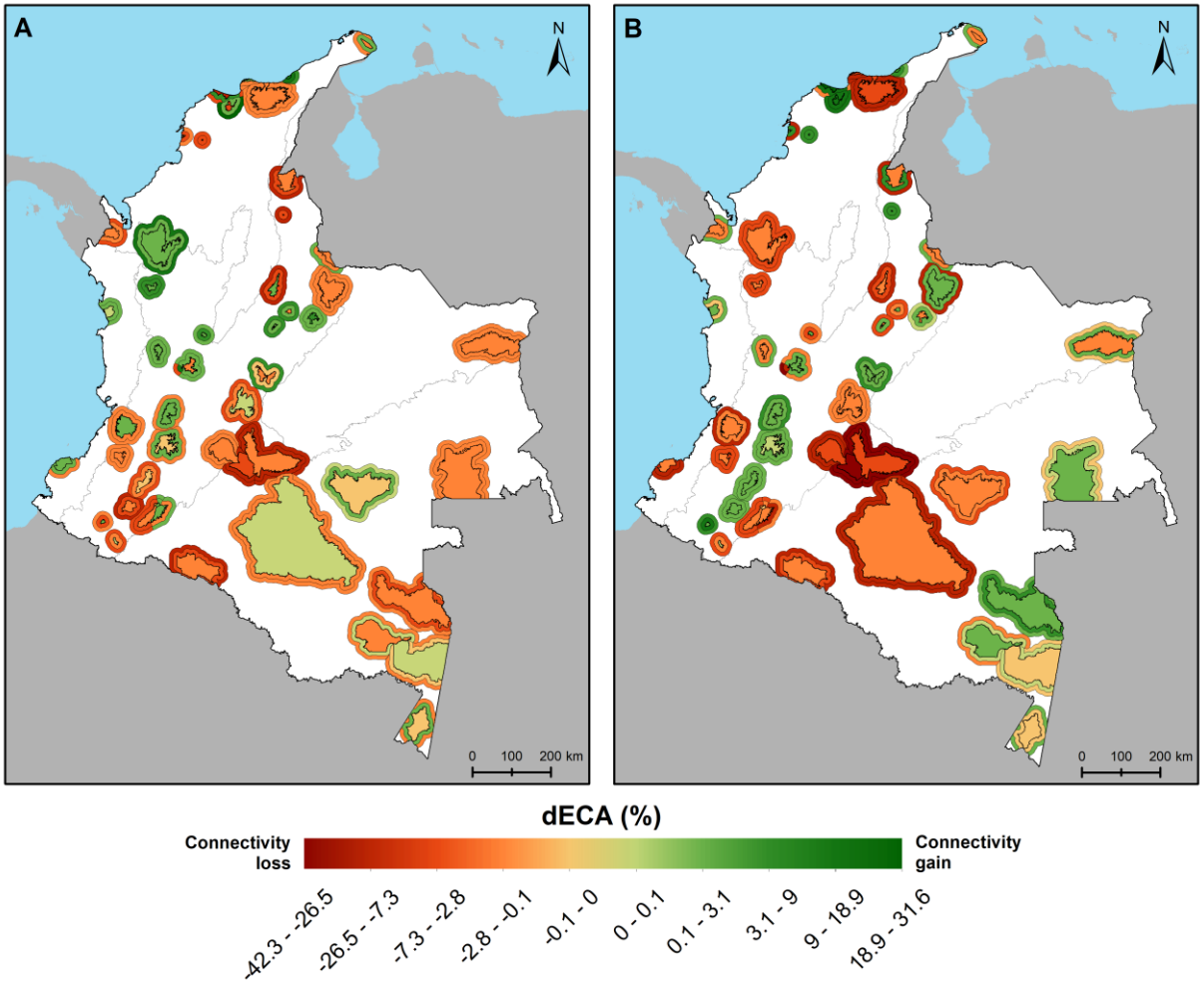

Figure S5. Spatial distribution of changes in ECA (dECA) for 2009–2016 (A) and 2016–2023 (B) across PAs and their surrounding buffers. See table S10 for detailed values.

Chapter 3

The Future of Colombian Andean Forests Under Different Deforestation Scenarios

Published in *Ecological Indicators* (2026): 183, https://doi.org/10.1016/j.ecolind.2026.114605

The Future of Colombian Andean Forests Under Different Deforestation Scenarios

Kristian Rubiano[1], Dennis Castillo Figueroa[1], Nicolás Bernal Guatibonza[1], Nicola Clerici[1,*]

[1] School of Sciences and Engineering, Universidad del Rosario, Bogotá – Colombia.
*Corresponding Author – Nicola Clerici

Abstract

Deforestation is a major environmental threat in Colombia, particularly in the Andean region, which harbors exceptional biodiversity and provides critical ecosystem services. This study assessed the projected deforestation in Colombian Andean forests under two scenarios—Business as Usual -BAU- and Governance -GOV- for the 2018–2030 and 2030–2050 periods, using spatially explicit models. Forest types were classified based on national ecosystem maps, and changes were estimated for the Andes, and within National Natural Parks. Under the BAU scenario, deforestation is widespread, especially in Basal and Fragmented forests, which by 2050 show declines of up to 8% and 5.4%, respectively. In contrast, Andean and Sub-Andean forests exhibit lower losses, though still notable over time. The GOV scenario projects significantly lower deforestation rates across all forest types and periods, with total losses remaining below 0.5%. Within protected areas, forest loss is limited (<0.8%) under all scenarios, but higher under BAU, particularly in Catatumbo Barí and Cordillera de los Picachos parks. These findings highlight contrasting futures for Andean forests depending on governance pathways. While the BAU scenario reflects continued deforestation despite protection efforts, the GOV scenario underscores the positive impact of improved institutional frameworks and land-use policies. This study emphasizes the urgent need to strengthen governance and enforcement mechanisms, even within protected areas, to safeguard Colombian biodiversity and ecosystem services. Our projections offer a valuable tool for anticipating deforestation risks and inform adaptive, regionally tailored conservation strategies in one of South America's most ecologically important regions.

Keywords

Protected areas, land cover change, spatial pattern analysis, habitat fragmentation, forest loss.

1. Introduction

Deforestation is one of the most pressing global environmental issues, with far-reaching consequences for biodiversity, climate stability, and the provision of essential ecosystem services (Brockerhoff et al., 2017; Curtis et al., 2018; Smith et al., 2023). It is estimated that about 17% of tropical moist forests have disappeared since 1990, making the tropics the most affected area by deforestation globally (Vancutsem et al., 2021). Andean forests, particularly, are unique ecosystems characterized by high biodiversity and play a crucial role in regulating climate and the hydrological cycle (Myster, 2021). They extend along the tropical Andes and include an important biodiversity hotspot, which harbors the greatest diversity and endemism of plants and vertebrate species (Myers et al., 2000; Orme et al., 2005; Mittermeier, 2011). Andean Forests also act as important sinks of aboveground carbon, estimated at 0.67 ± 0.08 Mg C ha−1 y−1 (Duque et al., 2021), having an important role in regulating and mitigating climate change (Spracklen & Righelato, 2014; Castillo-Figueroa, 2021). Similarly, around 84 million people in and around the Andes rely on water resources from forests and other Andean ecosystems (Aparecido et al., 2018; Célleri & Feyen, 2009; Carilla et al., 2023). In fact, about 40% of the South American population benefits from the ecosystem services that the tropical Andes provide (Calderón-Caro & Benavides, 2022). Nevertheless, these forests are being rapidly transformed by human activities, such as agriculture and pasture expansion, mining, and infrastructure development, threatening their integrity and functions, as well as the provision of essential ecosystem services (Hansen et al., 2013; Aide et al., 2019; Clerici, 2025).

In the case of Colombia, Andean forests have historically been subject to strong anthropogenic pressures (Etter & Van Wyngaarden, 2000; Correa Ayram et al., 2020; Etter et al., 2008; 2021). The Colombian Andes hosts some of the biggest urban settlements and the most populated region in the country (DANE, 2018), leading to a high population pressure on forests and a high demand for land, ecosystem services, and natural resources (Etter & Van Wyngaarden, 2000). As a result, drivers such as large-scale cattle ranching, agriculture, linear infrastructure development, and, more recently, mining and illegal cropping have been largely identified as direct causes of deforestation and forest degradation (Aide et al., 2019; González et al., 2018; Rodríguez Eraso et al., 2013; Etter et al., 2008; Etter & Villa, 2000). These pressures do not operate uniformly across the Andean region: previous studies have shown that their intensity and combination vary with elevation, accessibility, and proximity to the agricultural frontier, leading to highly heterogeneous patterns of forest loss and degradation along the Andean and Andean–Amazonian gradients (Etter et al., 2008; Rodríguez Eraso et al., 2013; Aide et al., 2019; González-González et al., 2021). Between 2001 and 2014, Colombia exhibited the most dynamic national patterns of Andean forest change, registering the largest gross loss of woody vegetation, particularly in the lower montane zone (1,000–1,499 m), but simultaneously experiencing extensive forest regeneration at higher elevations (>1,500 m). As a result, the overall balance was a net increase in forest cover, highlighting the contrasting and heterogeneous dynamics of land use and land cover change (LUCC) in these ecosystems. (Aide et al., 2019).

To reduce and mitigate the conversion and degradation of forests and other Andean ecosystems, several protected areas (PAs) have been declared under the System of National Natural Parks of Colombia (SPNN). Currently, nearly 17.17% of the country's terrestrial area is protected, including 61 PAs within the SPNN (IUCN categories I, II, and III), of which the Andean

region concentrates the largest number (Parques Nacionales Naturales de Colombia, 2025). At the national level, PAs have been found to reduce an average of 40% of deforestation compared to non-protected areas, with the Andes region above the national average, reaching about 60% of avoided deforestation and being the Colombian region where PAs reduced most deforestation (Negret et al., 2020). By contrast, Heino et al. (2015) found higher deforestation rates inside Andean PAs than in protected areas from any other region of Colombia. Inside the Andes, previous studies have shown deforestation rates in PAs were almost half than in their buffers, with the lowest rates in the Eastern Mountain range-Amazonia foothills and highest rates in the Western Mountain range (Rodríguez et al., 2013). Recently, rapid socioeconomic and political changes in Colombia led to increases in deforestation rates inside parks, including the ones located in the Andes, highlighting the vulnerability of these areas and the need for environmental governance to maintain socioecological equilibrium and conserve Andean forests (Clerici et al., 2020).

Ecosystems in mountain areas such as the tropical Andes are highly vulnerable to global change, especially to climate change, LUCC, and their combined effects (Nogués-Bravo et al., 2007; Pepin et al., 2015; Peters et al., 2019; Resler & Gunya, 2022; Rubiano et al., 2025; Verrall & Pickering, 2020). Also, Andean forests are particularly exposed to global change due to their sharp altitudinal and climatic gradients (Bradley et al., 2004; Alberdi Nieves 2025). Being the impacts of anthropic changes on biodiversity and ecosystem functions expected to be more severe in the future while temperatures and population growth increase, spatially explicit modeling and projections of future climate change and LUCC in the tropical Andes are needed to inform environmental policy and decision-making (Bax et al., 2021; Tovar et al., 2022). Studies have recently deepened our understanding of the potential impacts of future climate change on Andean biodiversity and ecosystem services provision (e.g., Báez et al., 2016; Buytaert et al., 2011; Diazgranados et al., 2021; Helmer et al., 2019; Rubiano et al., 2025), also as a result of the wide availability and global coverage of spatial data on projected climate change scenarios (Harris et al., 2014). In the context of tropical Andes, available data on projections of LUCC have been developed at a global scale (e.g., Chen et al., 2020; Havlík et al., 2011; Hurtt et al., 2011; Popp et al., 2014), at a national scale for Colombia (González-González et al., 2021; Linero et al., 2020), and at regional and local scales at Ecuador (Ochoa-Cueva et al., 2015; Thies et al., 2014), Peru (Bax & Francesconi, 2018), and Colombia (Clerici et al., 2019; Rodríguez Eraso et al., 2013). In the Colombian Andes, these projections have been used, for instance, to assess potential changes in the distribution of species of mammals as a consequence of habitat loss and climate change (Linero et al., 2020), to identify areas potentially threatened by deforestation (Castellanos-Mora & Agudelo-Hz, 2021), to evaluate the potential effects of deforestation on PAs (Rodríguez et al., 2013b), and to evaluate the cumulative effects of LUCC and climate change on ecosystem services (Clerici et al., 2019). Nevertheless, projections of deforestation rates in Colombian Andean forests are scarce, especially those considering ecological variability and the distinct LUCC dynamics of forest types and protected areas.

In this work, we quantify and compare projected deforestation in Colombian Andean forests across ecosystem typologies and within PAs under two contrasting deforestation scenarios (Business as Usual, BAU, and Governance, GOV) for 2030 and 2050. More specifically, we aim (i) to estimate future forest loss at regional and ecosystem-typology levels, (ii) to assess the exposure of individual PAs to these projected changes, and (iii) to discuss the implications of

these trajectories for biodiversity conservation and landscape-level governance in the Colombian Andes. We used the national-scale spatially explicit deforestation projections developed by González-González et al. (2021) for BAU and GOV scenarios, combined with the spatial distribution of ecosystems of Colombia (IDEAM et al., 2017), to estimate deforestation rates for Andean forests overall, by forest typology and for the network of PAs.

2. Materials and Methods

2.1. Data

To identify and delineate the Colombian Andes spatial boundaries, we used the Global Mountain Biodiversity Assessment (GMBA) Mountain Inventory v2.0 (Snethlage et al., 2022), which provides a hierarchical and standardized delineation of 8616 world mountain ranges based on a generalized and consistent mountain definition for a wide range of applications on global comparative mountain science (Snethlage et al., 2022). We selected from the dataset the Andean cordillera within the Colombian territory, which includes the Northern Andes and the Sierra Nevada de Santa Marta mountain range (Figure 1).

For the deforestation scenarios, we used the national-scale dataset developed by González-González et al. (2021), who generated spatially explicit projections of forest loss for Colombia under two time periods (2018–2030 and 2030–2050) and two contrasting management scenarios. The BAU scenario represents a continuation of recent deforestation dynamics, assuming constant annual deforestation rates equal to the mean rate observed during 2013–2018 in each biogeographical region, with forest loss allowed both inside and outside protected areas. In contrast, the GOV scenario represents an enhanced-governance pathway consistent with Colombia's deforestation-reduction commitments: the same spatial structure of deforestation drivers is retained, but annual deforestation rates are reduced by 30% for 2018–2030 and by 50% for 2030–2050 relative to the 2013–2018 mean. In the modeling framework, governance is therefore not a generic institutional concept but a policy-based scenario that assumes strengthened enforcement of national environmental legislation and the implementation of Colombia's National Agricultural Frontier (NAF). Operationally, this is reflected in constraining regional deforestation rates to match the reductions pledged under the Paris Climate Agreement and related national climate policies, and assigning stronger protection to legally excluded areas and non-protected forests, while concentrating higher deforestation probabilities within the NAF (González-González et al., 2021; LEY 1844, 2017; UNFCCC, 2015). A detailed summary of the socio-political meaning of each scenario and the region-specific transition rates used in BAU and GOV is provided in Table S1.

The scenarios dataset was produced using as a base product the Hansen Global Forest Change database v.1.6 (Hansen et al., 2013) to derive forest cover and forest loss extension during 2001–2013 and 2001–2018. These two historical windows were used in González-González et al. (2021) to reconstruct forest cover maps for 2013 and 2018 from a common 2001 baseline and to quantify the forest loss that occurred during 2013–2018 in each biogeographical region. The 2013–2018 forest loss was then used to estimate mean annual deforestation rates and to calibrate the spatially explicit deforestation model in Dinamica EGO, which provided the region-specific transition rates that underpin the BAU and GOV scenarios. In the analyses, the 2018

forest map constitutes the baseline from which future forest loss is simulated for the periods 2018–2030 and 2030–2050 under both scenarios.

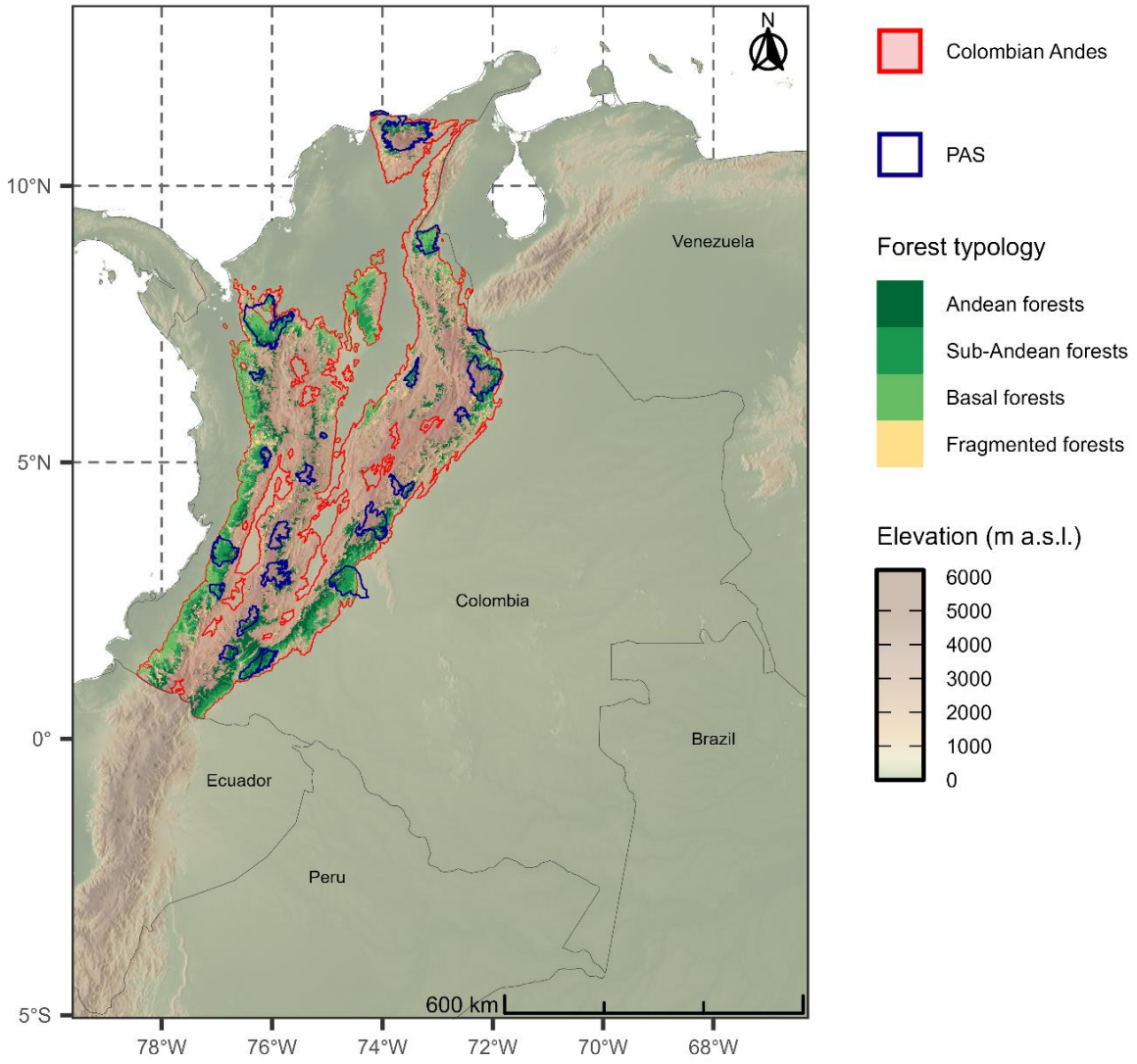

Figure 1. Location of the Andes and Sierra Nevada de Santa Marta in Colombia, showing the Andean national natural parks (NNPs) selected for analysis and the distribution of the four Andean general forest typologies as of 2018. Elevation data were obtained from the *elevatr* R package (Hollister et al., 2023).

The simulations of deforestation scenarios considered eleven spatially explicit variables representing potential drivers of deforestation in Colombia, according to the literature, from four general categories: ecological and geomorphological attributes, infrastructure, protected areas, and internal conflict. A variable-by-variable description, including data source, spatial resolution and conceptual justification, is provided in Table S2. According to González-González et al. (2021) these eleven variables were test by independence using the standard Cramér's V and the Joint Information Uncertainty diagnostics, satisfying the independence assumption required for analyses (Cramér's V < 0.5). The simulations of deforestation scenarios were performed in the Dinamica EGO platform, which focuses on cellular automata rules (Soares-Filho et al., 2009).

Additionally, to the deforestation scenarios layers, we also considered the extension of forests for the year 2018 as a time baseline, also provided by González-González et al. (2021). All forest layers have a spatial resolution of 1 km2.

To derive statistics of forest extension by forest typologies from the 2018 baseline and the different deforestation scenarios, we used the classification of the Map of Continental, Coastal and Marine Ecosystems of Colombia (IDEAM et al., 2017). We overlapped the map with the Colombian Andes boundaries and filtered for forest ecosystems, which led to the selection of 15 forest typologies, later aggregated into four general forest typologies based on transformation and elevation criteria, namely: Andean forests, Sub-Andean forests, Basal forests, and Fragmented forests (Table 1).

Table 1. Forest typologies considered in this study and classification criteria.

Forest typology*	General forest typology	Transformation category	Classification criteria	Elevation (m a.s.l.)
Humid Andean forests Dry Andean forests Flooded Andean forests	Andean forests	Natural	Elevation	1800 - 3700
Humid Sub-Andean forests Dry Sub-Andean forests Flooded Sub-Andean forests	Sub-Andean forests	Natural	Elevation	800 - 1800
Humid Basal forests Dry Basal forests Flooded Basal forests Humid Riparian forests Dry Riparian forests Flooded Riparian forests Flooded Coastal forests	Basal forests	Natural	Elevation	< 800
Fragmented forest with pastures and crops Fragmented forest with secondary vegetation	Fragmented forests	Transformed	Transformation category	< 3700

* According to IDEAM et al. (2017).

In IDEAM et al. (2017) the Andean Forests typology is located at an altitudinal range from 1800 to 3700 m a.s.l., with an annual average temperature ranging between 6°C to 18°C. It can be further classified into three subclasses: Humid, Dry and Flooded Andean forests. Here Lauraceae, Melastomataceae and Rubiaceae are the dominant plant families. Sub-Andean forests are distributed at an altitudinal range between 800 and 1800 m a.s.l., with annual average temperatures between 18°C and 24°C, approximately; the most diverse plant family in this forest typology is Fabaceae. Basal forests are found in an altitudinal range between 0 and 800 m a.s.l. (IDEAM et al., 2017); depending on the precipitation regime they can be further classified as Humid or Dry Basal forests. In Colombia, they are distributed in the Amazon, Pacific, Orinoquia and the Caribbean regions, with a small presence in the low Andes. They are represented by several subcategories, including flooded and riparian forests (Table 1). Fragmented forests

include several forest types, often characterized by patches of secondary vegetation established within a matrix of crops and pastures.

Finally, to derive statistics at the Protected Areas level, we obtained PAs boundaries in vector format from the Colombian National Natural Parks institution (PNNC, 2023). We filtered PAs from the National Natural Park (NNP; IUCN category II) category that intersects for at least 50% of the Colombian Andes spatial boundaries. As a result, 24 PAs were selected for the analysis (Figure 1).

2.2. Statistics extraction

The deforestation scenarios allowed us to derive an estimate of the future extension of the four different forest typologies by i) considering the Colombian Andes as a whole, and ii) inside the 24 PAs considered. Specifically, statistics were extracted for the 2018 baseline forest map, and the 2018-2030 and 2030-2050 BAU and GOV deforestation scenarios. Forest extensions were extracted considering the forest areas of every typology overlapped by the Colombian Andes and the PAs boundaries. Rates of forest loss were derived with respect to the 2018 and 2030 forest cover area, as follows (Puyravaud, 2003):

$$R = \left(\frac{A_{t1} - A_{t2}}{A_{t1}}\right) * 100$$

where A_{t1} and A_{t2} are the forest cover areas at years 1 and 2, respectively. All operations were performed in ArcGIS® 10.8.2.

3. Results

3.1. Deforestation scenarios of Andean forests

The limits of the Colombian Andes considered here enclose a surface of 28’597’897 ha. Within these boundaries, the extension of forests in 2018 was 9’047’524 ha. More than half of these are Sub-Andean and Andean forests (65.2%), followed by Basal forests (22%) and 12.8% Fragmented forests (Table 2).

In the BAU scenario for the 2018-2030 period, the overall extension of forests in the Andes is 8’927’381 ha, which corresponds to a decrease of 1.3% with respect to baseline year 2018. The most affected forest type in terms of proportions is Basal forest, with a 3.2% decrease (a loss of 63’064 ha; Table 2), followed by Fragmented forest, with a 2.5% decrease (a loss of 29’311 ha; Table 2). The coverages least affected by deforestation are the Andean forest and the sub-Andean forest, showing a decrease of 0.08% and 0.9% respectively (a loss of 2’439 ha for the Andean forest and 25’328 ha for the sub-Andean forest).

Table 2. Forest cover by general forest typology in year 2018, projected area and rate of forest loss (*R*) in the four different deforestation scenarios.

Forest typology	Forest cover 2018 (ha)	BAU				GOV			
		2018-2030		2030-2050		2018-2030		2030-2050	
		Forest loss (ha)	*R*	Forest loss (ha)	*R*	Forest loss (ha)	*R*	Forest loss (ha)	*R*
Basal forests	1,989,114	63,064	3.17	154,733	8.03	6,192	0.31	37,451	1.89
Sub-Andean forests	2,890,186	25,329	0.88	138,816	4.85	1,490	0.05	13,445	0.47
Andean forests	3,009,518	2,439	0.08	6,325	0.21	3	0.00	284	0.01
Fragmented forests	1,158,705	29,311	2.53	60,800	5.38	2,663	0.23	17,645	1.53
Overall	9,047,524	120,143	1.33	360,673	4.04	10,347	0.11	68,826	0.76

For the same period 2018-2030 but in the GOV scenario, the total extension of forest in the Andes is projected at 9’037’177 ha, which corresponds to a decrease of 0.1% with respect to the 2018 baseline. Also in this case, the most affected forest type in terms of proportions is Basal forest, with a 0.31% decrease (a loss of 6’192 ha), followed by Fragmented forest, with a 0.23% decrease (a loss of 2’663 ha; Table 2). As in the previous scenario, the coverages that were least affected by deforestation were the Andean Forest and the Sub-Andean forest. However, for the case of this scenario, the decrease was 8.69E-05% and 0.05% respectively (a loss of 3 ha for the Andean Forest and 1’490 ha for the Sub-Andean forest).

In the BAU scenario for the 2030-2050 period, the overall extension of forests in the Andes is 8’566’708 ha, which corresponds to a decrease of 4% with respect to 2030. Again, the most affected forest type in terms of proportions are Basal forests, with an 8% decrease, followed by Fragmented forest, with a 5.4% decrease, corresponding to a loss of 154’733 ha and 60’800 ha, respectively. In the case of the coverages with the lowest percentage of forest decrease, there is the Andean forest with 0.2% which represents a loss of 6’325 ha, followed by the Sub-Andean forest with a decrease of 4.85% representing a loss of 138’816 ha.

Finally, in the GOV scenario for the 2030-2050 period, the overall extension of forests in the Andes is 8’968’351 ha, which corresponds to a decrease of 0.11% with respect to 2030. Basal forests are the most affected forest type in terms of proportions with a 1.9% decrease, followed by Fragmented forest, with a 1.5% decrease, a loss of 37’451 ha and 17’645 ha, respectively. The coverages least affected by deforestation are the Andean forest and the Sub-Andean forest, showing a decrease of 0.01% and 0.47% respectively (a loss of 284 ha for the Andean forest and 13’445 ha for the Sub-Andean forest).

Forest loss in the BAU scenario is concentrated in the northern portions of the western and central mountain ranges (Figure 2A). In particular, Basal and Sub-Andean forests near the San Lucas mountain range and its surrounding areas are the most affected. Additional areas of high forest loss are found in the Catatumbo region and in the southern part of the Cordillera de los Picachos NNP in the eastern mountain range. Under the GOV scenario, the most significant

forest loss is also observed in the northern portions of the western and central mountain ranges (Figure 2B). The spatial configuration of current forest cover and projected deforestation for each forest typology under the BAU and GOV scenarios is shown in Supplementary Figures S1 and S2, respectively.

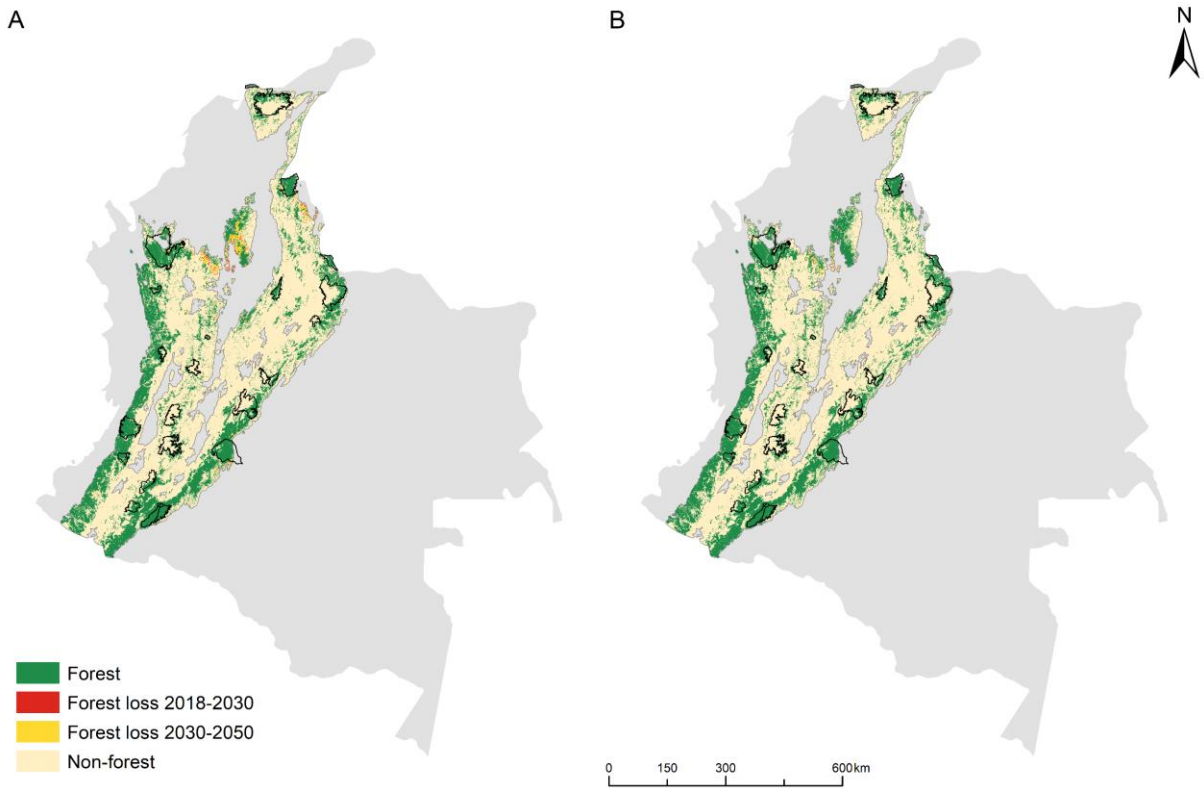

Figure 2. Maps showing the location of Andean forest loss by scenario and analysis period: (a) business as usual (BAU) scenario, and (b) governance (GOV) scenario, for the periods 2018–2030 and 2030–2050.

3.2. Deforestation scenarios within Andean PAs

We analyzed 24 protected areas in the Colombian Andes, all belonging to the National Natural Parks (NNP) conservation category. Within these PAs, the extension of forests in 2018 was 1'718'866 ha. Here, less than 0.8% of protected forest cover is lost in any of the four scenarios. BAU scenarios are the only ones that present rates of forest loss greater than 1% in any PA.

In the BAU scenario for the 2018-2030 period, the most affected park in terms of proportions is NNP Catatumbo Bari, with a 1.5% loss, followed by NNP Cordillera de los Picachos, with a 0.4% decrease (Table 3). In the BAU scenario for the 2030-2050 period, the same parks were the most affected but with a higher percentage of loss: Catatumbo Bari, with a 2.6% loss, and Cordillera de los Picachos, with a 1.7% loss. During this period, NNP Paramillo also reaches a 1.7% loss. Parks location is reported in Figure S3.

For the GOV scenario, it is evident that there was no decrease in forest in any of the 24 PAs greater than 0.1% from 2018 to 2030 (Figure 2b). However, for the period from 2030 to 2050, a decrease in forests is observed in some of them. Paramillo is the park with the highest

percentage of forest loss, with 0.32%, followed by Cordillera De Los Picachos and Catatumbo Bari, with 0.04% and 0.03%, respectively.

Table 3. Forest loss statistics for 24 National Natural Parks (NNPs), based on the Global Forest Change dataset (version 1.6) by Hansen et al. (2013). BAU refers to the Business as Usual scenario, while GOV represents the Governance scenario. *R* is the rate of forest loss.

Protected area	Forest cover 2018 (ha)	BAU				GOV			
		2018-2030		2030-2050		2018-2030		2030-2050	
		Forest loss (ha)	*R*	Forest loss (ha)	*R*	Forest loss (ha)	*R*	Forest loss (ha)	*R*
Alto Fragua - Indi Wasi	73,511	0	0	37	0.05	0	0	2	0
Catatumbo Bari	132,523	2,018	1.52	3,396	2.60	0	0	39	0.03
Chingaza	25,559	0	0	0	0	0	0	0	0
Complejo Volcánico Dona Juana Cascabel	41,184	0	0	0	0	0	0	0	0
Cordillera de los Picachos	206,761	764	0.37	3,558	1.73	0	0	78	0.04
Cueva de los Guacharos	6,938	0	0	0	0	0	0	0	0
El Cocuy	112,537	6	0.01	0	0	0	0	0	0
Farallones de Cali	172,845	0	0	0	0	0	0	0	0
Las Hermosas - Gloria Valencia de Castano	8,565	0	0	0	0	0	0	0	0
Las Orquídeas	21,195	0	0	11	0.05	0	0	0	0
Los Nevados	4,673	0	0	0	0	0	0	0	0
Munchique	40,803	0	0	0	0	0	0	0	0
Nevado del Huila	47,994	0	0	0	0	0	0	0	0
Paramillo	347,923	654	0.19	6,023	1.73	0	0	1,097	0.32
Pisba	2,988	0	0	0	0	0	0	0	0
Purace	33,332	0	0	0	0	0	0	0	0
Selva de Florencia	5,381	0	0	0	0	0	0	0	0
Serranía de los Churumbelos - Auka Wasi	96,275	0	0	0	0	0	0	0	0
Serrania de los Yariguies	47,661	0	0	33	0.07	0	0	0	0
Sierra Nevada de Santa Marta	141,698	0	0	0	0	0	0	0	0
Sumapaz	73,030	0	0	0	0	0	0	0	0
Tama	35,901	0	0	0	0	0	0	0	0
Tatama	31,093	0	0	0	0	0	0	0	0
Tayrona	8,495	0	0	0	0	0	0	0	0
Overall	1,718,866	3,442	0.20	13,060	0.76	0	0	1,217	0.07

4. Discussion

Deforestation remains a persistent and complex issue in Colombia, despite the implementation of public policies aimed at mitigating its impact (Bonilla & Higuera, 2016). Among the primary strategies adopted to address this challenge is the establishment of PAs, which contribute to reducing deforestation (Rodríguez et al. 2013); however, deforestation continues even within these zones, driven by pressures such as agricultural expansion, timber extraction, and mining activities (Etter et al., 2008; Armenteras et al., 2017; González-González et al., 2021). Our findings reflect this reality: forest loss within PAs of the Colombian Andes is consistently higher under the BAU scenario, regardless of the time period considered. These findings highlight the diverging trajectories that Andean forests may follow depending on the governance model adopted in the coming decades. While the BAU scenario projects sustained deforestation, particularly impacting Basal and Fragmented forests, the GOV scenario illustrates the potential of more robust policy implementation and institutional control to significantly reduce forest loss, thereby safeguarding critical ecosystems and their biodiversity. This contrast reinforces the urgency of strengthening land-use governance and monitoring mechanisms, even within officially PAs, if long-term conservation goals are to be achieved in the Colombian Andes.

4.1. Differential vulnerability among forest typologies

Among the four forest types assessed, Basal forests consistently emerged as the most vulnerable under both scenarios and time periods (Table 2). Their projected loss of up to 8% between 2030 and 2050 under the BAU scenario likely reflects the socioeconomic pressures associated with their geographic distribution at lower elevations, where anthropogenic activities such as agricultural expansion, cattle ranching, road development, and extractive activities are more intense (Rodríguez Eraso et al., 2013; Sanchez-Cuervo & Aide, 2013). Basal forests are generally located along the colonization frontier in flat areas, where rural populations often settle and convert natural forests into agricultural land for cattle grazing and crop production (Aide et al. 2019).

The fragmented forests typology also exhibited high deforestation rates, suggesting that landscape fragmentation not only reflects past degradation but also increases the likelihood of continued loss due to edge effects and reduced resilience (Haddad et al. 2015; Fischer et al. 2021; González-González et al. 2021). Forest fragmentation is often driven by the construction of roads and other infrastructure, which facilitates human access, land conversion, and ecological degradation (Laurence et al., 2009; Haddad et al. 2015; Ibisch et al., 2016). In fact, numerous studies have shown that proximity to roads and human settlements significantly increases deforestation risk by improving access to remote areas (Rodríguez Eraso et al., 2013; Bonilla & Higuera, 2016; Armenteras et al., 2017). Additionally, ongoing deforestation within Fragmented forests may lead not only to habitat loss but also to reduced landscape connectivity in key regions such as the Andes–Amazon transition belt (Murillo-Sandoval et al., 2022). This area hosts many species with limited dispersal capacity, making regional connectivity crucial for maintaining genetic exchange, metapopulation persistence, and evolutionary processes across neotropical ecosystems (Clerici et al., 2018).

By contrast, Andean and Sub-Andean forests showed significantly lower rates of deforestation, particularly under the GOV scenario. This relative stability may be attributed to a combination of factors, including land use and settlement history, steeper topography and higher altitudes that limits accessibility, the presence of existing conservation areas, and less pressure from large-scale LUCC (Sanchez-Cuervo y Aide 2013; Graesser et al. 2018). Since the Spanish colonization, the Andean mountains have been heavily transformed and have concentrated more than 70% of the country's economic activity and population, especially in the Andean trapeze (i.e., Bogotá, Medellín, Cali, Bucaramanga; DANE, 2024), where the largest cities are located. Since the second half of the twentieth century, the colonization frontier has shifted toward lower-elevation areas, particularly in the Andes–Amazon region (Etter et al., 2008), resulting in reduced pressure on Andean and Sub-Andean forests, as remaining forest fragments are often located in remote, inaccessible zones with steeper slopes (Myers, 1993; Rudel & Roper, 1997; Rubiano et al., 2017; Aide et al., 2019). Moreover, although PAs coverage in the Colombian Andes remains insufficient to safeguard the region's exceptional and unique biodiversity (González et al., 2018), there is a higher number of PAs in the mountain forests than in lowland regions, largely due to the concentration of highland parks in the Eastern Andes, which may also contribute to reduced deforestation rates (Rodríguez et al. 2013). However, even in these ecosystems, the BAU scenario projected continued losses, particularly in the Sub-Andean forest, which is often found in ecotones near human settlements or agricultural frontiers (Aide et al., 2019; Castellanos-Mora & Agudelo-Hz, 2021).

Taken together, our results suggest that deforestation and fragmentation in Andean protected forests are likely driven by a broadly similar set of processes, but that their relative importance varies among forest typologies and along the Andean gradient. At the core of these processes are the contagious expansion of deforestation from previously cleared areas, increased accessibility through road networks and other infrastructure, and the pressures associated with agricultural and cattle ranching frontiers, often coupled with land grabbing, illicit crops and, in some regions, post-conflict dynamics (Etter et al., 2008; Rodríguez Eraso et al., 2013; Bonilla & Higuera, 2016; Armenteras et al., 2017; Murillo-Sandoval et al., 2020, 2022; González-González et al., 2021). In Basal forests located along colonization frontiers and the Andes–Amazon transition, these drivers combine to produce high deforestation probabilities near roads, rural centres and mining concessions, consistent with the strong positive effects of distance to previous deforestation, road density and extractive activities documented for the Andean and Amazonian regions (Etter et al., 2008; Graesser et al., 2018; González-González et al., 2021). In Fragmented forests, the same drivers are likely amplified by high edge density and patch isolation, which enhance degradation processes and increase the likelihood of further loss (Haddad et al., 2015; Fischer et al., 2021). By contrast, in Andean and Sub-Andean forests, much of the historical conversion associated with long-term settlement and infrastructure development has already occurred, so current deforestation tends to be more localized and concentrated near agricultural ecotones and remaining accessible valleys, with steep slopes and remoteness acting as partial buffers (Sanchez-Cuervo & Aide, 2013; Rubiano et al., 2017; Graesser et al., 2018). Thus, while the underlying drivers are largely shared across regions (i. e. expansion of cattle and agriculture, infrastructure development, extractive activities and, in some areas, conflict-related pressures) their expression and intensity differ markedly among forest types and along the Andean–Amazonian transition.

4.2. Protected Areas

NNPs in the Colombian Andes currently serve as important refuges for forest conservation, with forest cover losses remaining below 1% in all scenarios. This agrees with other studies showing that deforestation is lower inside PAs (Rodríguez et al. 2013; Bonilla & Higuera, 2016; Negret et al. 2020). The GOV scenario particularly underscores the importance of effective policy enforcement, with almost no projected forest loss within PAs. Nevertheless, our results reveal that some parks, especially Catatumbo Bari and Cordillera de los Picachos (Figure S1), are already showing signs of vulnerability under the BAU scenario, with projected losses reaching up to 2.6% by 2050. This could be attributed to the socio-economic context surrounding these PAs, which is often linked to the presence criminal actors and large-scale land tenures that promote the expansion of livestock systems and illegal crops (Clerici et al., 2020), which are recognized as key drivers of deforestation (Etter et al., 2008; Armenteras et al., 2017; González-González et al., 2021). Unlike our study, which only considered the NNPs for the deforestation analysis, Bonilla & Higuera (2016) found that when normalizing by area, regional protected areas exhibited higher deforestation rates than NNPs during the 2001–2012 period.

Our results suggest that formal protection alone may be insufficient in areas where external pressures—such as armed conflict, illegal crops, or weak institutional presence—challenge the implementation and enforcement of conservation measures (Bonilla-Mejía & Higuera-Mendieta, 2016, 2019; Clerici et al. 2020; Murillo-Sandoval et al., 2022). Similar patterns have been documented, for instance for conservation units in the Brazilian Amazon, where some PAs have effectively become new deforestation frontiers under intense pressure from illegal loggers, cattle ranchers and small-scale farmers, despite their formal designation (Pedlowski et al., 2005). This is even more concerning given that different studies have shown that, following the 2016 peace agreement in Colombia, deforestation increased substantially within PAs due to the end of the so-called 'gunpoint conservation effect' (Clerici et al., 2020; Murillo-Sandoval et al., 2020). Forest loss within PAs, although relatively small in proportion, may have disproportionately large ecological consequences, especially if it compromises core habitats, protected species, or ecosystem connectivity (Hending et al. 2023; Yuan et al. 2024). It is therefore important to establish effective governance that supports not only conservation actions but also economic stabilization, providing viable alternatives for local communities to prevent illegal expansion and reduce forest degradation within PAs and their buffer zones (Clerici et al., 2020).

4.3. Implications for policy and landscape-level management

The stark contrast between the BAU and GOV scenarios highlights the transformative potential of improved governance in shaping future land-use outcomes. Strengthening institutional capacity, enforcing land-use regulations, promoting sustainable livelihoods, and integrating conservation goals into broader territorial planning are critical steps to reduce deforestation (Macura et al. 2015; Muñoz Brenes et al. 2018; Bonilla-Mejía & Higuera-Mendieta, 2019). The projected forest losses under BAU amount to hundreds of thousands hectares by 2050, underscoring the urgency of proactive interventions under this scenario.

From a policy perspective, the spatially explicit nature of our projections offers valuable inputs for prioritizing intervention areas. Identifying highly vulnerable forest types and pressure-prone PAs enables decision-makers to target conservation investments more effectively (Hoffmann et al., 2022). In addition, our findings can inform updates to Colombia's National Biodiversity Strategy, REDD+ implementation, and climate change mitigation strategies, particularly in the context of the country's commitments under the Kunming-Montreal Global Biodiversity Framework and the Paris Agreement (Nepstad et al. 2021). It is essential that the government establish incentives to promote the sustainable use of forests and reduce landscape transformation and deforestation. Establishing incentives to promote sustainable forest use and reduce landscape transformation is essential, and broader socioeconomic conditions—such as security, access to economic programs, financial grants, and technical support—must be ensured for local communities surrounding PAs (Clerici et al., 2020).

Importantly, these interventions are practically feasible through participatory monitoring programs and local land-use committees that enhance compliance with conservation regulations, increasing governance effectiveness (Evans & Guariguata, 2008; Mandeville et al., 2023). Financial incentives and technical support for sustainable land-use practices—such as payments for ecosystem services—further improve feasibility by aligning local livelihoods with ecosystem protection (Minambiente 2021). Engaging local communities in co-management of PAs fosters ownership and compliance, strengthening the prospects for long-term conservation success (Evans et al., 2019; Costa et al. 2018). While socioeconomic and security constraints may limit implementation, targeted support programs and conflict-resolution mechanisms can enhance the practicality of conservation actions (Evans et al., 2019). Moreover, regular monitoring of forest recovery and deforestation hotspots enables adaptive management, ensuring interventions remain effective under changing ecological and social conditions (IDEAM, 2024).

In addition to governance interventions, it is important to consider the role of secondary forests, which have been expanding in the Andean highlands due to demographic transitions such as rural population decline and the abandonment of agricultural activities (Rodríguez Eraso et al., 2013; Aide et al., 2019). These trends have facilitated natural Andean forest regeneration over recent decades (Rubiano et al., 2017; Calbi et al., 2020). In this context, it is also crucial to adopt a long-term conservation perspective that includes areas in early successional stages, as they can contribute to biodiversity recovery over time and improve landscape connectivity by linking with remnant old-growth forest patches (Sanchez-Cuervo & Aide, 2013). Accordingly, PAs should also encompass recently transformed landscapes undergoing regeneration, thereby reducing net forest loss through the promotion of secondary forest expansion.

At the same time, our scenario analysis focuses on deforestation and does not explicitly represent forest degradation processes. Nevertheless, long-term forest degradation has shown to affect areas comparable to or larger than those deforested, for instance in the Amazon forest, with important consequences for carbon emissions, biodiversity, water and energy balances, and forest resilience (Matricardi et al., 2020; Qin et al., 2021). In this sense, our deforestation-based projections should be interpreted as a conservative baseline that likely underestimates the full spectrum of anthropogenic impacts on Andean forest ecosystems and the services they provide.

5. Conclusion

Our study highlights the critical role of governance and socio-ecological factors in shaping the fate of Andean forests. By linking deforestation trajectories with different governance scenarios, we demonstrate that even modest improvements in policy implementation can yield substantial ecological benefits. These findings advance our understanding of how human and environmental drivers interact to influence forest conservation outcomes in montane ecosystems. Beyond biodiversity conservation, maintaining Andean forests is crucial for sustaining key ecosystem services, including water regulation, carbon storage, and cultural values for local communities. Our results provide actionable insights for forest management and conservation planning, offering a predictive framework that can guide adaptive strategies under climate change and ongoing land-use pressures. Future research could build on this work by integrating finer-scale socio-economic variables and exploring the long-term effectiveness of governance interventions on ecological resilience.

6. Data availability

The geospatial datasets of deforestation scenarios in Colombia (2018–2050) are available at https://doi.org/10.5281/zenodo.4559626. The GMBA Mountain Inventory v2 is available at https://doi.org/10.48601/earthenv-t9k2-1407. The map of continental, coastal, and marine ecosystems of Colombia v2.1 is available at http://archivo.ideam.gov.co/web/ecosistemas. The boundaries of the Colombian National Natural Parks can be downloaded from RUNAP at https://storage.googleapis.com/pnn_geodatabase/runap/latest.zip. The minimum derived datasets required to replicate the analyses, figures, and results presented in this manuscript are openly available at Zenodo https://doi.org/10.5281/zenodo.17080519.

7. Supplementary Material

Table S1. Definition, rationale and regional transition rates of the two deforestation scenarios (BAU and GOV) used in this study, based on González-González et al. (2021). Transition rates correspond to those reported in Table S4 of González-González et al. (2021) for each biogeographical region. They were used to parameterize the original Dinamica EGO simulations.

Scenario	Rationale	Governance assumptions	Time period	Deforestation rates assumption	Regional annual transition rates
BAU (Business as Usual)	Continuation of recent deforestation dynamics without additional governance efforts beyond current trends.	Forest loss is allowed in both inside and outside protected areas. Legal instruments (e.g. National Agricultural Frontier zoning) reduce, but do not completely eliminate, the probability of forest loss in legally protected zones.	2018–2050	Annual deforestation rates are kept constant and equal to the mean rate observed during 2013–2018 for each biogeographical region.	Andean: 0.006; Amazon: 0.005; Caribbean: 0.018; Orinoquia: 0.011; Pacific: 0.003.
GOV (Governance)	Enhanced environmental governance consistent with Colombia's deforestation-reduction commitments under the Paris Agreement.	Stronger enforcement and policy implementation; zoning categories strongly reduce the probability of forest loss in PAs and other legally protected areas, but do not eliminate it completely.	2018–2030	Same drivers as BAU, but annual deforestation rates are reduced by 30% relative to the 2013–2018 mean.	Andean 0.001; Amazon 0.001; Caribbean 0.005; Orinoquia 0.003; Pacific 0.001.
			2030–2050	Same drivers as BAU, but annual deforestation rates are reduced by 50% relative to the 2013–2018 mean.	Andean 0.003; Amazon 0.002; Caribbean 0.009; Orinoquia 0.005; Pacific 0.002.

Table S2. Spatially explicit variables used as drivers of deforestation in the scenario simulations, their data sources and conceptual justification, following González-González et al. (2021).

Variable	Data source	Justification	References
Distance to deforested areas	(Hansen et al., 2013)	Deforestation tends to expand outwards from existing clearings; proximity to previous forest loss is a strong predictor of new clearing in Colombia.	(Barber et al., 2014; Rubiano et al. 2017)
Distance to main roads Distance to paved municipal roads Distance to unpaved municipal roads Distance to roads accessible in dry periods Distance to other accessible roads	(Invías, 2020)	Road infrastructure increases accessibility, lowers transport costs and is a well-known facilitator of agricultural expansion and forest conversion in Colombia.	(Laurance et al., 2009; Rodríguez Eraso et al., 2013; Ibisch et al., 2016)
Distance to mining concessions	(Global Forest Watch, 2020)	Industrial and informal mining are documented drivers of deforestation and forest degradation in Colombia, affecting forests within and around concession areas.	(González-González et al., 2021)
Distance to administrative centers	(IGAC, 2020)	Urban centres represent demand hubs and administrative nodes that concentrate population and economic activities, increasing pressure on surrounding forests.	(Lambin et al., 2003; Etter et al., 2008)
Distance to water bodies		Rivers and other water bodies can act as transport corridors and sources of water for human settlements and agriculture, thereby shaping where deforestation can occur.	(Barber et al., 2014)
Slope	(Jarvis et al., 2008)	Terrain steepness limits mechanized agriculture and cattle ranching; deforestation is expected to concentrate on gentle to moderate slopes while steeper areas tend to be less accessible.	(IGAC, 2014; Rubiano et al., 2017)
Armed conflict	(FIP, 2016)	Armed conflict has shown contrasting effects on deforestation (deterrent or attractor) depending on the region.	(Clerici et al., 2019; Negret et al., 2019; Murillo-Sandoval et al., 2020)

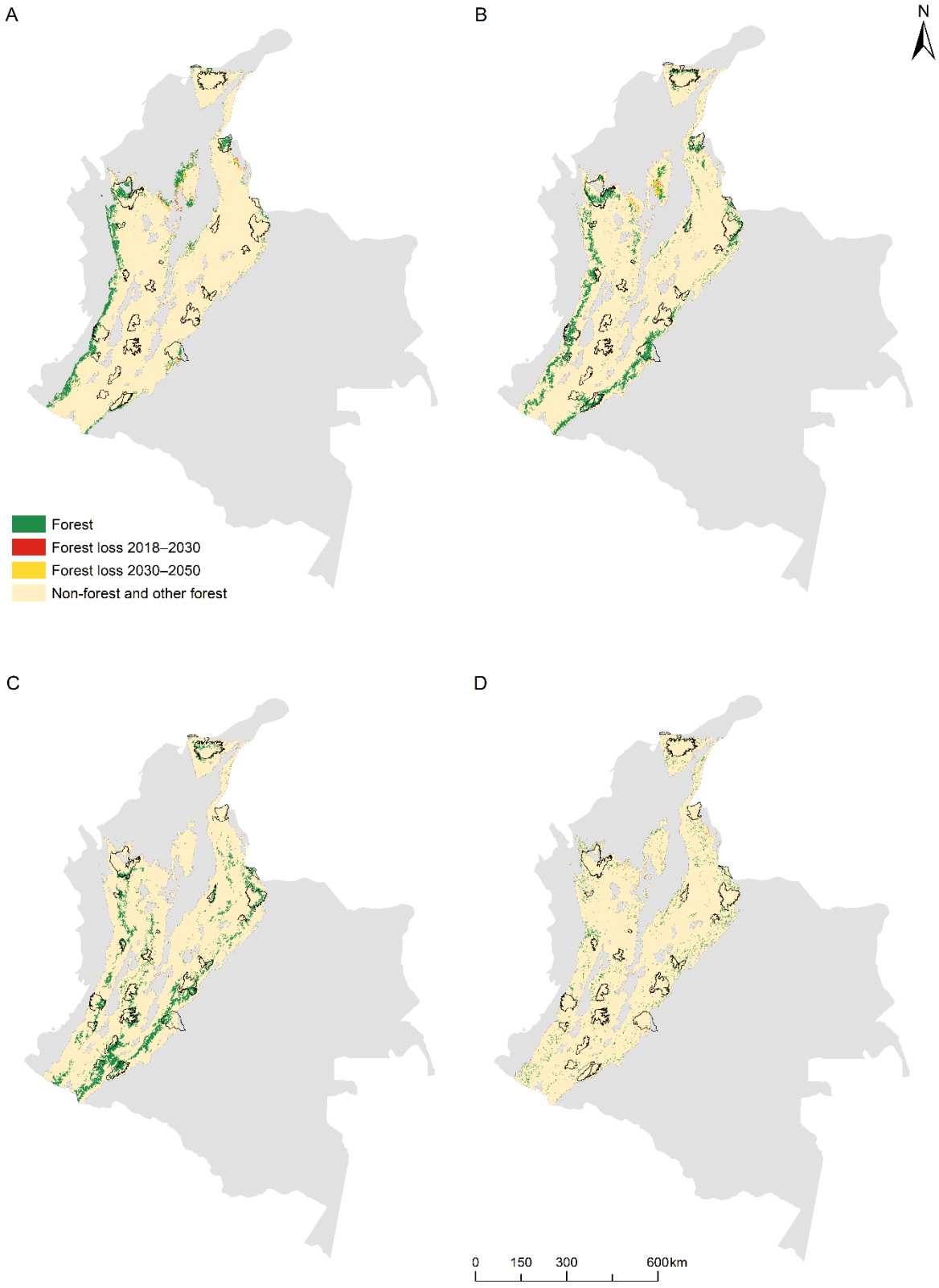

Figure S1. Maps depicting the spatial distribution and projected losses of the four forest typologies under the BAU deforestation scenario in the Colombian Andes. Each panel corresponds to one forest typology (A) Basal forest, (B) Sub-Andean forest, (C) Andean forest and (D) Fragmented forest.

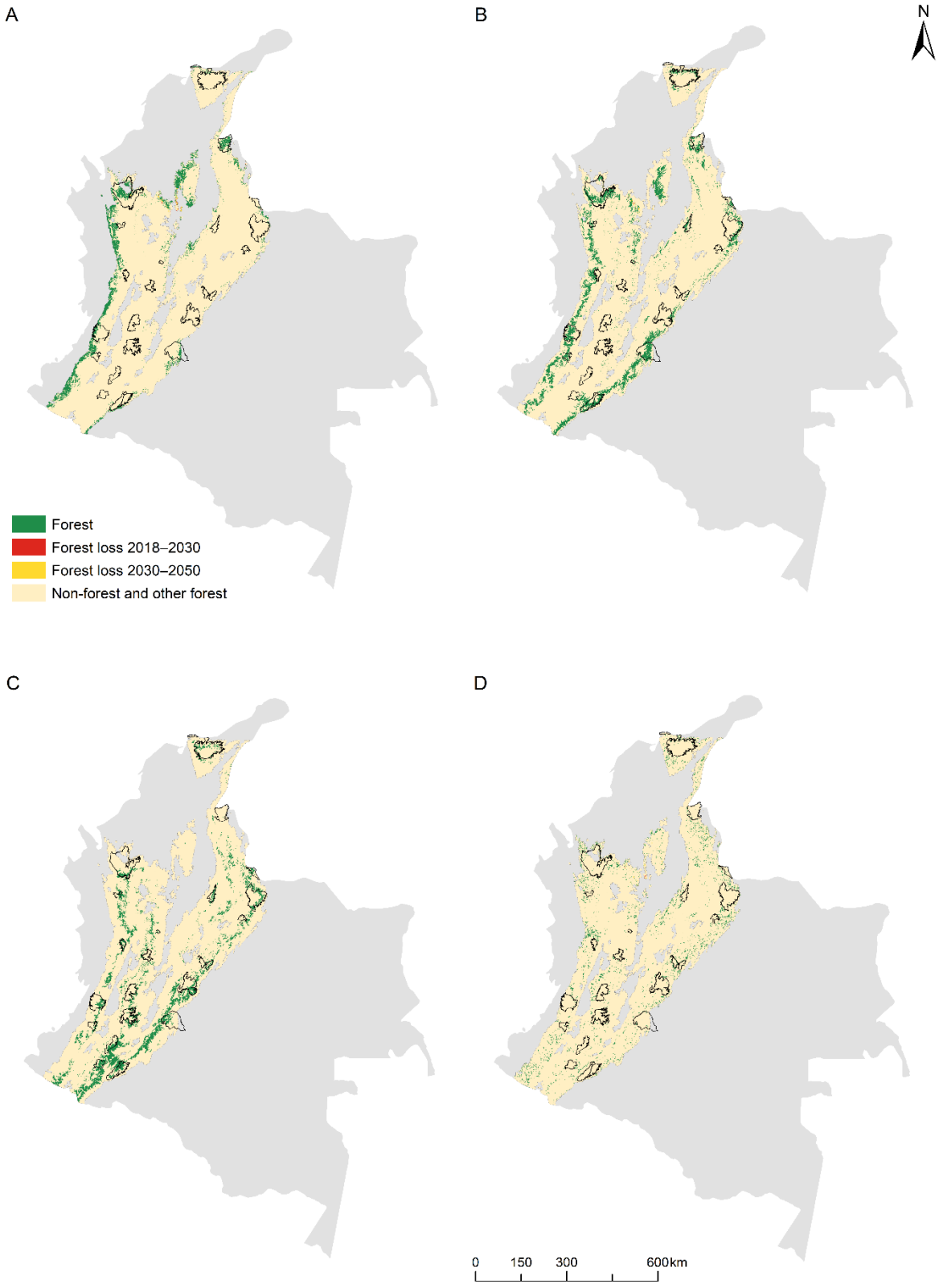

Figure S2. Maps depicting the spatial distribution and projected losses of the four forest typologies under the GOV deforestation scenario in the Colombian Andes. Each panel corresponds to one forest typology (A) Basal forest, (B) Sub-Andean forest, (c) Andean forest and (d) Fragmented forest.

Figure S3. National Natural Parks location and name, blue polygons (ID). Cueva de los Guácharos (1); Los Nevados (2); Alto Fragua - Indi Wasi (3); Tayrona (4); Catatumbo Barí (5); Chingaza (6); Cordillera de los Picachos (7); Complejo Volcánico Doña Juana Cascabel (8);El Cocuy (9); Farallones de Cali (10);Las Hermosas - Gloria Valencia de Castaño (11); Las Orquídeas (12); Tamá (13); Sumapaz (14); Sierra Nevada de Santa Marta (15); Serranía de los Yariguíes (16); Serranía de los Churumbelos - Auka Wasi (17); Munchique (18); Selva de Florencia (19); Nevado del Huila (20); Paramillo (21); Pisba (22); Puracé (23); Tatamá (24). Light tan polygons: Colombian Andes and Sierra Nevada de Santa Marta range.

Chapter 4

Current hydroclimatic spaces will be breached in half of the world's humid high-elevation tropical ecosystems

Published in *Communications Earth & Environment* (2025): 6(197), https://doi.org/10.1038/s43247-025-02087-6

Current hydroclimatic spaces will be breached in half of the world's humid high-elevation tropical ecosystems

Kristian Rubiano[1,2,3*], Nicola Clerici[1], Adriana Sanchez[1], Fernando Jaramillo[2]

[1] Faculty of Natural Sciences, Universidad del Rosario, Bogotá, Colombia
[2] Department of Physical Geography and Bolin Center for Climate Research, Stockholm University, Stockholm 10691, Sweden
[3] Jardín Botánico de Bogotá 'José Celestino Mutis', Bogotá, Colombia
[*]Corresponding author – Kristian Rubiano, kristian.rubiano@urosario.edu.co

Abstract

Humid high-elevation tropical ecosystems (HETEs), known as páramos, jalca, or moorlands, are essential for biodiversity conservation and water supply. Yet, a key question remains of how future climate change will affect their hydroclimatic spaces: the multidimensional hydroclimatic conditions in which they currently thrive. We use CMIP6-downscaled climate data to assess the potential breaching of these hydroclimatic spaces concerning the long-term means, extremes, and seasonality of temperature and precipitation. Our results show that HETEs in Northern South America will experience the largest increase in temperature and decrease in precipitation, leading to the breaching of their current hydroclimatic space by up to 100%. In the Afrotropics and Australasia, HETEs will experience a breaching of their hydroclimatic spaces related to long-term means and extremes. Our findings provide relevant information on the vulnerability of HETEs to climate change, offering insights to inform the integration of adaptation measures into policy development and management strategies for conserving these key ecosystems and their services.

Keywords

Humid high-elevation tropical ecosystems, hydroclimatic spaces, climate change, temperature, precipitation.

1. Introduction

Climate change is recognized as one of the major threats to global biodiversity (Hooper et al., 2012; Pereira et al., 2012). As the climate changes, the current distribution of hydroclimatic conditions and the range of the species will move and rearrange spatially (Pecl et al., 2017). High-elevation ecosystems are particularly vulnerable to this threat due to their narrow and strict elevational distribution (Nogués-Bravo et al., 2007; Tovar et al., 2022; Verrall & Pickering, 2020) and their restricted extent: they cover less than 3% of the global terrestrial area outside Antarctica (Testolin et al., 2020). These ecosystems are expected to shift rapidly poleward and upward in response to accelerating climate change in mountain regions (Pepin et al., 2015), potentially contracting or even disappearing altogether (Buytaert et al., 2011; Cresso et al., 2020; Helmer et al., 2019). This shift raises major concerns about the persistence of these invaluable ecosystems, the pressures on their biodiversity, and the resilience of their ecological functions to provide essential ecosystem services (Buytaert et al., 2006, 2011; Cresso et al., 2020; Diazgranados et al., 2021; La Sorte & Jetz, 2010; Nogués-Bravo et al., 2007; Tovar et al., 2022).

Humid high-elevation ecosystems in the tropics, hereafter HETEs (*sensu* Suárez et al., 2023), mainly occur in the Neotropic, Afrotropic, and Australasia between the upper treeline at about 3500 m.a.s.l (Flantua et al., 2019; Harsch et al., 2009) and the lower permanent snow line at approximately 5000 m.a.s.l. (Fig. 1A) (Burgess et al., 2004; Buytaert et al., 2011; Wikramanayake et al., 2002). These ecosystems have regional names, such as páramos and jalca in the Northern Andes or afroalpine and moorlands in East Africa (A. P. Smith & Young, 1987). HETEs are the most biodiverse among high-elevation ecosystems, hosting the highest species richness and endemism (Dimitrov et al., 2012; Llambí & Rada, 2019; Merckx et al., 2015; Sklenář et al., 2014). For instance, HETEs in the Northern Andes host about 3500 vascular plant species, of which approximately 60% are endemic, and thousands of vertebrate species (Llambí & Rada, 2019; Sklenář et al., 2014). The distribution of HETEs is naturally fragmented (Flantua et al., 2019), but land use changes have increased their isolation in recent decades (Gebrehiwot et al., 2021; Jacob et al., 2016; Tovar et al., 2012), further constraining the dispersal capacities of species (Chala et al., 2016; Tovar et al., 2020). The effects of climate change on biodiversity are then expected to be an interaction of movement, adaptation, or local extinction mechanisms at the specific level (Berg et al., 2010; Buytaert et al., 2011; La Sorte & Jetz, 2010).

HETEs are also crucial for their services to people and society (Anderson et al., 2011; Buytaert et al., 2011; Diazgranados et al., 2021; Mengist et al., 2020). They represent important carbon stocks due to topography and climate, promoting the formation of mineral soils and wetlands rich in organic carbon (Gebrehiwot et al., 2018; Hribljan et al., 2016; Yang et al., 2018). As a result of their climatic, edaphic, and vegetation properties, HETEs have an exceptional water regulation capacity, which is essential for water supply to millions of people in surrounding cities and communities (Buytaert et al., 2006; Buytaert & Bievre, 2012; Célleri & Feyen, 2009; Vuille, 2013). For instance, many large Andean cities depend on HETEs for up to 95% of their water supply (Buytaert et al., 2011; Flantua et al., 2019). This water supply also contributes to hydropower production, food security, and socio-economic development (Buytaert et al., 2006, 2011). Climate change is expected to impact the water balance of these ecosystems, their regulating capacity, and downstream water supply (Anderson et al., 2011; Bradley et al., 2006; Buytaert et al., 2006, 2011; Buytaert & Bievre, 2012; Célleri & Feyen, 2009; Vuille, 2013).

Although HETEs are highly vulnerable and crucial for biodiversity conservation and socio-economic development, they remain among the world's most understudied and poorly characterized ecosystems (Buytaert et al., 2011; Gleeson et al., 2016). Research on these ecosystems has increased in the last decades (Anderson et al., 2011; Buytaert et al., 2011; Cresso et al., 2020; Diazgranados et al., 2021; Tovar et al., 2013, 2022), primarily focused on the impacts of land use change and human activities in these ecosystems (Anderson et al., 2011; Buytaert et al., 2011; Cresso et al., 2020; Diazgranados et al., 2021; Tovar et al., 2013, 2022). However, understanding the implications of potential climate-related range shifts of HETEs worldwide is also necessary (Célleri & Feyen, 2009; Lenoir & Svenning, 2015; Verrall & Pickering, 2020) for impact assessment. It is also required to propose practical management approaches that ensure the conservation and resilience of HETEs, their services (Mengist et al., 2020) and the design and implementation of effective restoration (Christmann & Menor, 2021).

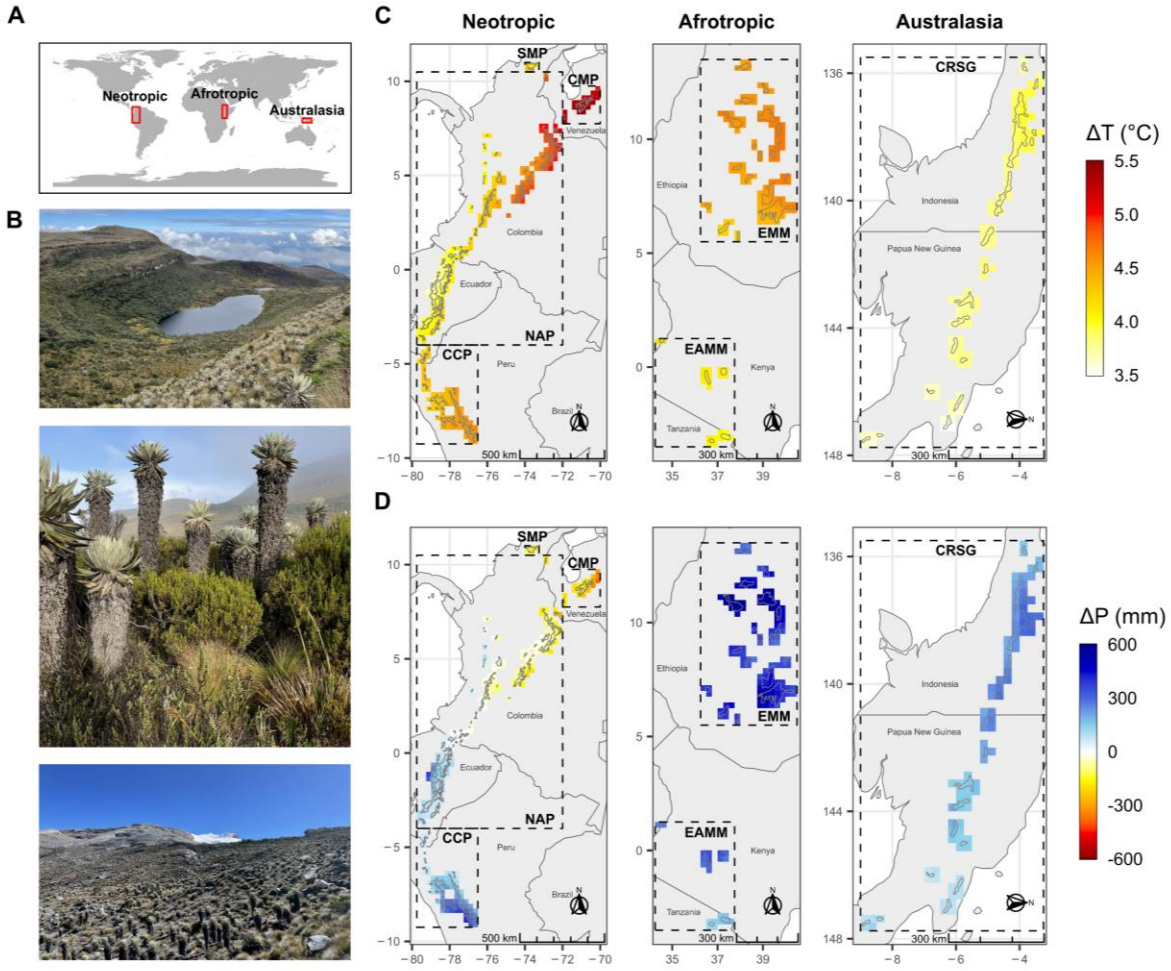

Figure 1. HETEs and their projections of hydroclimatic change between the baseline (1985-2014) and future (2071-2100) under SSP585. (A) General location of HETEs in the world, (B) examples of HETEs landscapes, (C) change in mean annual temperature T, and (D) change in total annual precipitation P in the seven high-elevation tropical ecoregions (SMP: Santa Marta Páramo; CMP: Cordillera de Merida Páramo; NAP: Northern Andean Páramo; CCP: Cordillera Central Páramo; EAMM: East African Mountain Moorlands; EMM: Ethiopian Mountain Moorlands; CRSG: Central Range sub-alpine Grasslands). The dotted lines mark the ecoregions. Photos in panel B from top to bottom: Chingaza Páramo, Colombia (Photo by Juanharveyc licensed under CC BY-SA 4.0); Giant Lobelia, Sanetti Plateau, Ethiopia (Photo by Rod

Waddington licensed under CC BY-SA 2.0); Mount Wilhelm, Papua New Guinea (Photo by Johannes Zielcke licensed under CC BY-NC-ND 2.0). Fig. S1 shows the spatial distribution of the standard errors among GCMs.

Predicting the potential impacts of future climate change on the extent and distribution of HETEs and identifying the most vulnerable and resilient HETEs to changes is thus crucial for biodiversity conservation and human well-being in and around these ecosystems. To do so, there is a need to understand the hydroclimatic spaces in which HETEs currently thrive; these present the thresholds within which these ecosystems can persist. Hydroclimatic spaces are the envelope of multidimensional water and energy-related conditions over a given period (Ohlemüller, 2011; Williams & Jackson, 2007). Since these hydroclimatic spaces are expected to change over time under climate change scenarios, one can compare current or baseline and future or projected ones to identify areas where baseline hydroclimates could be breached under the influence of climate change (Ohlemüller, 2011; Williams & Jackson, 2007).

Modeling of hydroclimatic spaces has been previously used to reconstruct and draw inferences about past climates from paleo-ecological data (Jackson & Williams, 2004; Roberts & Hamann, 2012; Veloz et al., 2012) and assess projected changes in temperature and precipitation from regional to global scales (Ackerly et al., 2010; Cresso et al., 2020; Ohlemüller et al., 2006; Tovar et al., 2022; Williams et al., 2007). The use of hydroclimatic spaces to analyze the potential impacts of climate change on HETEs has, to date, mainly focused on the Andes at local scales (Cresso et al., 2020; Tovar et al., 2022), leaving those of the Afrotropics and Australasia unassessed. Furthermore, these efforts have considered only the long-term mean temperature and precipitation, leaving aside seasonality and extremes of these variables, which are pivotal to predicting and understanding the ecosystem and biodiversity responses of HETEs to climate change (García-Robledo et al., 2016; Lancaster & Humphreys, 2020; Perez et al., 2016).

Here, we explore on an ecoregional basis the potential impacts of future climate change on the extent and distribution of HETEs globally based on the high emissions Shared Socioeconomic Pathway (SSP) scenario without carbon emission mitigation strategies, SSP585. Specifically, we use a multimodel ensemble of climate data from the latest NASA Global Daily Downscaled Projections archive (NEX-GDDP-CMIP6; Thrasher et al., 2022) and the Terrestrial Ecoregions of the World (TEOW) dataset Version 2.0 (Olson et al., 2001) by the World Wildlife Fund (WWF) to assess changes in temperature and precipitation (from 1985-2014 to 2071-2100) in HETEs across three continents and seven ecoregions (Fig. 1. A-C). We use this data on precipitation and temperature to define the baseline hydroclimatic spaces and their potential projected breaching. Lastly, we discuss the implications of our results for biodiversity conservation and ecosystem services provision.

2. Methods

2.1. Delimitation of humid high-elevation Tropical Ecoregions

We used the Terrestrial Ecoregions of the World (TEOW) dataset Version 2.0 (Olson et al., 2001) by the World Wildlife Fund (WWF) to delineate humid high-elevation tropical areas for subsequent spatial analyses. There, ecoregions are defined as land units that harbor particular

assemblages of species, and their limits represent the original extent of the natural communities before anthropogenic transformation (Olson et al., 2001). This dataset delineates the global terrestrial ecoregions based on the conciliation of previous studies and biogeographical classifications.

We filtered seven ecoregions from the TEOW dataset belonging to the Montane Grasslands and Shrublands biome. We followed the Humid Tropical Alpine Regions delimitation of (Buytaert et al., 2011) which specifies that HETEs occur in the northern Andes, in the Afro-alpine belt, and New Guinea. We defined four ecoregions for the Neotropics: Santa Marta Páramo (SMP), Cordillera de Mérida Páramo (CMP), Northern Andean Páramo (NAP), and Cordillera Central Páramo (CCP); one ecoregion for Australasia: Central Range Sub-alpine Grasslands (CRSG) located above 3000 m above sea level (m.a.s.l.) of elevation (Wikramanayake et al., 2002); and two ecoregions for the Afrotropics: East African Montane Moorlands (EAMM), and Ethiopian Montane Moorlands (EMM), which are located from 3000 m to over 4500 m.a.s.l. (Burgess et al., 2004). It is worth noting that some authors report the extension of the Andean HETEs southwards to the north of Peru (approximately ~5°S, where the páramo ends and the ecosystem known as Jalca begins; Buytaert et al., 2011). In contrast, others consider that páramo extends even more to the South (approximately 10°S; Hofstede et al., 2003). As the TEOW dataset agrees with the latter and locates the CCP between approximately 5°S and 10°S (Olson et al., 2001), we also include the CCP ecoregion in our analyses.

2.2. Climate data

We used downscaled climate raster data from the latest NASA Earth Exchange Global Daily Downscaled Projections archive for the Coupled Model Intercomparison Project Phase 6 (CMIP6), NEX-GDDP-CMIP6, with a horizontal resolution of 0.25° (~25 km) (Thrasher et al., 2022). Although the CMIP Global Climate Models (GCMs) have shown to be reliable and, therefore, widely used for producing climatic projections, their outputs have coarse spatial resolutions (~100-200 km) that make them unsuitable for regional to local analyses (Grose et al., 2023). However, GCM downscaling allows for data generation at finer temporal and spatial scales, which is more suitable for a broader range of applications where narrow ecosystems with a narrow spatial extent are considered (Iles et al., 2020). The NEX-GDDP-CMIP6 dataset was produced using a statistical downscaling algorithm that uses climate observations to adjust future climate projections to ~25 km spatial resolution (Thrasher et al., 2022). While there are very high-resolution global climate datasets (~1 km) such as WorldClim (Fick & Hijmans, 2017) and CHELSA (Karger et al., 2017), we selected the medium-resolution NEX-GDDP-CMIP6, looking for a trade-off between resolution and accuracy, as the capacity of high-resolution datasets to accurately represent the climate in topographically complex regions, such as tropical mountains, has been largely questioned (Bedia et al., 2013; Hemp & Hemp, 2024; Tovar et al., 2022). The NEX-GDDP-CMIP6 dataset has been used in climate change studies with various spatial and temporal scales and applications (Falchetta et al., 2024; Murali et al., 2023; Rao et al., 2024; Yin et al., 2023).

The NEX-GDDP-CMIP6 dataset compiles climatic data for five experiments produced from several GCMs for the CMIP6. The historical experiment extends from 1950 to 2014, which is

helpful as a climatic reference, while the four remaining experiments are based on the Shared Socioeconomic Pathways (SSPs), consisting of different scenarios of future greenhouse gas emissions, land use changes, and radiative forcing levels covering the period 2015 to 2100 (O'neill et al., 2016). The SSP585 is a high-emission climate change scenario representing the upper limit of feasible future climatic pathways, assuming continuous fossil-fuel development in the future and an 8.5 W/m^2 level of forcing by 2100 (Meinshausen et al., 2020). Continuing current trends and policies without successful efforts to reduce greenhouse gas emissions or mitigate climate change impacts in a business-as-usual and worst-case pathway make SSP585 an ideal scenario to explore the potential outcomes of no climatic action on HETEs (Kriegler et al., 2017; Tovar et al., 2022). We focused on the historical and SSP585 experiments from six widely used GCMs (i.e., ACCESS-ESM1-5 (Ziehn et al., 2020), EC-EARTH3 (Döscher et al., 2022), EC-EARTH3-Veg-LR (Döscher et al., 2022), HadGEM3-GC31-MM (Walters et al., 2019), IPSL-CM6A-LR (Boucher et al., 2020), and MPI-ESM1-2-HR (Müller et al., 2018)) to compute model ensemble-based data for each of the seven HETE ecoregions. We estimated the means for the baseline 30-year period (1985-2014) and the future 30-year period (2071-2100; Kriegler et al., 2017). These GCMs have been used in previous assessments of global hydroclimatic change and have different original spatial resolutions before downscaling, in some cases, integrating land surface and dynamic vegetation models (Jaramillo et al., 2022).

2.3.Data processing

For each of the six GCMs and the two experiments selected for the analyses, we downloaded daily precipitation (P), daily minimum near-surface air temperature (T_{min}), and daily maximum near-surface air temperature (T_{max}) data from the NASA Center for Climate Simulation (NCCS) data collections. We limited the spatial extent of the climate data by selecting every raster cell intersecting the previously filtered high-elevation Tropical Ecoregions' polygons from the TEOW dataset. Daily raster data were aggregated by cell to compute monthly climate time series for the baseline (1985-2014) and the future (2071-2100) 30-year periods. The T_{min} and T_{max} were averaged for every month and year. The daily P was aggregated to monthly precipitation (See next section). We then used the P, T_{min}, and T_{max} monthly time series to compute six selected bioclimatic variables (Table 1) using the *biovars* function from the *dismo* package in R (Hijmans et al., 2021). The *biovars* function takes as inputs P, T_{min}, and T_{max} monthly raster data for a specific year (i.e., one raster for each variable per month) and returns a single raster for each bioclimatic variable for a particular year. Bioclimatic variables are often used as covariates in potential species distribution models. They summarize annual climatic conditions, seasonal mean conditions, and intra-annual seasonality, providing information relevant to analyzing the species' response to climate changes due to ecological and physiological constraints (O'Donnell & Ignizio, 2012). We based the selection of the six bioclimatic variables on their importance for HETE functioning and their impact on animal and plant physiology (García-Robledo et al., 2016; Lancaster & Humphreys, 2020; Perez et al., 2016). Finally, we computed the six bioclimatic variables for every year and averaged their annual values across the baseline and future 30-year periods (Bede-Fazekas & Somodi, 2020). This procedure was repeated for each of the six GCMs.

2.4. Hydroclimatic changes in HETEs between 1985-2014 and 2071-2100

We refer to changes as the difference between the 30-year baseline and future values for each GCM. We used the spatial coverage of the seven ecoregions to extract spatial weighted means for the baseline, the future periods and their changes for every ecoregion. We used the pixel areas intersected by the ecoregion's spatial coverage as weights (See Fig. S6). We averaged them to compute model-based ensemble means for each ecoregion and HETEs overall, and the standard errors among GCMs. The model-based ensemble mean is a widely used approach to combine multiple GCMs to produce more robust and accurate climatic estimations than using individual GCMs, as each GCM has its own biases and errors, and by averaging their outputs the ensemble mean reduces the impact of these individual inaccuracies (Bellucci et al., 2015; Kim et al., 2012).

Table 1. Bioclimatic variables selected for the analysis.

Hydroclimatic space	Bioclimatic variable*	Name*	Units	Description
Long-term (LT)	Bio1	Mean annual temperature (T)	°C	The tmin and tmax monthly data are used to calculate the average temperature for each month, and then the latter are averaged across the year.
Long-term (LT)	Bio12	Total annual precipitation (P)	mm	The sum of the precipitation values of each of the 12 months in a year.
Extremes (SE)	Bio4	Temperature seasonality (Ts)	°C	The standard deviation of the 12 monthly temperature averages across the year times 100.
Seasonality (SE)	Bio15	Precipitation seasonality (Ps)	CV	The coefficient of variation of the 12 monthly precipitation values across the year.
Extremes (EX)	Bio5	Maximum temperature of warmest month (Tmw)	°C	The maximum temperature value across all months within a particular year.
Seasonality (EX)	Bio14	Precipitation of driest month (Pd)	mm	The minimum precipitation value across all months within a particular year.

*According to Hijmans et al., (2021).

Considering the spatial resolution of the data, we used bilinear spatial interpolation to obtain the baseline values of the variables (i.e., T, P, T_{mw}, P_d T_s, P_s) for each HETEs' areas from the 30-year climatic mean rasters. By HETEs' areas, we refer to the geometric intersections of the ecoregion's spatial extents and the raster data pixels (See Fig. S6). The interpolated values were assigned to the centroid of every HETEs' area, and later, we used them to compute the baseline hydroclimatic spaces as the 95% probability of 2-dimensional kernel densities. In this way, we reduced the potential noise of using cell values highly influenced by lower elevation areas, given the insular and fragmented distribution of HETEs. Due to the low number of pixels within the extent of the SMP ecoregion, we decided to merge them with the NAP pixels to build the

hydroclimatic spaces. We repeated this for the future period to construct the three 2-dimensional projected hydroclimatic spaces.

2.5. Baseline and projected hydroclimatic spaces

We used the 30-year means of the baseline period to build three 2-dimensional baseline hydroclimatic spaces for each ecoregion. The long-term (LT) baseline hydroclimatic space represents the annual climatic conditions and consists of the long-term means of T and P (Table 1). The extreme (EX) baseline hydroclimatic space corresponds to the extreme seasonal conditions and involves T_{mw} and P_d. The seasonality (SE) baseline hydroclimatic space denotes the intra-annual seasonality and consists of T_s and P_s. It is worth noting that HETEs have been previously found to be susceptible to the six variables comprising the three hydroclimatic spaces (LT, EX, and SE; Table 1), becoming critical environmental drivers of these ecosystems' occurrence and persistence (Lancaster & Humphreys, 2020; Perez et al., 2016).

2.6. Changes between current baseline and future hydroclimatic spaces

To quantify the trajectory of the changes in the hydroclimatic spaces (i.e., the change in LT, EX, and SE conditions in time), we computed the centroids of the baseline and projected hydroclimatic spaces and the vector resulting from their change in the 2-dimensional space (Destouni et al., 2013; Jaramillo et al., 2022; Jaramillo & Destouni, 2014). We then described and summarized the trajectories through the direction of change (θ) as follows:

$$\theta = \arctan\left(\frac{\Delta y}{\Delta x}\right) \quad (1)$$

where θ is the direction of change in degrees from the x-axis (i.e., depending on the variables selected). The pairs of Δy and Δx become the ΔT and ΔP for LT, ΔT_{mw} and ΔP_d for EX and ΔT_s and ΔP_s for SE, respectively, as computed from the normalized change vectors. Conversely, the I is calculated as:

$$I = \sqrt{\Delta y^2 + \Delta x^2} \quad (2)$$

The severity of the movement (S) can be defined as the percentage of the area of the future hydroclimatic space that does not intercept the baseline one, i.e., the percentage of the extent of the HETEs in which baseline hydroclimatic conditions are breached. Hence, S becomes an indicator of the impacts of the direction and intensity of the movement on the ecoregions, as the changes in the projected hydroclimatic conditions are a combination of them. S was calculated as:

$$S = \frac{A - (A \cap B)}{A} * 100 \quad (3)$$

where A is the area of the projected hydroclimatic space, and B is the area of the baseline hydroclimatic space.

2.7. Location and quantification of safe and breached hydroclimatic spaces

Hydroclimatic spaces were also used to locate the extension of the HETEs' areas (i.e. the geometric intersections of the ecoregion spatial extents and the raster data grids) within each ecoregion that will either remain in their safe hydroclimatic spaces or be breached, according to their trajectories of change. To that end, we identified and quantified the HETEs' areas whose projected future hydroclimatic values overlapped the baseline hydroclimatic spaces in the 2-dimensional space (see Fig. 3). When overlapping exists the HETEs's areas were classified as safe, and those whose projected values did not overlap were classified as breached.

Furthermore, the breached HETEs' areas were also reclassified by assessing if their projected future hydroclimatic values would overlap the baseline hydroclimatic space of any ecoregion. The HETEs' areas whose projected future hydroclimatic values did not overlap the baseline hydroclimatic space of any of the seven ecoregions were classified as novel, as their hydroclimatic conditions would not have been experienced before by any ecoregion. If the HETEs' areas were not classified as novel, we classified them as analog, because although the specific baseline hydroclimatic space of the ecoregion in question would be breached, their hydroclimatic conditions would still resemble baseline hydroclimatic conditions of other ecoregions.

We performed this classification for the three types of hydroclimatic space (i.e., LT, EX, and SE). Finally, we mapped and quantified the vulnerability to climate change of each ecoregion based on the data resulting from the number of breaches of the three types of hydroclimatic spaces. Then, we used four categories to determine the vulnerability of the HETEs' areas to climate change according to their number of breached spaces. Areas of the HETEs with no breaching were assigned with low vulnerability; areas breaching one of the three types of hydroclimatic space were assigned with medium vulnerability; those breaching two of the three types of hydroclimatic spaces were assigned with high vulnerability; and areas breaching the three hydroclimatic spaces were assigned as critically vulnerable.

3. Results

3.1. Projected hydroclimatic changes in global HETEs

Based on the mean of six Global Circulation Models (GCMs) of the historical and high-emission Shared Socioeconomic Pathways (SSP) 585 of the Climate Model Intercomparison Project Phase 6 (CMIP6), we find that temperature (T) will increase more in the ecoregions of the Northern Neotropics, with warming reaching about +5.5°C in the Northern Andean Páramo (NAP) and the Cordillera de Merida Páramo (CMP) (Fig. 1A-C). The change in total annual precipitation (P) is spatially less consistent than temperature (Fig. 1D), increasing in most ecoregions and mainly in the Ethiopian Mountain Moorlands (EMM), except for the ecoregions in Northern South America,

where drier conditions will emerge. Northern South America emerges as the region where HETEs will experience the most intense warming and drying across the Tropics.

Beyond the long-term (LT) changes in T and P, changes in climatic extremes (EX) and Seasonality (SE) are critical to understanding projected climate change impacts on HETEs. The long-term T (Fig. 2A) is expected to increase with a similar spatial pattern as the maximum temperature of the warmest month (T_{mw}; Fig. 2C), with the East African Mountain Moorlands (EAMM) in the Afrotropics and the Central Range sub-alpine Grasslands (CRSG) in Australasia experiencing the overall smallest changes. On the other hand, although P will increase in more than half of the ecoregions (Fig. 2B), the precipitation of the driest month (P_d; Fig. 2D) will decrease in most ecoregions, accentuating dry extremes, especially in the Neotropics. Precipitation seasonality (P_s; Fig. 2F) and temperature seasonality (T_s; Fig. 2E) will also increase consistently across most ecoregions and biogeographical realms, following the trends observed in the long-term means and extremes of temperature.

3.2. Baseline and projected hydroclimatic spaces

We have constructed a two-dimension hydroclimatic space for the baseline long-term (LT), extremes (EX), and Seasonality (SE) conditions in each HETE ecoregion based on the corresponding selected variables describing water and energy availability (See Table 1). By constructing them likewise for the future, we are able to calculate the changes in these hydroclimatic spaces over time and reveal the potential impacts of climate change on HETEs.

The magnitude and extent of the trajectories represented in the hydroclimatic space by these changes differ among ecoregions, as expressed by their direction (θ), intensity (I), and severity (S) of change (Fig. 3; Fig. S3): geometric parameters used to assess the characteristics of the change (see methods). For instance, the Central Range sub-alpine Grasslands of Australasia (CRSG; Fig. 3A) will experience conditions of energy and water availability in the future period 2071-2100 that fall outside of the three current baseline hydroclimatic spaces (i.e., LT, EX, SE) across half of the HETEs spatial extent (i.e., area of the yellow polygons without intersection with the blue polygon).

We refer to areas within both blue and yellow polygons as safe hydroclimatic spaces since the future hydroclimatic conditions experienced by the HETEs are within the envelope of conditions of the current baseline. Conversely, we refer to the areas of yellow polygons not intersected by the blue polygons as breached hydroclimatic spaces, as future hydroclimatic conditions will be outside of the envelope of current baseline hydroclimatic conditions.

In the case of the Cordillera de Merida Páramo in the Neotropics (CMP; Fig. 3B), the full ecosystem's spatial extent will experience conditions falling outside the envelope representing the baseline LT, EX, SE hydroclimatic spaces. In this sense, we refer to a full breach of the hydroclimatic space in CMP in the future (i.e., S=100%). In addition, the intensity (I) of the breaching is highest in CMP, judging by the separation between current and future envelopes of temperature and precipitation. Breaching the LT and EX baseline hydroclimatic spaces is primarily due to the increasing temperature rather than precipitation changes (lower θ) in both CRSG and CMP ecoregions.

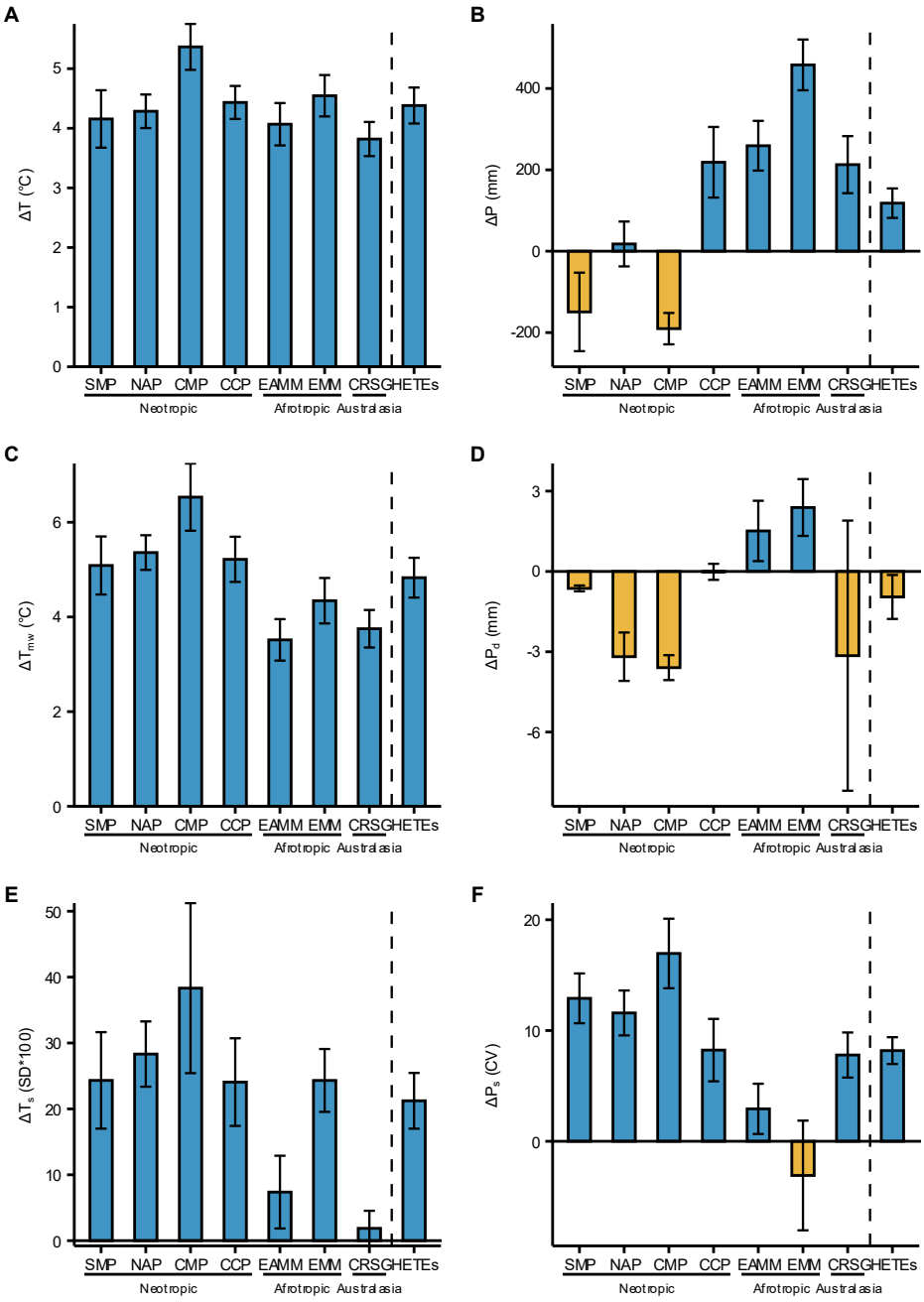

Figure 2. Change in the six hydroclimatic parameters that comprise the baseline hydroclimatic spaces of HETEs related to long-term means, extremes, and seasonality of temperature and precipitation. The parameters include: (A) mean annual temperature T, (B) total annual precipitation P, (C) maximum temperature of the warmest month T_{mw}, (D) precipitation of driest month P_d, (E) temperature seasonality T_s, and (F) precipitation seasonality P_s. Changes are calculated between 1985-2014 and 2071-2100 for each of the seven ecoregions and HETEs overall. Error bars show the standard errors of the six GCMs. Fig. S2 shows the reference (1985-2014) and the projected (2071-2100) mean values of the six hydroclimatic parameters for each ecoregion.

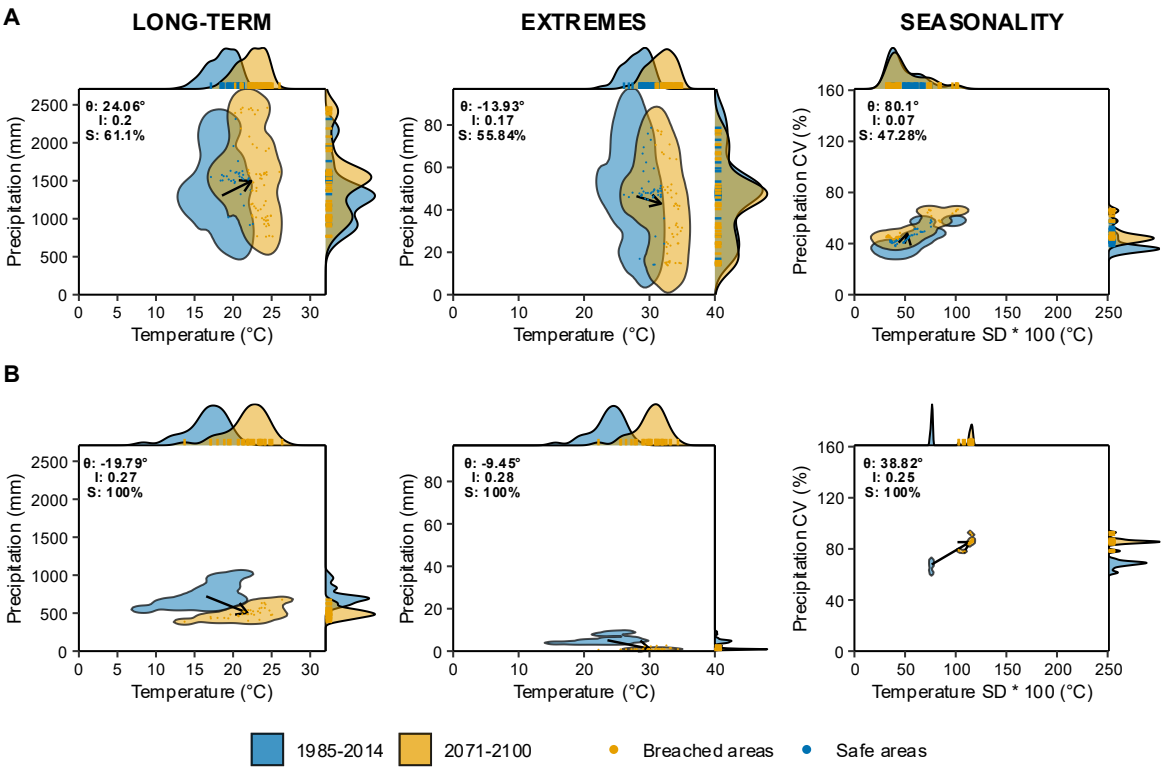

Figure 3. Case studies of current baseline (1985-2014) and future (2071-2100) hydroclimatic spaces of water and energy availability for long-term (LT), extreme (EX), and seasonality conditions (SE). (A) Central Range sub-alpine Grasslands (CRSG) and (B) Cordillera de Mérida Páramo (CMP). Polygons represent the hydroclimatic spaces, and arrows represent the mean trajectories of their change as expressed by the movement of the centroids of the polygons between 1985-2014 and 2071-2100. The direction of change in degrees (θ) is measured from the right horizontal, accompanied by the normalized intensity of change (I), and the severity of the change (S) is defined as the percentage of the future polygon breaching the boundaries of the current one (See Methods section). Points represent projected values of future hydroclimatic parameters and are colored according to their geometric intersection with the baseline hydroclimatic space of the respective ecoregion. Marginal plots show the 1-dimensional 95% Kernel Densities for the hydroclimatic parameters. Table S1 shows the 95% confidence intervals and standard errors of the indicators from the six CMIP6 GCMs used to build the multimodel ensemble of climate data.

As the hydroclimatic conditions change in the high-elevation tropical ecoregions, future temperature and precipitation will lead to conditions falling even beyond the baseline hydroclimatic spaces of any of the HETEs found globally. An extreme case is that of CRGS, where future hydroclimatic conditions in precipitation and temperature will surpass the current conditions of all HETEs. This will result in 41% and 26% of the ecoregion extent experiencing novel long-term and extreme hydroclimatic conditions, respectively (Fig. S4; Fig. S5). Hence, these HETEs will potentially be under novel hydroclimates and may become novel ecosystems (Hobbs et al., 2009; Ohlemüller, 2011; Starzomski, 2013; Williams et al., 2007; Williams & Jackson, 2007).

3.3. Vulnerability of HETEs to climate change

Locating and quantifying the safe and breached hydroclimatic spaces helps determine the overall vulnerability of HETEs to climate change. The most vulnerable HETEs are concentrated in the Neotropic, particularly the CMP and CCP ecoregions, where the three hydroclimatic spaces (LT,

EX, SE) will be simultaneously breached in 100% and 30% of their spatial extent, respectively (Fig. 4; dark red). In the Afrotropic, the vulnerability level is medium to high, with most of the ecoregion's extent experiencing breaching in one (yellow to light orange) or two safe hydroclimatic spaces (dark orange to red). On the contrary, 25% of the spatial extent of NAP and CRSG have low vulnerability to change as they will remain in safe hydroclimatic spaces across (green). Finally, it is worth noting that ecoregions such as NAP or CRSG present a varying range of vulnerability levels due to their ample spatial coverage and the variability of their orographic conditions.

Overall, only 15% of all the HETEs' spatial extent will have a low vulnerability to climate change, conserving their safe hydroclimatic conditions under the three hydroclimatic spaces. In contrast, about 10% of the spatial extent of HETEs will have their hydroclimatic space breached under all three dimensions, resulting in critical vulnerability, and around 40% will have at least two of their hydroclimatic spaces breached in the future (high vulnerability). This raises concerns for the survival of HETEs by the end of the century.

4. Discussion

Our results show the projected changes in hydroclimatic conditions of HETEs by 2100 under the SSP585 scenario. For instance, in the Neotropics, HETEs will experience regionally variable changes in precipitation, with increments in the south and reductions in the north. Ecoregions in the north will be the only ones to face simultaneous warmer and drier conditions. These patterns are consistent with previous studies that have explored the projected temperature and precipitation changes over the Andes and South America (Almazroui et al., 2021; Arias et al., 2021; Pabón-Caicedo et al., 2020; Tovar et al., 2022). Similarly, other studies agree with the increasing temperature and precipitation patterns we found for HETEs in Africa (Doherty et al., 2010; Engelbrecht et al., 2015) and Australasia (Cámara-Leret et al., 2019; I. Smith et al., 2013) at continental and regional scales. The consistent temperature increments and shifts in precipitation found in this study, which lead to the breaching of the hydroclimatic spaces in the seven ecoregions, could eventually reduce suitable climates for these ecosystems and drive the emergence of novel climates within HETEs. The capacity of high-elevation tropical species to face climate change impacts and avoid local extinctions could be conditioned by the persistence of safe hydroclimatic spaces, their dispersal abilities for reaching analog climates, as well as their capability to adapt to novel climates (Berg et al., 2010; La Sorte & Jetz, 2010; Loarie et al., 2009; Pecl et al., 2017).

Our findings suggest potential breaching within the safe hydroclimatic spaces and increased vulnerability to climate change that will likely affect the persistence of isolated populations and increase the extinction risk of species. This would be particularly impactful in ecoregions such as CMP where, according to our results, HETEs will virtually disappear by 2100. Some studies have indeed assessed the projected impacts of climate change on the biodiversity of HETEs. For instance, it has been reported that species such as *Polylepis quadrijuga* from the Northern Andean treeline or species from the emblematic *Espeletia* complex are highly vulnerable to climate change and will face large reductions in their distribution under future climate change scenarios (Caballero-Villalobos et al., 2021; Valencia et al., 2020). In the CMP, 28

Espeletiinae endemic species are projected to lose, on average, 77% of their geographical extent by 2070 (Mavárez et al., 2019). In the Afrotropic, tropical alpine giant rosette plants such as the endemic *Lobelia rhynchopetalum* are projected to face a very high risk of extinction and losing 82% of their genetic diversity by 2080 due to range reduction and isolation (Chala et al., 2016). Similarly, about 75 species from the humid high-elevation ecoregion in New Guinea will disappear by 2070 under RCP 8.5 scenario (Cámara-Leret et al., 2019).

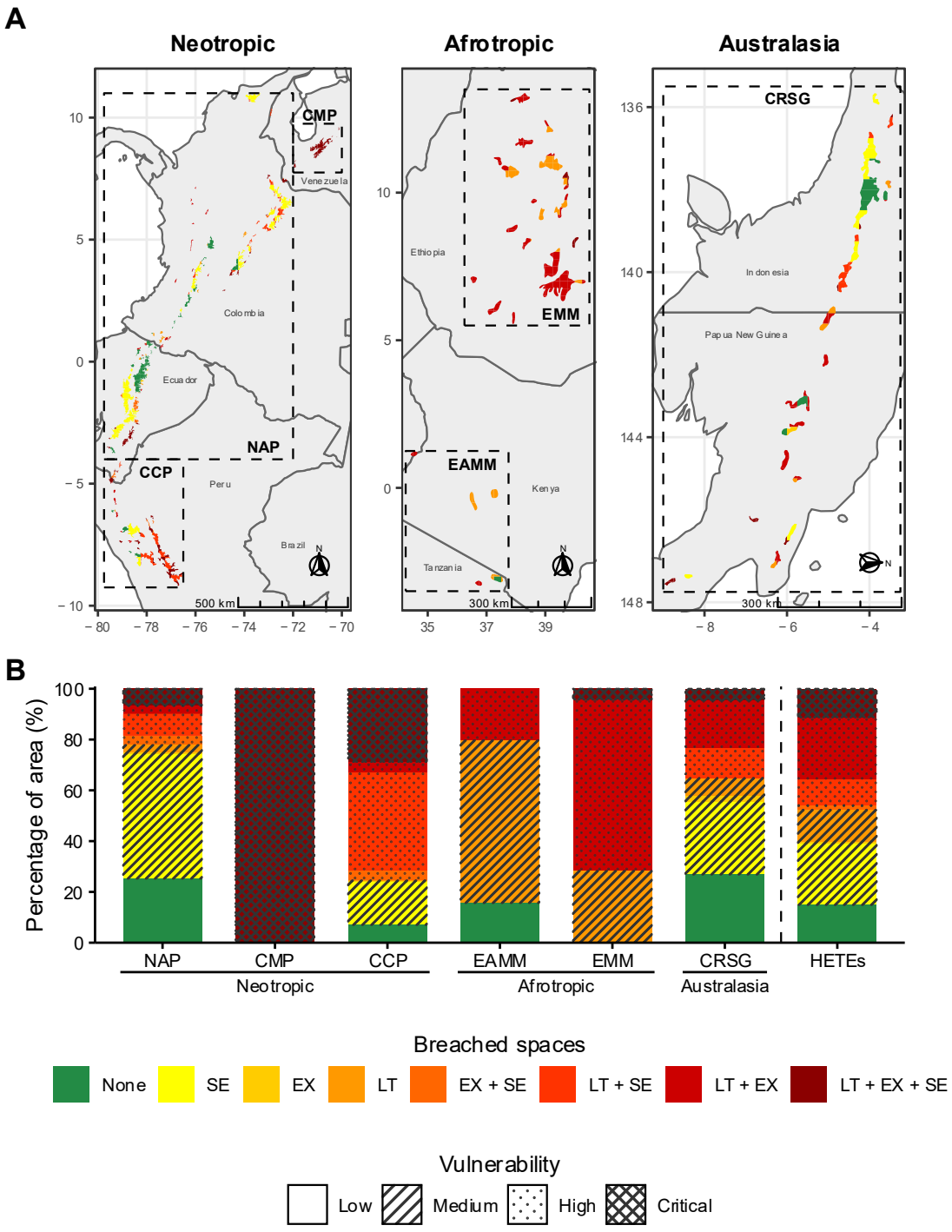

Figure 4. Vulnerability levels to climate change and breaching of hydroclimatic spaces. Classification of vulnerability to climate change in each ecoregion based on A) Location and B) percentage of spatial extent. Colors in A and B represent the combinations and severity of the breached hydroclimatic spaces: long-term (LT), extreme (EX), and seasonality (SE), with green representing no hydroclimatic space breached, and dark red for all three hydroclimatic spaces breached. The patterns translate the number of hydroclimatic spaces being breached into vulnerability categories.

This study also suggests that projected increments in temperature and the overall changes in hydroclimatic spaces toward novel conditions will likely produce upward shifts in the HETEs' vertical distribution in the search for suitable hydroclimatic conditions. With restricted cross-mountain dispersal opportunities due to the expected increment in fragmentation, the extent of elevational range and vertical dispersion capacities of high-elevation tropical species will become critical factors in determining their risk of extinction when facing this threat. These elevational climatic shifts impact birds and plant species with narrow vertical distributions and dispersal constraints because their thermal niches could be surpassed faster, and their capacity to track climate changes moving upward is limited (Freeman et al., 2018; Freeman & Class Freeman, 2014; La Sorte & Jetz, 2010; Polato et al., 2018). Furthermore, high-elevation tropical species have shown to be more responsive to warming by shifting their range upwards faster than high-latitude montane species (Freeman et al., 2021). For instance, it has been reported that Andean plant species can migrate upward from 7 m/decade (Sklenář et al., 2021) to 25 m/decade (Freeman et al., 2021). Therefore, in HETEs with lower maximum elevations, such as in the Afrotropic and Australasia, species with distributions limited to the highest elevations will face a higher extinction risk (Mavárez et al., 2019), as they will have less space to move upward and may be caught in climatic traps (La Sorte & Jetz, 2010).

The breaching of the safe hydroclimatic spaces in some HETEs (Fig. 3; e.g., CMP and CCP) will induce changes in the physiological and functional response of high-elevation tropical vegetation to climate stress and modulate species' adaptation. Temperature stress in HETEs is mainly mediated by the differences in the night-time freezing temperatures and the day-time high temperatures, as well as by the seasonal variations in temperature (Rada et al., 2019; Rundel et al., 1994). Our results show overall consistent increments in T and T_{mw} of about 4.5°C and 5°C in HETEs, respectively, which could increase stress (and plant death) by high day-time and dry-season temperatures. However, the increments could also alleviate night-time freezing stress as rising temperatures are expected to push the frost line upward. These changes will likely benefit the less freeze-resistant species while negatively impacting those more sensitive to high temperatures and evaporative demand.

Water stress in HETEs is mainly accentuated during the dry season when soil water availability decreases and the air evaporative demand increases (Rada et al., 2019; Rundel et al., 1994). Projected reductions in P and P_d in some ecoregions, such as CMP, will exacerbate water stress, particularly during the dry season. According to their stomatal response, water stress-tolerant species have shown to be more successful at dealing with droughts in the Andean Páramo than water stress-avoiding species, suggesting that species with the first strategy would be more likely to adapt to climate change (Sandoval et al., 2019). Similarly, experiments using open-top chambers in the Andes have shown changes in the plant's taxonomic and growth form diversity, mainly by a progressive increment of lower elevation species of tussock grasses and

shrubs and a reduction of rosettes (Duchicela et al., 2021; Lasso et al., 2021). Tree species and giant rosettes in HETEs will then be more susceptible to higher temperatures and lower precipitation than herbaceous and shrub species. We expect the CMP and the NAP to experience shifts in community structure and composition by increasing the dominance of herbaceous and shrub species with climate change (Llambí & Rada, 2019; Rada et al., 2019; Sandoval et al., 2019).

Differences in the thermal sensitivities and the dispersal capacities, among other traits at the specific level, will also produce changes at the community level, e.g., due to the disruption of biotic interactions through spatial and temporal mismatches in phenology and dispersal (Berg et al., 2010; Gilman et al., 2010; Rasmann et al., 2014; Tovar et al., 2020; Tylianakis et al., 2008). In addition, breaching baseline spaces toward novel hydroclimatic conditions could result in migration from lower elevations, inducing community changes or even generating novel ones (Hobbs et al., 2009; Lurgi et al., 2012; Williams & Jackson, 2007).

These changes in vegetation structure and composition can modify HETE functioning, impacting its hydrology and water regulation capacity. For instance, changes in the vegetation structure could alter the interception of fog and the contribution of occult or horizontal precipitation to the water balance of HETEs, which is up to ca. 30% of the precipitation inputs in Andean páramos (Cárdenas et al., 2017). In tropical montane cloud forests, cloud water interception can reach 5% to 75% of total precipitation (Bruijnzeel et al., 2011). Additionally, water yield for páramo ecosystems has been reported to be higher, with about 63% of rainfall compared to 57% for cloud forests and 42% for rainforests (Cárdenas et al., 2018; Tobón, 2009). It has been reported that projected changes in hydroclimatic conditions will also impact cloud immersion, reducing the area of both tropical montane cloud forests and páramo in South America by up to 86% and 98%, respectively, with some ecoregions in northern South America, such as CMP, reaching 100% of projected area reduction (Helmer et al., 2019). Despite the difference in methodologies, our results also show a worrying impact on CMP, although the outlook for the rest of South America is more optimistic.

Changes in the dominance of vegetation growth forms resulting from the high vulnerability in the Neotropics, Afrotropics and Australasia could also alter evapotranspiration as vegetation exhibits different response strategies to avoid excessive water losses (Cárdenas et al., 2018). Since vegetation reduces soil humidity loss depending on their cover density and structure (Rodríguez-Morales et al., 2019), changes in vegetation cover can further impact the water yield (Bonnesoeur et al., 2019; Mosquera et al., 2022; Ochoa-Tocachi et al., 2016). Projected changes in the hydroclimatic spaces of HETEs will also directly affect their hydrology and capacity to supply water downstream. Increments in temperature and changes in precipitation patterns and intensity will increase evapotranspiration and modify water inputs to the ecosystem, altering the water balance of HETEs and their water storage capacity. For the specific cases of extreme and seasonal hydroclimatic spaces, our results project that drier seasons and higher temperatures and precipitation seasonality will impact the ability of HETEs to provide continuous and regular water flow downstream (Viviroli et al., 2020). Together, these could affect the constant water requirements of cities and communities around these ecosystems (Viviroli et al., 2020) and water availability for hydropower production and agriculture, thus risking socioeconomic development and food security (Tito et al., 2018; Zhang & Cai, 2011). Beyond water regulation, the provision of other valuable ecosystem services will be impacted by climate change among HETEs in the

Neotropic (Anderson et al., 2011; Diazgranados et al., 2021), Afrotropic (Doherty et al., 2010; Midgley & Bond, 2015; Sintayehu, 2018), and Australasia (Cámara-Leret et al., 2019).

One limitation of our framework of breaching baseline hydroclimatic spaces and vulnerability to climate change is that it does not consider the implications of land use change. Beyond vulnerability to climate change, HETEs are vulnerable to land use and land cover changes (LULC). For instance, productive activities such as floriculture and potato crops can benefit from Andean HETEs' hydroclimatic conditions, which could increase interest in agricultural expansion (Guarderas et al., 2022). This has largely contributed to the degradation, habitat loss, and fragmentation of HETEs in recent decades. Some studies have reported these anthropogenic impacts in the Afro-Alpine Belt, where the main drivers of LULC are linked to increased human population pressure in higher-elevation areas due to high population pressures in lower regions. This has led to natural vegetation degradation by land clearing for farmland, woodcutting, and livestock grazing. The absence of land use policy and climate variability also contribute to LULC in these areas (Gebrehiwot et al., 2021; Jacob et al., 2016). In the Andes, the transformation of HETEs is also driven by agricultural expansion (Guarderas et al., 2022; Peyre et al., 2021; Thompson et al., 2021; Tovar et al., 2012), constraining the dispersal capacities of species by reducing landscape connectivity and threatens their ability to respond to climate change by moving to suitable climates (Chala et al., 2016; Feeley & Silman, 2010; Tovar et al., 2020). It also impacts the water regulation capacity of HETEs by modifying the land cover and the soil properties with alterations in evaporation, runoff, and water seepage rates (Bonnesoeur et al., 2019; Crespo et al., 2010; Ochoa-Tocachi et al., 2016). Due to climate change, farmers in and around HETEs may be forced to change agricultural practices and locations to track suitable climates upwards and maintain yields (Skarbø & VanderMolen, 2016; Tito et al., 2018; Tovar et al., 2012). Such interaction between climate and land use changes can potentially exacerbate the vulnerability of HETEs to global change (Feeley & Silman, 2010; Mantyka-pringle et al., 2012; Oliver & Morecroft, 2014), even beyond those found in this study. Incorporating land use changes and other stressors into the vulnerability analysis of HETEs could help improve the understanding of global change impacts on biodiversity in these ecosystems.

Our findings provide valuable spatially explicit information on the vulnerability of HETEs to climate change and allow for the overall comparison among ecoregions. This information is crucial for enhancing our ability to integrate climate change adaptation measures into policy development and management strategies and prioritize efforts to conserve these key ecosystems. For instance, knowledge of the extent and direction of hydroclimatic changes in HETEs provide criteria for a better selection and implementation of more suitable management strategies, accounting for the plausibility of these ecosystems to maintain their baseline biotic and abiotic features (Christmann & Menor, 2021; Hobbs et al., 2009).

The framework of vulnerability to climate change can also be used for other ecosystems, providing a valuable contribution to biogeography and conservation ecology. Nevertheless, even when we used a bilinear interpolation approach to mitigate the potential impacts of climate data spatial resolution on the definition of hydroclimatic spaces, the resolution of the climate data we employed could impact the accuracy of our modeling. Data with finer resolution can offer more detailed predictions on habitat loss and species distribution changes, particularly in topographically diverse regions. In contrast, coarse-resolution data are better suited for broader,

regional analyses but may overlook important microhabitats and local variations (Franklin et al., 2013; Kriticos & Leriche, 2010; Seo et al., 2009), such as topographically controlled climate variations crucial for certain species (Scherrer & Körner, 2011).

Fine-resolution climate datasets are available for HETEs and have been used in previous studies. However, their accuracy in tropical mountain regions is questionable because of the scarcity of climate monitoring stations and data availability (Hemp & Hemp, 2024). It is crucial to generate fine-resolution climate data for high-elevation ecosystems such as HETEs that account for the complex topography of those areas and allow for more detailed and accurate modeling. Integrated and multiscale monitoring of biodiversity and ecosystem services in HETEs is also key to improving our understanding of climate change's impacts on biodiversity and the functioning of these ecosystems (Llambí et al., 2019). To that end, we need to strengthen the climate and hydrological monitoring network and other current monitoring initiatives in HETEs (Grabherr et al., 2000; Llambí et al., 2019; Ochoa-Tocachi et al., 2018) to reduce data and information deficiencies.

It is worth noting that our results show the potential implications of the effects of climate change on HETEs under the SSP585 scenario. Although these results can seem bleak, analyzing this business-as-usual scenario warns about the impacts of continuing current trends and policies without significant efforts to reduce greenhouse gas emissions or mitigate climate change impacts. Accomplishing climatic goals and agreements is necessary to reduce these emissions and slow down the projected impacts of climate change on high-elevation ecosystems by changing the trajectory of climate change towards more optimistic scenarios.

5. Data availability

The TEOW dataset is available at https://www.worldwildlife.org/publications/terrestrial-ecoregions-of-the-world. The NEX-GDDP-CMIP6 is available at https://www.nccs.nasa.gov/services/data-collections/land-based-products/nex-gddp-cmip6. Data results are available at https://doi.org/10.5281/zenodo.14562653 (Rubiano et al., 2024).

6. Code availability

The R scripts used in this study to process and analyze data are available at https://doi.org/10.5281/zenodo.14559880 (Rubiano, 2024).

7. Acknowledgments

This work was funded by the Big Grants Program of Universidad del Rosario, Colombia, Project 2022-01570 of the Swedish Research Council for Sustainable Development (FORMAS), and Project 2021-05774 of the Swedish Research Council (VR). We thank the NCCS for making the NEX-GDDP-CMIP6 dataset available.

8. Supplementary information

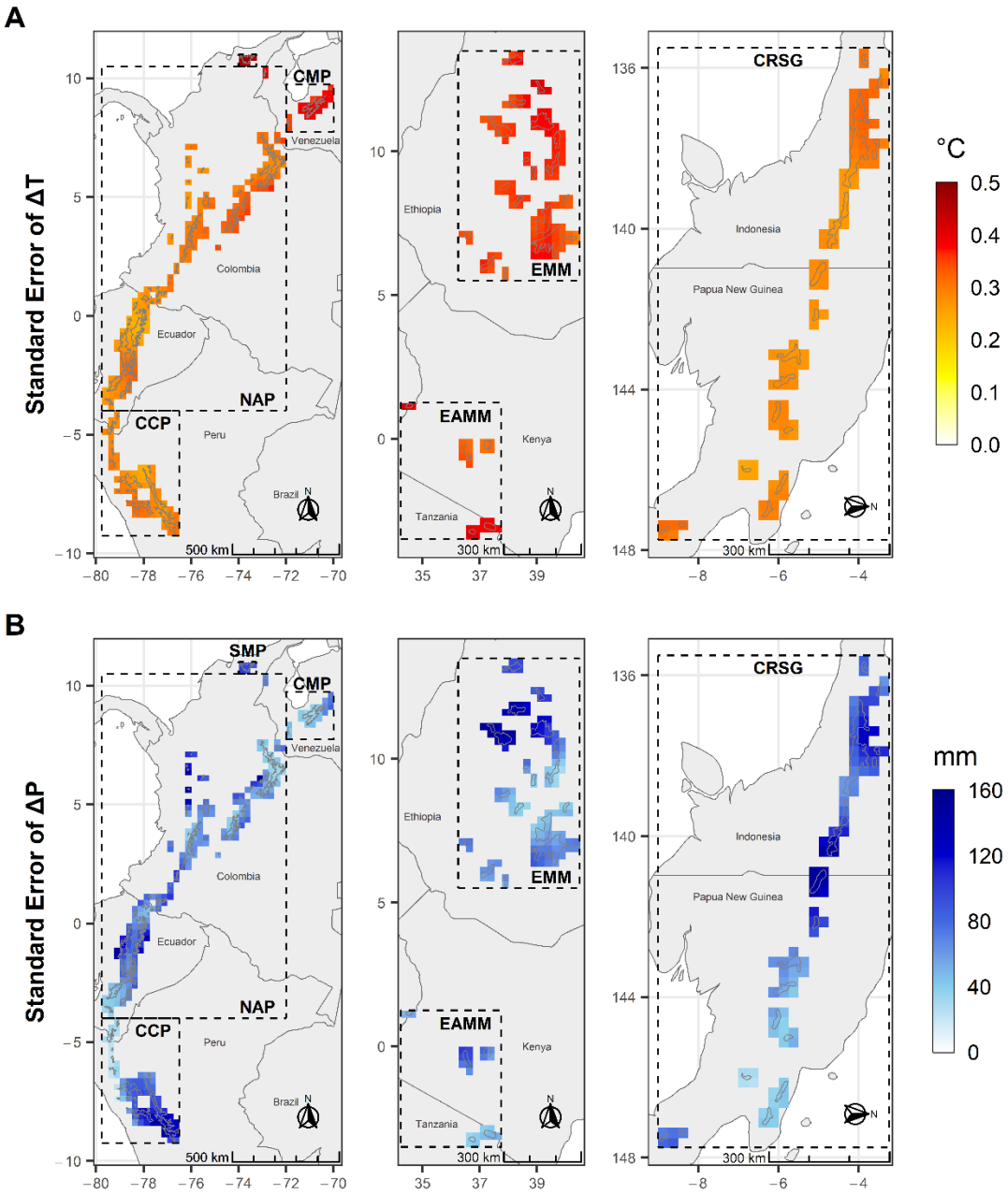

Figure S1. Spatial distribution of standard errors of change. (A) mean annual temperature (ΔT) and (B) total annual precipitation (ΔP) between the 30-year periods 1985-2014 and 2071-2100 for the six GCMs.

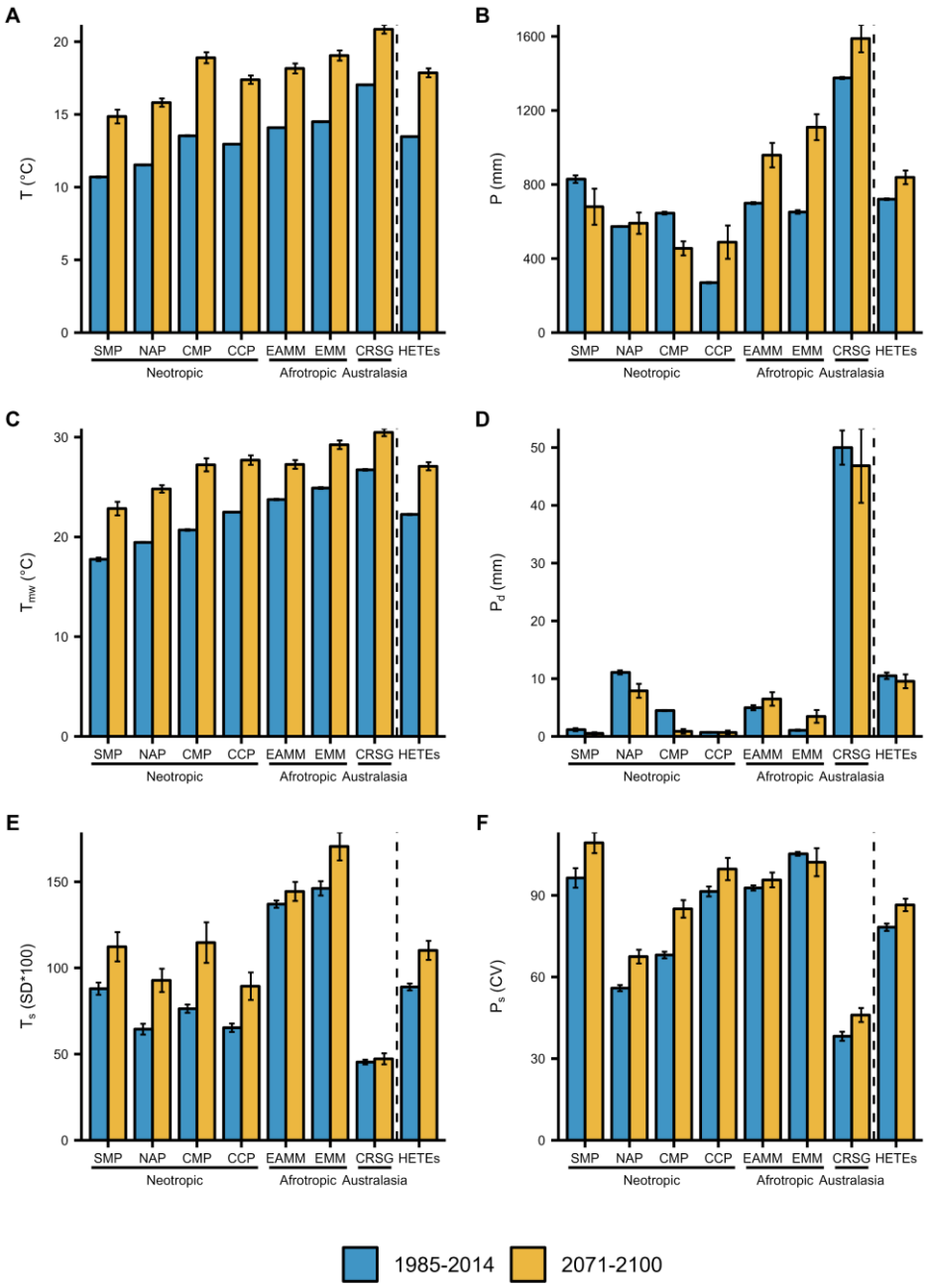

Figure S2. Mean values of (A) mean annual temperature (T), (B) total annual precipitation (P), (C) maximum temperature of the warmest month (T_{mw}), (D) precipitation of driest month (P_d), (E) temperature seasonality (T_s), and (F) precipitation seasonality (P_s) for 1985-2014 and 2071-2100 for each of the seven ecoregions (CRSG: Central Range sub-alpine Grasslands; CCP: Cordillera Central Páramo; CMP: Cordillera de Merida Páramo; EAMM: East African Mountain Moorlands; EMM: Ethiopian Mountain Moorlands; NAP: Northern Andean Páramo; SMP: Santa Marta Páramo) and HETEs overall. Error bars show the standard errors of the six GCMs.

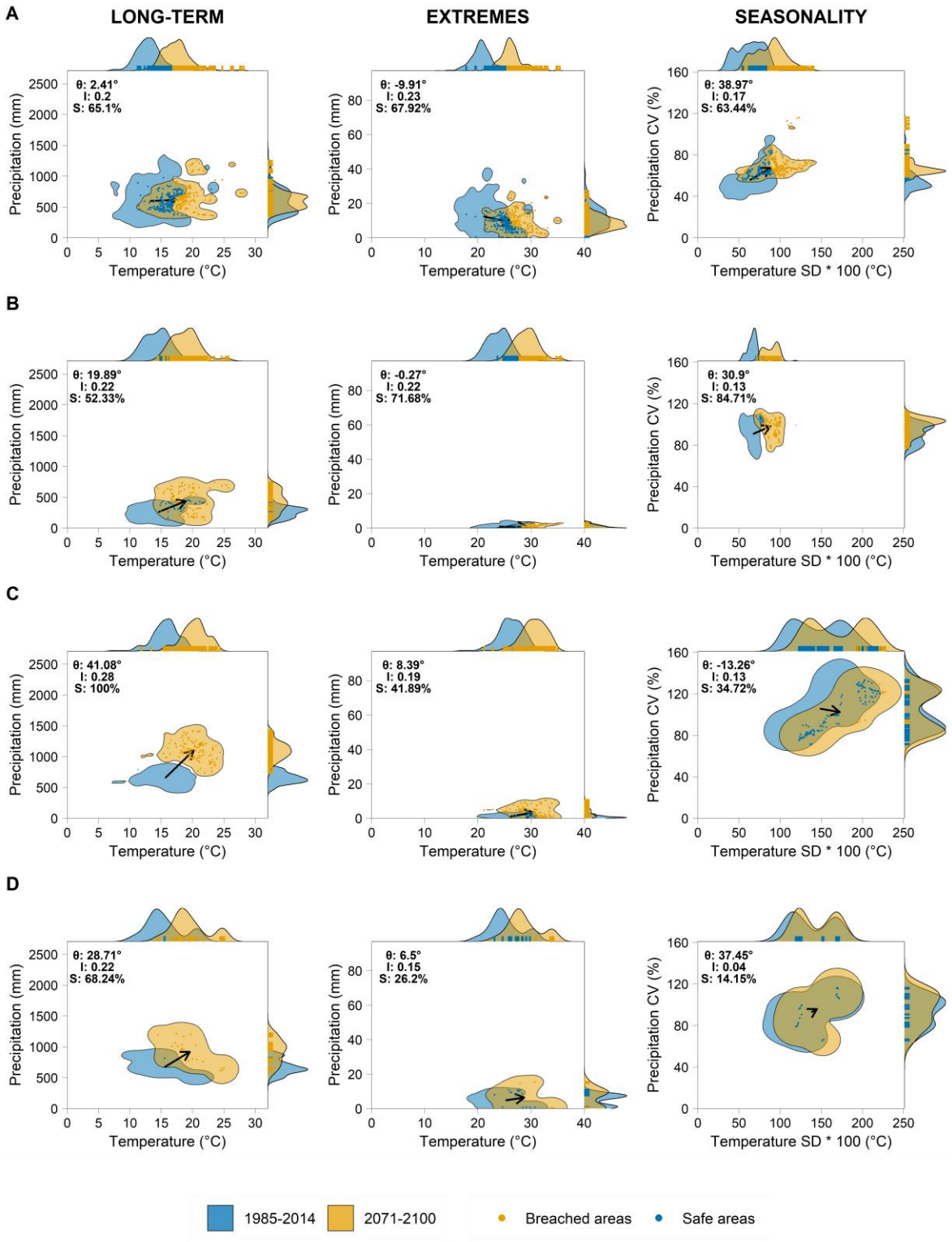

Figure S3. Changes among safe (1985-2014) and future (2071-2100) hydroclimatic spaces in four High-elevation tropical ecoregions. (A) NAP; (B) CCP; (C) EMM; (D) EAMM. Polygons represent the hydroclimatic spaces, and arrows represent the mean trajectory of change as expressed by the movement of the centroids of the polygons between periods. The direction of change in degrees (θ) is measured from the right horizontal, accompanied by the normalized intensity of change (I), and the severity of the change (S) is defined as the percentage of the future polygon breaching the boundaries of the current one. Points represent the projected values of the future hydroclimatic parameters for tropical alpine areas. Marginal plots show the 1-dimensional 95% Kernel Densities for the hydroclimatic parameters. Due to their low number, SMP areas were joined to NAP areas to define the Kernel Densities.

Table S1. 95% confidence intervals and standard errors for direction of change (θ), intensity of change (I), and severity of the change (S) from the six CMIP6 GCMs used to build the multimodel ensemble of climate data.

Hydroclimatic space	Ecoregion	θ			I			S		
		CI lower	CI upper	Std. Error	CI lower	CI upper	Std. Error	CI lower	CI upper	Std. Error
Long term	CRSG	7.42	36.01	5.56	0.16	0.24	0.01	47.89	71.90	4.67
	CCP	-0.70	36.80	7.29	0.18	0.28	0.02	41.95	65.97	4.67
	CMP	-25.86	-11.77	2.74	0.21	0.32	0.02	83.78	101.63	3.47
	EAMM	10.99	44.22	6.46	0.17	0.28	0.02	44.79	84.50	7.72
	EMM	28.37	51.02	4.41	0.22	0.36	0.03	77.59	106.45	5.61
	NAP	-15.26	19.69	6.80	0.18	0.23	0.01	51.58	66.38	2.88
Extremes	CRSG	-51.30	25.60	14.96	0.16	0.23	0.01	40.33	73.19	6.39
	CCP	-2.51	1.63	0.81	0.18	0.26	0.02	52.96	95.85	8.34
	CMP	-13.49	-5.20	1.61	0.21	0.35	0.03	93.67	102.78	1.77
	EAMM	-2.80	13.85	3.24	0.11	0.20	0.02	17.24	41.34	4.69
	EMM	-3.11	19.82	4.46	0.14	0.23	0.02	25.95	51.11	4.89
	NAP	-19.10	-2.02	3.32	0.20	0.26	0.01	57.27	74.84	3.42
Seasonality	CRSG	55.15	128.74	14.31	0.03	0.12	0.02	30.10	52.85	4.42
	CCP	-9.76	65.56	14.65	0.07	0.18	0.02	27.44	97.46	13.62
	CMP	20.46	64.94	8.65	0.10	0.39	0.06	89.99	104.39	2.80
	EAMM	-23.77	141.96	32.24	0.03	0.11	0.01	-0.12	49.82	9.71
	EMM	-63.06	22.71	16.68	0.10	0.19	0.02	18.38	42.69	4.73
	NAP	25.15	53.96	5.60	0.10	0.21	0.02	24.58	67.89	8.42

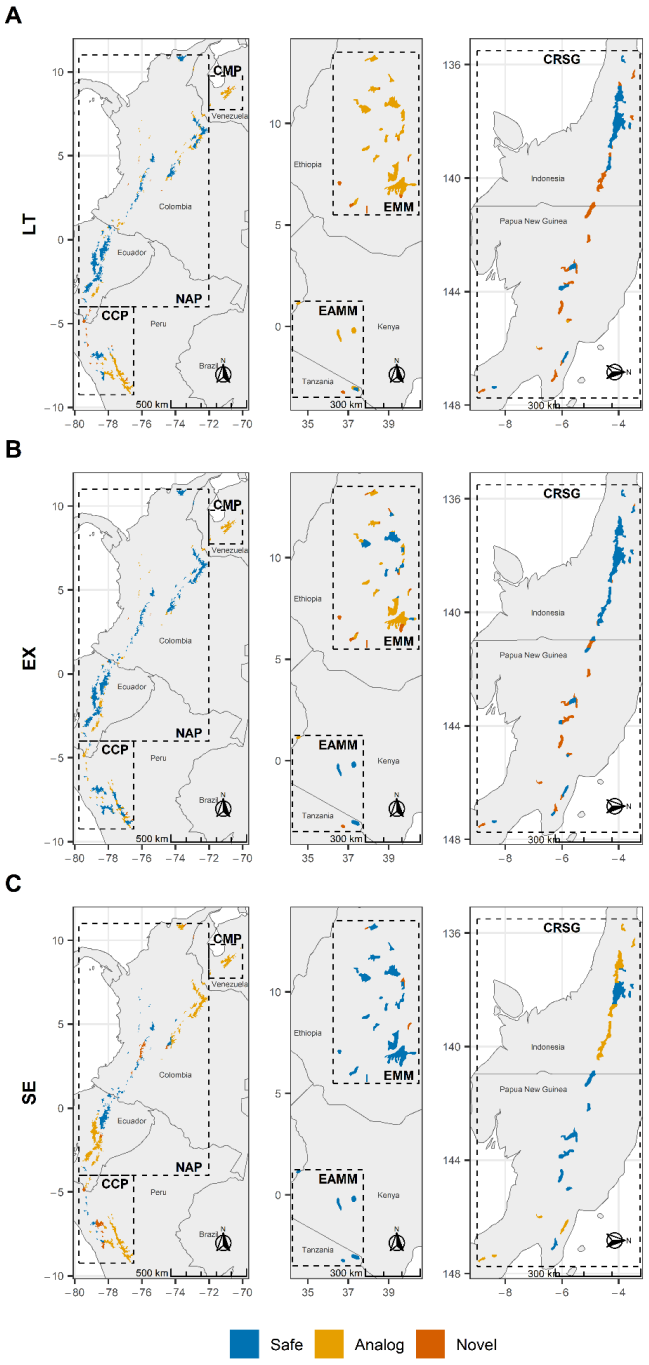

Figure S4. Location of safe and breached hydroclimatic spaces in HETEs between current (1985-2014) and future (2071-2100) 30-year periods. A) Long-term; B) Extreme; and C) Seasonality hydroclimatic spaces. Blue areas refer to areas regarded as safe hydroclimatic spaces since the conditions in the future remain within the envelope of those in the current time period. Yellow areas represent areas where hydroclimatic conditions in the future breach the envelope of conditions in the current period but only in that specific ecoregion. Orange areas represent areas where hydroclimatic conditions in the future breach the current conditions of any High-Elevation Tropical ecoregion. Hence, safe areas are those projected to keep inside their ecoregion's safe hydroclimatic spaces in the future, analog areas are expected to move to other ecoregions' safe hydroclimatic spaces, and novel areas are projected to move beyond any ecoregion's safe hydroclimatic space boundaries.

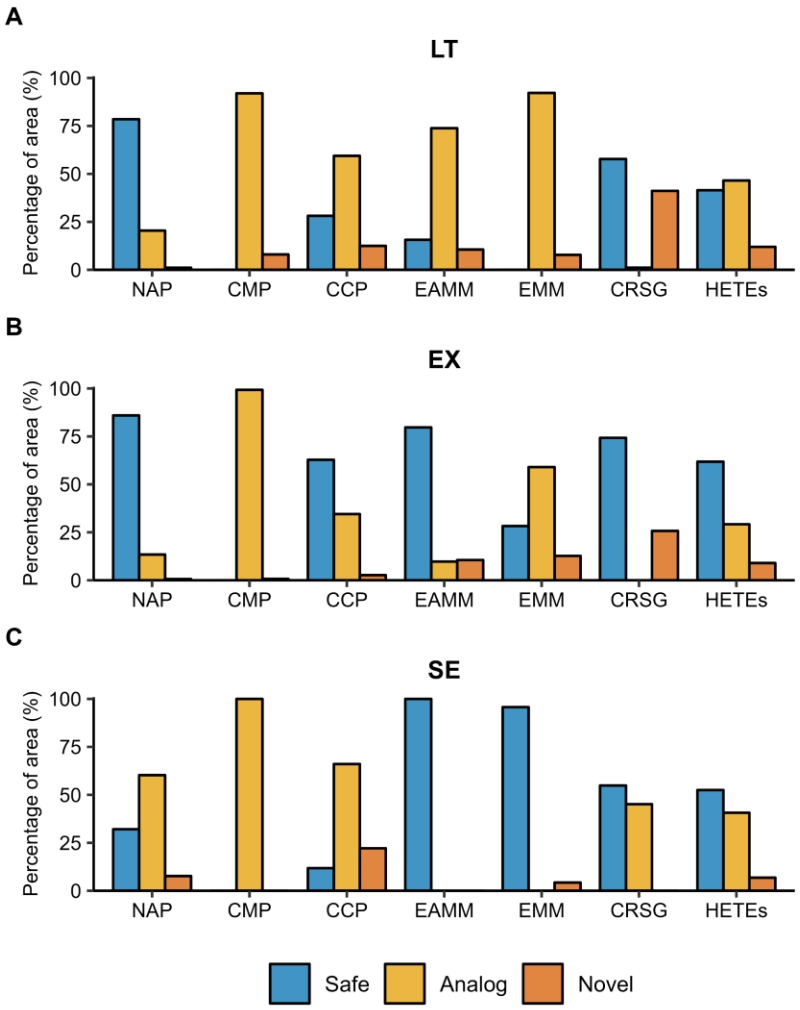

Figure S5. Quantification of safe and breached hydroclimatic spaces in high-elevation tropical ecoregions and HETEs overall between current (1985-2014) and future (2071-2100) 30-year periods. A) Long-term; B) Extreme; and C) Seasonality hydroclimatic spaces. Blue bars refer to areas regarded as safe hydroclimatic spaces since the conditions in the future remain within the envelope of those in the current time period. Yellow areas represent areas where hydroclimatic conditions in the future breach the envelope of conditions in the current period but only in that specific ecoregion. Orange bars represent areas where hydroclimatic conditions in the future breach the current conditions of any high-elevation tropical ecoregion. Hence, safe areas are those projected to keep inside their ecoregion's safe hydroclimatic spaces in the near future, analog areas are expected to move to other ecoregions' safe hydroclimatic spaces, and novel areas are projected to move beyond any HETEs' safe hydroclimatic space boundaries.

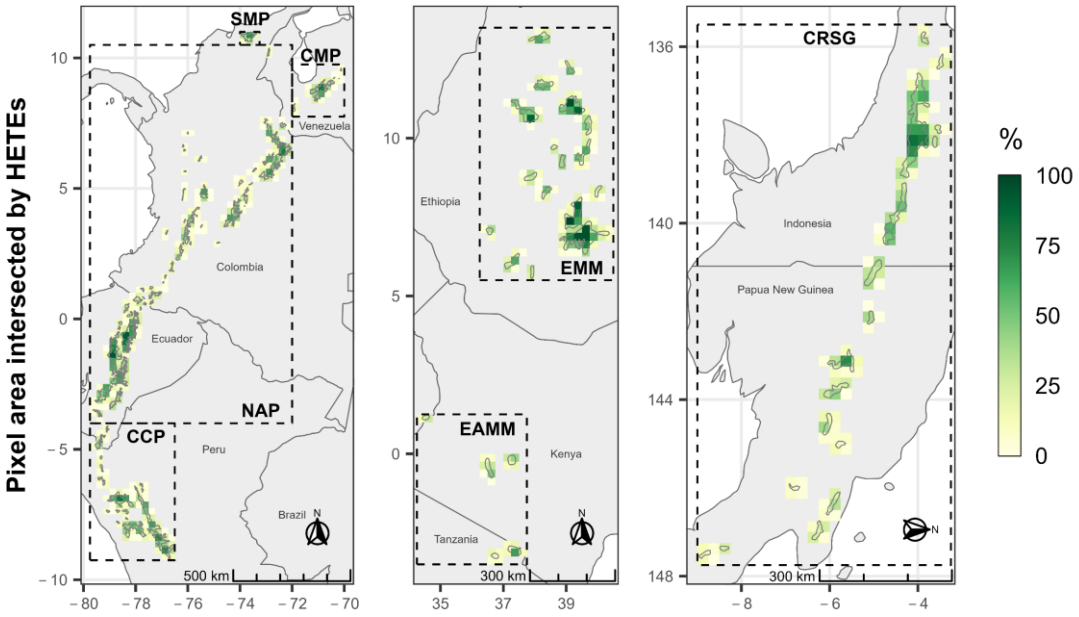

Figure S6. Percentage of climatic data pixels area intersected by HETEs according to TEOW dataset.

Chapter 5

General conclusions

General conclusions

First, we evaluated changes in natural habitat loss and landscape connectivity across Colombia's protected-area system and their buffer zones between the conflict (2009–2016) and post-conflict (2016–2023) periods. Overall, we found that following the 2016 Peace Agreement, both deforestation and the loss of NNFV accelerated, with the latter exceeding deforestation in relative terms. Habitat loss was greater in buffer zones than within PAs and was concentrated in the Andes–Amazon transition belt. We found that although extensive ranching and low-intensity agriculture remain the dominant proximate drivers of LULC change, new pressures such as mining and oil palm have emerged near PAs. These transformation processes led to declines in landscape connectivity that outpaced habitat loss, increasing the risk of ecological isolation for PAs. We also identified the locations most vulnerable to anthropogenic pressures in the post-conflict context.

Second, we estimated deforestation in the Andean region and within its PAs under BAU and GOV scenarios for 2018–2030 and 2030–2050. Under GOV, projected deforestation is lower across all forest types and in both periods, both across the Andes and inside PAs. Under BAU, projected deforestation is widespread, especially in Basal and Fragmented forests. We also identified the PAs most at risk of forest loss under BAU. Overall, the results indicate two clear futures for Andean forests: BAU aligns with continued loss despite formal protection, whereas GOV points to reduced loss under stronger institutions and land-use policies.

Third, focusing on Colombian páramo ecosystems, we found that the Eastern Cordillera is projected to experience the strongest warming and drying signals, with some areas breaching up to three dimensions of their current hydroclimatic space and reaching vulnerability levels from medium to critical (Chapter 4). Breaches are most widespread in the seasonality dimension, implying more irregular intra-annual precipitation and temperature regimes. These shifts may reduce the reliability of water supplies for cities and rural communities and constrain hydropower and agriculture. Overall, these findings provide decision-relevant evidence on the vulnerability of Colombian páramos to future hydroclimatic change.

Taken together, the results of this work advance understanding of the pressures and threats facing key ecosystems and high-value conservation areas in Colombia, notably PAs and Andean ecosystems, amid rapid socio-ecological change and plausible global-change scenarios. Observed declines in habitat amount and landscape connectivity undermine the capacity of PAs to mitigate climate-change impacts and to function as biodiversity refugia. Prospectively, our scenario analyses (BAU, SSP5-8.5) underscore the likely outcomes of maintaining current trajectories and policies without effective measures to curb habitat loss or offset hydroclimatic risks. As such, they provide informative no-action baselines to explore the consequences of inaction. Conversely, governance pathways aligned with improved institutions and land-use policy (GOV) indicate the potential to reduce projected habitat loss and help safeguard connectivity. Together, these insights support evidence-based decision-making and point to complementary priorities for conservation and adaptation. Priority actions

include restoring and maintaining connectivity in PA buffer zones, especially in the Andes–Amazon transition belt, targeting deforestation frontiers under BAU-like pressures, and protecting elevational corridors and headwater landscapes to sustain páramo resilience and downstream water security.

Other products and collaborations

Presentations in scientific conferences

Rubiano, K., Clerici, N., Bottin, M. & Boschetti, L. (2022, July 10-14). *Two decades of land change dynamics within and around the National Natural Park System of Colombia. A remote sensing approach*. In P. Negret & E. Cifuentes (Chairs), Analysing the effects of armed conflict on forest cover, land-use and biodiversity conservation in Colombia (Part 2/2) [Symposium]. 58th Annual Meeting of the Association for Tropical Biology and Conservation, Cartagena, Colombia. https://bit.ly/3kxAgxP

Rubiano, K., Clerici, N. & Jaramillo, F. (2022, December 12-16). *Reduction of Páramo Surface area under future climate change scenarios (B42J-1752)* [Poster presentation]. AGU 2022 Fall Meeting, Chicago, IL, United States. https://bit.ly/3iZmFir

Jaramillo, F., **Rubiano, K.**, Clerici, N., & Sánchez, A. (2023, mayo). *Tropical alpine ecosystems under climate change: Páramos and moorlands in peril*. En *EGU General Assembly Conference Abstracts* (p. EGU-13389). Copernicus Meetings. https://doi.org/10.5194/egusphere-egu23-13389

Popular articles

Rubiano, K., & Barragán Barrera, D. C. (2022). ¿Las áreas protegidas sí están protegiendo nuestra biodiversidad? *Revista Divulgación Científica*, 6(agosto de 2022). Universidad del Rosario. https://doi.org/10.12804/dvcn_10336.36920_num6

Articles published in peer reviewed journals as research collaborations during the PhD

Clerici, N., Cote-Navarro, F., Escobedo, F. J., **Rubiano, K.,** & Villegas, J. C. (2019). Spatio-temporal and cumulative effects of land use-land cover and climate change on two ecosystem services in the Colombian Andes. *Science of the Total Environment*, 685, 1181-1192. https://doi.org/10.1016/j.scitotenv.2019.06.275

Jaramillo, F., Aminjafari, S., Castellazzi, P., Fleischmann, A., Fluet-Chouinard, E., Hashemi, H., Hubinger, C., Martens, H. R., Papa, F., Schöne, T., Tarpanelli, A., Virkki, V., Wang-Erlandsson, L., Abarca-del-Rio, R., Borsa, A., Destouni, G., Di Baldassarre, G., Moore, M-L., Posada-Marín, J. A., Wdowinski, S., Werth, S., Allen, G. H., Argus, D., Elmi, O., Fenoglio, L., Frappart, F., Huggins, X., Kalantari, Z., Munier, S., Palomino-Ángel, S., Robinson, A., **Rubiano, K.**, Siles, G., Simard, M., Song, C., Spence, C., Tourian, M. J., Wada, Y., Wang, C., Wang, J., Yao, F., Berghuijs, W. R., Cretaux, J-F., Famiglietti, J., Fassoni-Andrade, A., Fayne, J. V., Girard, F., Kummu, M., Larson, K. M., Marañón, M., Moreira, D. M., Nielsen, K., Pavelsky, T., Pena, F., Reager, J. T., Rulli, M. C., & Salazar, J. F. (2024). The potential of hydrogeodesy to address water-related and sustainability challenges. *Water Resources Research*, 60(11), e2023WR037020. https://doi.org/10.1029/2023WR037020

Acknowledgments

I wish to thank Prof. Nicola Clerici for supervising this work, for his invaluable mentorship throughout the process, and for funding the project with his research funds.

I am grateful to Prof. Fernando Jaramillo for inviting me to carry out my doctoral research stay under his valuable guidance, and for helping to finance my stay in Sweden and my presentation of results at the AGU 2022 Fall Meeting (Chicago) with his research funds.

I thank Profs. Adriana Sánchez and Luigi Boschetti, and Dr. Marius Bottin, for their guidance on several key topics essential to this work.

I also thank the members of the evaluation committee Prof. Benjamin Quesada, Prof. Camilo Correa, and Prof. Cristian Echeverría for their willingness to review this work and for their valuable comments.

My thanks go to Universidad del Rosario for providing the financial support that made my PhD possible through the Sueño Ser scholarship program.

I am grateful to the Department of Physical Geography at Stockholm University for welcoming me during my research stay, which was crucial to my doctoral training, and for funding the publication of Chapter 3 of this work in Communications Earth & Environment.

I thank the Jardín Botánico de Bogotá, especially the Connectivity and Ecological Interactions team, for trusting in my research skills and allowing me to develop them.

My sincere thanks to Katarina von Greiff and her family for opening their home to me during my stay in Stockholm.

To my family, for their love and unconditional support at every moment, encouraging me to keep going and to complete this process.

To Blanca, for her personal and academic advice, her love, and for always being by my side and providing the energy boost I so often needed to finish this journey. You are a great inspiration for achieving any goal.

To my friends Daniel and Felipe, for their trust and for always making me laugh and encouraging me.

Finally, to all those who, in one way or another, contributed to and were part of this stage of my life: thank you.

Agradecimientos

Quiero agradecer al Prof. Nicola Clerici por la dirección de este trabajo, su valiosa mentoría durante el proceso y por financiar el proyecto con sus fondos de investigación.

Al Prof. Fernando Jaramillo por invitarme a desarrollar mi estancia doctoral bajo su valiosa tutela y por ayudarme a financiar mi estadía en Suecia y la presentación de resultados de investigación en la AGU 2022 Fall Meeting (Chicago) con sus fondos de investigación.

A los Prof. Adriana Sánchez, Prof. Luigi Boschetti y al Dr. Marius Bottin por su orientación en diversos temas clave para el desarrollo de este trabajo.

A los miembros del comité evaluador Prof. Benjamin Quesada, Prof. Camilo Correa y Prof. Cristian Echeverría por su disposición para revisar este trabajo y por sus valiosas observaciones.

A la Universidad del Rosario por brindarme el apoyo económico necesario para realizar mi doctorado mediante el programa de becas Sueño Ser.

Al Departamento de Geografía Física de la Universidad de Estocolmo por abrirme sus puertas durante mi pasantía, la cual fue clave para mi formación doctoral, y por financiar la publicación del capítulo 3 de este trabajo en la revista Communications Earth & Environment.

Al Jardín Botánico de Bogotá, en especial al equipo de Conectividad e Interacciones Ecológicas por confiar en mis habilidades de investigación y permitirme desarrollarlas.

A Katarina von Greiff y su familia por abrirme las puertas de su hogar durante mi estancia en Estocolmo.

A mi familia por todo el cariño y el apoyo incondicional que me brindaron en todo momento para animarme a avanzar y culminar este proceso.

A Blanca por sus consejos tanto personales como académicos, su amor y por estar siempre a mi lado y ser ese impulso de energía que tantas veces necesité para finalizar este proceso. Eres una gran inspiración para alcanzar cualquier meta.

A mis amigos Daniel y Felipe por su confianza y siempre hacerme reír y animarme.

A todos aquellos quienes de una u otra manera contribuyeron e hicieron parte de esta etapa.

References

Achard, F., Eva, H. D., Stibig, H. J., Mayaux, P., Gallego, J., Richards, T., & Malingreau, J. P. (2002). Determination of deforestation rates of the world's humid tropical forests. *Science*, *297*(5583), 999–1002. https://doi.org/10.1126/science.1070656

Ackerly, D. D., Loarie, S. R., Cornwell, W. K., Weiss, S. B., Hamilton, H., Branciforte, R., & Kraft, N. J. B. (2010). The geography of climate change: Implications for conservation biogeography. *Diversity and Distributions*, *16*(3), 476–487. https://doi.org/10.1111/j.1472-4642.2010654.x

Agudelo-Hz, W. J., Urbina-Cardona, N., & Armenteras-Pascual, D. (2019). Critical shifts on spatial traits and the risk of extinction of Andean anurans: an assessment of the combined effects of climate and land-use change in Colombia. *Perspectives in Ecology and Conservation*, *17*(4), 206–219. https://doi.org/10.1016/j.pecon.2019.11.002

Aide, T. M., Grau, H. R., Graesser, J., Andrade-Nuñez, M. J., Aráoz, E., Barros, A. P., Campos-Cerqueira, M., Chacon-Moreno, E., Cuesta, F., Espinoza, R., Peralvo, M., Polk, M. H., Rueda, X., Sanchez, A., Young, K. R., Zarbá, L., & Zimmerer, K. S. (2019). Woody vegetation dynamics in the tropical and subtropical Andes from 2001 to 2014: Satellite image interpretation and expert validation. *Global Change Biology*, *25*(6), 2112–2126. https://doi.org/10.1111/gcb.14618

Alberdi Nieves, V. (2025). Analysis of Climate Change Impacts on Andean Forests Using Potential Distribution Models (2010-2069). Cuadernos De Investigación Geográfica, 51(1), 89–104. https://doi.org/10.18172/cig.6341

Almazroui, M., Ashfaq, M., Islam, M. N., Rashid, I. U., Kamil, S., Abid, M. A., O'Brien, E., Ismail, M., Reboita, M. S., Sörensson, A. A., Arias, P. A., Alves, L. M., Tippett, M. K., Saeed, S., Haarsma, R., Doblas-Reyes, F. J., Saeed, F., Kucharski, F., Nadeem, I., … Sylla, M. B. (2021). Assessment of CMIP6 Performance and Projected Temperature and Precipitation Changes Over South America. *Earth Systems and Environment*, *5*(2), 155–183. https://doi.org/10.1007/s41748-021-00233-6

Anderson, E. P., Marengo, J., Villalba, R., Halloy, S., Young, B., Cordero, D., Gast, F., Jaimes, E., & Ruiz, D. (2011). Consequences of climate change for ecosystems and ecosystem services in the tropical Andes. In *Climate change and biodiversity in the tropical Andes* (pp. 1–18). Inter-American Institute for Global Change Research (IAI).

Aparecido, L. M. T., Teodoro, G. S., Mosquera, G., Brum, M., Barros, F. de V., Pompeu, P. V., Rodas, M., Lazo, P., Müller, C. S., Mulligan, M., Asbjornsen, H., Moore, G. W., & Oliveira, R. S. (2018). Ecohydrological drivers of Neotropical vegetation in montane ecosystems. In *Ecohydrology* (Vol. 11, Issue 3). John Wiley and Sons Ltd. https://doi.org/10.1002/eco.1932

Arias, P. A., Garreaud, R., Poveda, G., Espinoza, J. C., Molina-Carpio, J., Masiokas, M., Viale, M., Scaff, L., & van Oevelen, P. J. (2021). Hydroclimate of the Andes Part II: Hydroclimate Variability and Sub-Continental Patterns. *Frontiers in Earth Science*, *8*. https://doi.org/10.3389/feart.2020.505467

Armenteras D, Gast F, Villareal H. (2003). Andean forest fragmentation and the representativeness of protected natural areas in the eastern Andes, Colombia. Biol. Conserv. 113(2): 245-256. https://doi.org/10.1016/S0006-3207(02)00359-2

Armenteras, D., Espelta, J. M., Rodríguez, N., & Retana, J. (2017). Deforestation dynamics and drivers in different forest types in Latin America: Three decades of studies (1980–2010). *Global Environmental Change*, *46*, 139–147. https://doi.org/10.1016/j.gloenvcha.2017.09.002

Armenteras, D., Rodríguez, N., & Retana, J. (2009). Are conservation strategies effective in avoiding the deforestation of the Colombian Guyana Shield? Biological Conservation, 142(7), 1411–1419. https://doi.org/10.1016/j.biocon.2009.02.002

Armenteras, D., Rodríguez, N., Retana, J., & Morales, M. (2011). Understanding deforestation in montane and lowland forests of the Colombian Andes. *Regional Environmental Change*, *11*(3), 693–705. https://doi.org/10.1007/s10113-010-0200-y

Armenteras, D., Schneider, L., & Dávalos, L. M. (2019). Fires in protected areas reveal unforeseen costs of Colombian peace. Nature Ecology & Evolution, 3(1), 20–23. https://doi.org/10.1038/s41559-018-0727-8

Auffret, A. G., Plue, J., & Cousins, S. A. O. (2015). The spatial and temporal components of functional connectivity in fragmented landscapes. *Ambio, 44*(Suppl. 1), 51–59. https://doi.org/10.1007/s13280-014-0588-6

Báez, S., Jaramillo, L., Cuesta, F., & Donoso, D. A. (2016). Effects of climate change on Andean biodiversity: a synthesis of studies published until 2015. In *Neotropical Biodiversity* (Vol. 2, Issue 1, pp. 181–194). Taylor and Francis Ltd. https://doi.org/10.1080/23766808.2016.1248710

Baguette, M., Blanchet, S., Legrand, D., Stevens, V. M., & Turlure, C. (2013). Individual dispersal, landscape connectivity and ecological networks. *Biological Reviews, 88*(2), 310–326. https://doi.org/10.1111/brv.12000

Bailey, K. M., McCleery, R. A., Binford, M. W., & Zweig, C. (2016). Land-cover change within and around protected areas in a biodiversity hotspot. *Journal of Land Use Science*, *11*(2), 154-176. https://doi.org/10.1080/1747423X.2015.1086905

Bax, V., & Francesconi, W. (2018). Environmental predictors of forest change: An analysis of natural predisposition to deforestation in the tropical Andes region, Peru. *Applied Geography*, *91*, 99–110. https://doi.org/10.1016/j.apgeog.2018.01.002

Bax, V., & Francesconi, W. (2019). Conservation gaps and priorities in the Tropical Andes biodiversity hotspot: Implications for the expansion of protected areas. Journal of Environmental Management, 232, 387–396. https://doi.org/10.1016/j.jenvman.2018.11.086

Bax, V., Castro-Nunez, A., & Francesconi, W. (2021). Assessment of potential climate change impacts on montane forests in the peruvian andes: Implications for conservation prioritization. *Forests, 12*(3). https://doi.org/10.3390/f12030375

Bede-Fazekas, Á., & Somodi, I. (2020). The way bioclimatic variables are calculated has impact on potential distribution models. *Methods in Ecology and Evolution*, *11*(12), 1559–1570. https://doi.org/10.1111/2041-210X.13488

Bedia, J., Herrera, S., & Gutiérrez, J. M. (2013). Dangers of using global bioclimatic datasets for ecological niche modeling. Limitations for future climate projections. *Global and Planetary Change*, *107*, 1–12. https://doi.org/10.1016/j.gloplacha.2013.04.005

Beger, M., Metaxas, A., Balbar, A. C., McGowan, J. A., Daigle, R., Kuempel, C. D., Treml, E. A., & Possingham, H. P. (2022). Demystifying ecological connectivity for actionable spatial conservation planning. *Trends in Ecology & Evolution, 37*(12), 1079–1091. https://doi.org/10.1016/j.tree.2022.09.002

Bellucci, A., Haarsma, R., Gualdi, S., Athanasiadis, P. J., Caian, M., Cassou, C., Fernandez, E., Germe, A., Jungclaus, J., Kröger, J., Matei, D., Müller, W., Pohlmann, H., Salas y Melia, D., Sanchez, E., Smith, D., Terray, L., Wyser, K., & Yang, S. (2015). An assessment of a multi-model ensemble of decadal climate predictions. *Climate Dynamics*, *44*(9–10), 2787–2806. https://doi.org/10.1007/s00382-014-2164-y

Berg, M. P., Toby Kiers, E., Driessen, G., van der Heijden, M., Kooi, B. W., Kuenen, F., Liefting, M., Verhoef, H. A., & Ellers, J. (2010). Adapt or disperse: understanding species persistence in a changing world. *Global Change Biology*, *16*(2), 587–598. https://doi.org/10.1111/J.1365-2486.2009.02014.X

Bonilla-Mejía, L., & Higuera-Mendieta, I. (2019). Protected areas under weak institutions: Evidence from Colombia. *World Development*, *122*, 585-596. https://doi.org/10.1016/j.worlddev.2019.06.019

Bonnesoeur, V., Locatelli, B., Guariguata, M. R., Ochoa-Tocachi, B. F., Vanacker, V., Mao, Z., Stokes, A., & Mathez-Stiefel, S. L. (2019). Impacts of forests and forestation on hydrological services in the Andes: A systematic review. *Forest Ecology and Management*, *433*, 569–584. https://doi.org/10.1016/j.foreco.2018.11.033

Bottin, M. (2022). Non overlapping buffers for the Colombian parks. https://github.com/marbotte/ecolMisc/blob/main/nonOverlapBuffers/finalDoc/colombianParks.md

Boucher, O., Servonnat, J., Albright, A. L., Aumont, O., Balkanski, Y., Bastrikov, V., Bekki, S., Bonnet, R., Bony, S., Bopp, L., Braconnot, P., Brockmann, P., Cadule, P., Caubel, A., Cheruy, F., Codron, F., Cozic, A., Cugnet, D., D'Andrea, F., ... Vuichard, N. (2020). Presentation and Evaluation of the IPSL-CM6A-LR Climate Model. *Journal of Advances in Modeling Earth Systems*, *12*(7). https://doi.org/10.1029/2019MS002010

Bradley, R. S., Vuille, M., Diaz, H. F., & Vergara, W. (2006). Threats to water supplies in the tropical Andes. *Science*, *312*(5781), 1755-1756. https://doi.org/10.1126/science.1128087

Bradley, R.S., Keimig, F.T., & Diaz, H.F. (2004). Projected temperature changes along the American cordillera and the planned GCOS network. *Geophysical Research Letters* 31, L16210. https://doi.org/10.1029/2004GL020229.

Bradshaw, C. J., Sodhi, N. S., & Brook, B. W. (2009). Tropical turmoil: A biodiversity tragedy in progress. In *Frontiers in Ecology and the Environment* (Vol. 7, Issue 2, pp. 79–87). John Wiley & Sons, Ltd. https://doi.org/10.1890/070193

Brockerhoff, E. G., Barbaro, L., Castagneyrol, B., Forrester, D. I., Gardiner, B., González-Olabarria, J. R., Lyver, P. O. B., Meurisse, N., Oxbrough, A., Taki, H., Thompson, I. D., van der Plas, F., & Jactel, H. (2017). Forest biodiversity, ecosystem functioning and the provision of ecosystem services. In *Biodiversity and Conservation* (Vol. 26, Issue 13, pp. 3005–3035). Springer Netherlands. https://doi.org/10.1007/s10531-017-1453-2

Brodie, J. F., Gonzalez, A., Mohd-Azlan, J., Nelson, C. R., Tabor, G., Vasudev, D., Zeller, K. A., & Fletcher, R. J., Jr. (2025). A well-connected Earth: The science and conservation of organismal movement. *Science, 388*(6745), eadn2225. https://doi.org/10.1126/science.adn2225

Bruijnzeel, L. A., Mulligan, M., & Scatena, F. N. (2011). Hydrometeorology of tropical montane cloud forests: Emerging patterns. *Hydrological Processes*, *25*(3), 465–498. https://doi.org/10.1002/hyp.7974

Burgess, N., Hales, J., Underwood, E., Dinerstein, E., Olson, D., Itoua, I., Schipper, J., Ricketts, T., & Newman, K. (2004). *Terrestrial ecoregions of Africa and Madagascar: a conservation assessment*.

Buytaert, W., & Bievre, B. De. (2012). Water for cities: The impact of climate change and demographic growth in the tropical Andes. *Water Resources Research*, *48*(8). https://doi.org/10.1029/2011WR011755

Buytaert, W., Célleri, R., De Bièvre, B., Cisneros, F., Wyseure, G., Deckers, J., & Hofstede, R. (2006). Human impact on the hydrology of the Andean páramos. *Earth-Science Reviews*, *79*(1–2), 53–72. https://doi.org/10.1016/j.earscirev.2006.06.002

Buytaert, W., Cuesta-Camacho, F., & Tobón, C. (2011). Potential impacts of climate change on the environmental services of humid tropical alpine regions. *Global Ecology and Biogeography*, *20*(1), 19–33. https://doi.org/10.1111/j.1466-8238.2010585.x

Buytaert, W., Iñiguez, V., & Bièvre, B. De. (2007). The effects of afforestation and cultivation on water yield in the Andean páramo. Forest Ecology and Management, 251(1–2), 22–30. https://doi.org/10.1016/j.foreco.2007.06.035

Caballero-Villalobos, L., Fajardo-Gutiérrez, F., Calbi, M., & Silva-Arias, G. A. (2021). Climate Change Can Drive a Significant Loss of Suitable Habitat for Polylepis quadrijuga, a Treeline Species in the Sky Islands of the Northern Andes. *Frontiers in Ecology and Evolution*, *9*. https://doi.org/10.3389/fevo.2021.661550

Calabrese, J. M., & Fagan, W. F. (2004). A comparison-shopper's guide to connectivity metrics. *Frontiers in Ecology and the Environment, 2*(10), 529–536. https://doi.org/10.1890/1540-9295(2004)002[0529:ACGTCM]2.0.CO;2

Calbi M, Clerici N, Borsch T, Brokamp G (2020) Reconstructing long term high Andean forest dynamics using historical aerial imagery: a case study in Colombia. Forests 11(8):788. https://doi.org/10.3390/f11080788

Calderón-Caro, J., & Benavides, A. M. (2022). Deforestation and fragmentation in the most biodiverse areas in the Western Cordillera of Antioquia (Colombia). *Biota Colombiana*, *23*(1). https://doi.org/10.21068/2539200X.942

Calle-Rendón, B. R., Moreno, F., & Hilário, R. R. (2018). Vulnerability of mammals to land-use changes in Colombia's post-conflict era. Nature Conservation, 29, 79–92. https://doi.org/10.3897/natureconservation.29.28943

Cámara-Leret, R., Raes, N., Roehrdanz, P., De Fretes, Y., Heatubun, C. D., Roeble, L., Schuiteman, A., Van Welzen, P. C., & Hannah, L. (2019). Climate change threatens New Guinea's biocultural heritage. *Sci. Adv*, *5*. http://advances.sciencemag.org/

Canavire-Bacarreza, G., Diaz-Gutierrez, J. E., & Hanauer, M. M. (2018). Unintended consequences of conservation: Estimating the impact of protected areas on violence in Colombia. Journal of Environmental Economics and Management, 89, 46–70. https://doi.org/10.1016/j.jeem.2018.02.004

Cárdenas, M. F., Tobón, C., & Buytaert, W. (2017). Contribution of occult precipitation to the water balance of páramo ecosystems in the Colombian Andes. *Hydrological Processes*, *31*(24), 4440–4449. https://doi.org/10.1002/hyp.11374

Cárdenas, M. F., Tobón, C., Rock, B. N., & del Valle, J. I. (2018). Ecophysiology of frailejones (Espeletia spp.), and its contribution to the hydrological functioning of páramo ecosystems. *Plant Ecology*, *219*(2), 185–198. https://doi.org/10.1007/s11258-017-0787-x

Carilla, J., Araoz, E., Acosta, O. O., Malizia, A., Malizia, M., Jimenez, Y., ... & Llambí, L. D. (2023). Long-term environmental and social monitoring in the Andes: State of the art, knowledge gaps, and priorities for an integrated agenda. *Mountain Research and Development*, *43*(2), A1-A9. https://doi.org/10.1659/mrd.2022.00018

Castellanos-Mora, L., & Agudelo-Hz, W. (2021). Spatial Scenarios of Land-Use/Cover Change for the Management and Conservation of Paramos and Andean Forests in Boyacá, Colombia. *Environmental Sciences Proceedings*, *3*(1), 87. https://doi.org/10.3390/IECF2020-08023

Castiblanco, C., Etter, A., & Aide, T. M. (2013). Oil palm plantations in Colombia: A model of future expansion. Environmental Science and Policy, 27, 172–183. https://doi.org/10.1016/j.envsci.2013.01.003

Castillo, L. S., Correa Ayram, C. A., Matallana Tobón, C. L., Corzo, G., Areiza, A., González-M., R., Serrano, F., Chalán Briceño, L., Sánchez Puertas, F., More, A., Franco, O., Bloomfield, H., Aguilera Orrury, V. L., Rivadeneira Canedo, C., Morón-Zambrano, V., Yerena, E., Papadakis, J., Cárdenas, J. J., Golden Kroner, R. E., & Godínez-Gómez, O. (2020). Connectivity of Protected Areas: Effect of Human Pressure and Subnational Contributions in the Ecoregions of Tropical Andean Countries. *Land*, 9(8), 239. https://doi.org/10.3390/land9080239

Castillo-Figueroa, D. (2021). Carbon cycle in tropical upland ecosystems: A global review. *Web Ecology, 21*, 109–136. https://doi.org/10.5194/we-21-109-2021

Cavelier, J., & Etter, A. (1995). Deforestation of montane forests in Colombia as a result of illegal plantations of opium (Papaver somniferum). In P. ; Churchill, H. ; Baslev, E. ; Forero, & J. L. Luteyn (Eds.), *Biodiversity and conservation of Neotropical montane forests. Proc. symposium, New York Botanical Garden, 1993* (Issue June 2014, pp. 541–549).

Ceccherini, G., Duveiller, G., Grassi, G., Lemoine, G., Avitabile, V., Pilli, R., & Cescatti, A. (2021). Reply to Wernick, IK et al.; PalahÍ, M. et al. *Nature, 592*(7856), E18–E23.

Célleri, R., & Feyen, J. (2009). The hydrology of tropical andean ecosystems: Importance, knowledge status, and perspectives. *Mountain Research and Development*, *29*(4), 350–355. https://doi.org/10.1659/mrd.00007

Chala, D., Brochmann, C., Psomas, A., Ehrich, D., Gizaw, A., Masao, C. A., Bakkestuen, V., & Zimmermann, N. E. (2016). Good-bye to tropical alpine plant giants under warmer climates? Loss of range and genetic diversity in Lobelia rhynchopetalum. *Ecology and Evolution*, *6*(24), 8931–8941. https://doi.org/10.1002/ECE3.2603

Chaves, M. E., & Arango, N. (1998). Informe nacional sobre el estado de la biodiversidad: Diversidad biológica (Vol. 1). Instituto de Investigación de Recursos Biológicos Alexander von Humboldt.

Chen, M., Vernon, C. R., Graham, N. T., Hejazi, M., Huang, M., Cheng, Y., & Calvin, K. (2020). Global land use for 2015–2100 at 0.05° resolution under diverse socioeconomic and climate scenarios. *Scientific Data*, *7*(1). https://doi.org/10.1038/s41597-020-00669-x

Christmann, T., & Menor, I. O. (2021). A synthesis and future research directions for tropical mountain ecosystem restoration. *Scientific Reports 2021 11:1*, *11*(1), 1–17. https://doi.org/10.1038/s41598-021-03205-y

Clerici, N., Armenteras, D., Kareiva, P., Botero, R., Ramírez-Delgado, J. P., Forero-Medina, G., Ochoa, J., Pedraza, C., Schneider, L., Lora, C., Gómez, C., Linares, M., Hirashiki, C., & Biggs, D. (2020). Deforestation in Colombian protected areas increased during post-conflict periods. *Scientific Reports*, *10*(1), 4971. https://doi.org/10.1038/s41598-020-61861-y

Clerici, N., Bodini, A., Eva, H., Grégoire, J. M., Dulieu, D., & Paolini, C. (2007). Increased isolation of two Biosphere Reserves and surrounding protected areas (WAP ecological complex, West Africa). *Journal for Nature Conservation*, *15*(1), 26-40. https://doi.org/10.1016/j.jnc.2006.08.003

Clerici, N., Cote-Navarro, F., Escobedo, F. J., Rubiano, K., & Villegas, J. C. (2019). Spatio-temporal and cumulative effects of land use-land cover and climate change on two ecosystem services in the Colombian Andes. *Science of the Total Environment*, *685*, 1181–1192. https://doi.org/10.1016/j.scitotenv.2019.06.275

Clerici, N., ed. (2025). Conservation of Andean Forests. Springer. https://doi.org/10.1007/978-3-031-80805-0

Clerici, N., Richardson, J. E., Escobedo, F. J., Posada, J. M., Linares, M., Sanchez, A., & Vargas, J. F. (2016). Colombia: Dealing in conservation. Science, 354(6309), 190. https://doi.org/10.1126/science.aaj1459

Clerici, N., Salazar, C., Pardo-Díaz, C., Jiggins C.D., Richardson, J.E. (2018) Peace in Colombia is a critical moment for Neotropical connectivity and conservation: Save the northern Andes-Amazon biodiversity bridge. *Conservation Letters* 12, e12594. https://doi.org/10.1111/conl.12594

Convention on Biological Diversity. (2025). The Convention on Biological Diversity – Colombia: Country Profile. https://www.cbd.int/countries/profile/?country=co

Correa Ayram, C. A., Etter, A., Díaz-Timoté, J., Rodríguez Buriticá, S., Ramírez, W., & Corzo, G. (2020). Spatiotemporal evaluation of the human footprint in Colombia: Four decades of anthropic impact in highly biodiverse ecosystems. *Ecological Indicators*, *117*, 106630. https://doi.org/10.1016/j.ecolind.2020.106630

Correa-Ayram, C. A., Godínez-Gómez, O., & Murillo-Sandoval, P. J. (2025). Forest Connectivity Loss Surpasses Deforestation in the Colombian Andean Forests. In Conservation of Andean Forests (pp. 175–190). Springer.

Crespo, P., Célleri, R., Buytaert, W., Feyen, J., Iñiguez, V., Borja, P., & De Bievre, B. (2010). Land use change impacts on the hydrology of wet Andean páramo ecosystems. *IAHS-AISH Publication*, *336*, 71–76.

Cresso, M., Clerici, N., Sanchez, A., & Jaramillo, F. (2020). Future climate change renders unsuitable conditions for paramo ecosystems in Colombia. *Sustainability (Switzerland)*, *12*(20), 1–13. https://doi.org/10.3390/su12208373

Curtis, P. G., Slay, C. M., Harris, N. L., Tyukavina, A., & Hansen, M. C. (2018). Classifying drivers of global forest loss. *Science*, *361*, 1108–1111. https://doi.org/10.1126/science.aau3445

Cuyckens, G. A. E., & Renison, D. (2024). Identification of priority areas for the restoration of high Andean mountain forests under climate change: a case study using potential distribution models. *Restoration Ecology*, 32(7), e14193. https://doi.org/10.1111/rec.14193

Dávalos, L. M., Bejarano, A. C., Hall, M. A., Correa, H. L., Corthals, A., & Espejo, O. J. (2011). Forests and drugs: coca-driven deforestation in tropical biodiversity hotspots. *Environmental science & technology*, 45(4), 1219–1227. https://doi.org/10.1021/es102373d

Dávalos, L. M., Sanchez, K. M. & Armenteras, D. (2016). Deforestation and coca cultivation rooted in twentieth-century development projects. *Bioscience* 66, 974–982, https://doi.org/10.1093/biosci/biw118

de Almeida-Rocha, J. M., & Peres, C. A. (2021). Nominally protected buffer zones around tropical protected areas are as highly degraded as the wider unprotected countryside. Biological Conservation, 256. https://doi.org/10.1016/j.biocon.2021.109068

de la Fuente, B., Bertzky, B., Delli, G., Mandrici, A., Conti, M., Florczyk, A. J., Freire, S., Schiavina, M., Bastin, L., & Dubois, G. (2020). Built-up areas within and around protected areas: Global patterns and 40-year trends. Global Ecology and Conservation, 24. https://doi.org/10.1016/j.gecco.2020.e01291

DeFries, R., Hansen, A., Newton, A. C., & Hansen, M. C. (2005). Increasing isolation of protected areas in tropical forests over the past twenty years. Ecological Applications, 15(1), 19–26. https://doi.org/10.1890/03-5258

DeFries, R., Karanth, K. K., & Pareeth, S. (2010). Interactions between protected areas and their surroundings in human-dominated tropical landscapes. Biological Conservation, 143(12), 2870–2880. https://doi.org/10.1016/j.biocon.2010.02.010

Departamento Administrativo Nacional de Estadística (DANE), 2018. Censo Nacional de Población y Vivienda [Online]. https://www.dane.gov.co/index.php/estadisticas-por-tema/demografia-ypoblacion/censo-nacional-de-poblacion-y-vivenda-2018/dondeestamos (Accessed May 27, 2025).

Departamento Administrativo Nacional de Estadística (DANE), 2024. *Producto Interno Bruto (PIB) nacional trimestral*. Available at: https://www.dane.gov.co/index.php/estadisticas-por-tema/cuentas-nacionales/cuentas-nacionales-trimestrales/pib-informacion-tecnica (Accessed May 24, 2024).

Destouni, G., Jaramillo, F., & Prieto, C. (2013). Hydroclimatic shifts driven by human water use for food and energy production. *Nature Climate Change*, *3*(3), 213–217. https://doi.org/10.1038/nclimate1719

Di Gregorio, A., & Jansen, L. J. M. (2005). Land Cover Classification System (LCCS): Classification concepts and user manual. http://www.fao.org/docrep/003/x0596e/x0596e00.htm

Diazgranados, M., Tovar, C., Etherington, T. R., Rodríguez-Zorro, P. A., Castellanos-Castro, C., Rueda, M. G., & Flantua, S. G. A. (2021). Ecosystem services show variable responses to future climate conditions in the Colombian páramos. *PeerJ*, *9*. https://doi.org/10.7717/peerj.11370

Dilts, T. E., Weisberg, P. J., Leitner, P., Matocq, M. D., Inman, R. D., Nussear, K. E., & Esque, T. C. (2016). Multiscale connectivity and graph theory highlight critical areas for conservation under climate change. Ecological Applications, 26(4), 1223–1237. https://doi.org/https://doi.org/10.1890/15-0925

Dimitrov, D., Nogués-Bravo, D., & Scharff, N. (2012). Why Do Tropical Mountains Support Exceptionally High Biodiversity? The Eastern Arc Mountains and the Drivers of Saintpaulia Diversity. *PLOS ONE*, *7*(11), e48908. https://doi.org/10.1371/JOURNAL.PONE.0048908

Doherty, R. M., Sitch, S., Smith, B., Lewis, S. L., & Thornton, P. K. (2010). Implications of future climate and atmospheric CO2 content for regional biogeochemistry, biogeography and ecosystem services across East Africa. *Global Change Biology*, *16*(2), 617–640. https://doi.org/10.1111/j.1365-2486.2009.01997.x

Döscher, R., Acosta, M., Alessandri, A., Anthoni, P., Arsouze, T., Bergman, T., Bernardello, R., Boussetta, S., Caron, L.-P., Carver, G., Castrillo, M., Catalano, F., Cvijanovic, I., Davini, P., Dekker, E., Doblas-Reyes, F. J., Docquier, D., Echevarria, P., Fladrich, U., … Zhang, Q. (2022). The EC-Earth3 Earth system model for the Coupled Model Intercomparison Project 6. *Geosci. Model Dev*, *15*, 2973–3020. https://doi.org/10.5194/gmd-15-2973-2022

Duarte Ritter, C., Muñoz, J., Fabrício Machado, A., Albert, J. S., Ribas, C. C., Carnaval, A. C., Ulloa Ulloa, C., Carrillo, J. D., Tuomisto, H., Armenteras, D., & Guayasamin, J. M. (2025). Indigenous territories and protected areas are crucial for ecosystem connectivity in the Amazon basin. *Proceedings of the National Academy of Sciences of the United States of America*, 122(31), e2418189122. https://doi.org/10.1073/pnas.2418189122

Duchicela, S. A., Cuesta, F., Tovar, C., Muriel, P., Jaramillo, R., Salazar, E., & Pinto, E. (2021). Microclimatic Warming Leads to a Decrease in Species and Growth Form Diversity: Insights From a Tropical Alpine Grassland. *Frontiers in Ecology and Evolution*, *9*. https://doi.org/10.3389/fevo.2021.673655

Dudley, N. (2008). Guidelines for applying protected area management categories. https://doi.org/10.2305/iucn.ch.2008.paps.2.en

Duque, A., Peña, M. A., Cuesta, F., González-Caro, S., Kennedy, P., Phillips, O. L., Calderón-Loor, M., Blundo, C., Carilla, J., Cayola, L., Farfán-Ríos, W., Fuentes, A., Grau, R., Homeier, J., Loza-Rivera, M. I., Malhi, Y., Malizia, A., Malizia, L., Martínez-Villa, J. A., … Feeley, K. J. (2021). Mature Andean forests as globally important carbon sinks and future carbon refuges. *Nature Communications*, *12*(1). https://doi.org/10.1038/s41467-021-22459-8

Dytham, C. (2011). Choosing and using statistics: a biologist's guide. John Wiley & Sons.

Engelbrecht, F., Adegoke, J., Bopape, M. J., Naidoo, M., Garland, R., Thatcher, M., McGregor, J., Katzfey, J., Werner, M., Ichoku, C., & Gatebe, C. (2015). Projections of rapidly rising surface temperatures over Africa under low mitigation. *Environmental Research Letters*, *10*(8). https://doi.org/10.1088/1748-9326/10/8/085004

Espinoza, J. C., Garreaud, R., Poveda, G., Arias, P. A., Molina-Carpio, J., Masiokas, M., Viale, M., & Scaff, L. (2020). Hydroclimate of the Andes Part I: Main Climatic Features. In Frontiers in Earth Science (Vol. 8). Frontiers Media S.A. https://doi.org/10.3389/feart.2020064

Etter, A., & Van Wyngaarden, W. (2000). Patterns of landscape transformation in Colombia, with emphasis in the Andean region. *Ambio*, *29*(7), 432–439. https://doi.org/10.1579/0044-7447-29.7.432

Etter, A., & Villa, A. (2000). Andean Forests and Farming Systems in part of the Eastern Cordillera (Colombia). *Mountain Research and Development*, *20*(3), 236–243. https://doi.org/10.1659/0276-4741(2000)020[0236:AFAFSI]2.0.CO;2

Etter, A., Andrade, A., Saavedra, K., Amaya, P., Cortés, J., & Arévalo, P. (2021). *Ecosistemas colombianos: amenazas y riesgos*. Editorial Pontificia Universidad Javeriana.

Etter, A., McAlpine, C., & Possingham, H. (2008). Historical patterns and drivers of landscape change in Colombia since 1500: A regionalized spatial approach. *Annals of the Association of American Geographers*, *98*(1), 2–23. https://doi.org/10.1080/00045600701733911

Etter, A., McAlpine, C., Wilson, K., Phinn, S., & Possingham, H. (2006). Regional patterns of agricultural land use and deforestation in Colombia. Agriculture, Ecosystems and Environment, 114(2–4), 369–386. https://doi.org/10.1016/j.agee.2005.11.013

Falchetta, G., De Cian, E., Sue Wing, I., & Carr, D. (2024). Global projections of heat exposure of older adults. *Nature Communications*, *15*(1), 3678. https://doi.org/10.1038/s41467-024-47197-5

Feeley, K. J., & Silman, M. R. (2010). Land-use and climate change effects on population size and extinction risk of Andean plants. *Global Change Biology*, *16*(12), 3215–3222. https://doi.org/10.1111/j.1365-2486.2010.02197.x

Fick, S. E., & Hijmans, R. J. (2017). WorldClim 2: new 1-km spatial resolution climate surfaces for global land areas. *International Journal of Climatology*, *37*(12), 4302–4315. https://doi.org/10.1002/JOC.5086

Fischer, R., Taubert, F., Müller, M. S., Groeneveld, J., Lehmann, S., Wiegand, T., & Huth, A. (2021). Accelerated forest fragmentation leads to critical increase in tropical forest edge area. *Science advances*, *7*(37), eabg7012. https://doi.org/10.1126/sciadv.abg7012

Flantua, S., O'Dea, A., Onstein, R. E., Giraldo, C., & Hooghiemstra, H. (2019). The flickering connectivity system of the north Andean páramos. *Journal of Biogeography*, *46*(8), 1808–1825. https://doi.org/10.1111/jbi.13607

Franco, P., Saavedra-Rodríguez, C. A., & Kattan, G. H. (2007). Bird species diversity captured by protected areas in the Andes of Colombia: A gap analysis. ORYX, 41(1), 57–63. https://doi.org/10.1017/S0030605306001372

Franklin, J., Davis, F. W., Ikegami, M., Syphard, A. D., Flint, L. E., Flint, A. L., & Hannah, L. (2013). Modeling plant species distributions under future climates: How fine scale do climate projections need to be? *Global Change Biology*, *19*(2), 473–483. https://doi.org/10.1111/gcb.12051

Freeman, B. G., & Class Freeman, A. M. (2014). Rapid upslope shifts in New Guinean birds illustrate strong distributional responses of tropical montane species to global warming. *Proceedings of the National Academy of Sciences of the United States of America*, *111*(12), 4490–4494. https://doi.org/10.1073/pnas.1318190111

Freeman, B. G., Scholer, M. N., Ruiz-Gutierrez, V., & Fitzpatrick, J. W. (2018). Climate change causes upslope shifts and mountaintop extirpations in a tropical bird community. *Proceedings of the National Academy of Sciences of the United States of America*, *115*(47), 11982–11987. https://doi.org/10.1073/pnas.1804224115

Freeman, B. G., Song, Y., Feeley, K. J., & Zhu, K. (2021). Montane species track rising temperatures better in the tropics than in the temperate zone. *Ecology Letters*, *24*(8), 1697–1708. https://doi.org/10.1111/ele.13762

Fu, W., Liu, S.-L., Cui, B.-S., & Zhang, Z.-L. (2009). A review on ecological connectivity in landscape ecology. *Acta Ecologica Sinica, 29*(11), 6174–6182.

Fundación Gaia Amazonas. (2024). Documento de Bases Teóricas de Algoritmo (ATDB) RAISG-MapBiomas Colombia Colección 2, Apéndice Colombia – Colección 2 de Mapas Anuales de Cobertura y Uso del Suelo de Colombia. https://www.gaiaamazonas.org

García, H., Corzo, G., Isaacs, P., & Etter, A. (2014). Distribución y estado actual de los remanentes del bioma de bosque seco tropical en Colombia: insumos para su gestión. In El bosque seco tropical en Colombia (pp. 228–251). Instituto de Investigación de Recursos Biológicos Alexander von Humboldt.

García-Robledo, C., Kuprewicz, E. K., Staines, C. L., Erwin, T. L., & Kress, W. J. (2016). Limited tolerance by insects to high temperatures across tropical elevational gradients and the implications of global warming for extinction. *PNAS*, *113*(3), 680–685. https://doi.org/10.5883/DS-BOFCR

Garcia-Ulloa, J., Sloan, S., Pacheco, P., Ghazoul, J., & Koh, L. P. (2012). Lowering environmental costs of oil-palm expansion in Colombia. *Conservation Letters*, 5(5), 366–375. https://doi.org/10.1111/j.1755-263X.2012.00254.x

Gaynor, K. M., Fiorella, K. J., Gregory, G. H., Kurz, D. J., Seto, K. L., Withey, L. S., & Brashares, J. S. (2016). War and wildlife: linking armed conflict to conservation. *Frontiers in Ecology and the Environment, 14*(10), 533–542. https://doi.org/10.1002/fee.1433

Gebrehiwot, K., Desalegn, T., Woldu, Z., Demissew, S., & Teferi, E. (2018). Soil organic carbon stock in Abune Yosef afroalpine and sub-afroalpine vegetation, northern Ethiopia. *Ecological Processes*, *7*(6). https://doi.org/10.1186/s13717-018-0117-9

Gebrehiwot, K., Teferi, E., Woldu, Z., Fekadu, Mekbib, Desalegn, Temesgen, & Demissew, S. (2021). Dynamics and drivers of land cover change in the Afroalpine vegetation belt: Abune Yosef mountain range, Northern Ethiopia. *Environment, Development and Sustainability*, *23*, 10679–10701. https://doi.org/10.1007/s10668-020-01079-0

Geldmann, J., Barnes, M., Coad, L., Craigie, I. D., Hockings, M., & Burgess, N. D. (2013). Effectiveness of terrestrial protected areas in reducing habitat loss and population declines. *Biological Conservation* (Vol. 161, pp. 230–238). https://doi.org/10.1016/j.biocon.2013.02.018

Gilman, S. E., Urban, M. C., Tewksbury, J., Gilchrist, G. W., & Holt, R. D. (2010). A framework for community interactions under climate change. *Trends in Ecology & Evolution*, *25*(6), 325–331. https://doi.org/10.1016/j.tree.2010.03.002

Gleeson, E. H., Von Dach, S. W., Flint, C. G., Greenwood, G. B., Price, M. F., Balsiger, J., Nolin, A., & Vanacker, V. (2016). Mountains of Our Future Earth: Defining Priorities for Mountain Research—A Synthesis From the 2015 Perth III Conference. *Mountain Research and Development*, *36*(4), 537–548. https://doi.org/10.1659/MRD-JOURNAL-D-16-00094.1

Godínez-Gómez, O., Correa-Ayram, C., Goicolea, T., & Saura, S. (2025). Makurhini: An R package for comprehensive analysis of landscape fragmentation and connectivity. https://doi.org/10.21203/rs.3.rs-6398746/v1

González, I., Noguera-Urbano, E.A., Velásquez-Tibatá, J. Y J.M. Ochoa-Quintero (2018). Especies endémicas, áreas protegidas y deforestación. En Moreno, L. A, Andrade, G. I. y Goméz, M.F. (Eds.). 2019. Biodiversidad 2018. Estado y tendencias de la biodiversidad continental de Colombia. Instituto de Investigación de Recursos Biológicos Alexander von Humboldt. Bogotá, D. C., Colombia.

González, J., Cubillos, A., Chadid, M., Cubillos, A., Arias, M., Zuñiga, E., Joubert, F., Perez, I., & Berrio, V. (2018). *Caracterización de las principales causas y agentes de la deforestación a nivel nacional período 2005-2015*. Instituto de Hidrología, Meteorología y Estudios Ambientales – IDEAM-. Ministerio de Ambiente y Desarrollo Sostenible. Programa ONU-REDD Colombia.

González-González, A., Villegas, J. C., Clerici, N., & Salazar, J. F. (2021). Spatial-temporal dynamics of deforestation and its drivers indicate need for locally-adapted environmental governance in Colombia. *Ecological Indicators*, *126*. https://doi.org/10.1016/j.ecolind.2021.107695

González-González, A., Villegas, J. C., Clerici, N., & Salazar, J. F. (2021). Spatial-temporal dynamics of deforestation and its drivers indicate need for locally-adapted environmental governance in Colombia. Ecological Indicators, 126. https://doi.org/10.1016/j.ecolind.2021.107695

Grabherr, G., Gottfried, M., & Pauli, H. (2000). GLORIA: A Global Observation Research Initiative in Alpine Environments. *Mountain Research and Development*, *20*(2), 190 – 191. https://doi.org/10.1659/0276-4741(2000)020[0190:GAGORI]2.0.CO;2

Graesser, J., Ramankutty, N., & Coomes, O. T. (2018). Increasing expansion of large-scale crop production onto deforested land in sub-Andean South America. Environmental Research Letters, 13(8), 084021. https://doi.org/10.1088/1748-9326/aad5bf

Grose, M. R., Narsey, S., Trancoso, R., Mackallah, C., Delage, F., Dowdy, A., Di Virgilio, G., Watterson, I., Dobrohotoff, P., Rashid, H. A., Rauniyar, S., Henley, B., Thatcher, M., Syktus, J., Abramowitz, G., Evans, J. P., Su, C. H., & Takbash, A. (2023). A CMIP6-based multi-model downscaling ensemble to underpin climate change services in Australia. *Climate Services*, *30*. https://doi.org/10.1016/j.cliser.2023.100368

Guarderas, P., Smith, F., & Dufrene, M. (2022). Land use and land cover change in a tropical mountain landscape of northern Ecuador: Altitudinal patterns and driving forces. *PLoS ONE*, *17*(7 July). https://doi.org/10.1371/journal.pone.0260191

Haddad, N. M., Brudvig, L. A., Clobert, J., Davies, K. F., Gonzalez, A., Holt, R. D., Lovejoy, T. E., Sexton, J. O., Austin, M. P., Collins, C. D., Cook, W. M., Damschen, E. I., Ewers, R. M.,

Foster, B. L., Jenkins, C. N., King, A. J., Laurance, W. F., Levey, D. J., Margules, C. R., … Townshend, J. R. (2015). Habitat fragmentation and its lasting impact on Earth's ecosystems. *Science Advances*, 1(2), e1500052. https://doi.org/10.1126/sciadv.1500052

Hansen, A. J., & DeFries, R. (2007). Ecological mechanisms linking protected areas to surrounding lands. Ecological Applications, 17(4), 974–988. https://doi.org/10.1890/05-1098

Hansen, M. C., Potapov, P. V, Moore, R., Hancher, M., Turubanova, S. a, Tyukavina, A., Thau, D., Stehman, S. V, Goetz, S. J., Loveland, T. R., Kommareddy, A., Egorov, A., Chini, L., Justice, C. O., & Townshend, J. R. G. (2013). High-Resolution Global Maps of 21st-century forest cover change. *Science (New York, N.Y.)*, *850*(November), 2011–2014. https://doi.org/10.1126/science.1244693

Hanson, T. (2018). Biodiversity conservation and armed conflict: A warfare ecology perspective. *Annals of the New York Academy of Sciences, 1429*(1), 50–65. https://doi.org/10.1111/nyas.13689

Hanson, T., Brooks, T. M., Da Fonseca, G. A. B., Hoffmann, M., Lamoreux, J. F., MacHlis, G., Mittermeier, C. G., Mittermeier, R. A., & Pilgrim, J. D. (2009). Warfare in biodiversity hotspots. *Conservation Biology, 23*(3), 578–587. https://doi.org/10.1111/j.1523-1739.2009.01166.x

Harris, R. M. B., Grose, M. R., Lee, G., Bindoff, N. L., Porfirio, L. L., & Fox-Hughes, P. (2014). Climate projections for ecologists. *Wiley Interdisciplinary Reviews: Climate Change, 5*(5), 621–637. https://doi.org/10.1002/wcc.291

Harsch, M. A., Hulme, P. E., McGlone, M. S., & Duncan, R. P. (2009). Are treelines advancing? A global meta-analysis of treeline response to climate warming. *Ecology Letters*, *12*(10), 1040–1049. https://doi.org/10.1111/j.1461-0248.2009.01355.x

Havlík, P., Schneider, U. A., Schmid, E., Böttcher, H., Fritz, S., Skalský, R., Aoki, K., Cara, S. De, Kindermann, G., Kraxner, F., Leduc, S., McCallum, I., Mosnier, A., Sauer, T., & Obersteiner, M. (2011). Global land-use implications of first and second generation biofuel targets. *Energy Policy*, *39*(10), 5690–5702. https://doi.org/10.1016/j.enpol.2010.03.030

Hazzi, N. A., Moreno, J. S., Ortiz-Movliav, C., & Palacio, R. D. (2018). Biogeographic regions and events of isolation and diversification of the endemic biota of the tropical Andes. Proceedings of the National Academy of Sciences of the United States of America, 115(31), 7985–7990. https://doi.org/10.1073/pnas.1803908115

Heino, M., Kummu, M., Makkonen, M., Mulligan, M., Verburg, P. H., Jalava, M., & Räsänen, T. A. (2015). Forest loss in protected areas and intact forest landscapes: A global analysis. *PLoS ONE*, *10*(10), e0138918. https://doi.org/10.1371/journal.pone.0138918

Helmer, E. H., Gerson, E. A., Baggett, L. S., Bird, B. J., Ruzycki, T. S., & Voggesser, S. M. (2019). *Neotropical cloud forests and páramo to contract and dry from declines in cloud immersion and frost*. https://doi.org/10.1371/journal.pone.0213155

Hemp, A., & Hemp, J. (2024). Weather or not—Global climate databases: Reliable on tropical mountains? *PLoS ONE*, *19*(3 March). https://doi.org/10.1371/journal.pone.0299363

Hending, D., Randrianarison, H., Andriamavosoloarisoa, N.N.M. *et al.* Forest fragmentation and its associated edge-effects reduce tree species diversity, size, and structural diversity in Madagascar's transitional forests. *Biodivers Conserv* **32**, 3329–3353 (2023). https://doi.org/10.1007/s10531-023-02657-0

Hijmans, R. J., Phillips, S., Leathwick, J., & Elith, J. (2021). *dismo: Species Distribution Modeling*. https://CRAN.R-project.org/package=dismo

Hilty, J., Worboys, G. L., Keeley, A., Woodley, S., Lausche, B., Locke, H., Carr, M., Pulsford, I., Pittock, J., White, J. W., Theobald, D. M., Levine, J., Reuling, M., Watson, J. E. M., Ament, R., & Tabor, G. M. (2020). *Guidelines for conserving connectivity through ecological networks and corridors* (Best Practice Protected Area Guidelines Series No. 30). IUCN. https://doi.org/10.2305/IUCN.CH.2020.PAG.30.en

Hobbs, R. J., Higgs, E., & Harris, J. A. (2009). Novel ecosystems: implications for conservation and restoration. *Trends in Ecology and Evolution*, *24*(11), 599–605. https://doi.org/10.1016/j.tree.2009.05.012

Hoffmann, C., García Márquez, J. R., & Krueger, T. (2018). A local perspective on drivers and measures to slow deforestation in the Andean-Amazonian foothills of Colombia. Land Use Policy, 77, 379–391. https://doi.org/10.1016/j.landusepol.2018.04.043

Hoffmann, S. Challenges and opportunities of area-based conservation in reaching biodiversity and sustainability goals. *Biodivers Conserv* **31**, 325–352 (2022). https://doi.org/10.1007/s10531-021-02340-2

Hofstede, R., Mena V, P., & Segarra, P. (2003). *Los páramos del mundo: Proyecto Atlas Mundial de los Páramos*. IUCN: International Union for Conservation of Nature.

Hollister, J., Shah, T., Nowosad, J., Robitaille, A., Beck, M., & Johnson, M. (2023). *elevatr: Access Elevation Data from Various APIs*. doi:10.5281/zenodo.8335450, R package version 0.99.0, https://github.com/jhollist/elevatr/.

Hooper, D. U., Adair, E. C., Cardinale, B. J., Byrnes, J. E. K., Hungate, B. A., Matulich, K. L., Gonzalez, A., Duffy, J. E., Gamfeldt, L., & Connor, M. I. (2012). A global synthesis reveals biodiversity loss as a major driver of ecosystem change. *Nature 2012 486:7401*, *486*(7401), 105–108. https://doi.org/10.1038/nature11118

Hribljan, J. A., Suárez, E., Heckman, K. A., Lilleskov, E. A., & Chimner, R. A. (2016). Peatland carbon stocks and accumulation rates in the Ecuadorian páramo. *Wetlands Ecology and Management*, *24*(2), 113–127. https://doi.org/10.1007/s11273-016-9482-2

Hurtt, G. C., Chini, L. P., Frolking, S., Betts, R. A., Feddema, J., Fischer, G., Fisk, J. P., Hibbard, K., Houghton, R. A., Janetos, A., Jones, C. D., Kindermann, G., Kinoshita, T., Klein Goldewijk, K., Riahi, K., Shevliakova, E., Smith, S., Stehfest, E., Thomson, A., … Wang, Y. P. (2011). Harmonization of land-use scenarios for the period 1500-2100: 600 years of global gridded annual land-use transitions, wood harvest, and resulting secondary lands. *Climatic Change*, *109*(1), 117–161. https://doi.org/10.1007/s10584-011-0153-2

Ibisch, P. L., Hoffmann, M. T., Kreft, S., Pe'er, G., Kati, V., Biber-Freudenberger, L., DellaSala, D. A., Vale, M. M., Hobson, P. R., & Selva, N. (2016). A global map of roadless areas and their conservation status. Science (New York, N.Y.), 354(6318), 1423–1427. https://doi.org/10.1126/science.aaf7166

IDEAM (Instituto de Hidrología, Meteorología y Estudios Ambientales), Instituto de Investigación de Recursos Biológicos Alexander von Humboldt (Instituto Humboldt), Instituto de Investigaciones Marinas y Costeras José Benito Vives de Andréis (Invemar) e Instituto Geográfico Agustín Codazzi (IGAC). (2017) Memoria técnica. Mapa de ecosistemas continentales, costeros y marinos de Colombia (MEC), escala 1:1000. 170 pp.

IDEAM, & MADS. (2025). Actualización de cifras de monitoreo de la superficie de bosque – Año 2024: Resumen de resultados de monitoreo.

IDEAM. (2010). Leyenda nacional de coberturas de la tierra. Metodología CORINE Land Cover adaptada para Colombia escala 1:1000. Instituto de Hidrología, Metereología y Estudios Ambientales. http://siatac.co/c/document_library/get_file?uuid=a64629ad-2dbe-4e1e-a561-fc16b8037522&groupId=762

Iles, C. E., Vautard, R., Strachan, J., Joussaume, S., Eggen, B. R., & Hewitt, C. D. (2020). The benefits of increasing resolution in global and regional climate simulations for European climate extremes. *Geoscientific Model Development*, *13*(11), 5583–5607. https://doi.org/10.5194/gmd-13-5583-2020

Instituto Geográfico Agustin Codazzi. (2019). Planning and Land Management Geographical Information System of Colombia (SIGOT). https://sigot.igac.gov.co/

Jackson, S. T., & Williams, J. W. (2004). Modern analogs in quaternary paleoecology: Here today, gone yesterday, gone tomorrow? *Annual Review of Earth and Planetary Sciences*, *32*, 495–537. https://doi.org/10.1146/annurev.earth.32.101802.120435

Jacob, M., Romeyns, L., Frankl, A., Asfaha, T., Beeckman, H., & Nyssen, J. (2016). Land Use and Cover Dynamics Since 1964 in the Afro-Alpine Vegetation Belt: Lib Amba Mountain

in North Ethiopia. *Land Degradation & Development*, *27*(3), 641–653. https://doi.org/10.1002/LDR.2396

Jaramillo, F., & Destouni, G. (2014). Developing water change spectra and distinguishing change drivers worldwide. *Geophysical Research Letters*, *41*(23), 8377–8386. https://doi.org/10.1002/2014GL061848

Jaramillo, F., Piemontese, L., Berghuijs, W. R., Wang-Erlandsson, L., Greve, P., & Wang, Z. (2022). Fewer Basins Will Follow Their Budyko Curves Under Global Warming and Fossil-Fueled Development. *Water Resources Research*, *58*(8). https://doi.org/10.1029/2021WR031825

Jenkins, C. N., & Joppa, L. (2009). Expansion of the global terrestrial protected area system. *Biological Conservation*, 142(10), 2166–2174. https://doi.org/10.1016/j.biocon.2009.04.016

Karger, D. N., Conrad, O., Böhner, J., Kawohl, T., Kreft, H., Soria-Auza, R. W., Zimmermann, N. E., Linder, H. P., & Kessler, M. (2017). Climatologies at high resolution for the earth's land surface areas. *Scientific Data*, *4*. https://doi.org/10.1038/sdata.2017.122

Kattan, G. H., Franco, P., Rojas, V., & Morales, G. (2004). Biological diversification in a complex region: A spatial analysis of faunistic diversity and biogeography of the Andes of Colombia. *Journal of Biogeography*, 31(11), 1829–1839. https://doi.org/10.1111/j.1365-2699.2004.01109.x

Keeley, A. T. H., Beier, P., & Jenness, J. S. (2021). Connectivity metrics for conservation planning and monitoring. *Biological Conservation, 255*, 109008. https://doi.org/10.1016/j.biocon.2021.109008

Kim, H. M., Webster, P. J., & Curry, J. A. (2012). Evaluation of short-term climate change prediction in multi-model CMIP5 decadal hindcasts. *Geophysical Research Letters*, *39*(10). https://doi.org/10.1029/2012GL051644

Kindlmann, P., & Burel, F. (2008). Connectivity measures: A review. *Landscape Ecology, 23*(8), 879–890. https://doi.org/10.1007/s10980-008-9245-4

Kriegler, E., Bauer, N., Popp, A., Humpenöder, F., Leimbach, M., Strefler, J., Baumstark, L., Bodirsky, B. L., Hilaire, J., Klein, D., Mouratiadou, I., Weindl, I., Bertram, C., Dietrich, J. P., Luderer, G., Pehl, M., Pietzcker, R., Piontek, F., Lotze-Campen, H., … Edenhofer, O. (2017). Fossil-fueled development (SSP5): An energy and resource intensive scenario for the 21st century. *Global Environmental Change*, *42*, 297–315. https://doi.org/10.1016/J.GLOENVCHA.2016.05.015

Kriticos, D. J., & Leriche, A. (2010). The effects of climate data precision on fitting and projecting species niche models. *Ecography*, *33*(1), 115–127. https://doi.org/10.1111/j.1600-0587.2009.06042.x

La Sorte, F. A., & Jetz, W. (2010). Projected range contractions of montane biodiversity under global warming. *Proceedings of the Royal Society B: Biological Sciences*, *277*(1699), 3401–3410. https://doi.org/10.1098/RSPB.2010.0612

Lancaster, L. T., & Humphreys, A. M. (2020). Global variation in the thermal tolerances of plants. *PNAS*, *117*, 13580–13587. https://doi.org/10.1073/pnas.1918162117/-/DCSupplemental

Landholm, D. M., Pradhan, P., & Kropp, J. P. (2019). Diverging forest land use dynamics induced by armed conflict across the tropics. *Global Environmental Change*, 56, 86–94. https://doi.org/10.1016/j.gloenvcha.2019.03.006

Lasso, E., Matheus-Arbeláez, P., Gallery, R. E., Garzón-López, C., Cruz, M., Leon-Garcia, I. V., Aragón, L., Ayarza-Páez, A., & Curiel Yuste, J. (2021). Homeostatic Response to Three Years of Experimental Warming Suggests High Intrinsic Natural Resistance in the Páramos to Warming in the Short Term. *Frontiers in Ecology and Evolution*, *9*. https://doi.org/10.3389/fevo.2021.615006

Latorre Parra, J. P., Gualdrón Díaz, L., & Corredor Gil, L. (2022). Veinte años de monitoreo satelital de las coberturas de la tierra en los parques nacionales naturales continentales de Colombia (2000 - 2019). Parques Nacionales Naturales de Colombia.

Laurance, W. F., Camargo, J. L. C., Luizão, R. C. C., Laurance, S. G., Pimm, S. L., Bruna, E. M., Stouffer, P. C., Bruce Williamson, G., Benítez-Malvido, J., Vasconcelos, H. L., Van Houtan, K. S., Zartman, C. E., Boyle, S. A., Didham, R. K., Andrade, A., & Lovejoy, T. E. (2011). The fate of Amazonian forest fragments: A 32-year investigation. *Biological Conservation*, 144(1), 56–67. https://doi.org/10.1016/j.biocon.2010.09.021

Laurance, W. F., Goosem, M., & Laurance, S. G. (2009). Impacts of roads and linear clearings on tropical forests. *Trends in ecology & evolution*, 24(12), 659–669. https://doi.org/10.1016/j.tree.2009.06.009

Laurance, W. F., Useche, C., Rendeiro, J., Kalka, M., Bradshaw, C. J. A., Sloan, S. P., Laurance, S. G., Campbell, M., Abernethy, K., Alvarez, P., Arroyo-Rodriguez, V., Ashton, P., Benítez-Malvido, J., Blom, A., Bobo, K. S., Cannon, C. H., Cao, M., Carroll, R., Chapman, C., … Zamzani, F. (2012). Averting biodiversity collapse in tropical forest protected areas. *Nature*, 489(7415), 290–294. https://doi.org/10.1038/nature11318

Lenoir, J., & Svenning, J. C. (2015). Climate-related range shifts - a global multidimensional synthesis and new research directions. *Ecography*, *38*(1), 15–28. https://doi.org/10.1111/ecog.00967

Li, G., Fang, C., Watson, J.E.M. *et al.* Mixed effectiveness of global protected areas in resisting habitat loss. *Nat Commun* **15**, 8389 (2024). https://doi.org/10.1038/s41467-024-52693-9

Liang, J., Ding, Z., Jiang, Z., Yang, X., Xiao, R., Singh, P. B., Hu, Y., Guo, K., Zhang, Z., & Hu, H. (2021). Climate change, habitat connectivity, and conservation gaps: a case study of four ungulate species endemic to the Tibetan Plateau. *Landscape Ecology*, 36(4), 1071–1087. https://doi.org/10.1007/s10980-021-01202-0

Linero, D., Cuervo-Robayo, A. P., & Etter, A. (2020). Assessing the future conservation potential of the Amazon and Andes Protected Areas: Using the woolly monkey (Lagothrix lagothricha) as an umbrella species. *Journal for Nature Conservation*, *58*. https://doi.org/10.1016/j.jnc.2020.125926

Linero-Triana, D., Correa-Ayram, C. A., & Velásquez-Tibatá, J. (2023). Prioritizing ecological connectivity among protected areas in Colombia using a functional approach for birds. *Global Ecology and Conservation*, 48. https://doi.org/10.1016/j.gecco.2023.e02713

Llambí, L. D., & Rada, F. (2019). Ecological research in the tropical alpine ecosystems of the Venezuelan páramo: past, present and future. *Plant Ecology and Diversity*, *12*(6), 519–538. https://doi.org/10.1080/17550874.2019.1680762

Llambí, L. D., Becerra, M. T., Peralvo, M., Avella, A., Baruffol, M., & Flores, L. J. (2019). Monitoring Biodiversity and Ecosystem Services in Colombia's High Andean Ecosystems: Toward an Integrated Strategy. *Mountain Research and Development*, *39*(3), A8–A20. https://doi.org/10.1659/MRD-JOURNAL-D-19-00020.1

Loarie, S. R., Duffy, P. B., Hamilton, H., Asner, G. P., Field, C. B., & Ackerly, D. D. (2009). The velocity of climate change. *Nature*, *462*(7276), 1052–1055. https://doi.org/10.1038/nature08649

López, J., Qian, Y., Murillo-Sandoval, P. J., Clerici, N., & Eklundh, L. (2024). Landscape connectivity loss after the de-escalation of armed conflict in the Colombian Amazon (2011–2021). *Global Ecology and Conservation*, 54. https://doi.org/10.1016/j.gecco.2024.e03094

Lowe, W. H., & Allendorf, F. W. (2010). What can genetics tell us about population connectivity? *Molecular Ecology, 19*(15), 3038–3051. https://doi.org/10.1111/j.1365-294X.2010.04688.x

Lurgi, M., López, B. C., & Montoya, J. M. (2012). Novel communities from climate change. In *Philosophical Transactions of the Royal Society B: Biological Sciences* (Vol. 367, Issue 1605, pp. 2913–2922). Royal Society. https://doi.org/10.1098/rstb.2012.0238

Machlis, G. E., & Hanson, T. (2008). Warfare ecology. *BioScience, 58*(8), 729–736. https://doi.org/10.1641/B580809

Macura, B., Secco, L. & Pullin, A.S. What evidence exists on the impact of governance type on the conservation effectiveness of forest protected areas? Knowledge base and evidence gaps. *Environ Evid* **4**, 24 (2015). https://doi.org/10.1186/s13750-015-0051-6

Mantyka-pringle, C. S., Martin, T. G., & Rhodes, J. R. (2012). Interactions between climate and habitat loss effects on biodiversity: A systematic review and meta-analysis. *Global Change Biology*, *18*(4), 1239–1252. https://doi.org/10.1111/j.1365-2486.2011.02593.x

MapBiomas Colombia. (2024). MapBiomas Colombia Collection 2.0: Annual land cover and land use maps for Colombia (1985–2023). Fundación Gaia Amazonas. https://colombia.mapbiomas.org/en/productos

MapBiomas Colombia. (2026). *Accuracy assessment analysis of MapBiomas' land cover mapping*. https://colombia.mapbiomas.org/en/exactitud/

Marengo, J. A., Pabón, J. D., Díaz, A., Rosas, G., Ávalos, G., Montealegre, E., Villacis, M., Solman, S., & Rojas, M. (2011). Climate change: evidence and future scenarios for the Andean region. *Climate Change and Biodiversity in the Tropical Andes*, 110–127.

Martensen, A. C., Saura, S., & Fortin, M. J. (2017). Spatio-temporal connectivity: assessing the amount of reachable habitat in dynamic landscapes. *Methods in Ecology and Evolution*, 8(10), 1253–1264. https://doi.org/10.1111/2041-210X.12799

Mavárez, J., Bézy, S., Goeury, T., Fernández, A., & Aubert, S. (2019). Current and future distributions of Espeletiinae (Asteraceae) in the Venezuelan Andes based on statistical downscaling of climatic variables and niche modelling. *Plant Ecology and Diversity*, *12*(6), 633–647. https://doi.org/10.1080/17550874.2018.1549599

Meinshausen, M., Nicholls, Z. R. J., Lewis, J., Gidden, M. J., Vogel, E., Freund, M., Beyerle, U., Gessner, C., Nauels, A., Bauer, N., Canadell, J. G., Daniel, J. S., John, A., Krummel, P. B., Luderer, G., Meinshausen, N., Montzka, S. A., Rayner, P. J., Reimann, S., … Wang, R. H. J. (2020). The shared socio-economic pathway (SSP) greenhouse gas concentrations and their extensions to 2500. *Geoscientific Model Development*, *13*(8), 3571–3605. https://doi.org/10.5194/gmd-13-3571-2020

Mendoza, J. P. (2020). Colombia' s peace is enhancing coca-driven deforestation. *Environmental Research Letters*, 15, 1–12. https://doi.org/10.1088/1748-9326/abb331

Mendoza-Cifuentes, H., Cárdenas, D., Aguilar-Cano, J., Ramírez-Padilla, B., Dueñas-Cepeda, A., & Carbonó-Delahoz, E. (2018). Representatividad de plantas vasculares en los Parques Nacionales Naturales de Colombia: ¿cuántas especies alberga el sistema? *Biota Colombiana*, 19(2), 21–34. https://doi.org/10.21068/c2018.v19n02a03

Mengist, W., Soromessa, T., & Legese, G. (2020). Ecosystem services research in mountainous regions: A systematic literature review on current knowledge and research gaps. *Science of The Total Environment*, *702*, 134581. https://doi.org/10.1016/J.SCITOTENV.2019.134581

Merckx, V. S. F. T., Hendriks, K. P., Beentjes, K. K., Mennes, C. B., Becking, L. E., Peijnenburg, K. T. C. A., Afendy, A., Arumugam, N., De Boer, H., Biun, A., Buang, M. M., Chen, P. P., Chung, A. Y. C., Dow, R., Feijen, F. A. A., Feijen, H., Soest, C. F. Van, Geml, J., Geurts, R.,

... Schilthuizen, M. (2015). Evolution of endemism on a young tropical mountain. *Nature 2015 524:7565*, *524*(7565), 347–350. https://doi.org/10.1038/nature14949

Midgley, G. F., & Bond, W. J. (2015). Future of African terrestrial biodiversity and ecosystems under anthropogenic climate change. In *Nature Climate Change* (Vol. 5, Issue 9, pp. 823–829). Nature Publishing Group. https://doi.org/10.1038/nclimate2753

Mittermeier, R. A., Turner, W. R., Larsen, F. W., Brooks, T. M., & Gascon, C. (2011). Global biodiversity conservation: The critical role of hotspots. In F. E. Zachos & J. C. Habel (Eds.), *Biodiversity hotspots* (pp. 3–22). Springer–Verlag Berlin.

Molina, M. (2024). Amazon rights in focus: Peoples and forest protection. https://www.iucn.nl/app/uploads/2024/06/Drivers-of-deforestation-in-the-Colombian-Amazon_IUCN-NL-2024.pdf

Moreno, L. A., Rueda, C., & Andrade, G. (Eds.). (2018). Biodiversidad 2017. Estado y tendencias de la biodiversidad continental de Colombia.

Mosquera, G. M., Marín, F., Stern, M., Bonnesoeur, V., Ochoa-Tocachi, B. F., Román-Dañobeytia, F., & Crespo, P. (2022). Progress in understanding the hydrology of high-elevation Andean grasslands under changing land use. *Science of The Total Environment*, *804*, 150112. https://doi.org/10.1016/J.SCITOTENV.2021.150112

Müller, W. A., Jungclaus, J. H., Mauritsen, T., Baehr, J., Bittner, M., Budich, R., Bunzel, F., Esch, M., Ghosh, R., Haak, H., Ilyina, T., Kleine, T., Kornblueh, L., Li, H., Modali, K., Notz, D., Pohlmann, H., Roeckner, E., Stemmler, I., ... Marotzke, J. (2018). A Higher-resolution Version of the Max Planck Institute Earth System Model (MPI-ESM1.2-HR). *Journal of Advances in Modeling Earth Systems*, *10*(7), 1383–1413. https://doi.org/10.1029/2017MS001217

Muñoz Brenes, C. L., Jones, K. W., Schlesinger, P., Robalino, J., & Vierling, L. (2018). The impact of protected area governance and management capacity on ecosystem function in Central America. *PloS one*, *13*(10), e0205964. https://doi.org/10.1371/journal.pone.0205964

Murali, G., Iwamura, T., Meiri, S., & Roll, U. (2023). Future temperature extremes threaten land vertebrates. *Nature*, *615*(7952), 461–467. https://doi.org/10.1038/s41586-022-05606-z

Murillo-Sandoval, P. J., Clerici, N., & Correa-Ayram, C. (2022). Rapid loss in landscape connectivity after the peace agreement in the Andes-Amazon region. *Global Ecology and Conservation*, 38. https://doi.org/10.1016/j.gecco.2022.e02205

Murillo-Sandoval, P. J., Dexter, K. V., Hoek, J. V. D., Wrathall, D., & Kennedy, R. (2020). The end of gunpoint conservation: Forest disturbance after the Colombian peace agreement. *Environmental Research Letters*, 15(3), 034033. https://doi.org/10.1088/1748-9326/ab6ae

Murillo-Sandoval, P. J., Gjerdseth, E., Correa-Ayram, C., Wrathall, D., Van Den Hoek, J., Dávalos, L. M., & Kennedy, R. (2021). No peace for the forest: Rapid, widespread land changes in the Andes-Amazon region following the Colombian civil war. Global Environmental Change, 69, 102283. https://doi.org/10.1016/j.gloenvcha.2021.102283

Murillo-Sandoval, P. J., Hoek, J. Van Den, & Hilker, T. (2017). Leveraging multi-sensor time series datasets to map short- and long-term tropical forest disturbances in the Colombian Andes. Remote Sensing, 9(2), 179. https://doi.org/10.3390/rs9020179

Myers, N. (1993). Tropical forests: the main deforestation fronts. *Environmental conservation*, *20*(1), 9-16.

Myers, N., Mittermeier, R. A., Mittermeier, C. G., da Fonseca, G. A. B., & Kent, J. (2000). Biodiversity hotspots for conservation priorities. *Nature*, *403*(6772), 853–858. https://doi.org/10.1038/35002501

Myster, R. W. (2021). Introduction. In R. W. Myster (Ed.), *The Andean cloud forest* (pp. 1–23). Springer, Cham. https://doi.org/10.1007/978-3-030-57344-7_1

Nagendra, H., Lucas, R., Honrado, J. P., Jongman, R. H. G., Tarantino, C., Adamo, M., & Mairota, P. (2013). Remote sensing for conservation monitoring: Assessing protected areas, habitat extent, habitat condition, species diversity, and threats. *Ecological Indicators*, 33, 45–59. https://doi.org/10.1016/j.ecolind.2012.09.014

Negret, P., Di-Marco, M., Sonter, L., Rhodes, J., Possingham, H., & Maron, M. (2020). Effects of spatial autocorrelation and sampling design on estimates of protected area effectiveness. *Conservation Biology*, *00*(0), 1–11. https://doi.org/10.1111/cobi.13522

Negret, P., Maron, M., Fuller, R. A., Possingham, H. P., Watson, J. E. M., & Simmonds, J. S. (2021). Deforestation and bird habitat loss in Colombia. *Biological Conservation*, 257(May), 109044. https://doi.org/10.1101/2020.05.30.125849

Negret, P., Sonter, L., Watson, J., Possingham, H., Jones, K., Suarez, C., Ochoa-Quintero, J. M., & Maron, M. (2019). Emerging evidence that armed conflict and coca cultivation influence deforestation patterns. *Biological Conservation*, 239. https://doi.org/10.1016/j.biocon.2019.07.021

Nepstad, D., Ardila, J. P., Stickler, C., Barrionuevo, M. de los A., Bezerra, T., Vargas, R., & Rojas, G. (2021). Adaptive management of jurisdictional REDD + programs: a methodology illustrated for Ecuador. *Carbon Management*, *12*(3), 323–333. https://doi.org/10.1080/17583004.2021.1926331

Newbold, T., Hudson, L. N., Hill, S. L. L., Contu, S., Lysenko, I., Senior, R. A., Börger, L., Bennett, D. J., Choimes, A., Collen, B., Day, J., De Palma, A., Díaz, S., Echeverria-Londoño, S., Edgar, M. J., Feldman, A., Garon, M., Harrison, M. L. K., Alhusseini, T., … Purvis, A. (2015). Global effects of land use on local terrestrial biodiversity. *Nature*, 520(7545), 45–50. https://doi.org/10.1038/nature14324

Nogués-Bravo, D., Araújo, M. B., Errea, M. P., & Martínez-Rica, J. P. (2007). Exposure of global mountain systems to climate warming during the 21st Century. *Global Environmental Change*, *17*(3–4), 420–428. https://doi.org/10.1016/j.gloenvcha.2006.11.007

O'Donnell, M. S., & Ignizio, D. A. (2012). Bioclimatic Predictors for Supporting Ecological Applications in the Conterminous United States. *U.S Geological Survey Data Series 691*, 10.

O'neill, B. C., Tebaldi, C., Van Vuuren, D. P., Eyring, V., Friedlingstein, P., Hurtt, G., Knutti, R., Kriegler, E., Lamarque, J.-F., Lowe, J., Meehl, G. A., Moss, R., Riahi, K., & Sanderson, B. M. (2016). The Scenario Model Intercomparison Project (ScenarioMIP) for CMIP6. *Geosci. Model Dev*, *9*, 3461–3482. https://doi.org/10.5194/gmd-9-3461-2016

Ocampo-Peñuela, N., & Winton, R. S. (2017). Economic and Conservation Potential of Bird-Watching Tourism in Postconflict Colombia. *Tropical Conservation Science*, 10. https://doi.org/10.1177/1940082917733862

Ocampo-Peñuela, N., Garcia-Ulloa, J., Ghazoul, J., & Etter, A. (2018). Quantifying impacts of oil palm expansion on Colombia's threatened biodiversity. *Biological Conservation*, 224, 117–121. https://doi.org/10.1016/j.biocon.2018.05.024

Ocampo-Peñuela, N., Garcia-Ulloa, J., Kornecki, I., Philipson, C. D., & Ghazoul, J. (2020). Impacts of four decades of forest loss on vertebrate functional habitat on Borneo. *Frontiers in Forests and Global Change, 3*, Article 53. https://doi.org/10.3389/ffgc.2020.00053

Ochoa-Cueva, P., Fries, A., Montesinos, P., Rodríguez-Díaz, J. A., & Boll, J. (2015). Spatial Estimation of Soil Erosion Risk by Land-cover Change in the Andes OF Southern Ecuador. *Land Degradation and Development*, *26*(6), 565–573. https://doi.org/10.1002/ldr.2219

Ochoa-Tocachi, B. F., Buytaert, W., Antiporta, J., Acosta, L., Bardales, J. D., Célleri, R., Crespo, P., Fuentes, P., Gil-Ríos, J., Guallpa, M., Llerena, C., Olaya, D., Pardo, P., Rojas, G., Villacís, M., Villazón, M., Viñas, P., & De Bièvre, B. (2018). High-resolution hydrometeorological data from a network of headwater catchments in the tropical Andes. *Scientific Data*, *5*. https://doi.org/10.1038/sdata.2018.80

Ochoa-Tocachi, B. F., Buytaert, W., De Bièvre, B., Célleri, R., Crespo, P., Villacís, M., Llerena, C. A., Acosta, L., Villazón, M., Guallpa, M., Gil-Ríos, J., Fuentes, P., Olaya, D., Viñas, P., Rojas, G., & Arias, S. (2016). Impacts of land use on the hydrological response of tropical Andean catchments. *Hydrological Processes*, *30*(22), 4074–4089. https://doi.org/10.1002/hyp.10980

Oettel, J., Sachser, F., Martinez-Richart, A. I., & Kumar, M. (2025). Concepts, measures, and models for assessing connectivity. In K. Lapin, J. Oettel, M. Braun, & H. Konrad (Eds.),

Ecological connectivity of forest ecosystems (pp. 3–21). Springer. https://doi.org/10.1007/978-3-031-82206-3_1

Ohlemüller, R. (2011). Running Out of Climate Space. *Science*, *334*(6056), 613–614. https://doi.org/10.1126/science.1214215

Ohlemüller, R., Gritti, E. S., Sykes, M. T., & Thomas, C. D. (2006). Towards European climate risk surfaces: The extent and distribution of analogous and non-analogous climates 1931-2100. *Global Ecology and Biogeography*, *15*(4), 395–405. https://doi.org/10.1111/j.1466-822X.2006.00245.x

Oliver, T. H., & Morecroft, M. D. (2014). Interactions between climate change and land use change on biodiversity: Attribution problems, risks, and opportunities. *Wiley Interdisciplinary Reviews: Climate Change*, *5*(3), 317–335. https://doi.org/10.1002/wcc.271

Olson, D. M., Dinerstein, E., Wikramanayake, E. D., Burgess, N. D., Powell, G. V. N., Underwood, E. C., D'amico, J. A., Itoua, I., Strand, H. E., Morrison, J. C., & others. (2001). Terrestrial Ecoregions of the World: A New Map of Life on EarthA new global map of terrestrial ecoregions provides an innovative tool for conserving biodiversity. *BioScience*, *51*(11), 933–938.

Orme, C. D. L., Davies, R. G., Burgess, M., Eigenbrod, F., Pickup, N., Olson, V. A., Webster, A. J., Ding, T. S., Rasmussen, P. C., Ridgely, R. S., Stattersfield, A. J., Bennett, P. M., Blackburn, T. M., Gaston, K. J., & Owens, I. P. F. (2005). Global hotspots of species richness are not congruent with endemism or threat. *Nature*, *436*(7053), 1016–1019. https://doi.org/10.1038/nature03850

Pabón-Caicedo, J. D., Arias, P. A., Carril, A. F., Espinoza, J. C., Borrel, L. F., Goubanova, K., Lavado-Casimiro, W., Masiokas, M., Solman, S., & Villalba, R. (2020). Observed and projected hydroclimate changes in the Andes. *Frontiers in Earth Science*, *8*, 61.

Palahí, M., Valbuena, R., Senf, C., Acil, N., Pugh, T. A. M., Sadler, J., Seidl, R., Potapov, P., Gardiner, B., Hetemäki, L., & others. (2021). Concerns about reported harvests in European forests. *Nature, 592*(7856), E15–E17.

Parks, S. A., Holsinger, L. M., Abatzoglou, J. T., Littlefield, C. E., & Zeller, K. A. (2023). Protected areas not likely to serve as steppingstones for species undergoing climate-induced range shifts. *Global Change Biology, 29*, 2681–2696. https://doi.org/10.1111/gcb.16629

Parques Nacionales Naturales de Colombia. (2025). Registro Único Nacional de Áreas protegidas (RUNAP) en Cifras. Recuperado el 11 de agosto de 2025, de https://runap.parquesnacionales.gov.co/cifras

Pascual-Hortal, L., & Saura, S. (2006). Comparison and development of new graph-based landscape connectivity indices: Towards the prioritization of habitat patches and

corridors for conservation. *Landscape Ecology, 21*(7), 959–967. https://doi.org/10.1007/s10980-006-0013-z

Pecl, G. T., Araújo, M. B., Bell, J. D., Blanchard, J., Bonebrake, T. C., Chen, I. C., Clark, T. D., Colwell, R. K., Danielsen, F., Evengård, B., Falconi, L., Ferrier, S., Frusher, S., Garcia, R. A., Griffis, R. B., Hobday, A. J., Janion-Scheepers, C., Jarzyna, M. A., Jennings, S., … Williams, S. E. (2017). Biodiversity redistribution under climate change: Impacts on ecosystems and human well-being. *Science*, *355*(6332). https://doi.org/10.1126/SCIENCE.AAI9214/SUPPL_FILE/PECL.SM.PDF

Pepin, N., Bradley, R. S., Diaz, H. F., Baraer, M., Caceres, E. B., Forsythe, N., Fowler, H., Greenwood, G., Hashmi, M. Z., Liu, X. D., Miller, J. R., Ning, L., Ohmura, A., Palazzi, E., Rangwala, I., Schöner, W., Severskiy, I., Shahgedanova, M., Wang, M. B., … Yang, D. Q. (2015). Elevation-dependent warming in mountain regions of the world. *Nature Climate Change 2015 5:5*, *5*(5), 424–430. https://doi.org/10.1038/nclimate2563

Pereira, H. M., Navarro, L. M., & Martins, I. S. (2012). Global biodiversity change: The Bad, the good, and the unknown. *Annual Review of Environment and Resources*, *37*, 25–50. https://doi.org/10.1146/annurev-environ-042911-093511

Perez, T. M., Stroud, J. T., & Feeley, K. J. (2016). Thermal trouble in the tropics. *Science*, *351*(6280), 1392–1393. https://doi.org/10.1126/science.aaf3343

Perugini, L., Caporaso, L., Marconi, S., Cescatti, A., Quesada, B., de Noblet-Ducoudré, N., … & Arneth, A. (2017). Biophysical effects on temperature and precipitation due to land cover change. *Environmental Research Letters*, *12*(5), 053002.

Peters, M. K., Hemp, A., Appelhans, T., Becker, J. N., Behler, C., Classen, A., Detsch, F., Ensslin, A., Ferger, S. W., Frederiksen, S. B., Gebert, F., Gerschlauer, F., Gütlein, A., Helbig-Bonitz, M., Hemp, C., Kindeketa, W. J., Kühnel, A., Mayr, A. V., Mwangomo, E., … Steffan-Dewenter, I. (2019). Climate–land-use interactions shape tropical mountain biodiversity and ecosystem functions. *Nature*, *568*(7750), 88–92. https://doi.org/10.1038/s41586-019-1048-z

Peyre, G., Osorio, D., François, R., & Anthelme, F. (2021). Mapping the páramo land-cover in the Northern Andes. *International Journal of Remote Sensing*, *42*(20), 7777–7797. https://doi.org/10.1080/01431161.2021.1964709

PNNC. (2023). *Información cartográfica (Shapefile) Limites de otras categorías reconocidas por el SINAP*. http://www.parquesnacionales.gov.co/portal/es/servicio-al-ciudadano/datos-abiertos/

PNNC. (2024). Informacion cartografica (Shapefile) Limites de otras categorias reconocidas por el SINAP. http://www.parquesnacionales.gov.co/portal/es/servicio-al-ciudadano/datos-abiertos/

PNNC. (2025). Registro Unico Nacional de Areas Protegidas. https://runap.parquesnacionales.gov.co/cifras

Polato, N. R., Gill, B. A., Shah, A. A., Gray, M. M., Casner, K. L., Barthelet, A., Messer, P. W., Simmons, M. P., Guayasamin, J. M., Encalada, A. C., & others. (2018). Narrow thermal tolerance and low dispersal drive higher speciation in tropical mountains. *Proceedings of the National Academy of Sciences*, *115*(49), 12471–12476.

Popp, A., Humpenöder, F., Weindl, I., Bodirsky, B. L., Bonsch, M., Lotze-Campen, H., Müller, C., Biewald, A., Rolinski, S., Stevanovic, M., & Dietrich, J. P. (2014). Land-use protection for climate change mitigation. *Nature Climate Change*, *4*(12), 1095–1098. https://doi.org/10.1038/nclimate2444

Potapov, P. V, Turubanova, S. A., Hansen, M. C., Adusei, B., Broich, M., Altstatt, A., Mane, L., & Justice, C. O. (2012). Quantifying forest cover loss in Democratic Republic of the Congo, 2000-2010, with Landsat ETM+ data. *Remote Sensing of Environment*, *122*, 106–116. https://doi.org/10.1016/j.rse.2011.08.027

Prugh, L. R., Hodges, K. E., Sinclair, A. R. E., & Brashares, J. S. (2008). Effect of habitat area and isolation on fragmented animal populations. *Proceedings of the National Academy of Sciences of the United States of America*, 105(52), 20770–20775. https://doi.org/10.1073/pnas.0806080105

Puyravaud, J.-P. (2003). Standardizing the calculation of the annual rate of deforestation. *Forest Ecology and Management, 177*, 593–596.

Quesada, B., Arneth, A., & De Noblet-Ducoudré, N. (2017). Atmospheric, radiative, and hydrologic effects of future land use and land cover changes: A global and multimodel climate picture. *Journal of Geophysical Research*, *122*(10), 5113–5131. https://doi.org/10.1002/2016JD025448

Quesada, B., Arneth, A., Robertson, E., & De Noblet-Ducoudré, N. (2018). Potential strong contribution of future anthropogenic land-use and land-cover change to the terrestrial carbon cycle. *Environmental Research Letters*, *13*(6), 064023. https://doi.org/10.1088/1748-9326/aac4c3

Quintero-Gallego, M. E., Quintero-Angel, M., & Vila-Ortega, J. J. (2018). Exploring land use/land cover change and drivers in Andean mountains in Colombia: A case in rural Quindío. *Science of the Total Environment*, 634, 1288-1299.

R Core Team. (2024). R: A Language and Environment for Statistical Computing. https://www.r-project.org/

Rada, F., Azócar, A., & García-Núñez, C. (2019). Plant functional diversity in tropical Andean páramos. *Plant Ecology and Diversity*, *12*(6), 539–553. https://doi.org/10.1080/17550874.2019.1674396

Rao, K. K., Al Mandous, A., Al Ebri, M., Al Hameli, N., Rakib, M., & Al Kaabi, S. (2024). Future changes in the precipitation regime over the Arabian Peninsula with special emphasis on UAE: insights from NEX-GDDP CMIP6 model simulations. *Scientific Reports*, *14*(1). https://doi.org/10.1038/s41598-023-49910-8

Rasmann, S., Pellissier, L., Defossez, E., Jactel, H., & Kunstler, G. (2014). Climate-driven change in plant–insect interactions along elevation gradients. *Functional Ecology*, *28*(1), 46–54. https://doi.org/10.1111/1365-2435.12135

Resler, L. M., & Gunya, A. (2022). *Trends of Land Use and Land Cover Change in Mountain Regions* (pp. 151–167). https://doi.org/10.1007/978-3-031-13298-8_9

Restrepo, J. D., & Escobar, H. A. (2018). Sediment load trends in the Magdalena River basin (1980–2010): Anthropogenic and climate-induced causes. *Geomorphology*, 302, 76–91. https://doi.org/10.1016/j.geomorph.2016.12.013

Restrepo, J. D., Kettner, A. J., & Syvitski, J. P. M. (2015). Recent deforestation causes rapid increase in river sediment load in the Colombian Andes. *Anthropocene*, 10, 13–28. https://doi.org/10.1016/j.ancene.2015.09.001

Roberts, D. R., & Hamann, A. (2012). Predicting potential climate change impacts with bioclimate envelope models: A palaeoecological perspective. *Global Ecology and Biogeography*, *21*(2), 121–133. https://doi.org/10.1111/j.1466-8238.2011.00657.x

Rodríguez Eraso, N., Armenteras-Pascual, D., & Alumbreros, J. R. (2013). Land use and land cover change in the Colombian Andes: Dynamics and future scenarios. *Journal of Land Use Science*, *8*(2), 154–174. https://doi.org/10.1080/1747423X.2011.650228

Rodríguez, N., Armenteras, D., & Retana, J. (2013). Effectiveness of protected areas in the Colombian Andes: deforestation, fire and land-use changes. *Regional Environmental Change*, *13*(2), 423–435. https://doi.org/10.1007/s10113-012-0356-8

Rodríguez-Morales, M., Acevedo-Novoa, D., Machado, D., Ablan, M., Dugarte, W., & Dávila, F. (2019). Ecohydrology of the Venezuelan páramo: water balance of a high Andean watershed. *Plant Ecology and Diversity*, *12*(6), 573–591. https://doi.org/10.1080/17550874.2019.1673494

Romero-Ruiz, M. H., Flantua, S. G. A., Tansey, K., & Berrio, J. C. (2012). Landscape transformations in savannas of northern South America: Land use/cover changes since 1987 in the Llanos Orientales of Colombia. *Applied Geography*, 32(2), 766–776. https://doi.org/10.1016/j.apgeog.2011.08.010

Rubiano, K. (2024). krubiano/HETEs-Hydroclimatic-spaces: v1.0.0. In *Zenodo*. Zenodo. https://doi.org/10.5281/zenodo.14559880

Rubiano, K., Clerici, N., Norden, N., & Etter, A. (2017). Secondary Forest and Shrubland Dynamics in a Highly Transformed Landscape in the Northern Andes of Colombia (1985–2015). *Forests*, 8(6), 216. https://doi.org/10.3390/f8060216

Rubiano, K., Clerici, N., Sanchez, A., & Fernando, J. (2024). Breaching of hydroclimatic spaces in humid high-elevation tropical ecosystems by future climate change [Data set]. In *Zenodo*. Zenodo. https://doi.org/10.5281/zenodo.14562653

Rubiano, K., Clerici, N., Sanchez, A., & Jaramillo, F. (2025). Current hydroclimatic spaces will be breached in half of the world's humid high-elevation tropical ecosystems. *Communications Earth & Environment*, *6*(1), 197. https://doi.org/10.1038/s43247-025-02087-6

Rubiano, K., Clerici, N., Bottin, M., & Boschetti, L. (2026). Data for: Post-agreement acceleration of habitat loss and landscape connectivity decline in and around Colombian protected areas [Data set]. Zenodo. https://doi.org/10.5281/zenodo.19445808

Rudel, T., & Roper, J. (1997). The paths to rain forest destruction: crossnational patterns of tropical deforestation, 1975–1990. *World development*, *25*(1), 53-65.

Rudnick, D. A., Ryan, S. J., Beier, P., Cushman, S. A., Dieffenbach, F., Epps, C. W., Gerber, L. R., Hartter, J., Jenness, J. S., Kintsch, J., Merenlender, A. M., Perkl, R. M., Preziosi, D. V., & Trombulak, S. C. (2012). The role of landscape connectivity in planning and implementing conservation and restoration priorities. *Issues in Ecology, 16*, 1–20.

Ruiz-Díaz, N., Nitola-Duitama, Z. L., & Useche-de-Vega, D. S. (2025). Mapping Structural Connectivity in Andean Landscapes: Insights from El Malmo Reserve and Páramo de Rabanal (2012–2023). *Earth Systems and Environment*, 1-15.

Rundel, P. W., Smith, A. P., & Meinzer, F. C. (1994). *Tropical alpine environments: plant form and function*. Cambridge University Press.

Sanchez, A., & Rada, F. (2023). Ecofisiología de plantas de los páramos andinos. In C. Tobón (Ed.), Los Páramos de Colombia. Características biofísicas, Ecohidrología y Cambio climático. Universidad Nacional de Colombia, Editorial UN.

Sanchez, A., Posada, J., & Smith, W. (2014). Dynamic cloud regimes, incident sunlight, and leaf temperatures in espeletia grandiflora and Chusquea tessellata, two representative species of the Andean Páramo, Colombia. *Arctic, Antarctic, and Alpine Research*, 46(2), 371–378. https://doi.org/10.1657/1938-4246-46.2.371

Sánchez-Cuervo, A. M., & Aide, T. M. (2013). Consequences of the Armed Conflict, Forced Human Displacement, and Land Abandonment on Forest Cover Change in Colombia: A Multi-scaled Analysis. Ecosystems, 16(6), 1052–1070. https://doi.org/10.1007/s10021-013-9667-y

Sánchez-Cuervo, A. M., & Aide, T. M. (2013). Identifying hotspots of deforestation and reforestation in Colombia (2001–2010): implications for protected areas. Ecosphere, 4(11), art143. https://doi.org/10.1890/ES13-00207.1

Sandoval, D., Rada, F., & Sarmiento, L. (2019). Stomatal response functions to environmental stress of dominant species in the tropical Andean páramo. *Plant Ecology and Diversity*, *12*(6), 649–661. https://doi.org/10.1080/17550874.2019.1683094

Saura, S., & Pascual-Hortal, L. (2007). A new habitat availability index to integrate connectivity in landscape conservation planning: Comparison with existing indices and application to a case study. Landscape and Urban Planning, 83(2–3), 91–103. https://doi.org/10.1016/j.landurbplan.2007.03.005

Saura, S., & Rubio, L. (2010). A common currency for the different ways in which patches and links can contribute to habitat availability and connectivity in the landscape. *Ecography, 33*(3), 523–537. https://doi.org/10.1111/j.1600-0587.2009.05760.x

Saura, S., Bastin, L., Battistella, L., Mandrici, A., & Dubois, G. (2017). Protected areas in the world's ecoregions: How well connected are they? Ecological Indicators, 76, 144–158. https://doi.org/10.1016/j.ecolind.2016.12.047

Saura, S., Estreguil, C., Mouton, C., & Rodríguez-Freire, M. (2011). Network analysis to assess landscape connectivity trends: Application to European forests (1990-2000). Ecological Indicators, 11(2), 407–416. https://doi.org/10.1016/j.ecolind.2010.06.011

Scherrer, D., & Körner, C. (2011). Topographically controlled thermal-habitat differentiation buffers alpine plant diversity against climate warming. *Journal of Biogeography*, *38*(2), 406–416. https://doi.org/10.1111/j.1365-2699.2010.02407.x

Schloss, C. A., Cameron, D. R., McRae, B. H., Theobald, D. M., & Jones, A. (2022). "No-regrets" pathways for navigating climate change: Planning for connectivity with land use, topography, and climate. *Ecological Applications, 32*(1), e02468. https://doi.org/10.1002/eap.2468

Seo, C., Thorne, J. H., Hannah, L., & Thuiller, W. (2009). Scale effects in species distribution models: Implications for conservation planning under climate change. *Biology Letters*, *5*(1), 39–43. https://doi.org/10.1098/rsbl.2008.0476

Shen, Y., Liu, G., Zhou, W., Liu, Y., Cheng, H., & Su, X. (2022). Protected areas have remarkable spillover effects on forest conservation on the Qinghai-Tibet Plateau. *Diversity and Distributions, 28*(12), 2944–2955. https://doi.org/10.1111/ddi.13466

Sierra, C. A., Mahecha, M., Poveda, G., Álvarez-Dávila, E., Gutierrez-Velez, V. H., Reu, B., Feilhauer, H., Anáya, J., Armenteras, D., Benavides, A. M., Buendia, C., Duque, Á., Estupiñan-Suarez, L. M., González, C., Gonzalez-Caro, S., Jimenez, R., Kraemer, G., Londoño, M. C., Orrego, S. A., … Skowronek, S. (2017). Monitoring ecological change during rapid socio-economic and political transitions: Colombian ecosystems in the

post-conflict era. In *Environmental Science and Policy* (Vol. 76, pp. 40–49). https://doi.org/10.1016/j.envsci.2017.06.011

Sintayehu, D. W. (2018). Impact of climate change on biodiversity and associated key ecosystem services in Africa: a systematic review. In *Ecosystem Health and Sustainability* (Vol. 4, Issue 9, pp. 225–239). Taylor and Francis Ltd. https://doi.org/10.1080/20964129.2018.1530054

Skarbø, K., & VanderMolen, K. (2016). Maize migration: key crop expands to higher altitudes under climate change in the Andes. *Climate and Development*, *8*(3), 245–255. https://doi.org/10.1080/17565529.2015.1034234

Sklenář, P., Hedberg, I., & Cleef, A. M. (2014). Island biogeography of tropical alpine floras. *Journal of Biogeography*, *41*(2), 287–297. https://doi.org/10.1111/jbi.12212

Sklenář, P., Romoleroux, K., Muriel, P., Jaramillo, R., Bernardi, A., Diazgranados, M., & Moret, P. (2021). Distribution changes in páramo plants from the equatorial high Andes in response to increasing temperature and humidity variation since 1880. *Alpine Botany*, *131*(2), 201–212. https://doi.org/10.1007/s00035-021-00270-x

Smith, A. P., & Young, T. P. (1987). Tropical Alpine Plant Ecology. *Annual Review of Ecology and Systematics*, *18*, 137–158. https://about.jstor.org/terms

Smith, C., Baker, J. C. A., & Spracklen, D. V. (2023). Tropical deforestation causes large reductions in observed precipitation. *Nature 2023*, 1–6. https://doi.org/10.1038/s41586-022-05690-1

Smith, I., Moise, A., Katzfey, J., Nguyen, K., & Colman, R. (2013). Regional-scale rainfall projections: Simulations for the New Guinea region using the CCAM model. *Journal of Geophysical Research Atmospheres*, *118*(3), 1271–1280. https://doi.org/10.1002/jgrd.50139

Snethlage, M. A., Geschke, J., Ranipeta, A., Jetz, W., Yoccoz, N. G., Körner, C., Spehn, E. M., Fischer, M., & Urbach, D. (2022). A hierarchical inventory of the world's mountains for global comparative mountain science. *Scientific Data*, *9*(1). https://doi.org/10.1038/s41597-022-01256-y

Snethlage, M. A., Geschke, J., Spehn, E. M., Ranipeta, A., Yoccoz, N. G., Körner, Ch., Jetz, W., Fischer, M., & Urbach, D. (2022). *GMBA Mountain Inventory v2*. GMBA-EarthEnv. https://doi.org/10.48601/EARTHENV-T9K2-1407

Soares-Filho, B. S., Rodrigues, H. O., Costa, W., & Schlesinger, P. (2009). Modeling environmental dynamics with Dinamica EGO. *Centro de Sensoriamento Remoto. Universidade Federal de Minas Gerais. Belo Horizonte, Minas Gerais*, *115*.

Souza, C. M., Shimbo, J. Z., Rosa, M. R., Parente, L. L., Alencar, A. A., Rudorff, B. F. T., Hasenack, H., Matsumoto, M., Ferreira, L. G., Souza-Filho, P. W. M., de Oliveira, S. W.,

Rocha, W. F., Fonseca, A. V., Marques, C. B., Diniz, C. G., Costa, D., Monteiro, D., Rosa, E. R., Vélez-Martin, E., ... Azevedo, T. (2020). Reconstructing three decades of land use and land cover changes in brazilian biomes with landsat archive and earth engine. *Remote Sensing, 12*(17). https://doi.org/10.3390/RS12172735

Spracklen, D. V., & Righelato, R. (2014). Tropical montane forests are a larger than expected global carbon store. *Biogeosciences*, *11*(10), 2741–2754. https://doi.org/10.5194/bg-11-2741-2014

Starzomski, B. M. (2013). Novel Ecosystems and Climate Change. In *Novel Ecosystems* (pp. 88–101). John Wiley & Sons, Ltd. https://doi.org/https://doi.org/10.1002/9781118354186.ch10

Suarez, A., Árias-Arévalo, P. A., & Martínez-Mera, E. (2018). Environmental sustainability in post-conflict countries: insights for rural Colombia. Environment, Development and Sustainability, 20(3), 997–1015. https://doi.org/10.1007/s10668-017-9925-9

Suárez, E., Encalada, A. C., Chimbolema, S., Jaramillo, R., Hofstede, R., & Riveros-Iregui, D. (2023). On the Use of '"Alpine"' for High-Elevation Tropical Environments. *Mountain Research and Development*, *43*(1), V1–V4. https://doi.org/10.1659/mrd.2022.00024

Taylor, P. D., Fahrig, L., Henein, K., & Merriam, G. (1993). Connectivity is a vital element of landscape structure. *Oikos, 68*(3), 571–573. https://doi.org/10.2307/3544927

Testolin, R., Attorre, F., & Jiménez-Alfaro, B. (2020). Global distribution and bioclimatic characterization of alpine biomes. *Ecography*, *43*(6), 779–788. https://doi.org/10.1111/ecog.05012

Thies, B., Meyer, H., Nauss, T., & Bendix, J. (2014). Projecting land-use and land-cover changes in a tropical mountain forest of Southern Ecuador. *Journal of Land Use Science*, *9*(1), 1–33. https://doi.org/10.1080/1747423X.2012.718378

Thompson, J. B., Zurita-Arthos, L., Müller, F., Chimbolema, S., & Suárez, E. (2021). Land use change in the Ecuadorian páramo: The impact of expanding agriculture on soil carbon storage. *Arctic, Antarctic, and Alpine Research*, *53*(1), 48–59. https://doi.org/10.1080/15230430.2021.1873055

Thrasher, B., Wang, W., Michaelis, A., Melton, F., Lee, T., & Nemani, R. (2022). NASA Global Daily Downscaled Projections, CMIP6. *Scientific Data*, *9*(1), 262. https://doi.org/10.1038/s41597-022-01393-4

Tischendorf, L., & Fahrig, L. (2000). On the usage and measurement of landscape connectivity. *Oikos, 90*(1), 7–19. https://doi.org/10.1034/j.1600-0706.2000.900102.x

Tito, R., Vasconcelos, H. L., & Feeley, K. J. (2018). Global climate change increases risk of crop yield losses and food insecurity in the tropical Andes. *Global Change Biology*, *24*(2), e592–e602. https://doi.org/10.1111/gcb.13959

Tobón, C. (2009). *Los bosques andinos y el agua*. Programa Regional ECOBONA-INTERCOOPERATIÓN, CONDESAN.

Torres, A. C., Binda, E., Ochoa Quintero, J. M., Garcia, H., Gómez, B., Soto, C., Martínez, S., & Clerici, N. (2020). Answering the right questions. Addressing biodiversity conservation in post-conflict Colombia. *Environmental Science & Policy*, 104, 82–87. https://doi.org/10.1016/j.envsci.2019.11.012

Tovar, C., Arnillas, C. A., Cuesta, F., & Buytaert, W. (2013). Diverging Responses of Tropical Andean Biomes under Future Climate Conditions. *PLoS ONE*, *8*(5). https://doi.org/10.1371/journal.pone.0063634

Tovar, C., Carril, A. F., Gutiérrez, A. G., Ahrends, A., Fita, L., Zaninelli, P., Flombaum, P., Abarzúa, A. M., Alarcón, D., Aschero, V., Báez, S., Barros, A., Carilla, J., Ferrero, M. E., Flantua, S. G. A., Gonzáles, P., Menéndez, C. G., Pérez-Escobar, O. A., Pauchard, A., … Hollingsworth, P. M. (2022). Understanding climate change impacts on biome and plant distributions in the Andes: Challenges and opportunities. *Journal of Biogeography*, *49*(8), 1420–1442. https://doi.org/10.1111/JBI.14389

Tovar, C., Duivenvoorden, J. F., Sánchez-Vega, I., & Seijmonsbergen, A. C. (2012). Recent Changes in Patch Characteristics and Plant Communities in the Jalca Grasslands of the Peruvian Andes. *Biotropica*, *44*(3), 321–330. https://doi.org/10.1111/J.1744-7429.2011.00820.X

Tovar, C., Melcher, I., Kusumoto, B., Cuesta, F., Cleef, A., Meneses, R. I., Halloy, S., Llambí, L. D., Beck, S., Muriel, P., Jaramillo, R., Jácome, J., & Carilla, J. (2020). Plant dispersal strategies of high tropical alpine communities across the Andes. *Journal of Ecology*, *108*(5), 1910–1922. https://doi.org/10.1111/1365-2745.13416

Tylianakis, J. M., Didham, R. K., Bascompte, J., & Wardle, D. A. (2008). Global change and species interactions in terrestrial ecosystems. *Ecology Letters*, *11*(12), 1351–1363. https://doi.org/10.1111/j.1461-0248.2008.01250.x

UNODC-SIMCI. (2021). Monitoreo de territorios afectados por cultivos ilícitos 2020. https://www.unodc.org/documents/crop-monitoring/Colombia/Colombia_Monitoreo_de_territorios_afectados_por_cultivos_ilicitos_2020.pdf

Urban, D., & Keitt, T. (2001). Landscape connectivity: A graph-theoretic perspective. *Ecology, 82*(5), 1205–1218. https://doi.org/10.1890/0012-9658(2001)082[1205:LCAGTP]2.0.CO;2

Valencia, J. B., Mesa, J., León, J. G., Madriñán, S., & Cortés, A. J. (2020). Climate Vulnerability Assessment of the Espeletia Complex on Páramo Sky Islands in the Northern Andes. *Frontiers in Ecology and Evolution*, *8*. https://doi.org/10.3389/fevo.2020.565708

Valencia, J. B., Mesa, J., León, J. G., Madriñán, S., & Cortés, A. J. (2020). Climate Vulnerability Assessment of the Espeletia Complex on Páramo Sky Islands in the Northern Andes. *Frontiers in Ecology and Evolution*, 8. https://doi.org/10.3389/fevo.2020.565708

Vancutsem, C., Achard, F., Pekel, J. F., Vieilledent, G., Carboni, S., Simonetti, D., Gallego, J., Aragão, L. E. O. C., & Nasi, R. (2021). Long-term (1990–2019) monitoring of forest cover changes in the humid tropics. *Science Advances*, *7*(10), 1–22. https://doi.org/10.1126/sciadv.abe1603

Veloz, S. D., Williams, J. W., Blois, J. L., He, F., Otto-Bliesner, B., & Liu, Z. (2012). No-analog climates and shifting realized niches during the late quaternary: Implications for 21st-century predictions by species distribution models. *Global Change Biology*, *18*(5), 1698–1713. https://doi.org/10.1111/j.1365-2486.2011.02635.x

Verrall, B., & Pickering, C. M. (2020). Alpine vegetation in the context of climate change: A global review of past research and future directions. *Science of The Total Environment*, *748*, 141344. https://doi.org/10.1016/J.SCITOTENV.2020.141344

Vijay, V., Pimm, S. L., Jenkins, C. N., & Smith, S. J. (2016). The impacts of oil palm on recent deforestation and biodiversity loss. *PLoS ONE*, 11(7). https://doi.org/10.1371/journal.pone.0159668

Viviroli, D., Kummu, M., Meybeck, M., Kallio, M., & Wada, Y. (2020). Increasing dependence of lowland populations on mountain water resources. *Nature Sustainability*, *3*(11), 917–928. https://doi.org/10.1038/s41893-020-0559-9

Vuille, M. (2013). *Climate Change and Water Resources in the Tropical Andes*. https://doi.org/10.13140/2.1.3846.9124

Walters, D., Baran, A. J., Boutle, I., Brooks, M., Earnshaw, P., Edwards, J., Furtado, K., Hill, P., Lock, A., Manners, J., Morcrette, C., Mulcahy, J., Sanchez, C., Smith, C., Stratton, R., Tennant, W., Tomassini, L., Van Weverberg, K., Vosper, S., … Zerroukat, M. (2019). The Met Office Unified Model Global Atmosphere 7.0/7.1 and JULES Global Land 7.0 configurations. *Geosci. Model Dev*, *12*. https://doi.org/10.5194/gmd-12-1909-2019

Watson, J. E. M., Dudley, N., Segan, D. B., & Hockings, M. (2014). The performance and potential of protected areas. *Nature*, 515(7525), 67–73. https://doi.org/10.1038/nature13947

Wikramanayake, E., Dinerstein, E., Loucks, C. J., Olson, D. M., Morrison, J., Lamoreux, J., McKnight, M., & Hedao, P. (2002). *Terrestrial ecoregions of the Indo-Pacific: a conservation assessment*.

Williams, J. W., & Jackson, S. T. (2007). Novel climates, no-analog communities, and ecological surprises. *Frontiers in Ecology and the Environment*, *5*(9), 475–482. https://doi.org/10.1890/070037

Williams, J. W., Jackson, S. T., Kutzbach, J. E., & Schneider, S. H. (2007). Projected distributions of novel and disappearing climates by 2100 AD. *PNAS*, *104*(14), 5738–5742. https://doi.org/10.1073/pnas.0606292104

Willis, K. S. (2015). Remote sensing change detection for ecological monitoring in United States protected areas. *Biological Conservation*, 182, 233–242. https://doi.org/10.1016/j.biocon.2014.12.006

Xu, Q., Yordanov, V., Bruzzone, L., & Brovelli, M. A. (2025). High-Resolution Global Land Cover Maps and Their Assessment Strategies. In *ISPRS International Journal of Geo-Information* (Vol. 14, Issue 6). Multidisciplinary Digital Publishing Institute (MDPI). https://doi.org/10.3390/ijgi14060235

Yang, S., Cammeraat, E., Jansen, B., Den Haan, M., Van Loon, E., & Recharte, J. (2018). Soil organic carbon stocks controlled by lithology and soil depth in a Peruvian alpine grassland of the Andes. *Catena*, *171*, 11–21. https://doi.org/10.1016/j.catena.2018.06.038

Yin, P., Gao, Y., Chen, R., Liu, W., He, C., Hao, J., Zhou, M., & Kan, H. (2023). Temperature-related death burden of various neurodegenerative diseases under climate warming: a nationwide modelling study. *Nature Communications*, *14*(1). https://doi.org/10.1038/s41467-023-44066-5

Yuan, R., Zhang, N., & Zhang, Q. (2024). The impact of habitat loss and fragmentation on biodiversity in global protected areas. *Science of the total environment*, 931, 173004. https://doi.org/10.1016/j.scitotenv.2024.173004

Zhang, X., & Cai, X. (2011). Climate change impacts on global agricultural land availability. *Environmental Research Letters*, *6*(1). https://doi.org/10.1088/1748-9326/6/1/014014

Ziehn, T., Chamberlain, M. A., Law, R. M., Lenton, A., Bodman, R. W., Dix, M., Stevens, L., Wang, Y.-P., Srbinovsky, J., Ziehn, T., Chamberlain, M. A., Law, R. M., Lenton, A., Bodman, R. W., Dix, M., Stevens, L., Wang, Y.-P., & Srbinovsky, J. (2020). The Australian Earth System Model: ACCESS-ESM1.5. *Journal of Southern Hemisphere Earth Systems Science*, *70*(1), 193–214. https://doi.org/10.1071/ES19035